Exploring a New Immunological Niche: How Fibroblastic Reticular Cells Tune T Cell Immunity Through Notch Signals

by

Eric T. Perkey

A dissertation submitted in partial fulfillment
of the requirements for the degree of
Doctor of Philosophy
(Cellular and Molecular Biology)
At the University of Michigan
2020

Doctoral Committee:

Professor Roman Giger, Co-Chair
Professor Ivan P. Maillard, Co-Chair
Assistant Professor Kaushik Choudhuri
Associate Professor Irina L. Grigorova
Professor Pavan R. Reddy

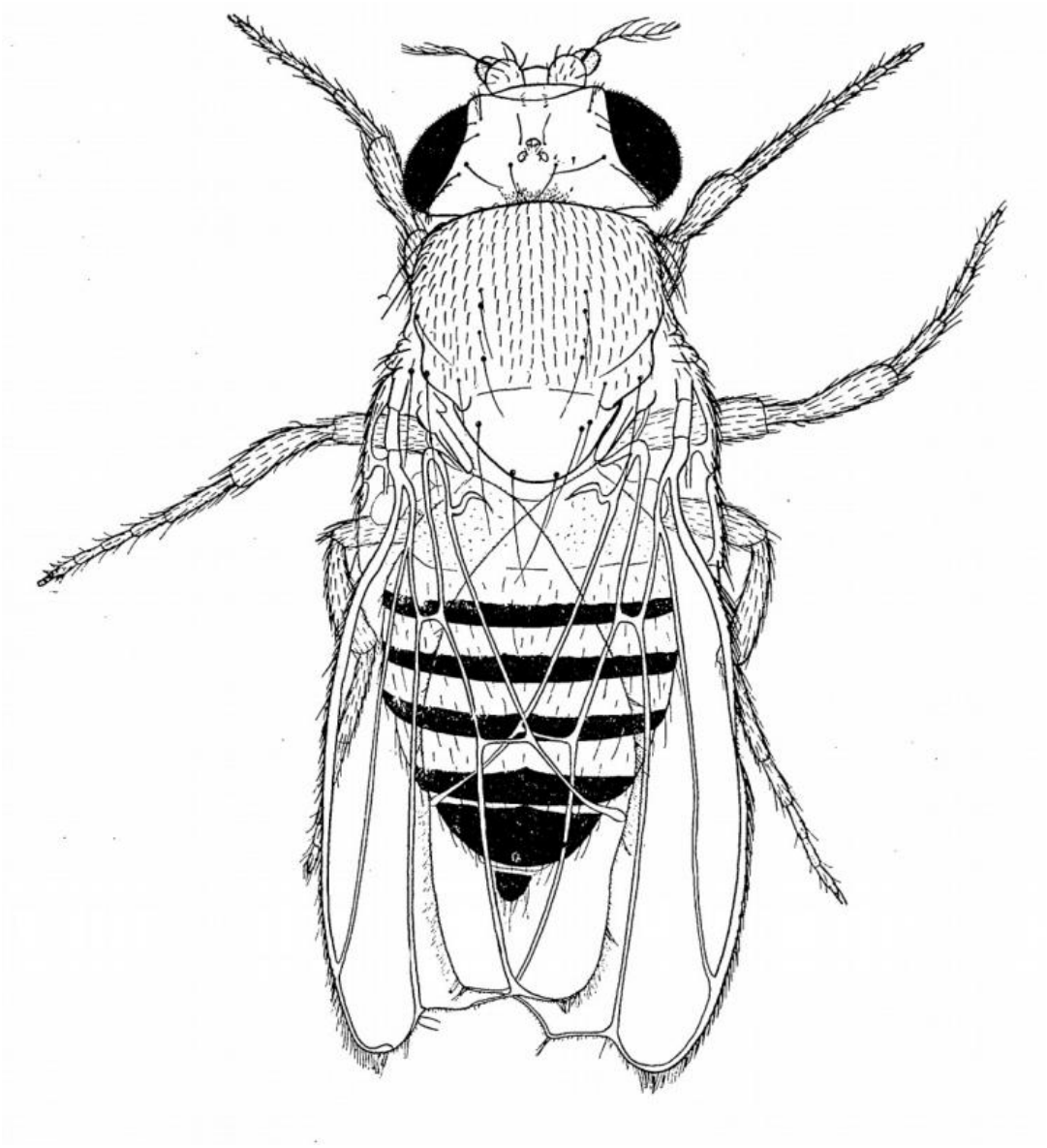

Notch mutant female

From T.H. Morgan. 1917. The Theory of the Gene. *American Naturalist* 51:513-544.

Eric T. Perkey

eperkey@umich.edu

ORCID iD: 0000-0003-3275-3181

Dedication

To my parents, Renay and Jim. And to my partner, Amelia.

Acknowledgements

I am eternally grateful to my mentor, Dr. Ivan Maillard, who I followed from Ann Arbor to Philadelphia to pursue the work described in this dissertation. The time, generosity, and effort he has put into my training cannot be overestimated. I look to him as a model of a physician-scientist. I am also sincerely grateful to my dissertation committee members: Drs. Kaushik Choudhuri, Roman Giger, Irina Grigorova, and Pavan Reddy for providing guidance in my studies and taking time to read and critique this work.

I would like to acknowledge the essential role that current members and alumni of the Maillard laboratory have had in laying the foundation of this dissertation and my scientific development. While many have contributed to the completion of this work, particular thanks to: Dr. Jooho Chung, Dr. Vedran Radojcic, Ann Friedman, Dr. Jennifer Chase, Dr. Christen Ebens, Dr. Léolène Carrington, Dr. Gloria Jih, Dr. Fred Allen, Dr. Daniela Gómez-Atria, Dr. Joshua Brandstadter, Ashley Vanderbeck, Sam Kelly, and Anneka Allman. I would like to provide special recognition to David Granadier and Alexander Dils who both dedicated countless hours of physical and intellectual work on critical experiments with me.

I am indebted to Dr. Nathalie Labrecque, her student Dave de Sousa, and the rest of the Labrecque laboratory at the University of Montreal, who have been our scientific partners in much of this work. Many others have been critical to developing my science, including Dr. Brian Gaudette, Dr. Victor Tkachev, Dr. Leslie Kean, Dr. Denis Migliorini, Dr. Heejin Jun, Dr. Jun Wu, Dr. Gonzalo Garcia, and Dr. Richard Miller, among others.

I would like to thank my friends and family. My MSTP cohort has kept me sane and excited about science. My parents, Renay and Jim, have always supported and encouraged my curiosity from a young age. I cannot express how grateful I am to them for their dedication and belief in me. And to my partner Amelia: thank you for being with me through all of it. I am surprised you have not yet grown annoyed with me even as we are each other's only human contact in the midst of the COVID-19 pandemic. I am excited for what the rest of our life together has in store.

Table of Contents

Chapter 5

Chapter 6

Chapter 7

List of Figures

Chapter 1

Chapter 2

Chapter 3

Chapter 4

Chapter 5

Chapter 6

Abstract

Notch is an evolutionarily conserved cell-to-cell signaling pathway with important roles throughout biology that has emerged as a critical regulator of mature T cell responses. Pharmacological Notch inhibition is a promising candidate strategy to prevent T cell pathogenicity in graft-versus-host disease (GVHD), the limiting complication of allogeneic bone marrow transplantation (allo-BMT). We found that presentation of the critical Delta-like Notch ligands to T cells is restricted to a cellular niche of non-hematopoietic fibroblastic reticular cells (FRCs) in secondary lymphoid organs. Still, little is known about the nature and regulation of the FRC niche during allo-BMT. Beyond allo-BMT, it is unclear whether T cells receive Notch ligands from the FRC niche or alternative sources, such as professional antigen-presenting cells (APCs). In this thesis, I explored how the FRC niche regulates T cell responses through Notch signaling, both during allo-BMT and in other immunological contexts.

First, I uncovered a novel indicator of Notch signaling in activated T cells based on core-2 O-glycosylation of CD43. Using this indicator, I observed that the FRC niche remains the critical source of Notch signals that drive T cell pathology after allotransplantation with reduced intensity or no myeloablative conditioning, contexts in which recipient hematopoietic cells are not profoundly depleted. Next, I documented the role of FRC niches in priming a pathogenic gut-homing program in alloreactive T cells. Inhibiting Notch signals in T cells or eliminating Delta-like ligands in FRCs preferentially prevented the accumulation of effector T cells in the intestines while accumulation of T regulatory cells was relatively preserved. Notch signals were required for

the acquisition of the gut-tropic α4β7 integrin in effector, but not regulatory T cells. These findings provide possible mechanistic explanations for the role of Notch in gastrointestinal GVHD. Next, we explored how allo-BMT regulates the FRC niche. Allo-BMT enhanced inflammatory gene programs in FRCs, including upregulation of Delta-like4 and antigen-presentation machinery. Delta-like4 upregulation was restricted to a subset of $CD157^{hi}$ FRCs and depended on signals from alloantigen-activated T cells, suggesting that early crosstalk between T cells and FRC subsets establishes a pathogenic niche that drives GVHD. We then investigated whether FRCs could present MHC class II-restricted alloantigens in a $CD4^+$ T cell-driven model of GVHD. While FRCs were necessary to drive GVHD through the provision of Notch ligands, they were dispensable sources of alloantigens, suggesting that T cell activation requires distinct physical interaction with APCs and FRCs. We tested this model using dendritic cell (DC) immunization to control the source of antigen. Even when we immunized recipients with $Delta\text{-}like4^{hi}$ DCs, FRCs acted non-redundantly to drive Notch-dependent differentiation of $CD8^+$ T cells into $KLRG1^{hi}$ short-lived effector cells, suggesting that FRCs deliver Notch signals to T cells independently of antigen. We next studied the effects of Notch signaling in naïve T cells. Transcriptomic profiling revealed Notch-dependent regulation of naïve T cells, with FRCs as the source of Notch ligands. Collectively, these studies document the non-redundant role of the FRC niche in controlling Notch-dependent T cell activation and differentiation. We propose that the availability of Notch ligands in the FRC niche is dynamically regulated to control effector T cell responses during allo-BMT and potentially other immune responses. Further understanding T cell-FRC interactions will suggest novel therapies to dampen pathogenic or amplify protective immunity.

Chapter 1

Introduction[1]

This dissertation describes four interrelated studies that seek to better understand how T cell immune responses are governed by the local microenvironment through the Notch signaling pathway. As an introduction, I will describe several concepts central to this work and present background information on the pathophysiology of graft-versus-host disease (GVHD). GVHD is a major complication of bone marrow transplantation and the immunobiological context in which we primarily studied T cell responses in this dissertation, although we also expanded our work to include observations in other contexts. We highlight critical questions that each project was designed to answer. When considered together, results from these projects suggest a new model of immune regulation by Notch signaling: specialized fibroblastic reticular cells (FRCs) residing within distinct immunological niches in secondary lymphoid organs orchestrate T cell immune responses through Notch ligand-receptor interactions.

[1] Excerpts taken from: **Perkey, E.** Maillard, I. *New Insights in Graft-Versus-Host Disease and Graft Rejection.* Annual Review of Pathology: Mechanisms of Disease. 13:219-245. 2018. PMID: 29099560

1.1 Immunological niches

The concept of cellular niches was first proposed by Schofield to explain how hematopoietic stem cell behavior is controlled by their interaction with other cells at specific anatomical sites (1). Niches determine the number and behavior of resident stem cells through the provision of signals in a spatially limiting niche. Cells that leave the niche lose access to these limited signals and begin to differentiate into mature cells. Since then, extensive work has characterized how cellular niches regulate diverse areas of stem cell biology. This includes work on the germ cell niche in Drosophila testes (2), the hematopoietic stem cell niche in bone marrow (3), and niches for cancer stem cells (4).

Analogous to stem cell niches is the evolving concept of immunological niches. While stem cell niches control progenitor cells, distinct immunological niches differentially regulate mature immune cell homeostasis, activation, and differentiation into effector cells (5). Local microenvironmental signals vary between different organs, and this differential signaling often tips the balance between immune activation and tolerance. Even within secondary lymphoid organs (SLOs), multiple microanatomical niches exist where differential regulation of the immune response occurs. These niches are created at least in part by the underlying architecture of resident stromal cells, including lymphatic endothelial cells, blood endothelial cells, and fibroblastic reticular cells.

1.2 Overview of fibroblastic reticular cells

Fibroblastic reticular cells (FRCs) are a heterogenous group of cells that encompass several related non-hematopoietic and non-endothelial mesenchymal cell subsets in lymphoid tissues. While

FRCs do serve structural purposes, as other fibroblasts, they are also specialized in organizing and orchestrating innate and adaptive immune responses. FRCs first develop from local perivascular myofibroblast precursors in response to Lymphotoxin-α signals (6–8). In mature secondary lymphoid organs, multiple distinct FRC subsets regulate the microanatomical niches that they organize (8, 9). In lymph nodes, $CD157^{hi}$ T-zone fibroblastic reticular cells (TRCs) organize the paracortex and produce high levels of CCL19, CCL21, and IL-7 to attract and maintain naïve T cells as well as activated dendritic cells, thus orchestrating initial antigen-T cell encounter (10). In B-cell follicles of the outer cortex, specialized B-zone fibroblastic reticular cells produce CXCL13 and support B cells (11). Follicular dendritic cells (FDCs) are another subset of FRCs critical to organize on-going germinal center responses through capture and presentation of antibody-antigen complexes to B cells (12, 13). In the medulla of lymph nodes, specialized $CD157^{lo}$ FRCs support early plasma cell maintenance through the production of IL-6, BAFF, and CXCL12 (14). MAdCAM-1^{+} marginal reticular cells (MRCs) are present at the interface between the cortex and subcapsular sinus in lymph nodes or the marginal sinus in spleen and play key roles in antimicrobial defense, generating FDCs in lymph nodes in response to microbial challenge, and supporting marginal zone B cell populations in the spleen (15–17). New functional studies of FRCs have been greatly accelerated by the development of transgenic mice expressing a Cre recombinase under control of regulatory elements of the *Ccl19* promoter (6, 8). Using this tool, novel roles for FRCs are being increasingly defined. For example, FRCs have been shown to temper T cell immune activation through the production of nitric oxide (18, 19) or prostaglandins (20). Conversely, FRCs can drive T cell activation through signals such as IL-6 (21) and CD40 (22). It is likely that the balance between T cell activation and regulation is controlled by FRCs themselves, through sensing of both innate immune stimuli and signals from activated T cells (23,

24). Using these new genetic tools, our laboratory (25, 26) and others (17) uncovered a novel and necessary role of FRC subsets in controlling adaptive immune response through the provision of Delta-like Notch ligands to T cells in secondary lymphoid organs.

1.3 Overview of Notch signaling

Notch signaling is a highly evolutionarily conserved cell-to-cell communication pathway mediated by Notch ligand-receptor interactions between adjacent cells **(Fig 1.1**) (27). Four Notch receptors (NOTCH1–4) and five Notch ligands of the Jagged (JAG) and Delta-like (DLL) families (JAG1/2 and DLL1/3/4) have been identified in mammals. Among Delta-like ligands, only DLL1 and DLL4 have agonistic properties. Specific interactions between Notch ligands and receptors expressed in adjacent cells induce regulated proteolytic activation of the receptor by an ADAM family metalloprotease and then by the γ-secretase complex. γ-secretase-mediated intramembrane proteolysis releases intracellular Notch (ICN) into the cytoplasm. ICN migrates into the nucleus where it partners with the DNA-binding transcription factor CSL (CBF1/suppressor-of-hairless/Lag-1), also called RBP-Jκ and encoded by the *Rbpj* gene. ICN and RBP-Jκ become part of a large transcriptional activation complex in association with a Mastermind-like (MAML) family coactivator and multiple other proteins that cooperate to mediate transcriptional activation of Notch target genes. The majority of Notch's well-documented effects in the immune system are mediated by canonical ICN/RBP-Jκ/MAML-dependent transcriptional activation, although noncanonical mechanisms of Notch action have also been reported (26, 28–33).

In the hematopoietic system, Notch was first described as a oncogene in T-cell acute lymphoblastic leukemia (34). Additional work identified a physiological role of Notch as an essential signal in

the early stages of T cell development in the thymus. Interaction of DLL4 ligands in thymic epithelial cells with NOTCH1 receptors in T lineage progenitors is required for the production mature T cells (35–37). Notch signaling also regulates the differentiation, maintenance, or function of distinct subsets of B cells, dendritic cells, macrophages, and innate lymphoid cells (38). However, in many of these contexts, the cellular source and regulation of Notch ligands are not fully understood.

Notch transcriptional effects are context-dependent. Progress has been made to identify direct transcriptional targets of Notch signaling that mediate downstream biological effects of the pathway in specific contexts, especially in Notch-driven cancers (39, 40). Many Notch targets are regulated via Notch activity at enhancer regions and via cooperation with other context-specific transcription factors (41). While many direct Notch targets have been described in cancer, more work is needed to systematically uncover the cell-type and context-specific transcriptional networks regulated by Notch in both resting and activated immune cells.

1.4 Notch signaling in mature T cell immunobiology

In mature T cell biology, Notch was originally described as a positive regulator of proliferation and IFN-γ production in vitro (42). Further in vitro studies suggested that Notch signals control $CD4^+$ T helper differentiation fate, with Delta-like ligands reported to drive Th1 fate and Jagged ligands a Th2 fate (43). However, these early studies involved in vitro stimulation where Notch ligands were either not present or artificially overexpressed on antigen-presenting cells. More recent studies have utilized in vivo loss-of-function approaches, which has revealed many context-dependent roles of Notch signaling in mature $CD4^+$ and $CD8^+$ T responses (44). During viral or

intracellular bacterial infection, Notch signals delivered to $CD8^+$ T cells are critical to generate robust effector response and clear of acute infection, while being dispensable for long-term memory formation (45, 46). In $CD4^+$ T cells, Notch signals regulate diverse immunologic effector functions including Th1, Th2, Th17, Th22, T follicular helper, and $Foxp3^+$ T regulatory cell (Treg) responses (17, 25, 47–55, 28–32, 43, 45, 46). Importantly, the majority of these studies implied (although often did not directly test) that professional antigen-presenting cells (APCs), such as dendritic cells (DCs) were the critical source of Notch ligands regulating T cell function.

Our laboratory has studied the role of Notch signaling in models of T cell-mediated alloimmunity including graft-versus-host disease (GVHD) following allogeneic bone marrow (allo-BMT) and organ rejection **(See Section 1.11)**. Both alloreactive $CD4^+$ and $CD8^+$ T cells required MAML-dependent Notch transcriptional activation to produce inflammatory cytokines, traffic to target tissues, and mediate lethal GVHD. We observed a dominant role for the NOTCH1 receptor and the DLL4 ligand with minor roles for NOTCH2 and DLL1. Pathogenic Notch signals were delivered within the first 48 hours of transplantation (28–30, 47). We first hypothesized that Notch signals would be delivered to T cells by hematopoietic professional APCs. Instead, we discovered that FRCs in secondary lymphoid organs are the critical cellular source of Notch ligands that prime pathogenic T cell response during GVHD (25). This key finding, along with other reports that FRCs provide Notch signals to T cells in vivo (17), led us to further explore the secondary lymphoid organ FRC niche and how it regulates T cell activation and function. For many of these studies, we have used allo-BMT models as there is a critical role for Notch signaling in this context and major unmet clinical needs in defining novel immunosuppressive strategies to mitigate

GVHD. In further studies we have extended these observations beyond the GVHD models to test if the FRC niche regulates other T cell immune responses through Notch signaling.

1.5 Overview of transplantation and alloimmunity

In patients with failing organs or tissues, modern medical practice relies on transplantation procedures as an important clinical resource with lifesaving potential. Transplanted organs and tissues are defined as allogeneic when harvested from donors who are genetically nonidentical to the recipients, which is the case for the vast majority of donor-recipient pairs (with the rare exception of identical twins). Immune responses directed against foreign tissue antigens (or alloantigens) mediate key unique complications of allogeneic transplantation. These complications include graft rejection, which occurs after transplantation of allogeneic organs (e.g., heart, lung, liver, small intestine, or kidney), tissues (e.g., bone marrow or pancreatic islets), or composite grafts (e.g., limb or facial structures). Conversely, graft-versus-host disease (GVHD) can occur after transplantation of grafts containing large amounts of donor immune cells, most commonly bone marrow, mobilized peripheral blood, or cord blood. Graft rejection involves immune reactivity of the recipient against transplanted allografts, while GVHD is triggered by the reactivity of donor-derived immune cells against allogeneic recipient tissues.

1.5.1 Clinical Importance of Alloimmune Complications

An improved understanding of the cellular and molecular mechanisms mediating graft rejection and GVHD is essential, because both complications are major medical problems that cause significant morbidity and mortality, limiting the success of transplantation procedures. Historically, T cells have been considered the dominant cellular subset mediating graft rejection

and GVHD, and most efforts to prevent or treat these complications have focused on interventions that target T cell reactivity. To prevent graft rejection, transplantation recipients routinely receive lifelong immunosuppression with calcineurin inhibitors, with or without additional agents. Although this strategy supported major progress in modern transplantation medicine, especially in controlling acute rejection, it is linked to significant problems, including drug toxicity, increased risks of opportunistic infections, and an increased incidence of malignancy (posttransplant lymphoproliferative disorders and other cancers). In addition, current immunosuppressive regimens insufficiently control chronic rejection, a distinct immunopathological syndrome leading to steady attrition in the viability of transplanted allografts over time. As a result, many patients experience a need for re-transplantation, which can be medically challenging, limited by low organ availability, and particularly problematic in recipients of life-sustaining allografts (e.g., heart or lung). B lineage cells as well as other non–T cells are thought to play a major role in chronic rejection and chronic GVHD. As an alternative to immunosuppression based on calcineurin inhibitors, preclinical and early clinical research efforts have attempted to achieve states of true tolerance to the transplanted organ that allow allograft survival in the absence of lifelong immunosuppression. Strategies to induce tolerance currently under investigation include targeting costimulatory pathways and establishing allogeneic hematopoietic chimerism via nonmyeloablative bone marrow transplantation, followed by organ transplantation. Although promising in principle, the full real-life clinical potential of these strategies remains to be established.

1.5.2 Risks and Benefits of Alloimmunity in Allogeneic Bone Marrow Transplantation

Alloimmune rejection is uniformly detrimental after solid organ transplantation, but a delicate balance between immune complications and benefits needs to be considered after allogeneic bone

marrow, cord blood, or mobilized peripheral blood transplantation (jointly referred to as allogeneic hematopoietic cell transplantation, or allo-HCT). However, for the sake of consistency we will continue to refer to allo-HCT in general as allogeneic bone marrow transplantation (allo-BMT) throughout this dissertation. In this setting, graft rejection is relatively rare, except in patients with preexisting autoimmune or alloimmune reactivity. In contrast, GVHD is the prevailing clinical problem, with the potential to induce life-threatening, immune-mediated damage to target organs, such as the gut, skin, liver, thymus, and lung. Similar to chronic allograft rejection, chronic GVHD is a distinct entity that affects a large fraction of patients, can cause major lifelong morbidity, and remains poorly responsive to current treatments. In parallel to these complications, however, transplanted T cells and other immune cells induce beneficial anticancer effects referred to as graft-versus-tumor (GVT) activity. Because the majority of allo-BMT procedures are performed for patients with hematological malignancies (e.g., leukemias or lymphomas), and only a minority for benign disorders, it is essential to identify strategies to control GVHD that still preserve potent GVT activity. Another important problem unique to allo-BMT is the occurrence of delayed immune reconstitution and poor immune function, a prevalent problem often associated with chronic GVHD.

1.5.3 Evolving Concepts in the Pathogenesis of Alloimmune Injury

To understand the pathogenesis of alloimmune complications after transplantation, it is useful to consider elements borrowed from the immune system's responses to conventional antigens, as well as features that are unique to the artificial conditions induced by transplantation. Unlike most conventional exogenous antigens, alloantigens are broadly expressed either in the transplanted allograft (rejection) or in the allo-BMT recipient (GVHD), and they are persistent in the sense that they can never be completely eliminated. In this regard, alloimmunity shares important features

with autoimmunity and chronic viral infections. Nevertheless, much remains to be learned about the molecular nature, tissue distribution, and cellular presentation of alloantigens. Another determinant of alloimmune reactivity is the delivery of context-dependent innate signals during the priming of the immune response. For example, ischemic injury during the harvest and processing of the allograft exerts major effects on the induction of alloimmunity via exposure to damage-associated molecular patterns, for example, DNA, RNA and other molecules released by damaged cells. Microbe-associated molecular patterns have also been reported to influence alloreactivity, with a recent focus on the role played by the microbiome in both solid organ rejection and GVHD. During allo-BMT, damage to recipient tissues is caused by myeloablative or, to a lesser extent, nonmyeloablative conditioning regimens involving total body irradiation or chemotherapy. In turn, tissue damage generates inflammatory signals that enhance the adaptive immune response to recipient alloantigens. Another key feature of GVHD pathogenesis is the preeminence of the gut, as both a site of immune priming and a target of the disease, with the potential for a self-reinforcing pathogenic loop. Although basic and clinical researchers have been focusing on this question for years, recent work has brought new insights into a complex cross talk among innate lymphoid cells (ILCs), intestinal epithelial cells, microbiota, and T cells that regulates the onset of GVHD. Finally, nonhematopoietic cells in secondary lymphoid organs (SLOs) and other tissues have recently come into focus as a source of alarmins [e.g., interleukin (IL)-33] and innate signals (e.g., Notch ligands) that control key aspects of alloimmunity during graft rejection and GVHD. Thus, although there is no doubt that T cells are essential in alloimmunity, T cell function is influenced by interactions with a complex microenvironmental niches and by the unique conditions induced by transplantation procedures.

1.6 Alloantigen presentation

After allogeneic transplantation, APCs stimulate alloreactive T cells through the provision of alloantigens and costimulatory signals. In recent years, intense scrutiny has been devoted to defining the mechanisms and the cellular subsets involved in alloantigen presentation **(Fig 1.1).** Importantly, both hematopoietic and nonhematopoietic APCs can be activated by innate immune stimuli that are associated with the transplantation procedure, including ischemic damage, tissue damage secondary to myeloablative conditioning, and exposure to signals from the microbiome. In a positive feedback loop, signals from activated alloreactive T cells drive further activation of professional APCs, as well as increased antigen presentation capacity in other APCs. These mechanisms, as well as the nature and distribution of alloantigens, determine how alloreactive T cells get activated and mediate the immune complications of transplantation.

1.6.1 Nature of Alloantigens

During microbial infections, naïve T cells encounter peptide antigens loaded on major histocompatibility complex (MHC) molecules. Costimulatory and coinhibitory signals regulate whether antigen encounter leads to productive immune responses or tolerance. Individual cellular subsets have variable capacities to provide these signals to T cells, but hematopoietic conventional dendritic cells (cDCs) appear to be the critical professional APCs that prime naïve T cells in SLOs in response to most infections. $CD8^+$ T cells recognize endogenous molecules presented on MHC class I, while $CD4^+$ T cells recognize exogenous molecules processed after uptake of extracellular pathogens and presented on MHC class II. However, it is now clear that overlap exists between endogenous and exogenous pathways, allowing presentation of exogenous peptides on MHC class I (cross presentation), and endogenous peptides on MHC class II.

In allogeneic transplantation, genetic polymorphisms between donor and recipient exist both within and outside the MHC locus. Critical differences exist between T cell activation in MHC-matched and MHC-mismatched transplants. In MHC-mismatched allogeneic responses, a large proportion of T cells are thought to react with polymorphic regions of allogeneic MHC, irrespective of which peptide is loaded (56). Alternatively, allogeneic MHC loaded with specific endogenous peptides can function as a molecular mimic of self-MHC loaded with foreign peptides (57, 58). MHC-mismatched transplantation induces strong alloimmune responses, and as a result, lethal GVHD and acute rejection of skin transplants can be driven by single polymorphisms in either MHC class I or class II (59). In solid organ transplantation, MHC matching increases allograft survival but is difficult to achieve in practice (60). In contrast, allo-BMT is often fully MHC-matched, although several types of mismatched allo-BMT are performed when MHC-matched donors are not available.

In MHC-matched transplants, polymorphisms at non-MHC loci encode alloantigens that are processed and presented on syngeneic MHC [minor histocompatibility antigens (MiHAs)]. Similar to microbial antigens, MiHAs are recognized by rare T cell clones with T cell receptors cognate to processed MiHA loaded on MHC molecules. For example, H-Y MiHAs encoded by the Y chromosome cause higher risks of alloimmunity when female T cells encounter male target cells (61). Among hundreds of potential MiHAs in human transplantation, only a few are known to date. However, analysis of single nucleotide polymorphisms encoding putative MiHA epitopes demonstrated that the degree of genetic mismatch correlates with the incidence of severe GVHD after allo-BMT (62). MiHAs that are restricted to the hematopoietic compartment can selectively drive GVT over GVHD (63), presumably because they induce responses against residual

hematological malignancies but not target epithelial organs. In mouse models, potent alloimmune responses can also be driven by virally encoded endogenous MiHAs that act as superantigens (64), although the role of similar mechanisms in human transplantation is unknown.

1.6.2 Antigen-Presenting Cells in Graft-Versus-Host Disease

Unlike most responses to pathogens in which specialized hematopoietic APCs prime T cells, in allo-BMT both recipient hematopoietic and nonhematopoietic cells have independently been shown to be sufficient to prime alloreactive T cell responses in distinct mouse GVHD models (65–67). Recipient-derived APCs are essential to initiate acute GVHD; however, donor APC subsets can amplify later disease states. For example, cDCs derived from the donor bone marrow restimulate alloreactive $CD4^+$ T cells in target GVHD organs (68, 69). After T cells are initially primed by recipient cells, donor $CD103^+$ cDCs seed the gut, capturing alloantigens and becoming activated by innate inflammatory signals before migrating to mesenteric lymph nodes, driving a potent positive feedback loop of T cell alloactivation through the provision of recipient alloantigen, IL-12, IL-6, and CD40 costimulatory signals (70, 71). Further dysregulation of donor-derived APCs after allo-BMT sustains the seemingly paradoxical autoimmunity and immunosuppression observed in chronic GVHD (72, 73).

During MHC-mismatched allo-BMT, $CD4^+$ T cells or, to a lesser extent, $CD8^+$ T cells can induce lethal GVHD regardless of whether target epithelial tissues express MHC class II or MHC class I, respectively (74). Consistent with the rapid kinetics of disease, MHC-mismatched allo-BMT likely triggers an inflammatory cytokine storm that induces disease irrespective of alloantigen expression in target cells. In these models, cDCs appeared sufficient to prime alloreactive T cells. This was based on an experimental add-back strategy in which recipients genetically lacking the ability to

present allogeneic MHC alloantigens received cDCs with an intact antigen presentation machinery just prior to transplantation. However, the authors of this study transferred unirradiated cDCs into recipients conditioned with myeloablative regimens, which may not accurately recapitulate the state of endogenous conditioned recipient cDCs (75). While cDCs or plasmacytoid dendritic cells (DCs) were sufficient to drive GVHD in this context, neither appeared necessary, as profound depletion of cDCs, plasmacytoid DCs, and B cell subsets did not protect recipients from MHC-mismatched $CD4^+$ T cell–driven GVHD (75–77). Due to the ubiquitous distribution of alloantigens and high frequency of alloreactive T cells in MHC-mismatched bone marrow transplantation, a single APC subset may not be critical to prime alloreactive T cells in these models. In fact, recipient cDCs can exert tolerogenic functions in GVHD; newer studies using multiple different genetic methods to deplete cDCs showed that recipients lacking cDCs displayed accelerated GVHD in both MHC-matched and mismatched models (66, 78). Similarly, expansion of recipient $CD8\alpha^+$ cDCs with recombinant FLT3L protected mice from GVHD (79).

In MHC-matched GVHD, Shlomchik et al. (65) used a $CD8^+$ T cell–driven allo-BMT model to show that eliminating MHC class I presentation in the recipient hematopoietic compartment prevented GVHD. As in MHC-mismatched GVHD, cDCs were inferred to be the critical hematopoietic APC subset, although this was not formally proven in vivo with cell-specific loss-of-function experiments (80). Subsequent work indicated that MHC class I expression in nonhematopoietic tissues was also necessary to drive disease (81), which suggests that reexposure to MiHA in target tissues drives $CD8^+$ T cell–mediated GVHD pathology in MHC-matched models of GVHD. In $CD4^+$ T cell–driven models of MHC-matched GVHD, conflicting evidence implicates both hematopoietic and nonhematopoietic APCs as the critical priming subset. In one

model, recipient mice lacking MHC class II in nonhematopoietic cells had similar or worse tissue GVHD compared to controls (81). More recently, other groups showed that MHC class II expressed only on nonhematopoietic cells (66) or that alloantigen mismatch only in the nonhematopoietic compartment (67, 82) is sufficient to drive $CD4^+$ T cell–mediated GVHD in several MiHA models, while depletion of recipient cDCs prior to allo-BMT actually worsened GVHD (66). Furthermore, when MHC class II was eliminated from the hematopoietic compartment, recipient mice lacked the ability to expand regulatory T cells (Tregs), suggesting tolerogenic roles for recipient hematopoietic APCs (83). Together, these findings suggest that nonhematopoietic APCs can be key stimulators of alloreactive $CD4^+$ T cells, while hematopoietic APCs can prime pathogenic $CD8^+$ T cell and both pathogenic and protective $CD4^+$ T cell responses in MHC-matched allo-BMT. However, it remains debated which nonhematopoietic cellular subsets serve as important APCs in $CD4^+$ T cell–driven GVHD and if they reside in target tissues or in SLOs, where classical priming is thought to occur.

Expression of MHC class II and other molecules important for exogenous antigen presentation in both hematopoietic and nonhematopoietic cells is regulated by the class II transactivator (*CIITA*) (84). *CIITA* expression itself is controlled by several promoters that are differentially active in various cellular subsets. Professional APC subsets, such as cDCs and B cells, drive *CIITA* from constitutively active promoters, while nonhematopoietic tissues utilize the IFNγ-inducible promoter IV of *CIITA* (85). This regulation pattern suggests that inducible MHC class II could participate in GVHD pathogenesis after alloreactive T cells or other immune cells release IFNγ. Additionally, nonhematopoietic cells may respond to local damage and microbe-associated danger signals after myeloablative conditioning by upregulating costimulatory molecules. In fact,

nonhematopoietic cells may be the critical responders to innate signals in GVHD pathogenesis, as recipient mice genetically lacking signal transduction machinery downstream of all Toll-like receptors in their hematopoietic compartment were not protected from GVHD (86).

In the small intestine and colon, two critical GVHD target organs, both lamina propria myofibroblasts (66, 87–89) and intestinal epithelial cells (90) have been implicated as key subsets that upregulate MHC class II and costimulatory molecules to prime alloreactive $CD4^+$ T cells after allo-BMT. Intestinal epithelial cells express MHC class II on their basolateral surface, with upregulated expression during GVHD, although they typically have been considered to have tolerogenic functions through DC-independent expansion of Tregs (91–93). However, a recent study identified that Villin-Cre^+ intestinal epithelial cells but not mesenchymal or endothelial cells were a necessary source of MHC class II alloantigen presentation required to drive lethal GVHD (90). If intestinal epithelial cells are converted to pro-inflammatory antigen-presenting cells by the allo-BMT environment, this could explain the why the GI tract is such a dominant target tissue during GVHD.

1.6.3 Sites of T Cell Priming in Graft-Versus-Host Disease

Where alloreactive T cells first get primed in GVHD remains debated. Naïve T cells typically traffic to SLOs, such as spleen and lymph nodes. Consistent with a role for SLOs in priming alloreactive T cells, splenectomized *aly/aly* mice that lacked lymph nodes had delayed and blunted GVHD (94). In another study, Lymphotoxin-α null mice (lacking lymph nodes and Peyer's patches) that had also been splenectomized were protected from gastrointestinal GVHD (95). This is consistent with luciferase reporter-based tracking of alloreactive T cells, which revealed that alloreactive T cells were first detected in secondary lymphoid organs before accumulating in target

tissues including the GI tract (96). Nonhematopoietic cells in SLOs, including blood endothelial cells, lymphatic endothelial cells, and fibroblastic reticular cells (FRCs), harbor MHC class II and upregulate its expression during adaptive immune responses (97). Antigen presentation from these cell types appears to be tolerogenic in many contexts (24, 98). However, in the context of allo-BMT, FRCs and other fibroblastic stromal cells were shown to drive GVHD through presentation of Delta-like Notch ligands within the first 48 h after transplantation (25), suggesting that these cells can be proinflammatory. FRCs were also shown to display peptide-loaded MHC class II from exosomes released from cDCs, although in this context it was tolerogenic (99). One intriguing possibility is that, prior to their elimination by myeloablative conditioning, recipient hematopoietic APCs may transfer intact MHC molecules to non-hematopoietic cells such as FRCs for presentation to alloreactive T cells. Fibroblasts infected with lymphocytic choriomeningitis virus were also shown to prime $CD8^+$ T cells in the absence of effective cross presentation by hematopoietic APCs but only in the setting of SLOs (100). Thus, the alloantigen-presenting functions of nonhematopoietic stromal cells, especially FRCs, in SLOs needs to be explored (see **Chapter 5**). High-endothelial venules (HEVs), FRCs, and likely follicular DCs also appear to be direct targets of acute GVHD, which in turn contributes to the dysregulation of humoral immunity (101) and breakdown of tolerance (102) during chronic GVHD.

While much evidence indicates that the primary site of initiation of GVHD resides in secondary lymphoid organs, competing reports have suggested that alloreactive T cells can be primed directly in target tissues without needing to migrate to secondary lymphoid organs. When MHC class II was conditionally deleted in intestinal epithelial cells, mice were protected from $CD4^+$ T cell mediated GVHD. Furthermore, intestinal epithelial cells isolated from irradiated mice could prime

alloreactive T cells in vitro (90). Still, mice lacking MHC class II in intestinal epithelial cells developed severe skin GVHD, indicating that not all priming occurred in the GI tract.

The requirement for alloantigen presentation in secondary lymphoid organs versus target tissues could depend on the chemokine receptors and integrin molecules that donor T cell subsets express combined with the integrins and chemokines expressed by the endothelium of target tissues versus HEVs **(See Chapter 3)**. The nature and subset of donor T cells (e.g. naïve vs. memory) could influence these trafficking molecules on T cells, while the conditioning regimen could influence expression of trafficking molecules on target and lymphoid tissue endothelium.

1.7 Gastrointestinal Graft-Versus-Host Disease

Damage to epithelial surfaces is a critical feature of GVHD that has attracted the attention of many researchers, as it is linked to the most dangerous clinical features of the disease. Disruption of the intestinal epithelium plays a critical role at the onset of GVHD as a result of both conditioning-related toxicity and immune-mediated injury (96, 103). However, epithelial damage in the gut is counterbalanced by repair and protective mechanisms regulated by ILCs, a family of lymphoid cells that do not express antigen receptors but have evolved to sense and respond to a broad range of innate signals (104) **(Fig 1.3)**. In the intestine and in other target organs such as the thymus, ILC-derived signals such as IL-22 protects epithelial tissues from GVHD damage (105, 106).

In experimental models and in clinical allo-BMT, the intensity of radiation or chemotherapy-based conditioning regimens is linked to the incidence and severity of GVHD (103, 107). Although multiple direct or indirect effects could be involved, the use of higher intensity conditioning

regimens is associated with increased histological evidence of gut epithelial damage after allo-BMT, increased abundance of lipopolysaccharide in the serum (suggesting defective intestinal barrier function and bacterial translocation), and increased serum levels of inflammatory cytokines such as TNF-α and IL-1β (consistent with a cytokine storm) (103, 108). Trafficking studies revealed evidence of early and prominent infiltration of the gut by donor-derived T cells within days after allo-BMT, only shortly after initial priming in SLOs (96). Dysregulation of the intestinal microbiome is also a prominent feature of allo-BMT that plays a role in GVHD onset (108–111). Altogether, these studies have shown the intestine to be at the center of a self-reinforcing pathogenic loop leading to GVHD.

Recent work has revealed detailed features of intestinal epithelial damage after allo-BMT that appear important for GVHD pathogenesis. In mouse allo-BMT models, profound loss of $Lgr5^+$ crypt-based intestinal stem cells (ISCs) was detected at disease onset, suggesting that ISCs themselves can be targeted by the combination of conditioning and alloimmune injury (105, 112, 113). The crypt-based ISC niche is located close to endothelium expressing the Mucosal addressin cell adhesion molecule 1 (MAdCAM1). In a recent study, GVHD led to preferential infiltration of this niche, but not other parts of the intestinal epithelium, by α4β7-expressing alloreactive T cells (114). Damage to $Lgr5^+$ intestinal epithelial cells was mediated by donor T cell derived IFN-γ which caused programmed cell death (115). Both in mice and in human patients, acute GVHD was also associated with loss of intestinal Paneth cells (108, 116). Paneth cells are specialized epithelial cells that sit at the basis of intestinal crypts and have been reported to function as a niche for ISCs by producing agonists of the Wnt and Notch signaling pathways (117). Paneth cells produce a range of antibacterial peptides including α-defensins and REG3 family proteins that regulate the

intestinal microbiome (118). Paneth cell loss in allo-BMT models was associated with dysbiosis even in the absence of irradiation-based conditioning (108). In patients, low Paneth cell numbers in intestinal biopsies at the onset of GVHD predicted a high risk for GVHD-related nonrelapse mortality (116). Interestingly, unbiased proteomic analysis identified serum levels of the C-type lectin REG3α as a sensitive and specific biomarker of intestinal acute GVHD with a role in risk stratification (119), possibly after release into the circulation upon Paneth cell injury. Thus, damage to ISCs and their niche may play a specific role at the core of GVHD pathogenesis.

1.8 Notch Signaling in T cell alloimmunity

Notch signaling has emerged as a key regulator of T cell alloimmunity, in the setting of both GVHD and allograft rejection (25, 28–31, 47, 48, 52, 120, 121). Recent data identified nonhematopoietic radioresistant FRCs as the critical source of Notch ligands at the onset of GVHD (25, 26).

1.8.1 Early Insights on Notch Signaling in Alloimmunity

Early studies relying heavily on artificial gain-of-function strategies were the first to draw attention to a potential role of Notch in tolerance and alloreactivity (122–125). Adoptive transfer of DCs engineered to overexpress the Notch ligand JAG1 induced antigen-specific T cell hyporesponsiveness to a house dust mite antigen (123). Similar observations were then made when studying T cell responses to alloantigens or viral antigens using JAG1-transduced Epstein–Barr virus–transformed B lymphoblastoid cell lines as APCs (124, 125). In a heart allograft model, Dallman and colleagues (122) reported a $CD8^+$ T cell–dependent tolerogenic effect of adoptively transferred L cell fibroblasts overexpressing the Notch ligand DLL1 and allogeneic MHC

molecules. Taken together, these studies suggested that inducing artificially high levels of Notch signaling could create a state of antigen-specific T cell tolerance. However, interpretation was difficult given possible non-cell-autonomous effects of overexpressed Notch ligands, the lack of direct genetic demonstration, and the artificial nature of the gain-of-function experimental systems. More recently, several laboratories used in vivo loss-of-function strategies to evaluate the role of Notch signaling in alloimmunity (25, 26, 121, 28–31, 47, 48, 52, 120). These studies reached concordant conclusions that Notch functions as a major proinflammatory signaling pathway promoting pathogenic alloreactivity, in both GVHD and transplant rejection. Thus, the actual in vivo function of Notch signaling in alloimmunity turns out to be opposite from that initially suggested by artificial gain-of-function strategies.

1.8.2 Notch and Graft-Versus-Host Disease

In multiple mouse models of allo-BMT and GVHD, genetic inhibition of canonical Notch signaling in T cells led to profoundly decreased GVHD severity and GVHD-associated mortality (28, 29, 47). The effects of Notch signaling were dependent on NOTCH1/2 receptors in T cells and DLL1/4 ligands in the recipient, with dominant effects of NOTCH1 and DLL4 (29, 52, 121). Transient systemic inhibition of DLL1/4 with neutralizing antibodies in the peri-transplant period was sufficient to confer long-term protection (25, 29). These findings suggested the existence of an early pathogenic pulse of Notch signaling in alloreactive T cells during their priming and initial activation. Upon Notch inhibition, protection from GVHD was associated with decreased production of multiple inflammatory cytokines, including IFN-γ and TNF-α, as well as increased expansion of preexisting Tregs. Upon in vivo priming in the absence of Notch signaling, alloreactive T cells acquired a state of acquired hyporesponsiveness to restimulation through their T cell receptor and CD28 coreceptor (47). Yet, some aspects of T cell function were preserved in

Notch-deprived alloreactive T cells, including in vivo proliferation and expansion in lymphopenic recipients as well as expression of cytotoxic molecules. Ex vivo cytotoxicity and in vivo anticancer activity were also preserved. As a result, Notch inhibition allowed long-term posttransplant survival without severe GVHD and without recurrent cancer in mouse models of allo-BMT and leukemia. The relative importance of conventional T cells and Tregs in mediating Notch's effects remains to be determined, as do the precise mechanisms of Notch action in T cells. Genetic data point at canonical RBP-Jk/MAML-dependent transcriptional effects of Notch signaling as the critical effectors of Notch signaling in alloreactive T cells, although functionally essential transcriptional targets need to be identified (26, 28, 31). In addition, Notch may also exert important effects in B cells during chronic GVHD (126).

1.8.3 Cellular Sources of Notch Ligands in Alloimmunity

Early studies of Notch in T cell immunity documented that professional APCs, such as DCs, increased Notch ligand expression in response to inflammatory stimuli and established the potential of these cells to function as a source of Notch ligands to T cells (43). Subsequent studies in alloreactivity and other immune contexts postulated that Notch ligands are derived from hematopoietic APC subsets, although most of these studies were based on correlation and ex vivo coculture systems without in vivo genetic data (49, 121, 127, 128). Radtke and collaborators (17) were the first to identify a nonhematopoietic cellular source of DLL1/4 Notch ligands for the differentiation of Notch-dependent T follicular helper cells, $ESAM^{hi}$ DCs, and marginal zone B cells in SLOs. In mouse models of acute GVHD, Chung et al. (25) discovered that hematopoietic sources of DLL1 and DLL4 Notch ligands were not essential for disease pathogenesis **(Fig1.1b).** Instead, a population of nonhematopoietic fibroblastic stromal cells lineage traced with a *Ccl19-Cre* transgene was the critical source of DLL1/4 ligands at GVHD onset, with essential Notch

signals delivered within days after allo-BMT (25) **(Fig 1.1c)** *Ccl19-Cre* is expressed in the fibroblastic stromal cell compartment of spleen and lymph nodes as well as in Peyer's patches (6). After irradiation-based conditioning and allo-BMT, *Ccl19-Cre* activity was detected predominantly in a population of FRCs with high CD157 expression and in follicular dendritic cells of spleen and lymph nodes, as well as, to a minor extent, in lymphatic endothelial cells (25). These findings identify a fibroblastic niche that plays a critical role in the pathogenesis of acute GVHD through the delivery of Notch signals.

1.9 Focus of the current studies

The Notch signaling pathway is emerging as a critical regulator of adaptive immunity via T cell–FRC interactions in specialized immunological niches in SLOs. However, we still have limited understanding of how T cell-FRC interactions are regulated in the context of allotransplantation. Furthermore, we do not understand the extent to which T cell-FRC interactions are required in other immunological contexts to provide Notch signals. Thus, we focused our exploration on four inter-related studies that seek to answer critical questions about T cell-FRC interactions and Notch signaling.

Chapter 2: Can we develop a generalizable tool to monitor Notch signals in antigen-activated T cell subsets? And can we use this tool to determine if the FRC niche provides Notch signals in different immunological contexts?

Whether FRCs also function as the dominant source of Notch ligands in nonmyeloablative allo-BMT, in allograft rejection, and in other types of immune response remains to be determined. In order to answer this question, we developed a novel and generalizable indicator of Notch signals

in antigen-activated T cells, based on expression of the core-2 O-glycoform of CD43. Using this indicator, we determined that FRCs remain the dominant source of Notch ligands that drive T cell pathogenicity after allotransplantation with reduced intensity or no myeloablative conditioning (26).

Chapter 3: How do Notch signals drive gastrointestinal GVHD?

The immunobiological mechanisms explaining how Notch signaling drives gastrointestinal GVHD pathogenesis remain to be determined. It is unclear if alloreactive T cells require Notch signaling in immunological niches in SLOs, in the GI tract, or both to mediate gastrointestinal GVHD. These are critical questions to answer to advance pharmacological Notch blockade to the clinic as a GVHD prophylaxis strategy. We used genetic loss-of-function studies to ask key questions about the role of FRC niches and Notch signaling in gastrointestinal GVHD.

Chapter 4: How does allo-BMT regulate the FRC niche? And can FRCs present alloantigens?

It is unclear if cross-talk occurs between alloreactive T cells and FRCs and if it is important for acquisition of pathogenic T cell function in GVHD. Furthermore, due to their role in providing Notch signals to T cells early during activation, FRCs may also be presenting alloantigen. To answer these questions, we studied alloreactive T cells and FRCs after allo-BMT and used genetic loss-of-function strategies to determine the role of alloantigen presentation from FRCs during GVHD. Furthermore, we used DC immunization to understand if FRCs are relevant sources of Notch signals to T cells when antigen presentation is restricted to another cellular subset.

Chapter 5: Can Notch signals be delivered to naïve T cells by the FRC niche?

Others have suggested that Notch is delivered at the immune synapse by APCs. Our findings that FRCs function as the critical source of Notch ligands during allo-BMT and DC immunization **(Chapter 4)** independently of antigen presentation led us to question this model. To understand if Notch and antigen signals can be dissociated, we studied the effects of Notch signaling in naïve $CD4^+$ T cells that have not yet encountered antigens.

Together, these interrelated studies explore an emerging paradigm of adaptive immune response: regulation by microenvironmental signals derived from localized stromal niche cells. We demonstrated in multiple new immunological contexts that Notch signaling derived from FRC-T cell interactions determines subsequent T cell activation and function. These interactions control pathogenic T cell function during allo-BMT, in part through controlling trafficking of alloreactive effector T cells to the GI tract. Furthermore, we show that FRCs are dynamically regulated by allo-BMT. Alloantigen-primed T cells controlled the abundance of DLL4 Notch ligands expressed by the FRC niche, suggesting that a very early cross-talk between activated T cells and FRCs may determine the subsequent magnitude of Notch-dependent T cell immune responses. We proved that FRCs, while necessary in their role as sources of Notch ligand, are dispensable sources of alloantigen presentation in allo-BMT. Instead, we propose a model where T cells engage in distinct cell-to-cell interactions with both FRCs and APCs. We tested this hypothesis during DC immunization and found that FRCs were necessary sources of Notch ligands for driving $CD8^+$ T cell effector function. Confirming that Notch signaling in mature T cells could be spatiotemporally separated from antigen presentation, we showed that naïve $CD4^+$ T cells experienced active Notch signaling from FRCs. In light of these studies, we propose that Notch ligand expressing FRCs

represent a dynamically regulated, spatially limited niche that controls the magnitude of inflammatory T cell responses in both allogeneic BMT and other immunological contexts.

1.10 Figures

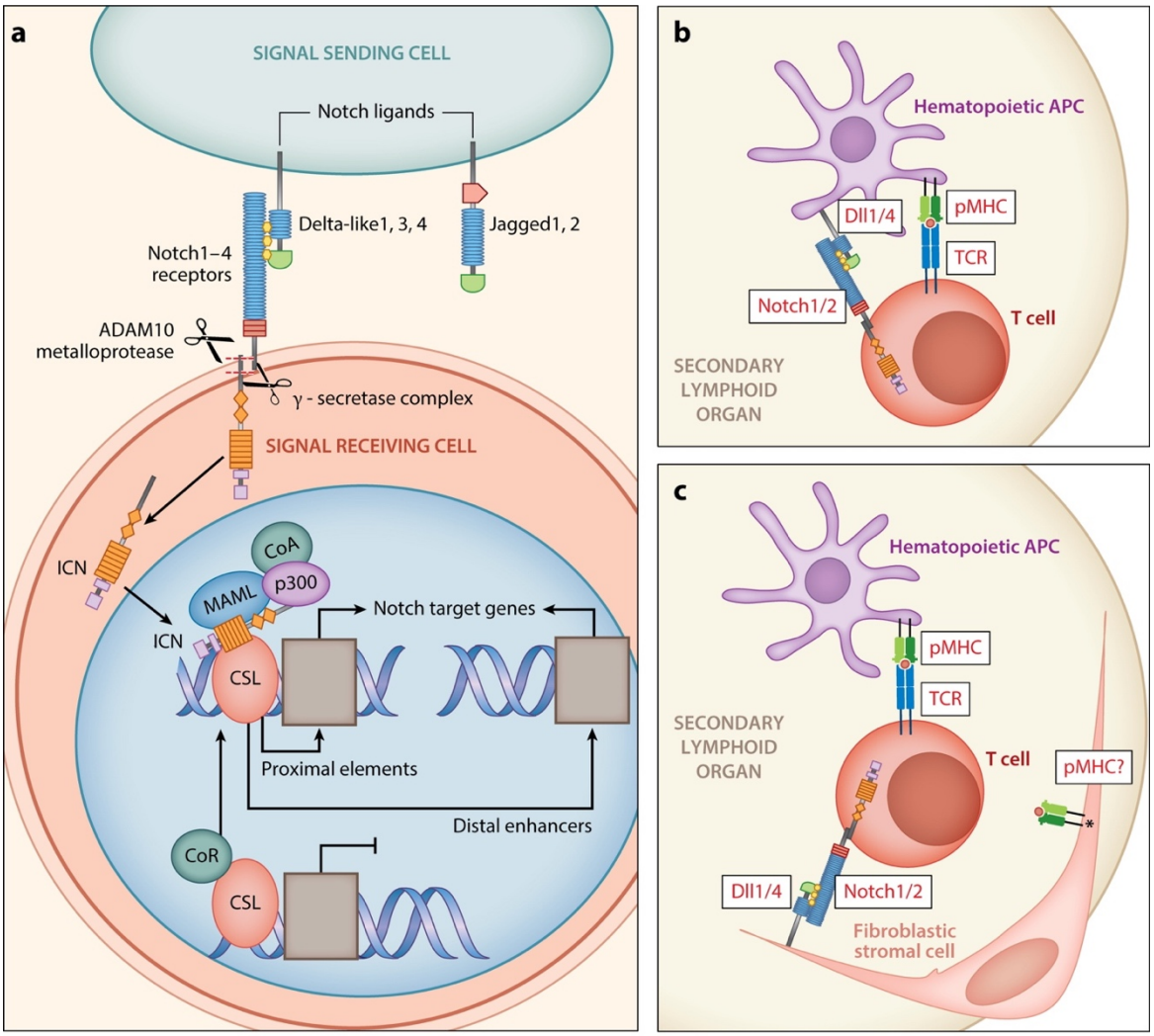

Perkey E, Maillard I. 2018.
Annu. Rev. Pathol. Mech. Dis. 13:219–45

Fig 1.1 Overview of Notch signaling and sources of Notch signals in alloimmunity. (a) Notch signaling occurs via the physical interaction between Notch receptors (Notch1–4) and Notch ligands (Delta-like 1,3, and 4; Jagged 1 and 2). Ligand-receptor binding allows two cleavage events to occur, which are mediated by the ADAM10 metalloprotease and the γ-secretase complex, releasing ICN into the cytosol. After entry into the nucleus, ICN forms a transcriptional activation complex with the transcription factor RBP-Jκ (alias CSL), a MAML coactivator, and other partners including p300. ICN/RBP-Jκ /MAML transcriptional complexes can regulate Notch target genes at promoter proximal regions or through binding at distal enhancer sites. (b) Classical model of Notch involvement in T cell alloactivation. A naïve T cell is activated by a hematopoietic APC that provides both antigen-specific signals and Notch signals through Delta-like1/4-Notch1/2 interactions. (c) New model of Notch signaling and T cell alloactivation. Delta-like1/4 Notch signals are derived from nonhematopoietic fibroblastic stromal cells such as fibroblastic reticular cells or follicular dendritic cells in secondary lymphoid organs. Fibroblastic stromal cells may also present alloantigens through the expression of allopeptide-loaded MHC complexes. Abbreviations: APC, antigen-presenting cell; CoA, coactivator; CoR, corepressor; RBP-Jκ, CBF1/suppressor-of-hairless/Lag-1; DLL1/4, Delta-like 1,4; ICN, intracellular Notch; MAML, mastermind-like; pMHC, peptide-loaded major histocompatibility complex; TCR, T cell receptor.

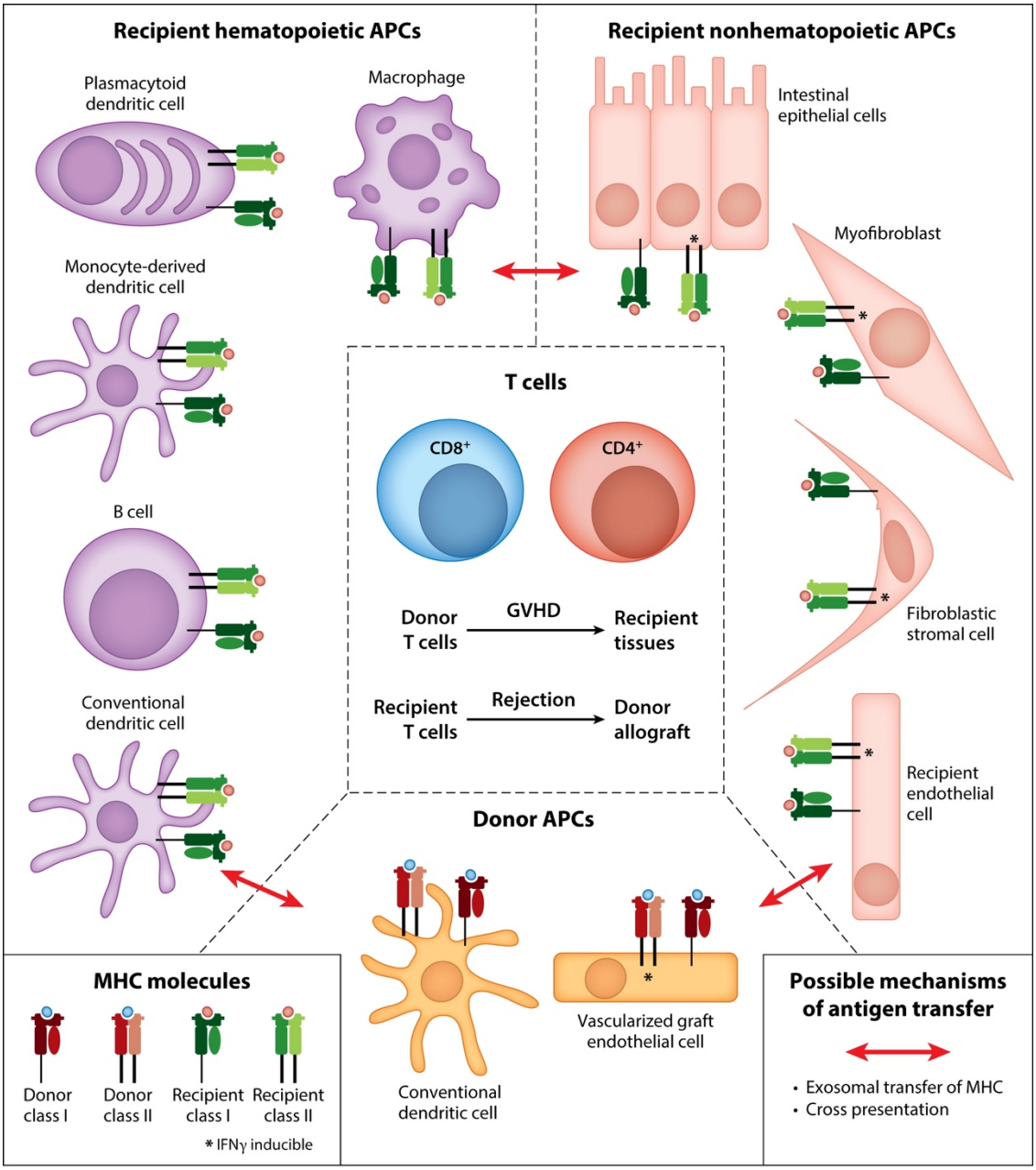

Perkey E, Maillard I. 2018. *Annu. Rev. Pathol. Mech. Dis.* 13:219–45

Fig 1.2 Potential inflammatory or tolerogenic alloantigen-presenting cells after allogeneic transplantation. (Center) After allogeneic hematopoietic cell transplantation, donor T cells become activated by recipient alloantigens, leading to graft-versus-host disease (GVHD). After solid organ transplantation, recipient T cells become activated by donor alloantigens, leading to allograft rejection. (Left) Potential recipient hematopoietic antigen-presenting cells (APCs). (Right) Potential recipient nonhematopoietic APCs. (Bottom) Potential donor APCs. All nucleated cell types express major histocompatibility complex (MHC) class I. Only some cell types constitutively express MHC class II, while others express MHC class II in response to IFNγ (inducible), denoted by the asterisk. Red arrows indicate potential mechanisms of alloantigen transfer: exosomal transfer of intact allopeptide-MHC complexes and endocytosis of cellular material followed by cross presentation of peptide alloantigens by another cellular subset.

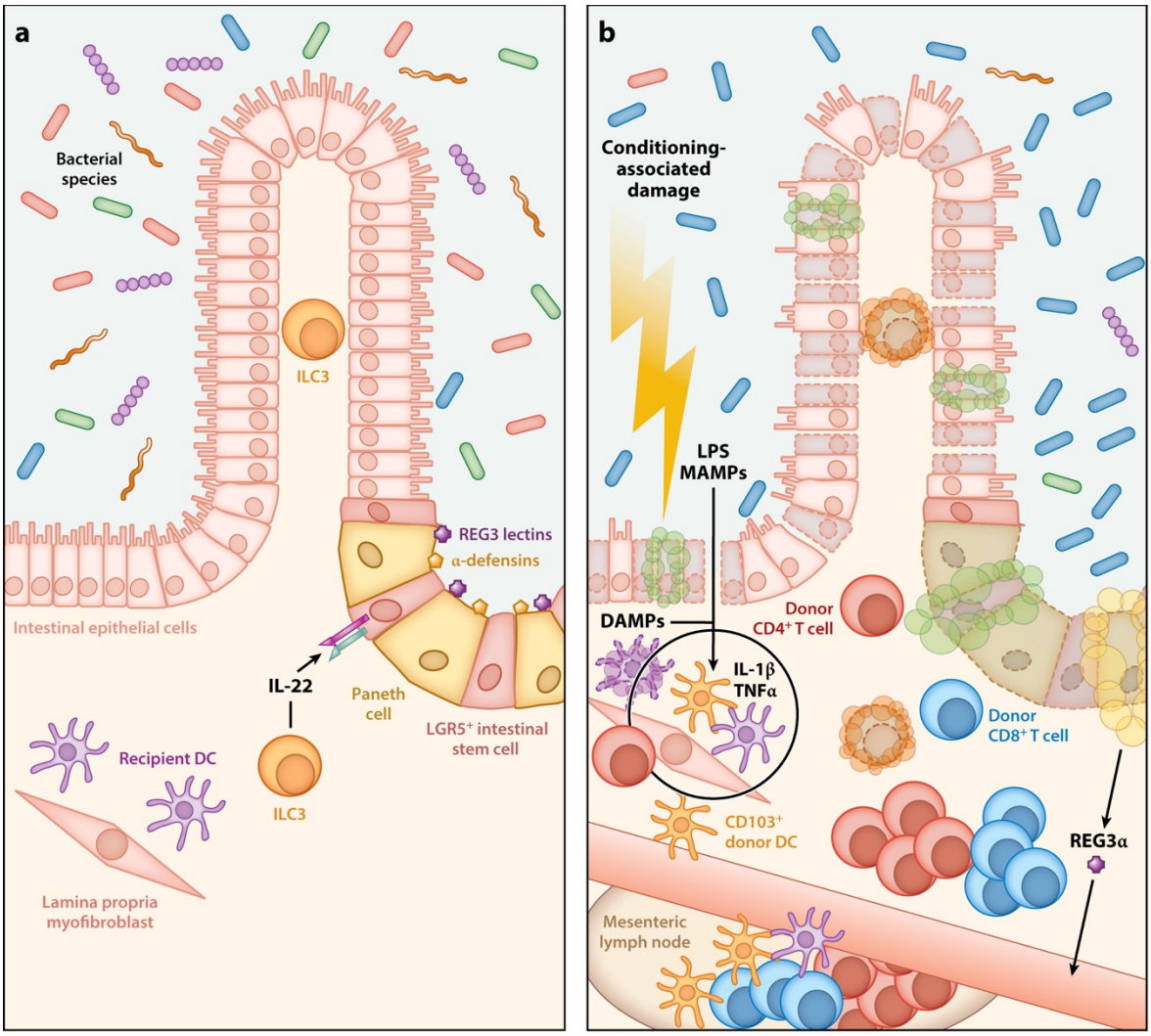

Perkey E, Maillard I. 2018. *Annu. Rev. Pathol. Mech. Dis.* 13:219–45

Fig 1.3 Loss of epithelial integrity and intestinal dysbiosis during acute GVHD. (a) Small intestine during homeostasis. The intestinal epithelium is constantly regenerated by LGR5+ ISCs. ILC3s release IL-22 to support epithelial repair after injury. Paneth cells secrete α-defensins and REG3 proteins to regulate the intestinal microbiome. (b) Small intestine during acute GVHD. Damage from myeloablative conditioning, including irradiation and chemotherapy, injures the intestinal epithelium, including Paneth cells and ISCs, leading to loss of mucosal integrity. LPS and other MAMPs translocate across the gut epithelium, activating recipient and donor innate immune cells, which in turn release inflammatory cytokines (IL-1β, TNFα). Alloimmune activation of donor T cells occurs in the mesenteric lymph node and locally in the lamina propria, leading to alloimmune reactivity that further damages the intestinal epithelium. REG3α release into the blood is associated with intestinal GVHD and loss of Paneth cells. Recipient ILC3s are lost through a combination of conditioning-associated and alloimmune damage preventing IL-22-mediated maintenance of ISCs and leading to impaired regeneration of the gut epithelium. GVHD and intestinal injury also dysregulate the microbiome, leading to dysbiosis, which reinforces GVHD pathogenesis. Abbreviations: DAMPs, damage-associated molecular patterns; DC, dendritic cell; GVHD, graft-versus-host disease; IL, interleukin; ILC3, type 3 innate lymphocyte; ISC, intestinal stem cell; LPS, lipopolysaccharide; MAMPs, microbe-associated molecular patterns; TNFα, tumor necrosis factor alpha.

Chapter 2

GCNT1-Mediated O-Glycosylation of the Sialomucin CD43 is a Sensitive Indicator of Notch Signaling in Activated T Cells[2]

2.1 Abstract

Notch signaling is emerging as a critical regulator of T cell activation and function. However, there is no reliable cell surface indicator of Notch signaling across activated T cell subsets. Here we show that Notch signals induce upregulated expression of the *Gcnt1* glycosyl-transferase gene in T cells mediating graft-versus-host disease (GVHD) after allogeneic bone marrow transplantation (allo-BMT) in mice. To determine if *Gcnt1*-mediated O-glycosylation could be used as a Notch signaling reporter, we quantified the core-2 O-glycoform of CD43 in multiple T cell subsets during GVHD. Pharmacological blockade of Delta-like Notch ligands abrogated core-2 O-glycosylation in a dose-dependent manner after allo-BMT, both in donor-derived $CD4^+$ and $CD8^+$ effector T cells, and in $Foxp3^+$ regulatory T cells. CD43 core-2 O-glycosylation depended on cell-intrinsic canonical Notch signals and identified $CD4^+$ and $CD8^+$ T cells with high cytokine-producing

[2] Reproduced from: **Perkey, E**., D. Maurice De Sousa, L. Carrington, J. Chung, A. Dils, D. Granadier, U. Koch, F. Radtke, B. Ludewig, B. R. Blazar, C. W. Siebel, T. V. Brennan, J. Nolz, N. Labrecque, and I. Maillard. 2020. GCNT1-Mediated O -Glycosylation of the Sialomucin CD43 Is a Sensitive Indicator of Notch Signaling in Activated T Cells. *J. Immunol.* 204: 1674–1688.

ability. *Gcnt1*-deficient T cells still drove lethal alloreactivity, showing that core-2 O-glycosylation predicted, but did not cause Notch-dependent T cell pathogenicity. Using core-2 O-glycosylation as a marker of Notch signaling, we identified Ccl19-Cre^{+} fibroblastic stromal cells as critical sources of Delta-like ligands in graft-versus-host responses irrespective of conditioning intensity. Core-2 O-glycosylation also reported Notch signaling in CD8^{+} T cell responses to dendritic cell immunization, *Listeria* infection, and viral infection. Thus, we uncovered a role for Notch in controlling core-2 O-glycosylation and identified a cell surface marker to quantify Notch signals in multiple immunological contexts. Our findings will help refine our understanding of the regulation, cellular source, and timing of Notch signals in T cell immunity.

2.2 Introduction

Notch signaling is an evolutionarily conserved juxtracrine signaling pathway. Interaction of Notch receptors (Notch1-4) with agonistic ligands of the Delta-like or Jagged families leads to proteolytic release of the Notch intracellular domain, followed by its translocation to the nucleus where it mediates the transcriptional activation of Notch target genes. T cell development requires Delta-like4/Notch1 interactions in the thymus. In addition, Notch has emerged as a critical regulator of mature CD4^{+} and CD8^{+} T cell activation, differentiation, and effector function in the periphery (129). T cells incapable of receiving Notch signals showed reduced acute protective functions in mouse models of intracellular bacterial (45), viral (46), fungal (55), and parasitic infection (32), as well as in selected tumor models (130, 131). Notch also drives pathogenic T cell functions in mouse models of T cell-mediated acute GVHD (25, 28, 29, 31), chronic GVHD (132), organ rejection (30, 48, 120), and multiple sclerosis (133, 134). Despite the multiple immunological effects of Notch signaling in T cells, it has remained impossible to prospectively identify individual

cells experiencing active Notch signaling, a major limitation to studying the detailed impact and regulation of the Notch pathway in vivo.

In mouse models of allogeneic bone marrow transplantation (allo-BMT) after myeloablative conditioning, donor T cells received critical Delta-like1 (DLL1) and Delta-like4 (DLL4)-mediated Notch signals within the first 48 hours after transplant. The cellular niche providing DLL1/4 ligands was restricted to nonhematopoietic Ccl19-Cre^{+} fibroblastic stromal cells and not hematopoietic cells in secondary lymphoid organs (25). Additionally, both Ccl19-Cre^{+} fibroblastic stromal cells (17) and CD11c^{+} classical dendritic cells (135) have been shown to provide DLL4 signals to drive T follicular helper cell differentiation. These findings highlight fine spatial and temporal regulation of Notch signaling induction to mature T cells in these contexts. However, outside of these observations, little is known about when and where T cells receive Notch signals, and about the essential cellular sources of Notch ligands in a broader range of immune responses. Identifying a common specific and sensitive surface indicator of Notch signaling across different activated T cell subsets and immunologic contexts would aid in answering these important questions.

CD43 (sialophorin, leukosialin) is a transmembrane sialomucin with an extensively O-glycosylated extracellular domain that is highly expressed on T cells (136). Dynamic regulation of glycosyltransferases during T cell development and activation results in the expression of two CD43 glycoforms (137). Mature naïve T cells express a 115 kDa glycoform characterized by core-1 O-glycans capped by sialic acid. During T cell activation, upregulated expression of *Gcnt1* and its protein product the core-2 GlcNAc transferase-1 (C2GlcNAcT-I) occurs. In concert with

reciprocal downregulation of *St3gal1,* which encodes the sialyltransferase that caps core-1 glycans, these changes generate an activation-associated 130 kDa glycoform of CD43 characterized by core-2 O-glycans (138). The switch from core-1 to core-2 O-glycosylation of surface glycoproteins, including CD43 and P-selectin glycoprotein ligand-1 (PSGL-1), increases the affinity of immune cells for P- and E-selectins, thus allowing initial rolling of activated (139) and memory T cell subsets (140, 141) on inflamed endothelium. Glycoform-specific antibodies to CD43 enable the detection of unique glycosylated forms of CD43, correlating with the overall O-glycosylation status of surface proteins. The mAb S11 recognizes CD43 regardless of glycosylation (136), while 1B11 specifically recognizes the core-2 activation-associated O-glycoform (138). Others have used core-2 O-glycoform CD43 reactivity to identify recently activated effector, as opposed to memory $CD8^+$ T cells in response to lymphocytic choriomeningitis virus (LCMV) infection (142). Furthermore, alloreactive T cells upregulate the core-2 O-glycoform of CD43, but not other glycoforms of CD43 during GVHD (143, 144). Regulation of *Gcnt1* expression and core-2 O-glycosylation, in turn, is context-dependent. Central memory $CD8^+$ T cells upregulate *Gcnt1* expression and subsequent CD43 core-2 O-glycoform reactivity in a TCR-independent but IL-15-dependent manner in vivo (140). In vitro studies have shown that naïve $CD4^+$ and $CD8^+$ T cells require TCR signals in cooperation with diverse cytokines, such as IL-2 and IL-12, to drive *Gcnt1* expression (145–147). However, IL-2 and IL-12 were dispensable in vivo for activated $CD8^+$ T cells (148). Thus, our understanding of the essential inputs that regulate *Gcnt1* expression and CD43 glycosylation remains limited.

Recently, we reported a transcriptional program activated by Notch signaling in alloantigen-specific $CD4^+$ T cells in a mouse model of allo-BMT and GVHD (149). Notch signaling was

required for inflammatory cytokine production and lethal T cell alloreactivity (25, 28, 47). Interestingly, induction of *Gcnt1* mRNA depended on both alloantigenic stimulation and Notch signals. These findings suggested that core-2 O-glycosylation of CD43 and other surface proteins may serve as a new surface marker to indicate the receipt of functional Notch signals. To establish whether core-2 O-glycosylation of CD43 depended on Notch signals, we used flow cytometric analysis with glycoform-specific antibodies to CD43. Blockade of the DLL1/4 Notch ligands decreased the core-2 O-glycosylation of CD43 in a dose-dependent manner, while overall CD43 expression remained stable or even increased slightly. Regulation was cell-intrinsic, depended on canonical Notch signaling, and was observed across all recently activated T cell subsets. However, *Gcnt1*-deficient T cells with intact Notch still drove lethal GVHD, indicating that Notch signaling instructs a wider pathogenic program than core-2 O-glycosylation. Instead, core-2 O-glycosylation serves as a sensitive and simple flow cytometric indicator of Notch signaling in recently antigen-activated T cells. Core-2 O-glycosylation status successfully predicted whether T cells had received critical Notch signals in multiple models of allotransplantation, immunization, bacterial infection, and viral infection. Together these data show that Notch signals are critical to drive *Gcnt1*-dependent core-2 O-glycosylation in recently activated T cells, although *Gcnt1*-dependent core-2 O-glycosylation is not required for GVHD lethality. We propose that the core-2 O-glycoform of CD43 can be used as a simple flow cytometric readout to map how Notch signaling regulates T cell activation, differentiation, and effector function, opening new avenues for a deeper understanding of Notch signaling's contribution to immune responses.

2.3 Results

2.2.1 Delta-like Notch signals drive *Gcnt1* expression and core-2 O-glycosylation of CD43 in alloreactive CD4$^+$ T cells.

Hallmarks and transcriptional consequences of Notch signaling have been investigated systematically in developing T cells and in T cell leukemia (150, 151), but only recently in mature T cells in the context of allo-BMT (149). To identify potential functional targets of Notch signals in antigen-activated T cells that can be used as indicators of Notch signaling, we built on our discovery that Notch signaling plays a critical role to drive T cell pathogenicity and GVHD after allo-BMT (25, 28, 29, 31, 47, 149). To capture the effects of Notch signaling specifically in alloantigen-reactive T cells, and not in bystander T cells, we studied the transcriptome of 4C CD4$^+$ TCR Tg T cells transplanted in syngeneic or allogeneic mouse recipients, with or without blocking antibodies to DLL1/4 Notch ligands. In this model, 4C CD4$^+$ T cells are activated by the host MHC class II I-A^d alloantigen, while intact DLL11/4-mediated signaling is critical to drive lethal GVHD (149). Transcriptomic profiling showed that the expression of canonical Notch target genes such as *Hes1, Dtx1,* and *Il2ra* was downregulated with pharmacologic Delta-like ligand blockade (149) (**Fig. 2.1A)**. Interestingly, upregulation of *Gcnt1* transcripts induced by allogeneic T cell activation was completely abrogated by Delta-like ligand blockade (149) (**Fig. 2.1A**). This was confirmed by qRT-PCR validation in a separate experiment **(Fig. 2.1B),** indicating that increased *Gcnt1* mRNA expression required both alloantigenic stimulation and Notch signals. Conversely, Delta-like ligand blockade induced a trend for increased expression of *St3gal1,* which encodes the sialyltransferase that adds a terminal sialic acid cap on core-1 O-glycans, making them inaccessible for modification by core-2 glycosyltransferases **(Fig 2.2A-B)**. Other core-2 GlcNAc transferases were not highly expressed in 4C alloreactive T cells **(Fig 2.2C)**.

As others showed that *Gcnt1* expression is critical for core 2 O-glycosylation of CD43 (138), we hypothesized that Notch signals would regulate cell surface expression of the core-2 glycoform of CD43 in recently activated T cells. We used a pan-CD43 (S11) and a core 2 O-glycoform specific (1B11) anti-CD43 antibody (**Fig. 2.1C**) to evaluate if Notch signaling regulates core 2 O-glycosylation in 4C $CD4^+$ T cells after transplantation into lethally irradiated (11Gy) CBF1 recipients ($H2\text{-}^{b/d}$). By flow cytometric analysis, the proportion of 4C $CD4^+$ T cells reactive with 1B11 decreased upon DLL1/4 inhibition in a dose-dependent manner (**Fig. 2.1D-E**). However, mean S11 reactivity, which reflects total CD43 levels, was not negatively affected by Notch blockade, instead increasing slightly with the highest dose of DLL1/4 inhibitors (**Fig. 2.1F**). These data correlated with increased mRNA levels of *Spn,* the gene encoding CD43, with Notch blockade **(Fig 2.2D).** To correct for any overall changes in CD43 expression, the ratio of 1B11 to S11 reactivity was calculated in individual cells. The 1B11/S11 reactivity ratio was dependent on Delta-like Notch signaling (**Fig. 2.1F-G**). To test if this regulation depended on the transcriptional functions of Notch signaling, we transplanted CBF1 recipients as in (D) with wild-type 4C cells or 4C cells expressing the pan-Notch inhibitor dnMAML, which blocks canonical RBP-Jκ/MAML-dependent signaling downstream of all Notch ligands and receptors (152). Importantly 4C and 4C-dnMAML cells showed similar levels of alloantigen-specific activation as indicated by similar CD44 levels **(Fig 2.2 E-F)**. However, 4C-dnMAML cells had significantly decreased 1B11 reactivity **(Fig. 2.1 H)** and 1B11/S11 ratios **(Fig. 2.1 I)** barely higher than isotype control staining levels. In contrast, cell surface CD25 in 4C-dnMAML cells, while lower than in wild-type 4C cells, remained above isotype control staining levels (**Fig. 2.1 J-K).** This is consistent with our transcriptional profiling showing that Notch blockade decreased but did not eliminate all

alloreactivity-induced *Il2ra* expression **(Fig. 2.1A).** To test which Delta-like ligand could drive 1B11 reactivity, we used an in vitro system where Notch ligands were provided by OP9 stromal cell line expressing either DLL1 (OP9-DL1) or DLL4 (OP9-DL4). Co-cultured wild-type 4C and 4C-dnMAML T cells were plated at a 1:1 ratio on this stroma. When plated on either OP9-DL1 or OP9-DL4 stromal lines, wild-type 4C cells showed increased 1B11/S11 ratios, which was blocked by ligand-specific antibodies (**Fig. 2.1H**). Thus, in concert with alloantigenic stimulus, either DLL1 or DLL4 could drive core-2 O-glycosylation of CD43 in vitro. Altogether, measuring 1B11 or the 1B11/S11 reactivity ratio quantified Notch signaling intensity in T cells through a simple flow cytometry-based assay of cell surface glycoproteins. When plated on either OP9-DL1 or OP9-DL4 stromal lines, wild-type 4C cells showed increased 1B11/S11 ratios, which was blocked by ligand-specific antibodies (**Fig. 2.1H**). Thus, in concert with alloantigenic stimulus, either DLL1 or DLL4 could drive core-2 O-glycosylation of CD43 in vitro. Altogether, measuring 1B11 or the 1B11/S11 reactivity ratio quantified Notch signaling intensity in T cells through a simple flow cytometry-based assay of cell surface glycoproteins.

2.2.2 Core-2 O-glycosylation of CD43 depends on cell-intrinsic canonical Notch signaling in multiple alloreactive polyclonal T cell subsets.

Next, we evaluated the abundance of CD43 core-2 O-glycoforms in multiple polyclonal donor-derived T cell subsets after allo-BMT with high-intensity conditioning (11 Gy). We transplanted $1x10^6$ T-cell depleted bone marrow (TCD BM) plus B6 ($H2^{b/b}$, Thy1.1/2) wild-type or B6-dnMAML T cells labeled with the eFluor450 cell proliferation dye into partially MHC-mismatched CBF1 ($H2^{b/d}$, Thy1.2) hosts (**Fig. 2.3A**). 1B11 reactivity in proliferated eFluor450 dilute $CD4^+$ conventional T cells (Tconv) and Treg was significantly reduced among dnMAML T

cell subsets from day 4 until day 14 post-transplant. 1B11 reactivity was also significantly reduced in dnMAML $CD8^+$ T cells, but to a lesser extent than in $CD4^+$ T cells. Maximum differences occurred on day 4, suggesting higher dependence on Notch signaling at early time points for core-2 glycosylation **(Fig. 2.3 A-B)**. Notch-dependent regulation of core-2 glycosylation was seen in both secondary lymphoid organs **(Fig. 2.3 C)** where Notch signals are received, but also in GVHD target tissues **(Fig 2.3 C)**. These signals were imprinted early during T cell activation, as a single dose of DLL1/4 blocking antibodies at the time of transplant was sufficient to prevent upregulation of 1B11 reactivity, but not when delayed to day 2 **(Fig 2.4 A-C)**. To establish if regulation of 1B11 reactivity by Notch was cell-intrinsic, we co-transplanted wild-type and *Notch1/2*-deficient T cells, or wild-type and dnMAML T cells into MHC-mismatched CBF1 recipients. Both wild-type and Notch-deficient T cells proliferated similarly post-transplant **(Fig 2.4 D-E)**, as shown previously (28, 29). However, compared to co-transplanted wild-type T cells, both *Notch1/2*-deficient and dnMAML T cells had significantly diminished 1B11 reactivity (**Fig. 2.3 D-E**). Furthermore, 1B11 reactivity predicted the ability of proliferated wild-type $CD4^+$ T cells to produce IL-17 and IFNγ (**Fig. 2.3 F)** and the ability of $CD8^+$ T cells to produce IFNγ **(Fig. 2.3 G)**. Thus, across allogeneic polyclonal T cell subsets, core-2 O-glycosylation of CD43 requires cell-intrinsic canonical Notch signals and identifies alloreactive T cells of high cytokine-producing potential.

2.2.3 Notch loss-of-function impacts core-2 O-glycosylation to a similar degree as *Gcnt1* deficiency, but Notch signaling can drive GVHD through *Gcnt1*-independent mechanisms.

Upregulated *Gcnt1* expression is critical for core-2 O-glycosylation of mucin-like glycoproteins including CD43, as well as other selectin ligands such as PSGL-1. In fact, core-2 modifications are required for PSGL-1 to bind P-selectins (153) and perhaps E-selectins (146, 154). Interestingly,

P-selectin-deficient mice were protected from GVHD, but T cells from PSGL-1 deficient mice still caused GVHD (155). This suggests that core-2 O-glycosylation of other selectin ligands, such as CD43, may mediate trafficking of alloreactive T cells in GVHD target organs. Loss of Notch signaling also blunted trafficking of alloreactive T cells into target GVHD tissues including the intestinal lamina propria in a model of acute GVHD (28) and skin in a model of chronic GVHD (132). Since Notch signaling regulates *Gcnt1* expression and core-2 glycosylation of CD43 and likely other selectin ligands, we evaluated if *Gcnt1* expression mediated trafficking to target tissues or other pathogenic effects of Notch signaling in T cells during GVHD. To compare the impact of Notch inhibition and *Gcnt1* loss in T cells, we transplanted wild-type, dnMAML, or *Gcnt1*-deficient B6 T cells into CBF1 recipients. dnMAML $CD4^+$ Tconv phenocopied $Gcnt1^{-/-}$ T cells, while dnMAML Treg and $CD8^+$ T cells nearly fully phenocopied $Gcnt1^{-/-}$ T cells in terms of 1B11 reactivity and 1B11/S11 ratio after allo-BMT **(Fig. 2.5 A-B).** These effects were seen both in lymphoid organs and in target organs including liver, GI epithelium and lamina propria (**Fig. 2.6 3 A-B**). Thus, Notch signals were the dominant input driving *Gcnt1* expression and core-2 O-glycosylation in this context. Consistent with previously published results, dnMAML $CD4^+$ **(Fig. 2.5 C)** and $CD8^+$ **(Fig. 2.5 D)** T cells had impaired accumulation in target tissues, but not lymphoid tissues. However, $Gcnt1^{-/-}$ T cells accumulated in similar numbers as wild-type T cells in both lymphoid organs and target tissues, except for the small intestine epithelium. Thus, while trafficking and/or accumulation of alloreactive T cells in liver or GI target tissues relies on Notch signals, these effects of Notch signaling are not driven by *Gcnt1* expression and core-2 O-glycosylation. Furthermore, the production of inflammatory cytokines was blunted in dnMAML but not $Gcnt1^{-/-}CD4^+$ (**Fig. 2.5 E, Fig. 2.6 C)** and dnMAML but not $Gcnt1^{-/-}$ $CD8^+$ T cells (**Fig. 2.5 F, Fig. 2.6 D)**. $Foxp3^+$ Tregs were also significantly expanded among dnMAML but not $Gcnt1^-$

$^{-/-}$ CD4^{+} T cells **(Fig. 2.6 E)**. Consistent with these results, *Gcnt1*$^{-/-}$ T cells transplanted into wild-type recipients mediated GVHD lethality and morbidity with similar if not increased kinetics as compared to wild-type T cells (**Fig. 2.5 G,** solid lines).

Notch appeared to drive GVHD pathogenicity independently of core-2 O-glycosylation, as mice receiving *Gcnt1*$^{-/-}$ T cells could be protected from GVHD by inactivating the *Dll1/4* ligand genes in Ccl19-Cre^{+} host fibroblastic stromal cells **(Fig. 2.5 G,** dotted lines**)**, as shown previously with wild-type T cells (25). Together, these data show that Notch signals are crucial for *Gcnt1*-mediated core-2 O-glycosylation of CD43 in alloreactive T cell subsets. However, Notch can drive GVHD pathogenesis through mechanisms independent of *Gcnt1*.

2.2.4 Core-2 O-glycosylation of CD43 in T cells predicts the cellular source of Notch ligands that drive lethal T cell alloreactivity after allo-BMT with myeloablative and nonmyeloablative conditioning.

Because Notch signals were necessary for cell-intrinsic upregulation of 1B11 reactivity, we hypothesized that 1B11 reactivity could be used as a surrogate marker of Notch signaling in activated T cells. As a corollary, 1B11 reactivity should predict which cellular subset is the critical source of Notch ligands that drive lethal T cell alloreactivity across multiple allo-BMT models. We previously reported that in fully MHC-mismatched allogeneic BMT with prior myeloablative conditioning, nonhematopoietic lymphoid tissue fibroblastic stromal cells lineage traced by the Ccl19-Cre transgene provided the critical DLL1/4 ligands to drive GVHD (25). However, nothing is known about the source of Notch ligands that drive lethal alloimmunity after transplantation with reduced-intensity conditioning (52), a clinically relevant scenario. Indeed, radiation-sensitive

hematopoietic cells, eliminated in myeloablative models, may provide a critical source of Notch ligands to drive lethal T cell alloreactivity. To test this question, we used a "parent into F1" model of allo-BMT where expression of parental alloantigens by the recipient causes tolerance to donor cells, allowing transplantation with titratable conditioning intensity (103). In a model with high-intensity irradiation-based conditioning (11 Gy), mice that received dnMAML T cells were protected from GVHD, similarly to recipient mice lacking *Dll1/4* in Ccl19-Cre^{+} fibroblastic stromal cells (**Fig. 2.7 A**), in concordance with our previous results in a fully MHC-mismatched model (25). To test if 1B11 reactivity could predict this outcome, we co-transplanted wild-type and dnMAML T cells into Ccl19-Cre^{+}*Dll1*$^{f/f}$*Dll4*$^{f/f}$ or littermate control mice. Wild-type recipients showed striking differences between co-transplanted dnMAML and wild-type CD4^{+} Tconv in 1B11 expression and 1B11/S11 ratios (**Fig. 2.7 B**). In contrast, these differences disappeared in Ccl19-Cre^{+}*Dll1*$^{f/f}$*Dll4*$^{f/f}$ recipients, indicating that no additional source of Notch ligands was available to CD4^{+} Tconv beyond the critical source in fibroblastic stromal cells (**Fig. 2.7 B-C**). Alloreactive CD8^{+} T cells showed similar effects, with the vast majority of Notch inputs driving 1B11 reactivity from Ccl19-Cre^{+} cells (**Fig. 2.7 B-C**). We next studied GVHD in a parent into F1 model with non-myeloablative irradiation-based conditioning (3 Gy). The differences in 1B11 reactivity and 1B11/S11 ratio of co-transplanted wild-type and dnMAML T cells indicated that Notch signals were received by wild-type T cells in wild-type recipients. However, in Ccl19-Cre^{+}*Dll1*$^{f/f}$*Dll4*$^{f/f}$ recipients, these differences in 1B11 reactivity disappeared, except for CD8^{+} T cells in skin draining lymph nodes (pLN) where minor differences in 1B11 expression remained **(Fig. 2.7 D-E),** suggesting another cellular source of Notch ligand available to CD8^{+} T cells in these lymphoid organs. Consistent with these flow cytometric results, Ccl19-Cre^{+} *Dll1*$^{f/f}$ *Dll4*$^{f/f}$ recipient mice were protected from lethal GVHD (**Fig. 2.7 F**). Thus, even after allotransplantation

with reduced-intensity conditioning, non-hematopoietic fibroblastic stromal cells were the critical source of Notch ligands that drive GVHD.

2.2.5 Core-2 O-glycosylation of donor T cells predicts a fibroblastic source of Notch ligands that drives lethal alloreactivity after donor lymphocyte infusion without prior conditioning.

In models with no prior conditioning, Notch also drives lethal alloimmunity, but the source of ligand remains unknown (28). To test the key cellular source of Notch ligands after allotransplantation with no prior conditioning, we created four-way bone marrow chimeric recipient mice with loss of Delta-like ligands in different cellular compartments. Wild-type or Ccl19-Cre^{+}*Dll1$^{f/f}$Dll4$^{f/f}$* CBF1 mice were transplanted after lethal irradiation with bone marrow from poly(I:C)-induced Mx-Cre^{+} *Dll1$^{f/f}$Dll4$^{f/f}$* or *Cre^{-}* control CBF1 mice. Chimeras were allowed to reconstitute for six weeks, generating recipients lacking Delta-like ligands in the hematopoietic compartment (**Fig. 2.8 A, recipient ii)**, fibroblastic stromal compartment **(recipient iii)**, both **(recipient iv)**, or neither **(recipient i)**. These mice then received a parental donor lymphocyte infusion of co-transferred 5x10^{6} wild-type and 5x10^{6} dnMAML B6 T cells (H2$^{b/b}$) without prior conditioning– a model capable of triggering alloimmune-mediated hematopoietic failure in CBF1 recipients (H2$^{b/d}$) (**Fig. 2.8 A**). To predict the critical cellular source(s) of Notch signaling, we examined 1B11 and S11 reactivity in these co-transferred T cells (**Fig. 2.8 B-C**) at day 6 post-infusion. Presence of DLL1/4 in the hematopoietic compartment had no impact on CD4^{+} Tconv Notch-dependent 1B11 reactivity **(Fig. 2.8 B-C, recipient i vs. recipient ii)**. However, loss of DLL1/4 ligands in the fibroblastic stromal compartment eliminated Notch-dependent 1B11 reactivity (**Fig. 2.8 B-C, recipient i vs. recipient iii**). Alloreactive CD8^{+} T cells also depended on

a fibroblastic source of DLL1/4 to show increased Notch-dependent 1B11 reactivity (**Fig. 2.8 D-E**).

Thus, we hypothesized that a fibroblastic source of Delta-like Notch ligands would be critical to drive lethal alloreactivity. To test this hypothesis, we transplanted CBF1 recipients as in **Fig. 4F**, but with no prior conditioning and 50^6 lymph node cells from wild-type or dnMAML parental B6 mice. In this model, lethal T cell alloreactivity depended on canonical Notch signaling and was rescued when the fibroblastic stromal source of DLL1/4 was eliminated (**Fig. 5F**). Thus, 1B11 reactivity predicted the functionally relevant source of Notch ligands, and fibroblastic stromal cells remained the essential source even in the absence of irradiation conditioning.

2.2.6 Delta-like Notch signals drive core-2 O glycosylation of CD43 and CD8+ T cell effector differentiation after dendritic cell immunization.

To assess if Notch-dependent regulation of CD43 core-2 O-glycosylation applied to other types of antigen-activated T cells, we used a model of BMDC immunization pulsed with OVA peptide (DC-OVA). In this model, $CD8^+$ T cell differentiation into $KLRG1^+IL7R^-$ short-lived effector cells (SLECs) depends on cell-intrinsic Notch signals (45, 46). However, the generation of $KLRG1^-IL7R^-$ early effector cells (EECs) and $KLRG1^-IL7R^+$ memory precursor cells (MPECs) remains intact. At the time of adoptive DC-OVA transfer, mice were treated with anti-DLL1/4 or isotype control antibodies as noted in **Fig. 2.9 A**. On day 10, Ag-specific $CD8^+$ T cells were assessed by K^b-OVA tetramer staining (**Fig. 2.9 A**). The overall percentage (**Fig. 2.9 A**) and total number (not shown) of Ag-specific $CD44^+CD8^+$ T cells were not affected by DLL1/4 blockade. However, differentiation into SLECs was blunted by anti-DLL1/4 antibodies (**Fig. 2.9 B**). Consistent with the effects of Notch on core-2 O-glycosylation, 1B11 reactivity of OVA-specific $CD8^+$ T cells

depended on DLL1/4 Notch signals (**Fig. 2.9 C**). The Notch-dependent 1B11 reactivity was not restricted to SLECs, but was also seen in OVA-specific $CD8^+$ T cells MPECs and EECs, suggesting that these cellular subsets have also received Notch signals (**Fig. 2.9 D**). Concordant results were observed when the response of adoptively transferred OT-I cells to DC-OVA was examined (**Fig. 6E-G**). These data show that Notch regulates short-lived effector cell differentiation and 1B11 reactivity in polyclonal and monoclonal models of OVA responsiveness.

2.2.7 Delta-like Notch signals control core-2 O-glycosylation of CD43 in Ag-specific $CD8^+$ T cells after *Listeria* infection.

Compared to infection, DC-OVA immunization does not trigger robust innate immune stimuli. Thus, it is possible that additional cytokine pathways, such as IL-12, that have been shown to drive core-2 O-glycosylation in vitro (31) may not be triggered in this model. To determine if *Gcnt1* expression was also regulated by Notch during an anti-infectious response, we studied control vs. *Notch1/2*-deficient OT-I $CD8^+$ T cells in naïve mice and on day 3 after a sublethal dose of *Listeria monocytogenes* expressing ovalbumin (Lm-OVA). *Gcnt1* expression was induced after Lm-OVA infection in control, but not in Notch-deficient OT-I cells (**Fig. 2.10 A**). Next, we administered Lm-OVA to wild-type or E8I-Cre^+ $Notch1^{f/f}$ $Notch2^{f/f}$ mice (lacking *Notch1/2* in all $CD8^+$ T cells). In parallel, we treated a group of wild-type mice with anti-DLL1/4 antibodies. Eliminating Notch signals either through loss of Notch1/2 receptors or through antibody-mediated DLL1/4 blockade did not impair or even slightly increased the overall expansion of antigen-specific $CD8^+$ T cells after Lm-OVA infection (**Fig. 2.10 B**). However, differentiation into SLECs depended on $CD8^+$ T cell-intrinsic Notch signals, which was recapitulated by blocking Delta-like ligands (**Fig. 2.10 C**). Consistently, 1B11 reactivity in bulk Ag-specific $CD8^+$ (**Fig. 2.10 D)** and fractionated SLEC, EEC

and MPEC subsets **(Fig. 2. 10 E)** depended on cell-intrinsic Notch signals and Delta-like Notch ligands **(Fig. 2.10 C-D)**. Compared to wild-type or E8I-Cre^{+} *Notch1$^{f/f}$ Notch2$^{f/f}$* mice, CD44^{+}CD4^{+} T cells from mice receiving anti-DLL1/4 treatment had decreased 1B11 reactivity, indicating that Notch also regulates core-2 O-glycosylation in activated CD4^{+} T cells after Lm-ova infection **(Fig. 2.10 F).** Furthermore, 1B11 reactivity was higher in wild type compared to E8I-Cre^{+} *Notch1$^{f/f}$Notch2$^{f/f}$* mice at day 8 and day 30 after LCMV clone 13 infection (**Fig 2.11)**. Altogether, our data identify core-2 O-glycosylation and 1B11 reactivity as conserved and sensitive readouts of Notch signaling activity in T cells in multiple types of T cell responses.

2.4 Discussion

Multiple studies have shown that Notch signals regulate T cell differentiation and function during adaptive immune responses with context-specific effects. However, in most contexts, little is known about the cellular source, regulation, and timing of Notch signals received by T cells. Identification of a simple and generalizable cell surface marker of Notch signaling in activated T cell subsets will enhance our understanding of how Notch shapes T cell responses in specific immune contexts.

In this study, we report that *Gcnt1*-dependent core-2 O-glycosylation of CD43 behaves as a new cell surface marker to indicate whether a T cell has received Notch signals after antigen activation. This marker was quantitative, as it directly correlated with dose-dependent pharmacologic blockade of Notch ligands and could be easily monitored by flow cytometry with the mAb 1B11. Upregulated core-2 O-glycosylation of CD43 was cell-intrinsically controlled by Notch signaling within multiple T cell subsets and depended on Notch signals mediated via its canonical

transcriptional activation complex. Importantly, the usefulness of this new surface marker was generalizable from alloimmunity to immunization, bacterial, and viral infection models. Furthermore, monitoring CD43 glycosylation status could predict the critical cellular sources of Notch ligands that drove lethal alloimmunity.

We and others previously relied on CD25 as a marker of Notch signaling, as its expression is regulated by Notch in developing as well as mature T cells (156). However, 1B11 functioned as a superior marker for Notch signaling over CD25 for three reasons. First, blocking Notch signaling after allo-BMT expanded the proportion of $Foxp3^+$ Tregs, which highly express CD25 irrespectively of Notch signals (8, 11). Instead, 1B11 reactivity in Tregs was regulated by Notch, as it was in $Foxp3^-CD4^+$ conventional T cells. Second, 1B11 reactivity appears more sensitive and less transient than CD25 expression. For example, we had previously not observed decreased CD25 expression among dnMAML T cells in unirradiated allotransplantation models (28). Furthermore, only a small fraction of Ag-specific $CD8^+$ T cells express CD25 at day 8 post-infection (26) or day 6 post-DC immunization (157). Instead, we have shown that 1B11 remains highly detectable on $CD8^+$ T cells until day 14 post activation in transplantation, while others have shown its presence until at least day 14 after acute viral infection (142). In fact, virus-specific Notch-deficient $CD8^+$ T cells still had reduced 1B11 reactivity at day 30 after inoculation with LCMV clone 13, a model of chronic infection. Third, 1B11 reactivity had a stricter requirement for Notch signals than CD25, as we observed small but significant CD25 upregulation in dnMAML 4C T cells. Thus, 1B11 reactivity provides both more sensitive and more specific information than CD25 expression as a readout of Notch signaling activity.

In addition to its increased expression in GVHD (144, 158), 1B11 reactivity has previously been proposed as a marker to distinguish $CD8^+$ effector T cells from memory T cells in response to viral infection (142). Similar to our studies where high 1B11 reactivity correlated with cytokine production, the authors showed that high 1B11 reactivity correlated with cytolytic function. Because of the centrality of Notch signaling in driving $CD8^+$ T cell effector differentiation and short-lived effector functions, we speculate that Notch orchestrates both *Gcnt1*-dependent 1B11 reactivity and effector T cell differentiation during early stages of T cell activation. Whether other signals can bypass Notch signaling to drive activation-associated *Gcnt1* upregulation, core-2 O-glycosylation, and effector T cell differentiation remains to be seen. In contrast to in vitro experiments, in vivo findings showed that IL-12, IL-2, and IL-15 were dispensable for functional P-selectin ligand formation and thus likely for *Gcnt1* induction and core-2 O-glycosylation in effector $CD8^+$ T cells (139). In $CD4^+$ T cells, *Gcnt1* expression depended on TCR signaling in concert with STAT4-dependent IL-12 signaling or other diverse cytokines in vitro (145, 147). However, little was known about the regulation of *Gcnt1* in $CD4^+$ T cells in vivo. Given that dnMAML CD4 Tconv fully recapitulated and dnMAML CD8 T cells largely recapitulated the impact of *Gcnt1* deficiency on 1B11 expression, Notch signals appear critical for *Gcnt1* upregulation and core-2 O-glycosylation at least in the context of allo-BMT. We show that a short pulse of Notch signaling in cooperation with antigen activation drives 1B11 reactivity in effector T cells. Over time, 1B11 reactivity tends to decay in antigen-activated $CD4^+$ and $CD8^+$ T cells. In contrast, memory $CD8^+$ T cells were reported to express *Gcnt1* in an IL-15-dependent and antigen-independent manner (140). It would be interesting to test if Notch signals also cooperate with IL-15 in this context to regulate *Gcnt1* expression.

To show the utility of 1B11 reactivity as a surrogate surface marker of Notch signaling, we asked whether it could be used to predict the cellular source of Notch ligands that drive lethal alloimmunity. We previously showed that non-hematopoietic fibroblastic stromal cells lineage traced by the Ccl19-Cre transgene were the source of Delta-ligands after allo-BMT with high-intensity myeloablative conditioning (25). However, in models of allotransplantation with reduced or no prior conditioning, it was unclear if viable hematopoietic cells could substitute for fibroblastic stromal cells as a source of Notch ligands. By comparing 1B11 reactivity in co-transferred wild-type and dnMAML T cells, we predicted that in both models of allotransplantation with reduced or no prior conditioning, fibroblastic stromal cells were necessary and hematopoietic cells dispensable to drive lethal Notch-mediated T cell pathogenicity. Additionally, we used 1B11 reactivity as a surrogate marker to compare Notch signals received by $CD8^+$ T cells during *L. monocytogenes* infection. Using 1B11, we predicted that pharmacologic blockade of DLL1/4 ligands would recapitulate cell-intrinsic loss of Notch1/2 receptors in $CD8^+$ T cells. This was confirmed when studying the differentiation of Ag-specific $CD8^+$ T cells into SLECs. Together, these findings show for the first time that Delta-like Notch ligands are essential and Jagged ligands are dispensable during Notch-dependent $CD8^+$ T cell differentiation. This is consistent with recent findings that dendritic cells lacking *Dll1* but not *Jag1* had decreased ability to support anti-tumor T cell response (128). Furthermore, the fact that pharmacologic blockade of DLL1/4 ligands fully recapitulated the loss of 1B11 reactivity and effector differentiation seen in Notch1/2 deficient $CD8^+$ T cells suggests there is a limited role for ligand-independent Notch signaling in vivo, in contrast to suggestions by other groups based on in vitro findings (42, 159).

What is the functional significance of Notch-dependent *Gcnt1*-mediated core-2 O-glycosylation in activated T cell subsets during GVHD? *Gcnt1* is crucial for the creation of functional ligands for P- and E-selectin in leukocytes and their trafficking into some inflamed non-lymphoid tissues. In our model of partially MHC-mismatched allo-BMT, *Gcnt1*-deficient T cells could still traffic into liver and GI target tissues and mediate lethal GVHD in a Notch-dependent manner. Thus, *Gcnt1* function is likely not central to T cell pathogenicity in this context. Interestingly, others have shown that P-selectin-deficient recipients had decreased lethality in GVHD models, although PSGL1-deficient T cells did not induce reduced mortality (155). Together with our data, these findings suggest that T cells can traffic into the GI tract and liver independently of functional P-selectin ligands. Other mechanisms such as α4β7/MAdCAM-1 interactions may also be involved in T cell trafficking into the gut during GVHD (114). P-selectin deficient mice may be protected from GVHD as subsequent migration of donor bone-marrow-derived myeloid cells into target tissues, which is necessary to sustain GVHD (68, 71), may require P-selectin to traffic into target tissues. Additionally, because morbidity in our allo-BMT model is predominantly driven by early GI damage, we did not examine skin-homing T cells, which may have a more stringent requirement for expression of P- and E-selectin ligands. In fact, we recently showed in a model of chronic GVHD that Notch-deprived T cells had significantly impaired accumulation in the skin (132).

In humans, a core-2 O-glycan-specific mAb for CD43, 1D4, recognizes a subset of what has been described as memory $CD4^+CD45RO^+$ mature T cells (160). Another mAb, T305, specific for core-2 O-glycosylated CD43 showed increased reactivity in T cells of patients with GVHD, autoimmunity or viral infection (161). These findings suggest that similar regulation of core-2 O-glycans may exist in recently activated human effector T cells in humans.

Much remains to be understood about Notch signaling during T cell activation. Our work defining a cell-intrinsic generalizable indicator of Notch signals in activated T cell subsets will help answer pressing questions in the field. For example, the cellular source of Notch ligands remains unknown in immunization and infection models. Also, little is known about the dynamic regulation of Notch ligand expression and activity in antigen-presenting cells vs. fibroblastic stromal cells. Assessing surface core-2 O-glycosylation of CD43, a simple marker correlated to Notch-dependent T cell function, will help decipher the immunobiology of Notch signaling in T cell immunity.

2.5 Figures

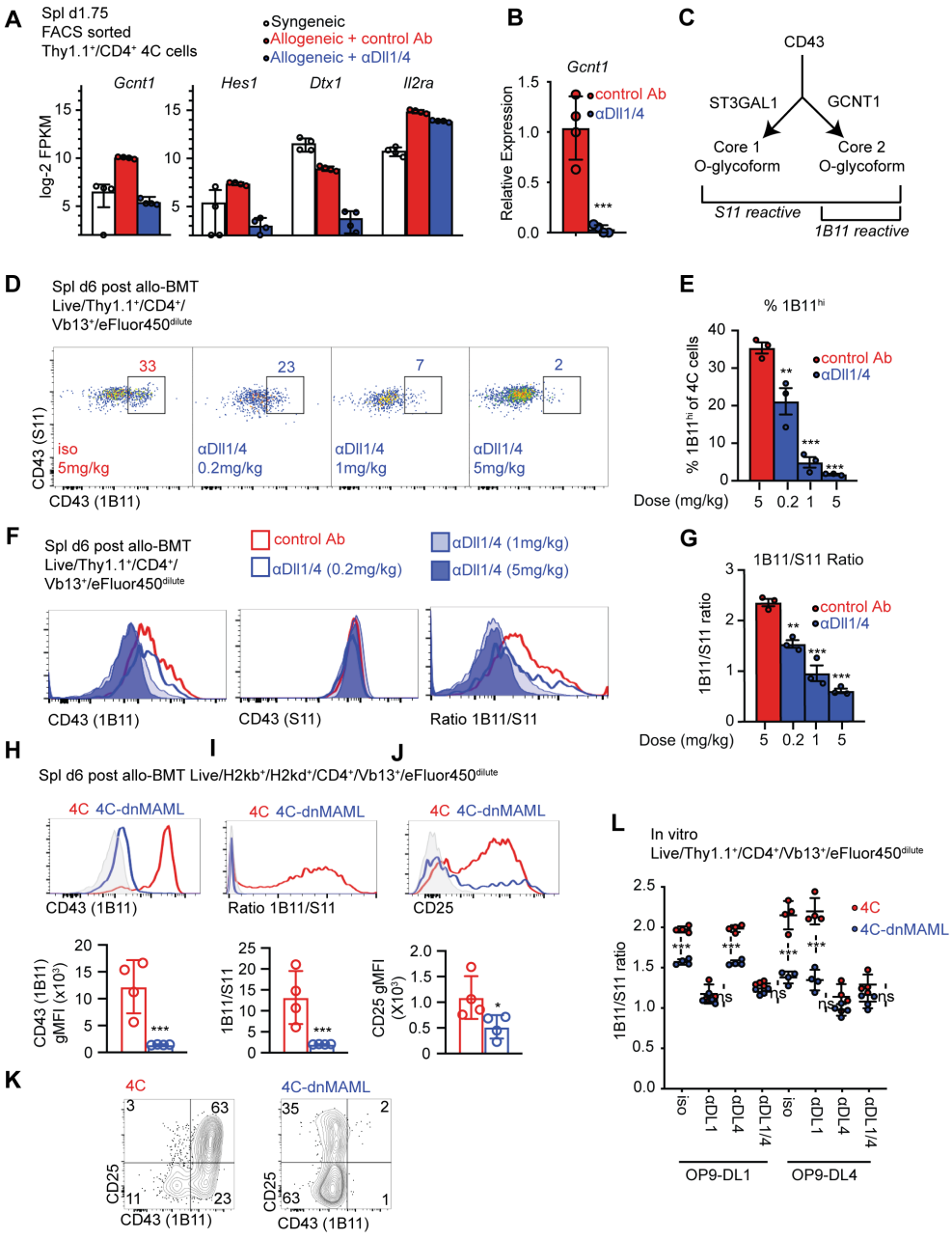

Figure 2.1. Notch signaling drives Gcnt1-mediated core-2 O-glycosylation of CD43 in alloreactive CD4+ T cells. (A-B) Purified IAd alloantigen-specific Vβ13+ Thy1.1+ 4C CD4+ T cells were transplanted into lethally irradiated (11 Gy) B6 MHC-matched (syngeneic) or BALB/c MHC-mismatched (allogeneic) hosts with or without neutralizing antibodies to Delta-like1/4 (DLL1/4) Notch ligands, then sort purified at day 1.75 post-transplant. (A) Fragments per kilobase per million mapped reads (FPKM) for Gcnt1 and highlighted Notch target gene transplanted into lethally irradiated MHC-mismatched CBF1 (H-2Kb/d) recipients receiving titrated doses of anti-DLL1/4 Abs. *(Figure legend continues on next page)*

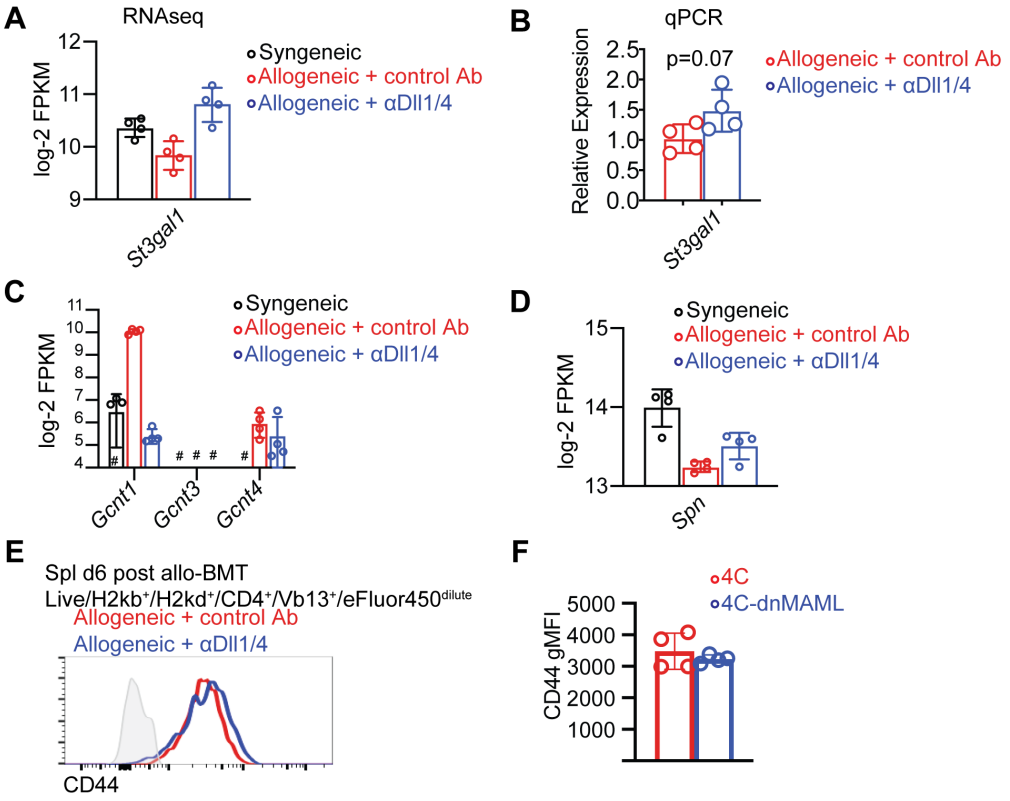

Figure 2.2. Related to Fig 2.1. Effects of Notch blockade on expression of sugar modifying enzymes. Expression of *St3gal1* by transcriptomic profiling **(A)** and qRT-PCR **(B).** Transcriptomic profiling of core-2 GlcNAc transferases **(C)** and *Spn,* the gene encoding CD43 **(D)**. # = no mapped reads. **(E-F)** CD44 expression in alloreactive 4C or 4-dnMAML T cells from Fig 2.1 H-K.

(Fig 2.1 legend, continued) Glycoform-specific flow cytometric analysis of CD43 was performed on day 6 on fully divided 4C cells. DLL1/4 blockade (αDLL1/4) induced dose-dependent downregulation of the percentage of 1B11hi 4C T cells (D-E) and 1B11 staining intensity (F, left panel), without loss in overall CD43 abundance (S11 staining intensity) (F, middle panel). The core-2 glycosylation status of CD43 could be examined on a single-cell basis by calculating a ratio of 1B11/S11. The core-2 glycosylation status of CD43 could be examined on a single-cell basis by calculating a ratio of 1B11/S11 staining intensity (F-G). (H-K) Purified CD4+ 4C or 4C-dnMAML were transplanted into CBF1 recipients as in (D). Proliferated alloreactive T cell subsets were assayed for 1B11 (H), S11, 1B11/S11 ratios (I) and CD25 (J). Among 4C-dnMAML T cells 1B11 reactivity was blunted in both CD25+ and CD25- populations (K). (L) Wild-type 4C T cells mixed 1:1 with 4C-dnMAML T cells were co-cultured on OP9-DL1 or OP9-DL4 stromal cells and stimulated in vitro with LPS matured bone-marrow-derived dendritic cells from poly(I:C)-induced *Mx-Cre+ Dll1$^{f/f}$Dll4$^{f/f}$* mice. Either OP9-DL1 or DL4 could increase core-2 CD43 O-glycosylation in a Notch ligand-dependent fashion. Mean and one standard deviation plotted in bar graphs.**p<0.01, ***p<0.001 by Student's t-test (B, H, J), one-way (E, G) or two-way (L) ANOVA with post-hoc Tukey's tests to assess differences in means.

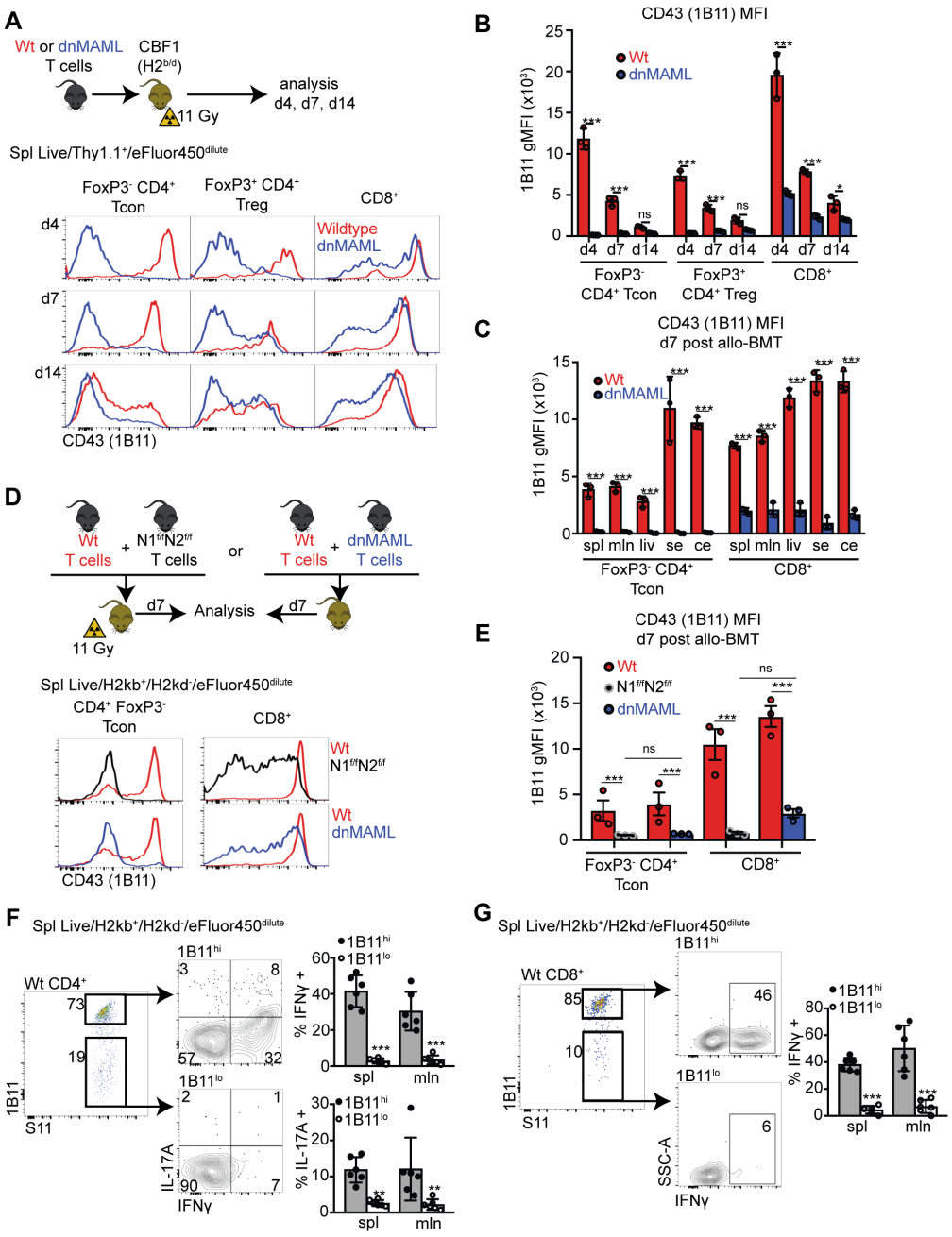

Figure 2.3. CD43 core-2 O-glycosylation requires cell-intrinsic canonical Notch signals in multiple alloreactive polyclonal T cell subsets. (A-C) 5 x 10^6 purified B6 (H-$2^{b/b}$, Thy$1^{1/2}$) wild-type or dnMAML T cells were labeled with eFluor450 proliferation dye and transplanted separately into lethally irradiated (11 Gy) MHC-mismatched CBF1 (H-$2^{b/d}$, Thy$1^{2/2}$) recipients with analysis at day 4, 7 and 14. Core-2 O-glycosylation of CD43 in proliferated Foxp3$^-$CD4$^+$ Tconv, Foxp3$^+$ Treg, and CD8$^+$ T cells was blunted by dnMAML-mediated Notch blockade at day 4 and day 7 (A-B), both in secondary lymphoid organs and GVHD target tissues (C). (D-G) 2.5 x 10^6 B6 wild-type plus 2.5 x 10^6 dnMAML-GFP T cells or 2.5 x 10^6 B6 wild-type plus 2.5x10^6 N1$^{f/f}$N2$^{f/f}$ *Rosa*^{eYFP} T cells were co-transplanted as in (A). For both N1$^{f/f}$ N2$^{f/f}$ and dnMAML T cells, 1B11 reactivity was significantly blunted in alloreactive CD4$^+$ Tconv and CD8$^+$ T cells (D-E). Among wild-type CD4$^+$ (F) and CD8$^+$ (G) cells, 1B11^{hi} status predicted cytokine production. spl = spleen, mln = mesenteric lymph node, liv = liver, se = small intestinal epithelium, ce = colonic epithelium. **p<0.01, ***p<0.001, one-way ANOVA with Tukey's post-hoc-tests.

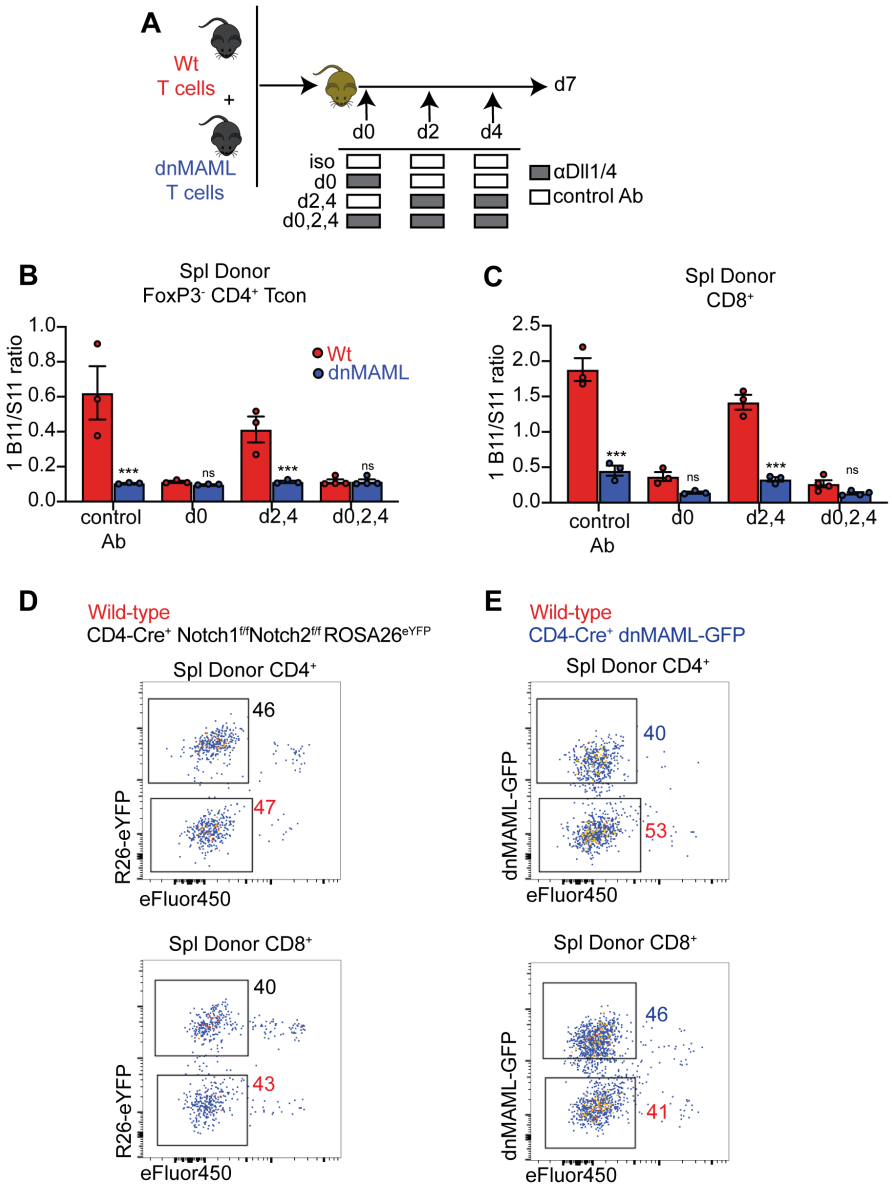

Figure 2.4 Related to Figure 2.3 **(A)** 1B11 reactivity in donor alloreactive T cell subsets at day 28 post allo-BMT **(B-D)** 2.5 x 106 purified B6 (H-$2^{b/b}$, $Thy1^{1/2}$) wild-type and dnMAML-GFP T cells (H-$2^{b/b}$, $Thy1^{1/2}$) were labeled with proliferation dye and co-transplanted into lethally irradiated (11 Gy) MHC-mismatched CBF1 (H-$2^{b/d}$, $Thy1^{2/2}$) recipients receiving DLL1/4-blocking or isotype control antibodies as indicated in **(B)**. A single dose of DLL1/4-blocking antibodies at day 0 (control Ab vs. d0) was sufficient to block Notch-dependent upregulation of 1B11 reactivity in both $CD4^+$ **(C)** and $CD8^+$ **(D)** T cells. In contrast, delaying blockade until day 2 did not block upregulated1B11 reactivity (control Ab vs. d2,4). **(E-F)** Related to Fig. 2D-E. Representative flow cytometry plots of proliferation as tracked by eFluor450 dilution in co-transplanted wild-type and CD4-Cre^+ $Notch1^{f/f}Notch2^{f/f}$ ROSA26eYFP **(E)** and in co-transplanted wildtype and $CD4^+$ dnMAML-GFP^+ cells **(F).**

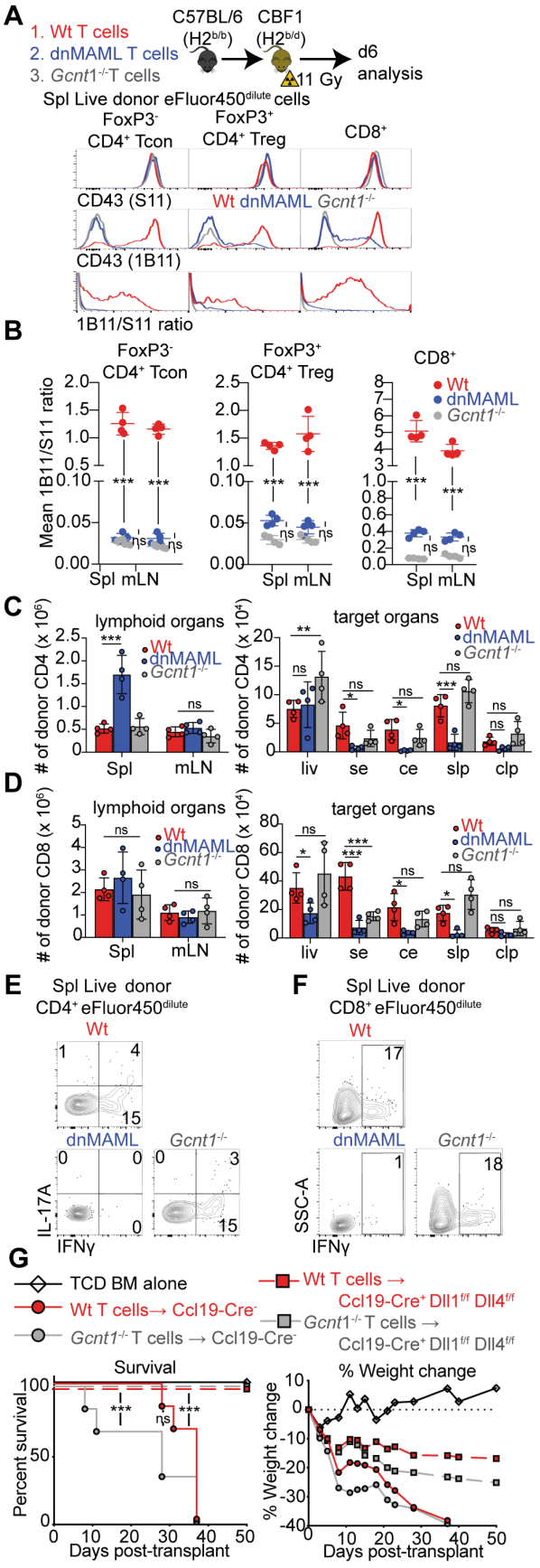

Figure 2.5 Notch blockade and Gcnt1 loss abrogate CD43 core-2 O-glycosylation in alloreactive T cells, but Gcnt1 loss does not decrease GVHD severity. (A-F) 2.5 x 10^6 Wild-type, dnMAML, or *Gcnt1*$^{-/-}$ T cells (H-2$^{b/b}$) were transplanted into lethally irradiated CBF1 recipients (H-2$^{b/d}$) as in Fig 2. (A-B) Core-2 O-glycosylation of CD43 was monitored in lymphoid organs by flow cytometry at day 6. dnMAML CD4$^+$ Tconv fully recapitulated, while dnMAML CD4$^+$ Treg and CD8$^+$ T cells nearly fully recapitulated the loss of 1B11 reactivity seen in *Gcnt1*$^{-/-}$ T cells. Accumulation of alloreactive donor CD4$^+$ (C) and CD8$^+$ (D) T cells in lymphoid and GVHD target organs. slp = small intestinal lamina propria. clp = colonic lamina propria. Cytokine production of representative alloreactive CD4$^+$ (E) and CD8$^+$ (F) T cell subsets. n=4 per group, flow panels from representative samples. (G) Survival and % weight change of lethally irradiated Ccl19-Cre$^+$*Dll1*$^{f/f}$*Dll4*$^{f/f}$ or Cre$^-$ littermate control CBF1 recipients transplanted with 5 x 10^6 T cell-depleted bone marrow (TCD BM) plus 5 x 10^6 wild-type or *Gcnt1*-deficient T cells. n=6 per group from one experiment. *p<0.05, **p<0.01, ***p<0.001, one-way (B) or two-way (C, D) ANOVA with Tukey's post-hoc-tests. For (G), a log-rank test was used to compare groups.

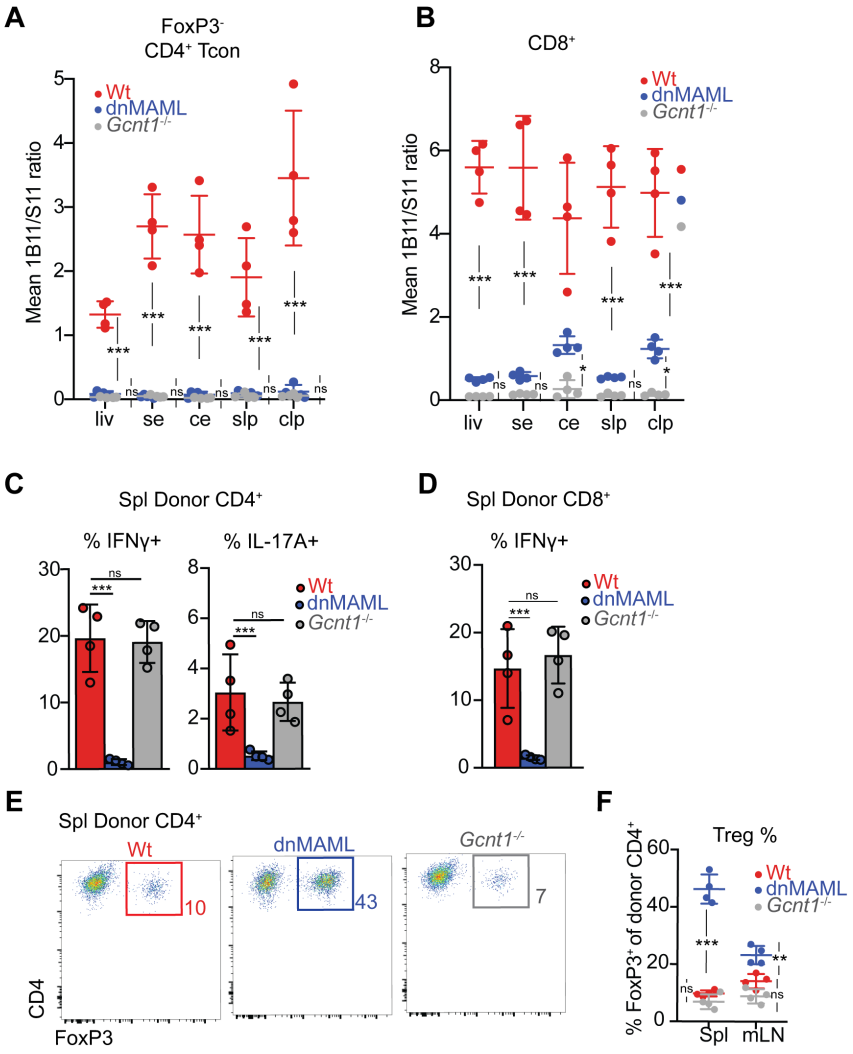

Figure 2.6 Related to Figure 2.5
Flow cytometric measurement of 1B11/S11 ratios in wild-type, Gcnt1$^{-/-}$, and dnMAML CD4^{+} **(A)** and **(B)** CD8+ T cells from GVHD target organs. liv = liver, se = small intestinal epithelium, ce = colonic epithelium, slp = small intestinal lamina propria, clp = colonic lamina propria. **(C, D)** Summary data from Fig. 3E and Fig. 3F. (E-F) Foxp3^{+} Treg abundance among donor CD4^{+} T cells.

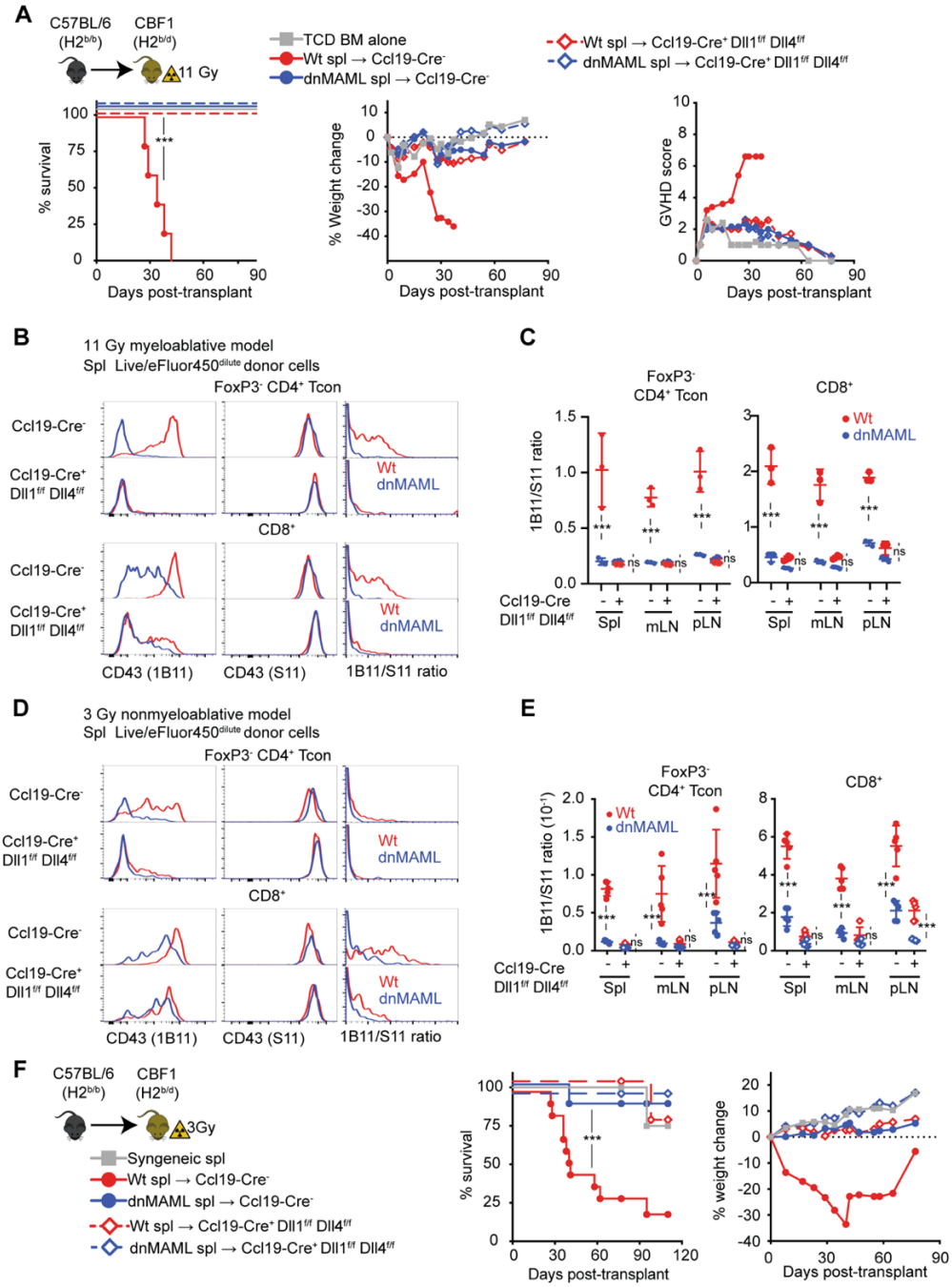

Figure 2.7. CD43 core-2 O-glycosylation reports Notch-dependent alloreactivity and identifies the critical Ccl19-Cre+ fibroblastic cell source of Delta-like ligands in GVHD. (A) Survival, % weight change, and clinical GVHD score of lethally irradiated (11 Gy) *Ccl19-Cre*$^{+}$*Dll1*$^{f/f}$ *Dll4*$^{f/f}$ vs. Cre- littermate control CBF1 recipients transplanted with 5 x 10^6 TCD BM and 2 x 10^7 wild-type or dnMAML splenocytes. n=5 mice per group, data representative of two independent experiments. (B-C) Flow cytometric analysis of CD43 core-2 O-glycosylation in co-transplanted wild-type and dnMAML T cell subsets harvested from *Ccl19-Cre*$^{+}$*Dll1*$^{f/f}$*Dll4*$^{f/f}$ or Cre^{-} littermate controls at day 6 post-transplant. (D-E) Flow cytometric analysis of CD43 core-2 O-glycosylation as in (B-C). (F) Survival and % weight change in a non-myeloablative model of allo-BMT (3 Gy) where recipients received 4 x 107 splenocytes. Survival curve represents pooled data from three independent experiments of n=5 mice per group. Weight loss data are shown from one experiment. *p<0.05, **p<0.01, ***p<0.001, (A, F) log-rank test and (C, E) two-way ANOVA with Tukey's post-hoc-tests.

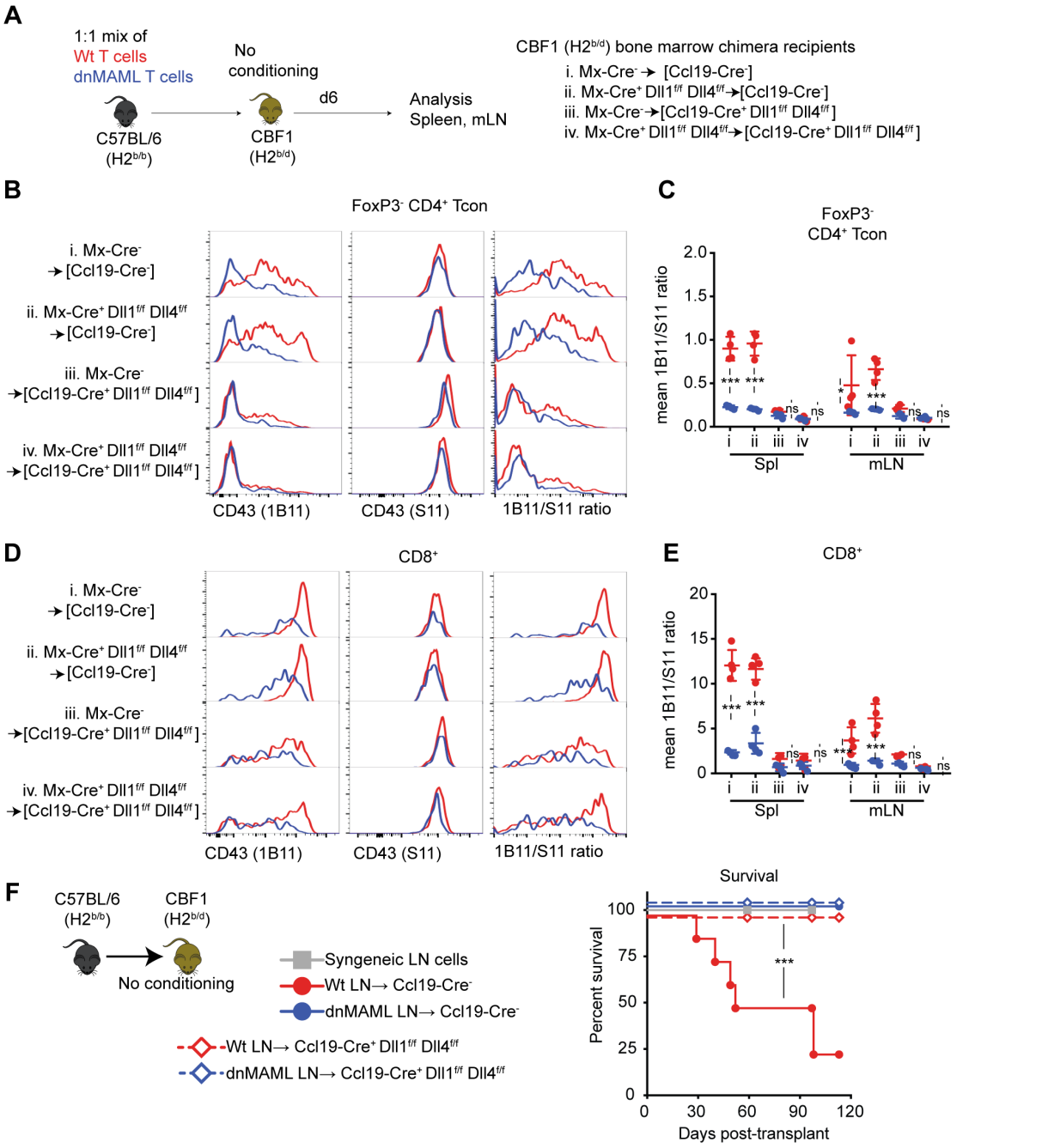

Figure 2.8 CD43 core-2 O-glycosylation in alloreactive T cells identifies a critical role for Ccl19-Cre+ fibroblastic cells as a source of Delta-like ligands even in the absence of prior conditioning. (A) Experimental scheme. Four-way bone marrow chimeras were generated by transplanting bone marrow from poly(I:C) induced *Mx-Cre+ Dll1$^{f/f}$Dll4$^{f/f}$* or Cre- CBF1 littermate controls into syngeneic *Ccl19-Cre+ Dll1$^{f/f}$Dll4$^{f/f}$* or Cre- littermate controls. After 8 weeks of reconstitution, recipients received a donor lymphocyte infusion of 5 x 106 purified wild-type and 5 x 106 dnMAML T cells. Flow cytometric analysis of core-2 O-glycosylation of CD43 in alloreactive CD4+ Tconv (B-C) and CD8+ T cells (D-E). (F) Survival of non-irradiated *Ccl19-Cre+ Dll1$^{f/f}$Dll4$^{f/f}$* or Cre- littermate control CBF1 recipients transplanted with 60 x 106 wild-type or dnMAML B6 lymph node cells. Survival data are from two pooled independent experiments with a total of n=8 mice per group. *p<0.05, **p<0.01, ***p<0.001, (C, E) two-way ANOVA with Tukey's post-hoc-tests and (F) log-rank tests.

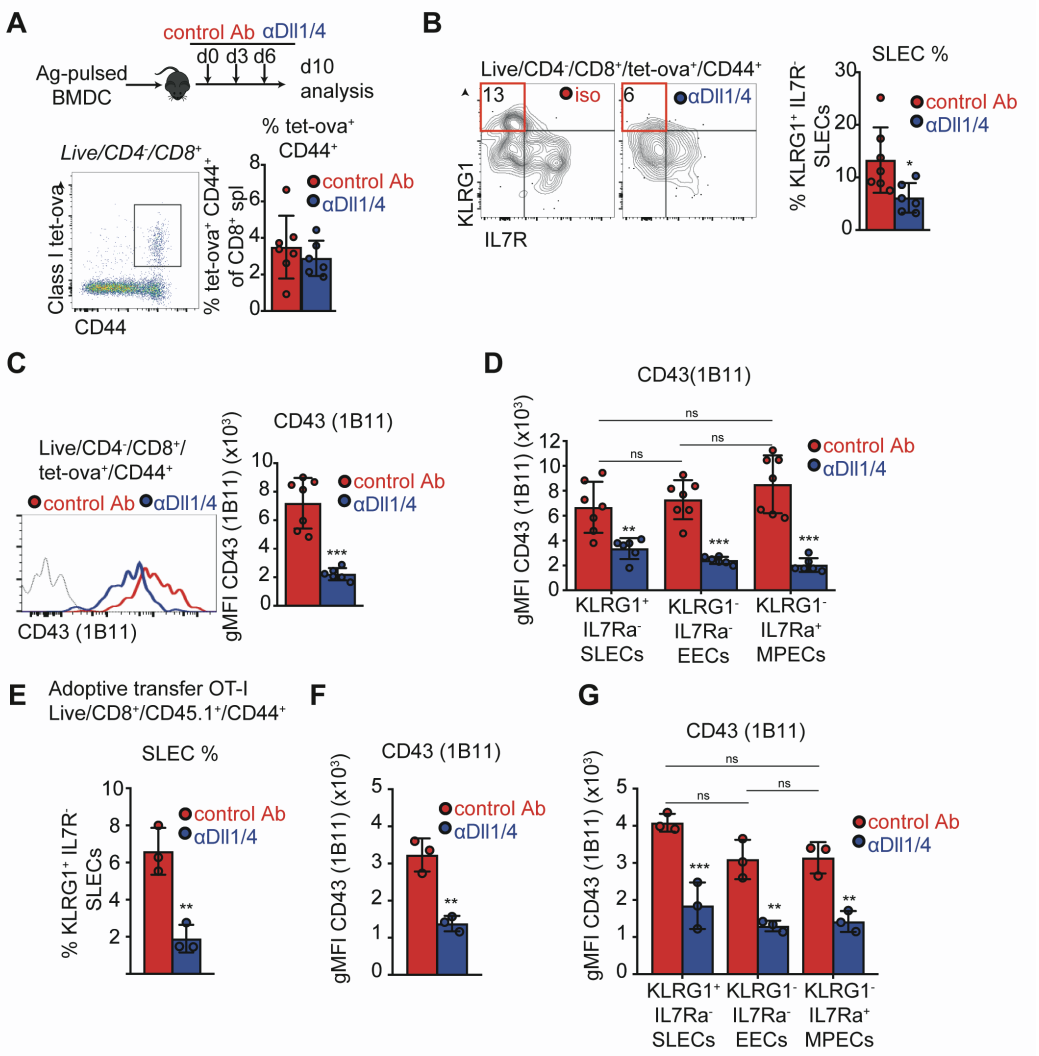

Figure 2.9. Delta-like Notch ligands drive Klrg1$^+$ short-lived effector T cell differentiation and CD43 core-2 O-glycosylation in antigen-specific CD8$^+$ T cell subsets after dendritic cell immunization.(A-D) B6 mice treated with anti-DLL1/4 or isotype control antibodies were immunized with 5 x 10^5 bone marrow-derived dendritic cells (BMDC) pulsed with OVA peptide (SIINFEKL). Antigen-specific CD8$^+$ T cells were monitored by flow cytometry with K^b-OVA tetramer. (A) Blockade of Delta-like ligands did not negatively affect the expansion of antigen-specific CD8$^+$ T cells, but markedly blunted differentiation into KLRG1$^+$ILR7$^-$ short-lived effector cells (SLECs). (B) Abundance of the CD43 core-2 O-glycoform in bulk antigen-specific CD8$^+$ T cells (C) or in SLEC, KLRG1$^-$ ILR7$^-$ early effector cell (EEC), and KLRG1$^-$ILR7$^+$ memory precursor cell (MPEC) subsets (D). Data representative of two experiments with n=6 mice per group. (E-G) BMDC immunization was performed as in (A-D), but mice received 5 x 10^4 purified CD45.1$^+$ OT-I CD8$^+$ T cells by adoptive transfer one day before immunization. Data are representative of two experiments with n=3 mice per group. *p<0.05, **p<0.01, ***p<0.001, (A-C, E-F) student's *t*-test and (D, G) two-way ANOVA with Tukey's post-hoc-tests.

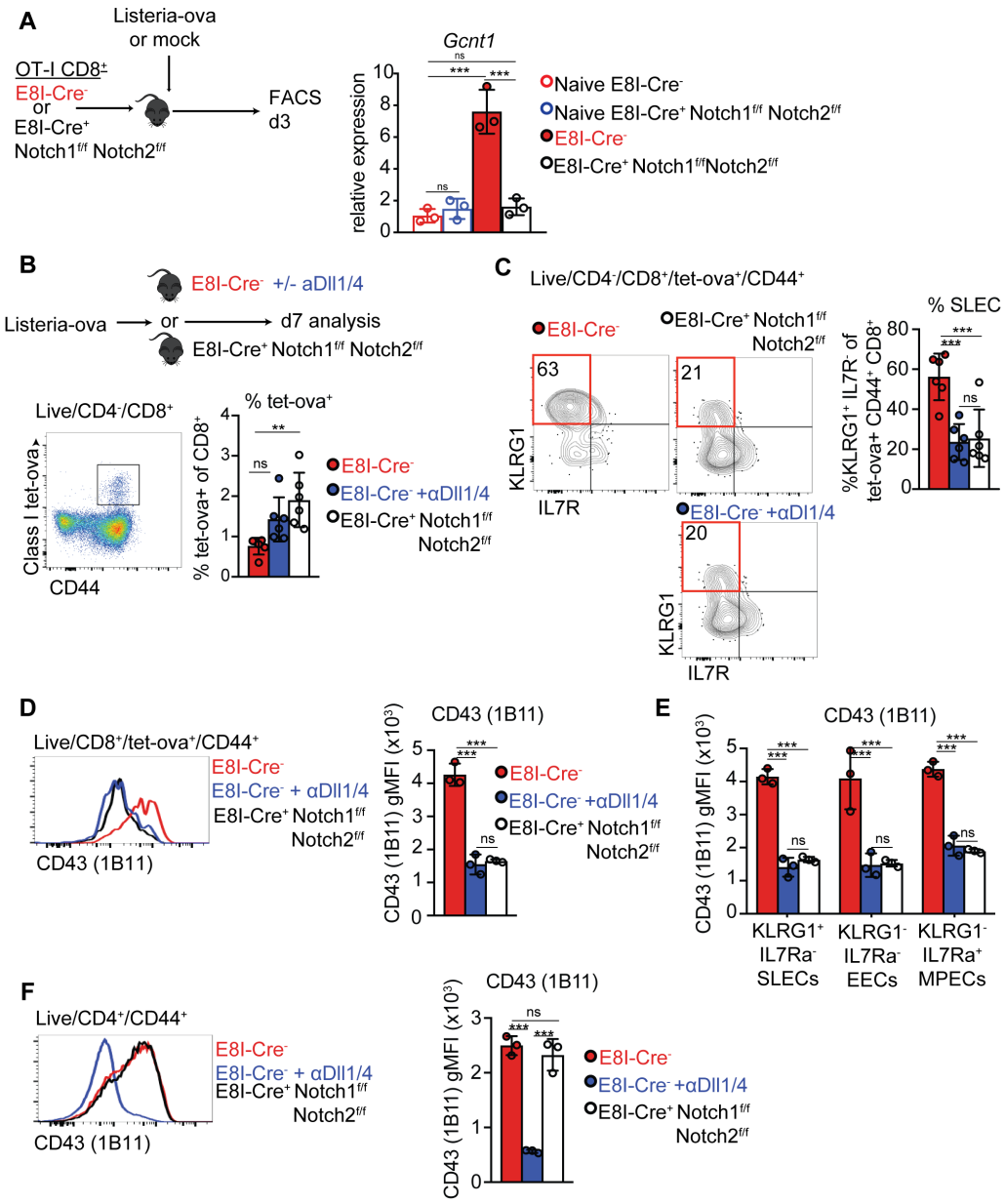

Figure 2.10 Delta-like Notch ligands control CD43 core-2 O-glycosylation in antigen-specific CD8$^+$ T cells during immune response to *Listeria* infection. (A) 10^6 purified wild-type or E8I-Cre$^+$ *Notch$^{f/f}$Notch2$^{f/f}$* CD8$^+$ OT-I (CD45.2$^+$) cells were transplanted into B6.SLJ recipients (CD45.1$^+$) followed by infection with *Listeria monocytogenes* expressing ovalbumin (Lm-OVA) or mock infection. On day 3 post-infection activated CD8$^+$CD45.2$^+$CD44^{hi} were sorted from infected mice and naïve CD8$^+$CD45.2$^+$CD44^{lo} FACS were sorted from non-infected mice and analyzed for *Gcnt1* mRNA by qRT-PCR. (B-F) Wild-type or E8I-Cre$^+$ *Notch$^{f/f}$Notch2$^{f/f}$* mice were infected with a sublethal dose of 2 x 10^3 CFUs of Lm-OVA. A subset of wild-type mice received anti-DLL1/4 antibodies. The antigen-specific CD8$^+$ T cell response was monitored as in Fig. 6. SLEC differentiation (B) and core-2 O-glycosylation of CD43 (C) depended on intact DLL1/4-mediated Notch signals and expression of the Notch1/2 receptors in CD8$^+$ T cells. Notch-dependent core-2 O-glycosylation of CD43 was independent of early differentiation state in CD8$^+$ T cells (D) and also affected CD4$^+$ T cells, as activated CD44$^+$CD4$^+$ T cells showed decreased 1B11 reactivity in mice treated with anti-DLL1/4 antibodies, but not mice lacking Notch receptors only in CD8$^+$ T cells (E). Data representative from two-independent experiments of n=3 per group. *p<0.05, **p<0.01, ***p<0.001, one-way (A-D, F) or two-way (E) ANOVA with Tukey's post-hoc-tests.

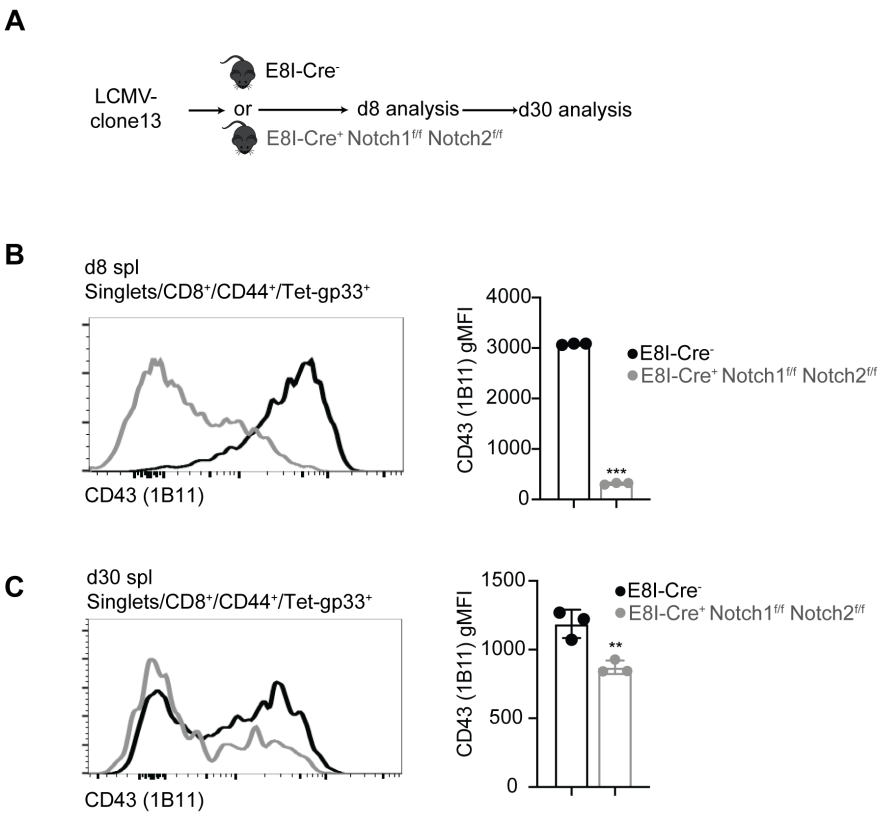

Figure 2.11. CD43 core-2 O-glycosylation is an indicator of Notch signals in viral-specific CD8$^+$ T cells during chronic LCMV infection. Flow cytometric measurement of 1B11 in wild-type and E8I-Cre$^+$ Notch1$^{f/f}$ Notch2$^{f/f}$ infected with 2 x 10^6 PFUs of LCMV clone 12. **(A)** Experimental scheme and 1B11 fluorescence intensity of LCMV specific CD8$^+$ T cells at day 8 **(B)** and day 30 **(C)** post infection.

Chapter 3

Notch Signals from Fibroblastic Reticular Cells Drive Alloreactive T Cell Gut Tropism During GVHD

3.1 Abstract

Graft-versus-host disease targeting the gastrointestinal tract (GI-GVHD) is one of the most feared complications of allogeneic bone marrow transplantation (allo-BMT), with high morbidity and mortality. A growing body of evidence indicates that genetic or pharmacological blockade of the Notch signaling pathway in donor T cells prevents lethal GI-GVHD. In established transplantation models, we used genetic loss-of-function to study how Notch signaling regulated GI-GVHD. We observed decreased accumulation of donor $CD8^+$ and $CD4^+$ conventional T cells (Tcon) but relative preservation of $Foxp3^+$ Treg in the GI-tract. Notch loss-of-function selectively blunted expression of the gut-homing integrin α4β7 in alloreactive $CD8^+$ and $CD4^+$ Tcon, while Notch-deprived Treg showed preserved or increased expression of α4β7. Notch-dependent induction of α4β7 in alloreactive T cells required Notch ligand expression in secondary lymphoid organ fibroblastic reticular cells lineage traced by a Ccl19-Cre transgene. Notch-deprived T cells co-transplanted with Notch-sufficient T cells accumulated in the gut with higher numbers than Notch-deprived T cells transplanted alone, indicating Notch can control gut-trafficking in part through non-cell intrinsic mechanisms. However, co-transfer experiments also revealed that Notch-sufficient effector T cells (but not Treg) preferentially accumulated in the gut compared to Notch-

deprived cells, revealing Notch also controls gut trafficking through cell-intrinsic mechanisms. Compared to pan-T cell loss of the β7 integrin chain, Notch blockade was more protective in our mouse model of allo-BMT. Thus, we defined a critical mechanism for how Notch signaling controls gut tropism of pathogenic donor T cells after allo-BMT. These findings provide key mechanistic insight into the striking protection from GI-GVHD that we observed in a non-human primate (NHP) model of allo-BMT with single-agent blockade of the Delta-like4 Notch ligand. These observations and continued work will uncover novel roles and mechanisms for Notch-dependent regulation of pathogenic T cell gut tropism, while suggesting clinical strategies to prevent GI-GVHD.

3.2 Introduction

The Notch signaling pathway is a critical regulator of pathogenic T cell activation and function in multiple mouse allo-BMT models (25, 28, 29, 31). Importantly, Notch signals exert differential effects on T cell subsets in a context-dependent manner. For example, Notch blockade blunts inflammatory cytokine production from effector $CD4^+$ and $CD8^+$ T cells (47), but expands $Foxp3^+$ regulatory T cells (Tregs) and enhances their function (28, 31). However, the collective contribution of these individual effects to overall survival in GVHD models is unknown. In humans, gastrointestinal GVHD (GI-GVHD) is a primary driver of morbidity and mortality after allo-BMT (162). In $CD4^+$ T cell-mediated models of GVHD, we previously showed that Notch-deficient $CD4^+$ T cells fail to accumulate in the GVHD target organs of the gastrointestinal tract (28), corresponding to decreased histopathologic scoring for GI-GVHD in this model. However, it is unknown whether decreased T cell accumulation in the gut contributes to the protective effects

of Notch blockade during allo-BMT or if other effects of Notch signaling on alloreactive T cell function explain this protection.

Immune cell trafficking from the circulation into lymphoid and non-lymphoid tissues is a step-wise, highly regulated process. First, immune cells diverge from laminar blood flow and roll/tether to the endothelium via weak interactions between selectins on the endothelium and selectin ligands on the immune cell. Notch signaling might be critical for this initial process, because Notch is a crucial regulator of *Gcnt1* expression. *Gcnt1,* a T-cell activation associated glycosyltransferase, controls the core-2 O-glycosylation of P-selectin ligands, determining their ability to interact with P-selectin (26). After rolling/tethering, a second firm adhesion stage occurs. During this stage, stable contacts are formed through specific integrin interaction with integrin ligands expressed by the endothelium, such as α4β1/VCAM-1, LFA-1/ICAM1, and α4β7/MAdCAM-1. This process may require integrin activation through chemokine receptor signaling triggered by chemokines released in the micro-environment. After firm adhesion, signals in part mediated by integrin binding allow the immune cell to traverse the endothelium into the parenchyma. This multi-step process with specific selectin/selectin ligand pairs, chemokine/chemokine receptor pairs, and integrin/integrin ligand pairs allows combinatorial control of tissue tropism, as both immune cell subsets and tissue-specific endothelium express different molecules. Gut tropism in T cell subsets relies on the expression of the integrin heterodimer α4β7 (or lymphocyte Peyer's patch adhesion molecule 1, LPAM-1) and the chemokine receptor CCR9. α4β7 was described as the preferential ligand for MAdCAM-1 (mucosal vascular addressin cell adhesion molecule 1) (163) compared to other integrins such as α4β1 (VLA-4) and αLβ2 (LFA-1). MAdCAM-1 is expressed by high-endothelial venules in mucosal tissue secondary lymphoid organs including mesenteric lymph

nodes and Peyer's patches. MAdCAM-1 is also expressed by other venules in mucosal tissues, including intestinal lamina propria and mammary glands (164). Although MAdCAM-1 was first described as a mucosa-specific molecular gate, it is also expressed on marginal reticular cells (MRCs) present in all secondary lymphoid organs (16) and specialized lymphatic endothelial cells that line the floor of the subcapsular sinus in lymph nodes (165), raising the possibility that it is involved in trafficking within lymphoid organs as well. Given α4β7/MAdCAM-1's critical role in T cell mucosal tissue tropism, its function has been explored in GI-GVHD. Many of these studies relied on genetic excision of *Itgb7*, the gene that encodes the β7 integrin. In one study, *Itgb7*$^{-/-}$ T cells mediated moderately reduced GVHD with decreased histopathological GVHD scores in the small intestine, colon, and liver. *Itgb7*$^{-/-}$ T cells had decreased accumulation in the gut and increased accumulation in secondary lymphoid organs and blood (166). A second study reported greater protection from clinical GVHD corresponding with lower donor T cell infiltration in the intestines and liver (167). In GI-GVHD, α4β7/MAdCAM-1 interactions are particularly critical to allow access of alloreactive T cells to the intestinal crypt base where they mediate damage to intestinal stem cells (114). Importantly, it remains debated whether donor T cells have direct access to the intestinal niche or first need to traffic to secondary lymphoid organs. One group reported that donor CD4^{+} T cells were directly primed by MHC class II molecules in intestinal epithelial cells within days after transplantation (90). In another study, direct transfer of α4β7^{+} T cells mediated worse GI-GVHD than α4β7^{-} T cells (168), suggesting that a pre-existing gut-homing program might bypass priming in secondary lymphoid organs. It is unclear from this study, however, if donor α4β7^{+} T cells trafficked directly into the intestine or first to Peyer's patches or mesenteric lymph nodes where α4β7 could help T cells extravasate across MAdCAM-1^{+} HEV. Conversely, another group that carefully tracked donor T cells using luciferase reporters and

bioluminescence imaging showed that donor T cells first arrive in secondary lymphoid organs where they are primed, acquire gut-homing properties, and then migrate to the GI tract (96, 169).

Careful in vitro studies showed that retinoic acid (RA) signaling controls T cell expression of both α4β7 and CCR9, the receptor for the chemokine CCL25 expressed by intestinal epithelial cells (170). Mucosal tissue-resident dendritic cells (171) and stromal cells present in mesenteric lymph nodes (172) have been shown to express the RA-producing enzymatic machinery that imprints this gut-homing phenotype. RA induction of 'gut-homing' molecules appears to be shared among other SLO immune cells. For instance, splenic MAdCAM-1^+ MRC are capable of producing RA under conditions of TLR agonism, which lead to upregulated α4β7 and CCR9 expression in marginal zone B cells (173). In addition to supporting gut homing, RA has been shown to cooperate with TGF-β to suppress pro-inflammatory Th17 cells and drive $Foxp3^+$ induced Tregs (174). However, it is unknown what signals might convert this normally tolerogenic RA-induced gut-homing program to a pathogenic response in an inflammatory setting like inflammatory bowel disease (IBD) or allo-BMT, where inhibiting the RA pathway in donor T cells protected mice from GVHD (175, 176).

In this study, we used a mouse model of MHC-mismatched allo-BMT to further explore the mechanisms underlying the effects of Notch signaling on alloreactive T cell gut trafficking. We report several key findings, including decreased accumulation of alloreactive T cells in the small intestine and especially the colon, with relatively preserved Treg frequencies in these organs. In mouse models, Notch loss-of-function also blunted α4β7 expression in effector $CD4^+$ T cells early post-transplant and $CD8^+$ T cells throughout the course of disease, while not negatively affecting

the expression of α4β7 in Tregs. These gut-tropic effects of Notch were imprinted by Delta-like ligands from non-hematopoietic secondary lymphoid organ fibroblastic reticular cells. Mixed transplants of wild type T cells and T cells expressing the pan-Notch inhibitor dnMAML (dominant negative Mastermind-like) revealed that cell-intrinsic effects of Notch signaling drove T cell α4β7 expression and accumulation in the gut, although non-cell intrinsic effects of Notch signaling also likely played a role. Finally, in contrast to global loss of integrin β7, Notch loss-of-function selectively blunted α4β7 in alloreactive $CD8^+$ cells but not Tregs and provided greater protection from GVHD. Together these results show that Notch signals, likely delivered to alloreactive T cells by fibroblastic reticular cells in secondary lymphoid organs, program the gut tropism of pathogenic T cells and subsequent GI-GVHD. Our study recapitulates key effects seen in a recent non-human primate (NHP) model of allo-BMT, while providing additional mechanistic insights. Our data suggest strong evolutionary conservation of this effect and indicate that Notch blockade could be a strong candidate for the pharmacological prophylaxis of GI-GVHD.

3.3 Results

3.3.1 Notch loss of function causes relative accumulation of donor Tregs in lymphoid organs and GVHD target tissues

Because mice receiving large doses of T cells succumb early to acute GVHD, we established a model of sub-lethal GVHD to assess the effects of Notch signaling on alloreactive T cell trafficking over a long course of disease. We showed previously that CBF1 mice receiving allo-BMT with $5x10^6$ B6 wild-type T cells and high-intensity conditioning (11 Gy) experienced near-uniform lethality by day 40 post-transplant (**Chapter 2)** (26). To avoid this high lethality but still trigger

acute GVHD, we transplanted eFluor450 labeled 1x10^6 B6 wild-type or dnMAML T cells (H-$2^{b/b}$, Thy1.1) into CBF1 recipients (H-$2^{b/b}$, Thy1.2). To distinguish the initial donor T cells in the inoculum from any donor bone marrow-derived T cells, we provided a source of T-cell depleted CD45.1^+ Thy1.2 bone marrow. As a negative control, we also transplanted a group of recipients with syngeneic T cells and bone marrow **(Fig 3.1 A).** This model led to noticeable clinical signs of acute GVHD, although it remained sub-lethal until at least day 28 post-transplant. Recipient mice receiving wild type allogeneic T cells but not syngeneic or dnMAML T cells had decreased frequency of bone marrow-derived $CD4^+CD8^+$ double-positive thymocytes at day 28 post-transplant **(Fig 3.1 B)**. This ongoing thymic damage indicated that we had established a Notch-sensitive model of sub-lethal GVHD. While we showed that Notch blockade causes expansion of Tregs in secondary lymphoid organs (25, 26, 28, 47), it was unclear if Notch loss-of-function would lead to preferential accumulation of Treg in GVHD target organs. Thus, we assessed Foxp3 staining in donor T cells at days 4, 7, 14, and 28 post-transplant. At day 4, donor T cells were not readily detectable in either small intestine or colon epithelial preparations, consistently with other reports (96). However, by day 7 post-transplant, $CD4^+$ $Foxp3^+$ made up a significantly higher fraction of donor T cells in both mesenteric lymph node and colon epithelium in mice receiving dnMAML T cells. **(Fig 3.2 A)**. The difference between wildtype and dnMAML donor T cells in percentage of Treg leveled off by day 28 post-transplant in secondary lymphoid organs **(Fig 3.2 B)**, but was maintained in both the liver, colon epithelium, and small intestine epithelium late in disease **(Fig 3.2 C).** Thus, Notch-deprived Treg expand in secondary lymphoid organs early post-transplant and may seed GVHD target organs.

3.3.2 Notch loss-of-function blunts α4β7 expression in effector CD8$^+$ and CD4$^+$ T cells but not Tregs

Expression of the activated heterodimeric form of the α4β7 integrin is critical for T cell interaction with MAdCAM1$^+$ gut endothelium and subsequent extravasation into the intestine from the blood. To evaluate if this effect was due to T-cell intrinsic Notch signals, we studied the expression of α4β7 in alloreactive donor T cell subsets. In mice, expression can be easily monitored by the antibody LPAM-1, which recognizes the heterodimeric form (177) or by dual staining with antibodies specific for α4 and β7. To determine when the upregulation of α4β7 occurs post allo-BMT, we examined the kinetics of individual α4 and β7 integrin expression in activated alloreactive T cell subsets. Consistent with other reports indicating acquisition of α4β7 only after several cell divisions (96), we found that α4β7 was only detectable in CD44$^+$ alloreactive T cell subsets >72hrs after allo-BMT **(Fig 3.3)** while CD44$^-$ subsets showed low levels and little upregulation of α4β7 (data not shown). Next, we evaluated how Notch loss-of-function affected longitudinal α4β7 expression in donor T cell subsets across the course of allo-BMT. At day 4 post-transplant, donor syngeneic T cells failed to upregulate α4β7 while allogeneic wild type T cells displayed marked upregulation of α4β7 in CD4$^+$ Foxp3$^-$ Tcon, CD4$^+$ Foxp3$^+$ Treg, and especially in CD8$^+$ T cells (**Fig 3.4 A)**. Notch loss-of-function blunted this upregulation, as a decreased fraction of donor CD8$^+$ and CD4$^+$ Tcon dnMAML cells expressed α4β7 as compared to wild type Tcon. In contrast to Tcon, however, dnMAML Treg showed increased rather than decreased α4β7 expression compared to wild type Treg in the spleen at day 4 post-transplant (**Fig 3.4 A)**. Notch was required to maintain α4β7 in donor CD8$^+$ T cells in the spleen (d4, d7, d14) and mLN (d7, d28) throughout the course of transplant **(Fig 3.4 B,** top panels), while Notch-deficient CD4$^+$ Tcon had significantly decreased α4β7 only at day 4 post-transplant α4β7 **(Fig 3.4 B,** middle panels).

However, α4β7 expression of Notch-deficient Treg was never significantly lower than wild type Treg (**Fig 3.4 B,** lower panels).

3.3.3 Secondary lymphoid organ resident fibroblastic reticular cells are the critical source of ligands to drive the Notch-dependent gut-homing program of effector T cells

We did not readily detect alloreactive donor T cells in the gut at day 4 but did detect them at day 7 post allo-BMT, consistent with findings from other groups (96, 169). Furthermore, upregulation of α4β7 expression in activated donor T cells in secondary lymphoid organs only occurred starting at day 3 post allo-BMT. This suggests that alloreactive T cells are primed and acquire a Notch-dependent gut-homing program in secondary lymphoid organs. This would be consistent with our previous finding that resident non-hematopoietic fibroblastic reticular cells in secondary lymphoid organs, traced by the Ccl19-Cre transgene, are the critical source of Delta-like ligands that drive lethal T cell alloreactivity after allo-BMT (25), even with no prior myeloablative conditioning (26). However, a recent study indicated that alloreactive $CD4^+$ cells can be primed directly by alloantigens presented by ileum intestinal epithelial cells (90). To identify the cellular source of Notch ligands that drives α4β7 expression, we performed allo-BMT into CBF1 recipients with Ccl19-Cre-mediated deletion of *Dll1* and *Dll4* ligand genes or Cre negative controls **(Fig 3.5 A)**. We then assessed α4β7 expression in alloreactive $CD8^+$ subsets in spleen, mesenteric lymph, and pooled peripheral (cervical, brachial, axial, and inguinal) lymph nodes at day 7 post allo-BMT **(Fig 3.5 B)**. Wild type alloreactive $CD8^+$ cells in peripheral and mesenteric lymph nodes had similar high expression of α4β7 with splenic $CD8^+$ expressing even higher levels of α4β7. However, $CD8^+$ cells transplanted into *Ccl19-Cre*$^+$*Dll1*$^{f/f}$*/Dll4*$^{f/f}$ recipients had significantly dampened expression of α4β7 in all three organs **(Fig 3.5 C)** suggesting that fibroblastic reticular cells are the critical

source of Notch signals that drive acquisition of gut homing properties. High expression of α4β7 in wild type pLN and spleen contrasts with previous reports in which alloreactive $CD8^+$ cells in the spleen and especially cervical lymph nodes had lower frequencies of α4β7 positivity than mesenteric lymph nodes (96). However, this could be dependent on the amount of inflammation in the model, as TLR signaling has been suggested to regulate RA production by the MAdCAM-1^+ MRC subset of FRCs (173) which also express high amounts of DLL4 post-transplant **(See Chapter 5)**. To understand if effects on α4β7 expression correlated with decreased T cell gut accumulation, we quantified donor $CD8^+$ T cells in secondary lymphoid organs **(Fig 3.5 D)** and small intestine epithelium (SIEL) and lamina propria (SILPL) **(Fig 3.5 E)**. *Ccl19-Cre*$^+$ *Dll1*$^{f/f}$*/Dll4*$^{f/f}$ recipients had dramatically decreased accumulation of donor $CD8^+$ cells in the small intestine. Reciprocally, there was an increased number of donor $CD8^+$ cells in the mesenteric lymph nodes of *Ccl19-Cre*$^+$*Dll1*$^{f/f}$*/Dll4*$^{f/f}$ mice consistent with what others have observed in secondary lymphoid organs with integrin β7 loss in T cells (166, 167). We also examined donor $CD4^+$ $CD25^-$ Tcon and observed less dramatic but similar effects of decreased α4β7 expression in the mLN and pLN, as well as a trend for lower expression in the spleen **(Fig 3.6 A)**. This correlated with increased accumulation of donor CD4 Tcon in mesenteric lymph nodes **(Fig 3.6 B)** and dramatically decreased accumulation in the small intestine **(Fig 3.6 C)** in *Ccl19-Cre*$^+$ *Dll1*$^{f/f}$*/Dll4*$^{f/f}$ recipients. $CD4^+$ $CD25^{hi}$ Treg frequency was increased in the spleen, mLN, and small intestine lamina propria of *Ccl19-Cre*$^+$*Dll1*$^{f/f}$*/Dll4*$^{f/f}$ mice **(Fig 3.6 D)**, consistent with the increased Treg frequency seen with dnMAML T cells in **Fig 3.2**. While more work needs to be done to explicitly rule out the effects of a Ccl19-Cre lineage-traced source of Notch ligands in the gut itself, these results suggest that FRCs in spleen, mLN, and pLN program gut homing in recently activated donor $CD8^+$ and $CD4^+$ Tcon through Delta-like Notch ligands.

3.3.6 Notch signals control alloreactive T cell gut tropism through both cell-intrinsic and non-cell intrinsic mechanisms

It is unclear if Notch signals drive the gut homing program of T cells through cell-intrinsic effects, non-cell-intrinsic mechanisms, or a combination of the two. First, it could be that Notch regulates α4β7 cell-autonomously, thus regulating entry into specific locations of the GI-tract through interaction with MAdCAM1$^+$ blood vessels (28). Notch could also cell-intrinsically control other molecules important for gut-homing, such as Gpr15 (178) or directly modulate specific signaling pathways, such as ERK signaling (47), mTOR, or Myc (149) that in turn regulate gut homing. If this is the case when wild type cells and dnMAML cells are co-transplanted, wild type cells should accumulate preferentially in the GI tract. Second, Notch signals could control gut homing through non-cell-intrinsic mechanisms. Notch signals control inflammatory cytokine production in donor CD4 and CD8 cells in secondary lymphoid organs (25, 28, 47), thus the Notch-driven inflammatory cytokine milieu may drive α4β7 and a gut homing program rather than Notch signals controlling it directly. Additionally, the Notch-dependent inflammatory cytokine environment, including TNFα, could also drive the endothelium to upregulate integrin ligands such as VCAM-1, MAdCAM-1, or ICAM-1 (179) allowing T cells easier entry into target tissues. In a model of experimental autoimmune encephalitis, we previously showed that Notch signals regulate the accumulation of autoreactive CD4$^+$ T cells in the CNS in part through non cell-intrinsic mechanisms (133). In the case of allo-BMT, this may be compounded by vascular leakiness as conditioning regimens directly damage the endothelium (180). Third, Notch effects on gut homing could be through a mixture of both cell-intrinsic and non-cell intrinsic mechanisms. Mixed mechanisms were apparent previously with Notch regulation of CD8$^+$ T cytokine production in

GVHD. In this context, Notch signals were required within $CD8^+$ T cells themselves and also helper $CD4^+$ T cells to induce high inflammatory cytokine production in $CD8^+$ T cells (47).

To dissect the roles of cell-intrinsic vs. non-cell-intrinsic Notch signals, we transplanted CBF1 recipients with $1x10^6$ allogeneic T cells either at a 1:1 ratio or a 0:1 ratio of wild type to dnMAML cells (i.e. $5x10^5$ wild type plus $5x10^5$ dnMAML T cells or $1x10^6$ dnMAML cells). We then monitored T cell accumulation in secondary lymphoid and target organs at day 7 post-transplant **(Fig 3.7 A)**. Consistent with previous findings, there was no negative effect of Notch inhibition on the expansion of $CD8^+$ and $CD4^+$ Tcon in spleen **(Fig 3.7B,** left and middle panels**)** or mLN (**Fig 3.8 A,** left and middle panels**)**, with wild type and dnMAML cells roughly maintaining the initial 1:1 ratio at which they were transplanted (solid line comparison). There were also no differences in overall cell numbers between recipients transplanted with a 1:1 ratio of wild type:dnMAML cells or transplanted only with dnMAML cells (dashed line comparison). dnMAML $Foxp3^+$ Tregs were much more likely to expand compared to wild type Tregs in both spleen **(Fig 3.7 B,** right panel**)** and mLN (**Fig 3.8 A,** right panel**)** consistent with previous findings, although this effect was much stronger when only dnMAML T cells were transplanted (solid versus dashed line comparison).

However, in colon lamina propria (top panels) and epithelium (bottom panels), both wild type $CD8^+$ T cells (left panels) and wild type $CD4^+$ Tcon (middle panels) represented a significantly higher fraction of donor T cells compared to co-transferred dnMAML T cells **(Fig 3.7 C**, solid line comparison**)**. We calculated the ratio of wild type:dnMAML cells for each T cell subset and organ and summarized them in **Fig 3.7 D**. $CD8^+$ T cells, indicated in the top panel, in spleen, mLN, and

liver remained close to the initial 1:1 transplantation ratio (black dotted line). In the GI-tract, $CD8^+$ T cells had higher wild type:dnMAML ratios in the small intestine epithelium (SIEL, ~1.5:1 ratio), colon epithelium (CEL, ~3:1 ratio), and colon lamina propria (CLPL, ~2.5:1 ratio) **(Figure 3.7 D,** top panel). When examining the wild type:dnMAML ratios in $CD4^+$ Tcon, there was an even more profound cell-intrinsic gut accumulation defect in dnMAML T cells, particularly in the colon. There was significant over-representation of wild type $CD4^+$ Tcon in the small intestine epithelium (~2.7:1 ratio), small intestine lamina propria (~3.2:1 ratio), colon epithelium (~7.5:1 ratio), and colon lamina propria (~9:1 ratio) **(Fig 3.7 D**, middle panel). There was minor over-representation of wild type $CD4^+$ Tcon in spleen, mLN and liver (~1.3:1 ratio), likely due to the fact that dnMAML $CD4^+$ cells are more likely to be $Foxp3^+$ Tregs than $Foxp3^-$ Tcon. Altogether, this competitive experiment suggested that Notch loss-of-function leads to cell-intrinsic defects in gut homing.

However, when comparing recipient mice that received a 1:1 mix of cells compared to recipients that received dnMAML alone (0:1), the recipients that received a mixture of cells had more dnMAML $CD8^+$ **(Fig 3.7 C** left panels, dashed line comparison**)** and $CD4^+$ Tcon (**Fig 3.7 C** middle panels, dashed line comparison**)** cells accumulate in the colon epithelium and lamina propria. This greater accumulation was more striking considering that recipients transplanted with a 1:1 mix initial had half ($5x10^5$) the absolute amount of dnMAML cells compared to recipients transplanted with a 0:1 ratio ($1x10^6$).

Altogether, these findings suggest that both cell-intrinsic and non-cell intrinsic effects of Notch signaling drive donor $CD8^+$ and $CD4^+$ Tcon cell accumulation in the GI-tract. Consistent with a

selective effect on $CD8^+$ and $CD4^+$ Tcon cells, $Foxp3^+$ Tregs maintained the initial 1:1 transplantation ratio in the colon **(Fig 3.7 C**, right panels) and small intestine (**Fig 3.7 D**, bottom panel). To further confirm the cell-intrinsic effects on $CD8^+$ and $CD4^+$ Tcon but not $CD4^+$ Treg cell accumulation in the gut, we conducted a similar experiment but with a 1:2 mixture of wild type:dnMAML T cells **(Fig 3.9 A).** Compared to dnMAML, wild type $CD8^+$ T cells accumulated preferentially in the colon **(Fig 3.9 B**, top panel), while wild type $CD4^+$ Tcon accumulated preferentially in the small intestine and colon **(Fig 3.9 B**, middle panel). In contrast, dnMAML Tregs maintained or expanded beyond the initial transplantation ratio in both secondary lymphoid organs and the gut **(Fig 3.9 B**, bottom panel).

To test whether the effects of Notch signaling on α4β7 expression were cell-intrinsic or non-cell intrinsic, we assessed α4β7 expression by flow cytometry in donor T cell subsets from recipients that received a 1:1 competitive transplant and recipients that received dnMAML T cells alone. Consistent with a cell-intrinsic effect in $CD8^+$ T cells, α4β7 was lower in co-transplanted dnMAML compared to wild type T cells in the spleen **(Fig 3.7 E**, left panel) and mLN **(Fig 3.8 B**, left panel). Additionally, dnMAML $CD8^+$ transplanted alone did not have significantly lower α4β7 expression than dnMAML $CD8^+$ T cells transplanted with wild type cells, indicating that non-cell intrinsic effects of Notch signaling did not regulate α4β7 expression in both spleen **(Fig 3.7 F** left panel) and mLN **(Fig 3.8 B**, left panel). Minor and no effects of cell-intrinsic Notch signals were seen on $CD4^+$ Tcon and Treg, respectively, in both spleen **(Fig 3.7 F**, middle and right panels) and mLN **(Fig 3.8 B**, middle and right panels). To assess whether dnMAML T cells present in the GI tract had a *bona fide* gut-resident phenotype, we studied CD103 expression in donor $CD8^+$ T cells in spleen, colon epithelium, and small intestinal epithelium. Cells in gut epithelium had higher levels

of CD103 compared to spleen consistent with gut-homed T cells **(Fig 3.7 G**), but there were no differences in CD103 expression in wild type vs. dnMAML T cells **(Fig 3.7 G/H)**. This demonstrates that Notch inhibition likely interferes with the entry and/or survival of gut-homed T cells but not with their acquisition or maintenance of a tissue-resident phenotype. Together, these results indicate that Notch signals control the gut-homing program of alloreactive effector T cells but not Tregs through both cell-intrinsic and non-cell intrinsic mechanisms.

3.3.7 Notch loss-of-function selectively modulates α4β7 expression in alloreactive T cell subsets and prevents GVHD to a higher extent than global integrin β7 loss

Other groups have shown that expression of integrin β7 is critical for GVHD in mice (166, 181, 182) and blocking antibodies to human α4β7 have been tested in the clinic as a prophylaxis for GVHD (183). Thus, we hypothesized that Notch signaling may mediate GI-GVHD at least in part through its effects on α4β7 expression. To test this hypothesis, we transplanted CBF1 recipients with wild type, *Itgb7*$^{-/-}$, dnMAML, or dnMAML/*Itgb7*$^{-/-}$ T cells **(Fig 3.10 A)**. Global β7 loss and Notch loss-of-function did not affect donor T cell frequency in the blood 14 days post-transplant **(Fig 3.10 B)**. β7 loss also did not affect the ability of T cells to experience Notch signals, as alloreactive wild type and *Itgb7*$^{-/-}$ CD4^{+} T cells had similar levels of the core-2 O-glycoform of CD43, a surrogate marker of Notch signaling (26) **(Fig 3.10 C**, left panel**)**. *Itgb7*$^{-/-}$ CD8^{+} T had a mild reduction in this Notch signaling marker, although to a much lesser extent as dnMAML and dnMAML/*Itgb7*$^{-/-}$ cells **(Fig 3.10C,** right panel). However, CD25 expression was blunted in dnMAML and dnMAML/*Itgb7*$^{-/-}$ CD8^{+} cells but not *Itgb7*$^{-/-}$ cells compared to wild type T cells **(Fig 3.11)**. Compared to *Itgb7* loss, Notch loss-of-function had T cell subset specific effects on α4β7 expression . *Itgb7*$^{-/-}$ and dnMAML/*Itgb7*$^{-/-}$ CD8^{+} T cells expressed no α4β7, as expected.

dnMAML $CD8^+$ had significantly blunted, but not fully abolished α4β7 expression **(Fig 3.10 D,** right panel). Furthermore, while *Itgb7*$^{-/-}$ and dnMAML/*Itgb7*$^{-/-}$ $CD4^+$ T cells lacked α4β7, dnMAML $CD4^+$ T cells had comparable levels of α4β7 compared to wild type cells in the blood **(Fig 3.10 D**, left panel) consistent with our previous data showing little Notch-dependent differences in $CD4^+$ T cells at day 14 post-transplant in secondary lymphoid organs (**Fig 3.4 B)**. In contrast to previous reports, *Itgb7*$^{-/-}$ T cells did not mediate less severe GVHD than wild type T cells **(Fig 3.10 E)**. In fact, *Itgb7*$^{-/-}$ T cell recipients showed trends for slightly increased weight loss early during the course of GVHD and had higher skin GVHD **(Fig 3.10 E)**. In contrast, recipients of dnMAML T cells were almost completed protected in terms of survival, weight loss, and GVHD scores compared to recipients receiving wild type or *Itgb7*$^{-/-}$ T cells. Any exacerbation of skin GVHD or early weight loss due to global integrin β7 was mitigated by the loss of Notch signals as recipients receiving dnMAML/*Itgb7*$^{-/-}$ were protected from GVHD similarly to recipients receiving dnMAML/*Itgb7*^{wt} T cells. Due to practical limitations, we were unable to assess the GI-tract and other GVHD target organs for histopathologic scoring or evaluate the accumulation of donor T cells. We plan to complete these experiments in the future. These results suggest that Notch blockade likely will have greater GVHD prophylactic activity in allo-BMT than pharmacologic blockade of α4β7.

3.4 Discussion

Notch signaling regulates pathogenic T cell alloimmunity in multiple GVHD models. Both in human GVHD and in mouse models of GVHD, tissue damage in the GI tract is a key driver of lethality. We observed that Notch loss-of-function prevents accumulation of alloreactive T cells in the gut in mice. Recently, our laboratory and collaborators have been investigating the efficacy of pharmacologic Delta-like4 (DLL4) Notch ligand blockade as a GVHD prophylaxis strategy in a

non-human primate (NHP) model of allo-BMT (184, 185). DLL4 blockade led to striking protection from clinical GI-GVHD, reduced GI histopathological scores, and significant improvement in overall survival (186). DLL4 blockade dramatically reduced the amount of alloreactive effector T cells accumulating in the colon with preferential preservation of Tregs over effector T cells. Anti-DLL4 treatment downregulated α4β7 expression in alloreactive $CD8^+$ T cells but not $Foxp3^+$ Tregs. However, the exact immunobiological mechanism for these highly conserved effects of Notch inhibition on GI-GVHD had not previously been documented.

In this study, we recapitulated in mice the key effects of Notch blockade observed in NHPs while providing mechanistic insights that would be impossible to obtain in the NHP model. In both NHP and mice, Notch loss-of-function led to decreased alloreactive effector T cell accumulation in the gut with relative preservation of donor Treg, and blunted α4β7 expression in effector T cells but not Tregs. In mice, we showed that these effects are likely due to a cellular source of Notch ligand derived from FRCs in secondary lymphoid organs. These trafficking effects depend on both cell-intrinsic and non-cell intrinsic effects of Notch signals. However, Notch loss-of-function did not block the acquisition of $CD103^+$ gut-resident phenotype in T cells that made it into the intestine, suggesting that Notch likely controls seeding of alloreactive T cells to the intestine or their survival rather than subsequent acquisition of a gut-resident phenotype. Finally, we showed that Notch loss-of-function likely mediates greater GI GVHD protection than global loss of integrin β7. However, many open questions still exist about how Notch signals control gut trafficking of T cells.

Notch loss-of-function was more protective than global deletion of integrin β7 in our mouse model, but others have shown that *Itgb7*$^{-/-}$ T cells mediate less severe GVHD (166, 167). Why might this

discrepancy exist? In certain models of allo-BMT, other integrins besides α4β7 may be important for alloreactive T cell arrest and adhesion to inflamed GI endothelium during GVHD. Controlled trials in Crohn's disease have indicated that natalizumab, which is specific for α4 and blocks both α4β1 and α4β7 has similar efficacy as vedolizumab, which is only specific for the α4β7 heterodimer (187). In some contexts, however, other integrins may regulate GI-specific T cell pathology (188). For example, α4β1 but not α4β7 has been shown to be critical for ileal homing of T cells in a humanized mouse model of Crohn's disease (189). Inflammatory cytokines such as TNFα are key drivers of upregulation of integrin receptors on endothelium (179). Interestingly, human colonic epithelial cell lines pre-treated with TNFα/IFNγ induced upregulation of ICAM-1 (the ligand for LFA-1) and VCAM-1 (the ligand for α4β1) in co-cultured endothelial cells (190). This may be particularly important during allo-BMT as both TNFα and IFNγ are produced early after the conditioning regimen in the gut (90). In fact, a prior allo-BMT study showed that irradiation drives global VCAM-1 upregulation in the ileum and colon, which was maintained in allo-BMT recipients. Additionally, ICAM-1 but not MAdCAM1 was strongly upregulated in the ileum at day 3 post allo-BMT (191). MAdCAM-1 was only mildly upregulated at day 9 post-allo-BMT. However, because of the lack of co-staining with cellular identity markers, it is difficult to conclude if this regulation is specific to the endothelium or the underlying lamina propria, which can express both VCAM-1 and ICAM-1, or the epithelium which expresses high levels of ICAM-1 during GVHD (192). One explanation for the non-intrinsic effects of Notch signaling on gut trafficking is that Notch-sufficient T cells produce more inflammatory cytokines such as TNFα that cause upregulation of integrin ligands on inflamed endothelium. Better resolution with new immunofluorescence and with flow cytometric studies is needed to dissect the dynamic landscape of integrin and adhesion molecule expression in the gut endothelium after allo-BMT. We have

started such studies by investigating the expression of these markers at baseline in secondary lymphoid organ and intestinal lamina propria stromal cells, which reveals that only a small proportion of endothelial cells in small intestinal lamina propria and mLN (~5%) express detectable levels of MAdCAM-1 **(Fig 3.12)**.

The integrin/adhesion molecule pairings that drive GI-GVHD likely vary depending on conditioning damage, the type of pathogenic T cell effector response, and the niche that pathogenic T cells require access to in order to mediate GI-GVHD. First, conditioning may damage endothelial cells, rendering them "leaky" and allowing extravasation of alloreactive T cells to become less dependent on specific integrins (180, 193). Second, if alloreactive T cells drive a strong, early, and lethal cytokine storm, pathogenicity may not strictly depend on trafficking into target tissues. In some models for example, alloreactive T cells do not need to re-encounter alloantigen in target tissues to mediate lethal GVHD (74). In other models that require re-exposure to alloantigen in target tissues (81)(66, 67, 90) , there may be greater requirement for integrins in GVHD pathogenesis. Third, pathogenic T cell access to specific adhesin-gated microanatomical niches likely matters. Careful imaging studies by Fu. et al. recently described that alloreactive T cells, irrespective of conditioning intensity, primarily invade the crypt base of the ileum epithelium, with fewer alloreactive T cells seen in the villi and upper crypt region. This distribution matches the location of MAdCAM-1^{+} blood vessels close to intestinal stem cells, which are then directly damaged by alloreactive T cells (114). However, the degree to which this infiltration into the crypt base depends upon α4β7/MAdCAM1 alone may vary if crypt base vessels also express VCAM-1 and ICAM-1. For example, transplantation of *Itgb7*$^{-/-}$ T cells or treatment with an anti-MAdCAM-1 antibody halved but did not eliminate the accumulation of alloreactive T cells in the

intestinal crypt, suggesting that there may be α4β7/MAdCAM1-independent access to this niche (114). Additionally, MAdCAM-1 can be glycosylated with sugar residues that allow binding of L-selectin, which may allow alternative entry mechanisms for naïve or central memory T cells into the intestinal crypt (194). It is also unknown if a similar microanatomical localization of alloreactive T cells occurs in the colon, where the effects of Notch signaling on alloreactive T cell accumulation appeared most profound, and other trafficking molecules such as Gpr15 might be involved in homing (178, 195, 196).

Migration across inflamed endothelium occurs in distinct stages. Integrin interaction and adhesion is the second stage preceded by selectin interaction, which mediates the initial rolling/tethering of immune cells. Inflammation-associated upregulation of E- and P-selectin in GI endothelium may cause increased rates of rolling/tethering of alloreactive T cells to the gut endothelium and subsequent trafficking. In fact, P-selectin-deficient mice are protected from GVHD (155). We recently reported a critical role of Notch signaling in regulating expression of the Ag-activation associated core-2 O-glycosyltransferase *Gcnt1* which decorates surface proteins with sugar residues required for their interaction with P-selectin (53, **Chapter 2**). However, T cells lacking *Gcnt1* were still able to accumulate in the GI tract in similar numbers as wild type T cells and mediate lethal GVHD (26). However, it could be that Notch regulation of both functional selectin ligand generation and integrin formation is a one-two punch that controls the early rolling/tethering interaction and the later adhesion/arrest stage of T cell trafficking across inflamed endothelium. Inhibiting this compound regulation could have much greater effects on T cell trafficking than blocking either step alone. Thus, it would be interesting to test if compound *Gcnt1*/*Itgb7* mutants better phenocopy the effects of Notch signaling on T cell trafficking.

Another intriguing possibility is that α4β7 expression may be important during T cell activation in secondary lymphoid organs. MAdCAM1$^+$ high-endothelial venules in mesenteric lymph node and Peyer's patches regulate initial entry or re-circulation of α4β7$^+$ T cells into secondary lymphoid organs. MAdCAM1$^+$ lymphatic endothelial cells line the floor of the capsular sinus of all lymph nodes. Fibroblastic MAdCAM1$^+$ marginal reticular cells exist in spleen and lymph nodes. Interestingly, we showed that in lymph nodes MAdCAM1$^+$ marginal reticular cells (MRCs) express very high levels of Delta-like4 that becomes upregulated within the first 12h post allo-BMT **(Chapter 4)**. Could α4β7 expression facilitate increased interactions with DLL4^{hi} MRCs and increase Notch signaling in a feed-forward loop? Our preliminary evidence indicates that this might be the case for CD8$^+$ T cells, as β7-deficient cells showed trends for blunted expression of the core-2 O-glycoform of CD43, a surrogate read-out of Notch signaling **(Fig 3.10)**. This will be interesting to explore further as α4β7/MAdCAM-1 in concert with retinoic acid signaling has been shown to provide strong costimulatory signals to naïve and memory T cells in a NHP model of HIV (197). In addition, others have suggested that MRCs upregulate RA-synthesis pathways in response to TLR signals that in turn drive α4β7/CCR9 expression in marginal zone B cells (173).

One simple explanation for the stronger protective effects of Notch loss-of-function compared to global β7 loss is suggested by our data that Notch inhibition selectively blunts α4β7 expression in effector CD8$^+$ and to a lesser extent CD4$^+$ effector cells, but not in Tregs. In fact, data from both the NHP model and our mouse model indicates that very early after allo-BMT, α4β7 levels may be higher in Notch-deprived Tregs. This observation could be critical as α4β7$^+$ Tregs correlated with GVHD protection in the clinic (198), while antigen-experienced CD45RO$^+$ α4β7$^+$ CD8$^+$ T

cells correlated with intestinal GVHD (199). What might be the mechanisms of this selective regulation of α4β7 in effector but not regulatory T cells? Differential regulation suggests that Notch does not directly regulate α4β7 transcriptionally. Instead, Notch might modulate signaling pathways and metabolism, e.g. via mTORC1 signals, that differentially regulate effector v. Treg function (200). We plan to assess the effects of Notch signaling on the transcriptomes of donor Tregs v. $CD8^+$ and $CD4^+$ Tcon to further our understanding of this differential regulation. We also plan to conduct experiments where we co-transfer wild type vs. dnMAML vs. *Itgb7*$^{-/-}$ effector T cells and Treg to dissect if differential gut homing of T cell subsets affects GVHD lethality.

Much remains to be understood about the role of Notch signaling in regulating T cell trafficking in the context of allo-BMT. It is unknown if Notch signaling controls α4β7 directly through transcription of *Itga4* and *Itgb7*, differentially regulates pairing with other integrins (201), or regulates expression through other post-translational mechanisms. Also, it is unknown if Notch signals regulate T cell gut-homing in other immunological contexts. Recently, a study dissected the role of Notch signaling in a Th2 model of house dust mite allergen. The authors found that Notch controlled the expression of S1PR1 and thus the ability of S1P to mediate *egress* of antigen-activated T cells from the draining lymph node to the lung (53). We saw a similar effect in our study with Notch-deprived T cells tending to accumulate more in secondary lymphoid organs. Together, our results in concert with complementary NHP data represent a critical and evolutionarily conserved role of Notch signals in regulating alloreactive T cell trafficking to GI target tissues and subsequent GI-GVHD. Altogether, we believe that these findings provide compelling evidence for pharmacologic Notch blockade as a potential therapeutic strategy for GVHD prophylaxis.

3.5 Figures

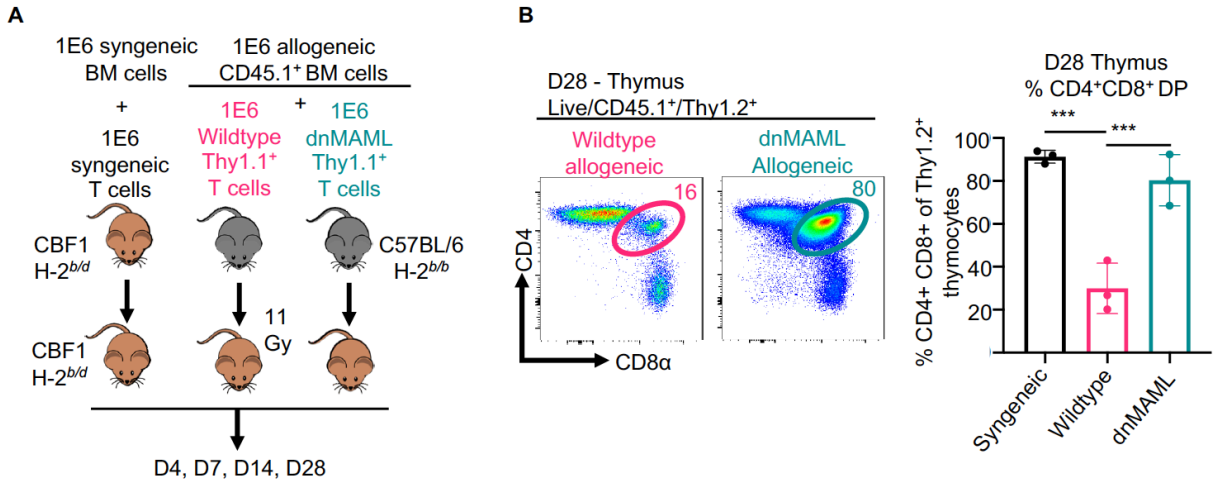

Figure 3.1 Establishing a sub-lethal model of GVHD. (A) 1x10^6 Thy1.1$^+$ allogeneic wildtype, allogeneic dnMAML T cells (H-2$^{b/b}$), or syngeneic (H-2$^{b/d}$) were labeled with eFluor450 cell proliferation dye and transplanted into lethally irradiated recipients (H-2$^{b/d}$). Recipients received CD45.1$^+$ Thy1.2$^+$ bone marrow to distinguish BM-derived cells from initial T-cell inoculum. (B) Percentage of CD4$^+$ CD8$^+$ cells among newly formed CD45.1$^+$ Thy1.2$^+$ thymocytes at d28 post-transplant. **p<0.01, ***p<0.001, one-way ANOVA with Tukey's post-hoc-tests.

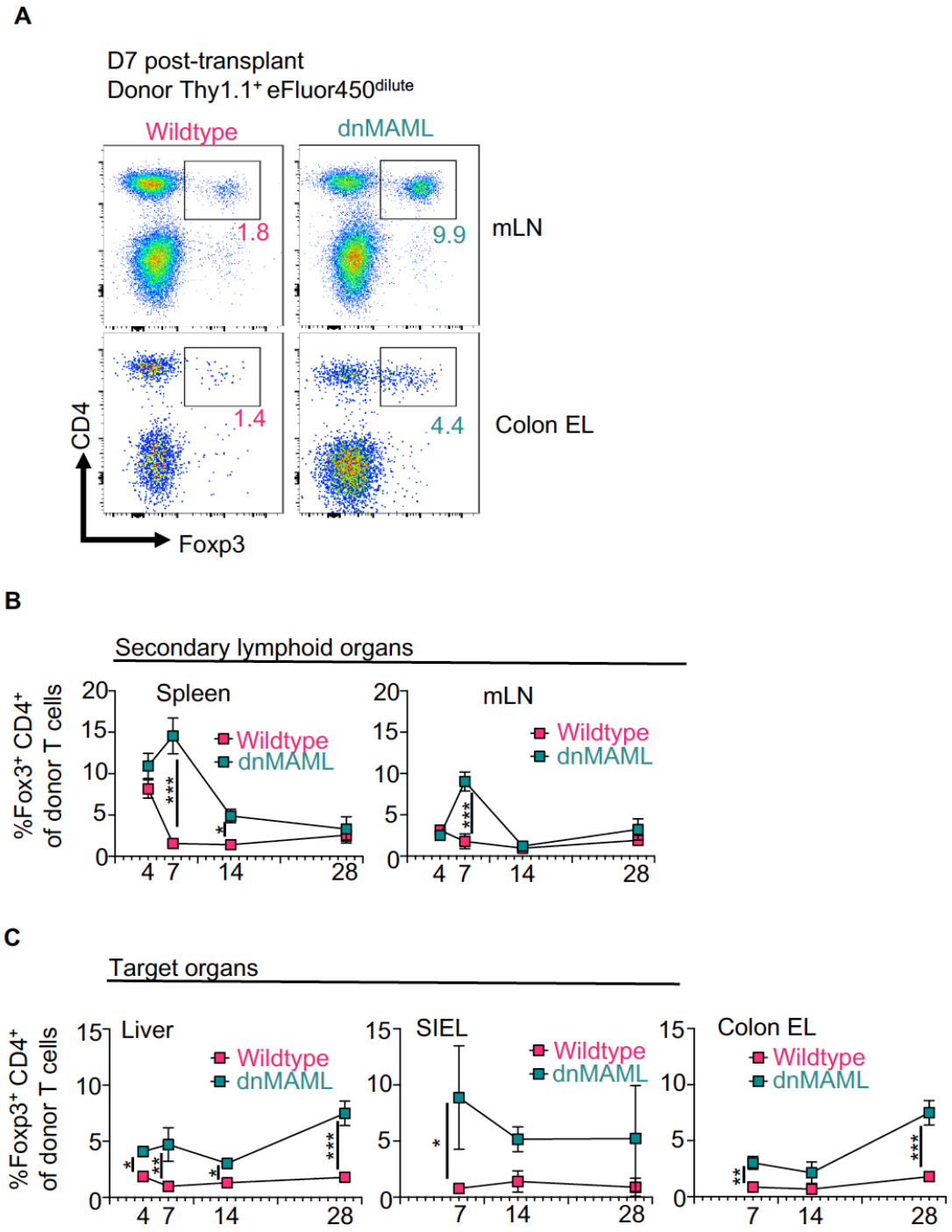

Figure 3.2 Notch loss of function leads to relative Treg accumulation in secondary lymphoid organs and GVHD target organs. Donor T cells at different timepoints from Fig 3.1 were assayed by flow cytometry. (A) Foxp3 expression of donor Thy1.1+ eFluor450 wildtype or dnMAML T cells summarized in (B). n=3 mice per group per timepoint. *p<0.05, **p<0.01, ***p<0.001, one-way ANOVA with Tukey's post-hoc-tests. mLN = mesenteric lymph node, SIEL = small intestine epithelium lymphocytes. Data at day 4,14,28 is from a single experiment. Data at d7 is representative of at least n=3 experiments.

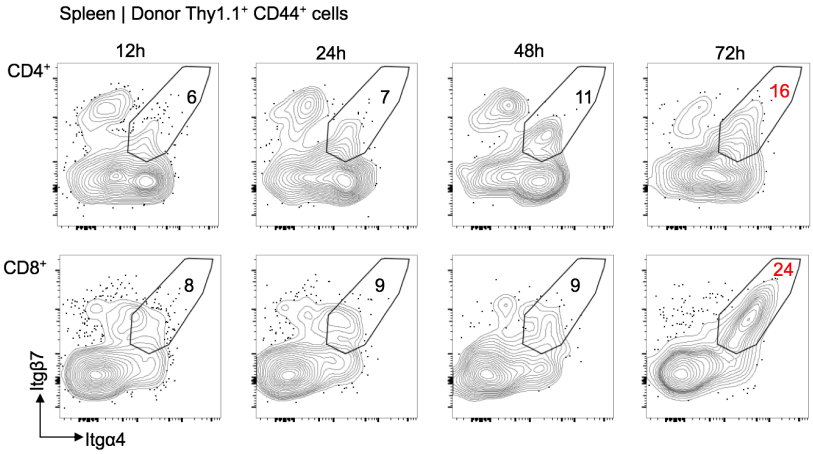

Fig 3.3. α4β7 upregulation occurs 72h post allo-BMT. Donor Thy1.1^{+} CD44^{+} T cell subsets were isolated from recipient spleens and assessed for integrin expression by flow cytometry.

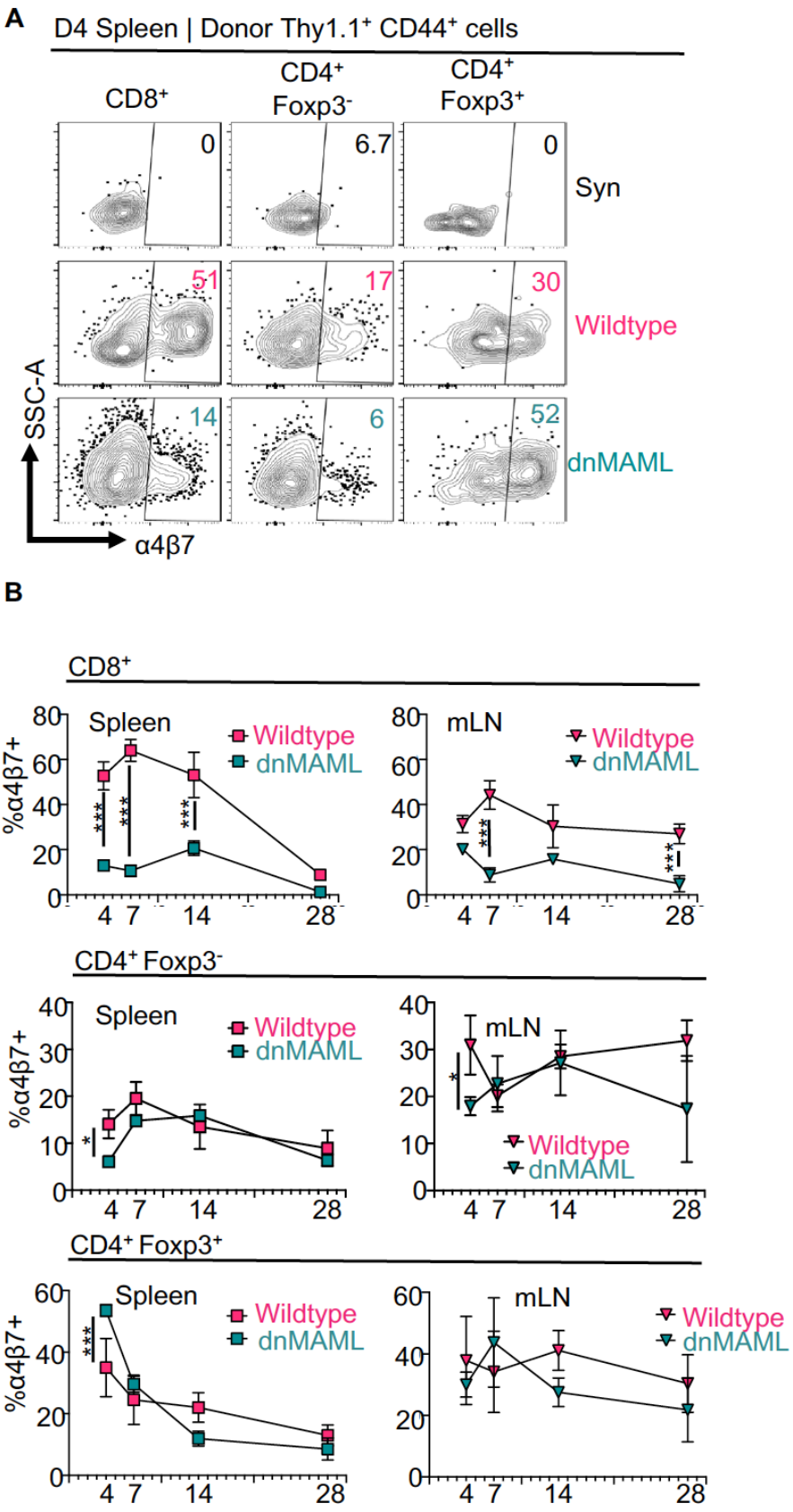

Figure 3.4. Notch loss of function blunts α4β7 expression in effector T cells. Donor T cell subsets from Fig 3.1 were assessed for α4β7 expression by flow cytometry after indicated timepoints. (A) Flow cytometry plots of $\alpha4\beta7^+$ donor T cell subsets isolated from spleen at day 4 post-transplant. (B) Summary data at indicated times post-transplant in spleen and mLN. n=3 mice per group per timepoint. *p<0.05, **p<0.01, ***p<0.001, one-way ANOVA with Tukey's post-hoc-tests. Syn = syngeneic. mLN = mesenteric lymph node.

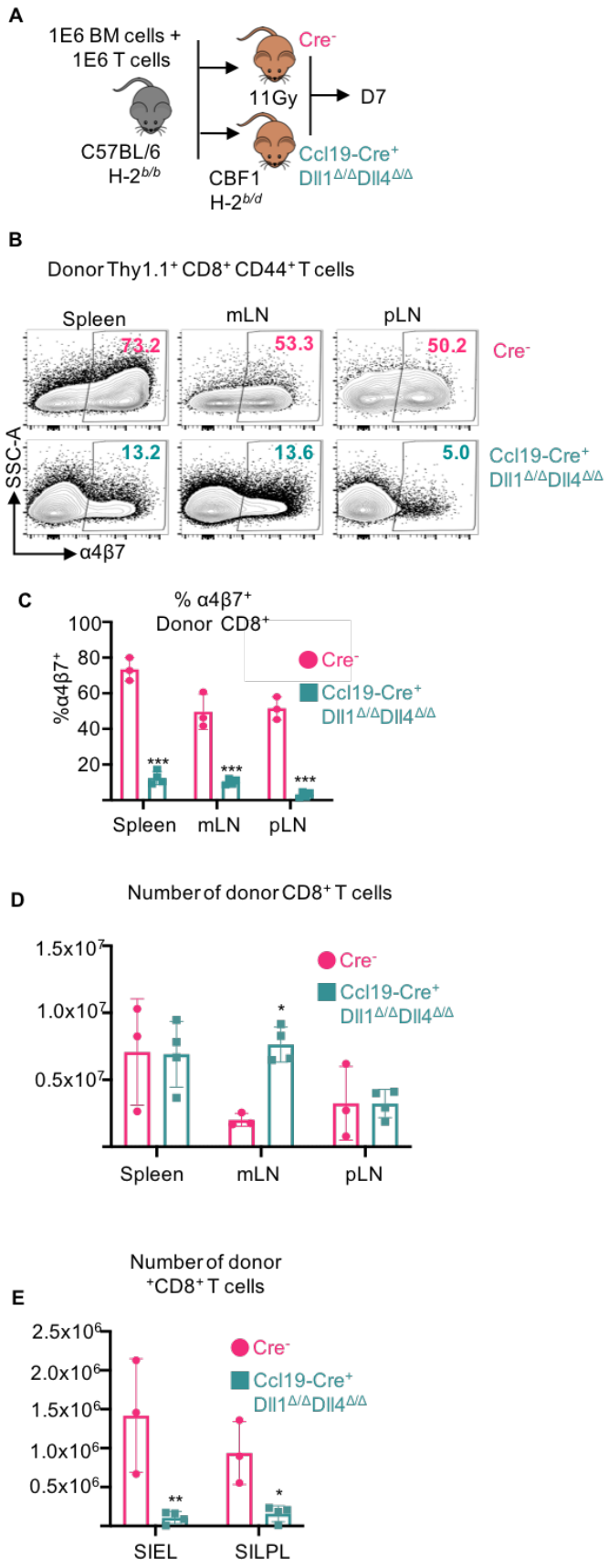

Fig 3.5. Delta-ligands from Ccl19-Cre lineage traced fibroblastic reticular cells are the critical source of Notch signals that drive the alloreactive T cell gut-homing.
(A) Experimental scheme. $1x10^6$ alloreactive T cells plus $1x10^6$ BM cells from C56BL/6 mice was transplanted into *Ccl19-Cre*$^+$ *Dll1*$^{\Delta/\Delta}$*Dll4*$^{\Delta/\Delta}$ or Cre$^-$ littermate control CBF1 mice after 11 Gy total body irradiation. Secondary lymphoid organs and small intestinal lymphocyte fractions were isolated at day 7 post-transplant. (B) Flow cytometry plots of α4β7 expression in donor Thy1.1+ CD8+ T cell subsets summarized in (C). transplant. Absolute number of donor CD8+ T cells was quantified in secondary lymphoid organs (D) and small intestinal lymphocyte fractions (E). n= at least 3 mice per group. *p<0.05, **p<0.01, ***p<0.001, one-way ANOVA with Tukey's post-hoc-tests. mLN = mesenteric lymph node. pLN = pooled peripheral (cervical, axial, brachial, inguinal) lymph nodes. SIEL = small intestinal epithelial lymphocyte fraction. SILPL = small intestinal lamina propria lymphocyte fraction.

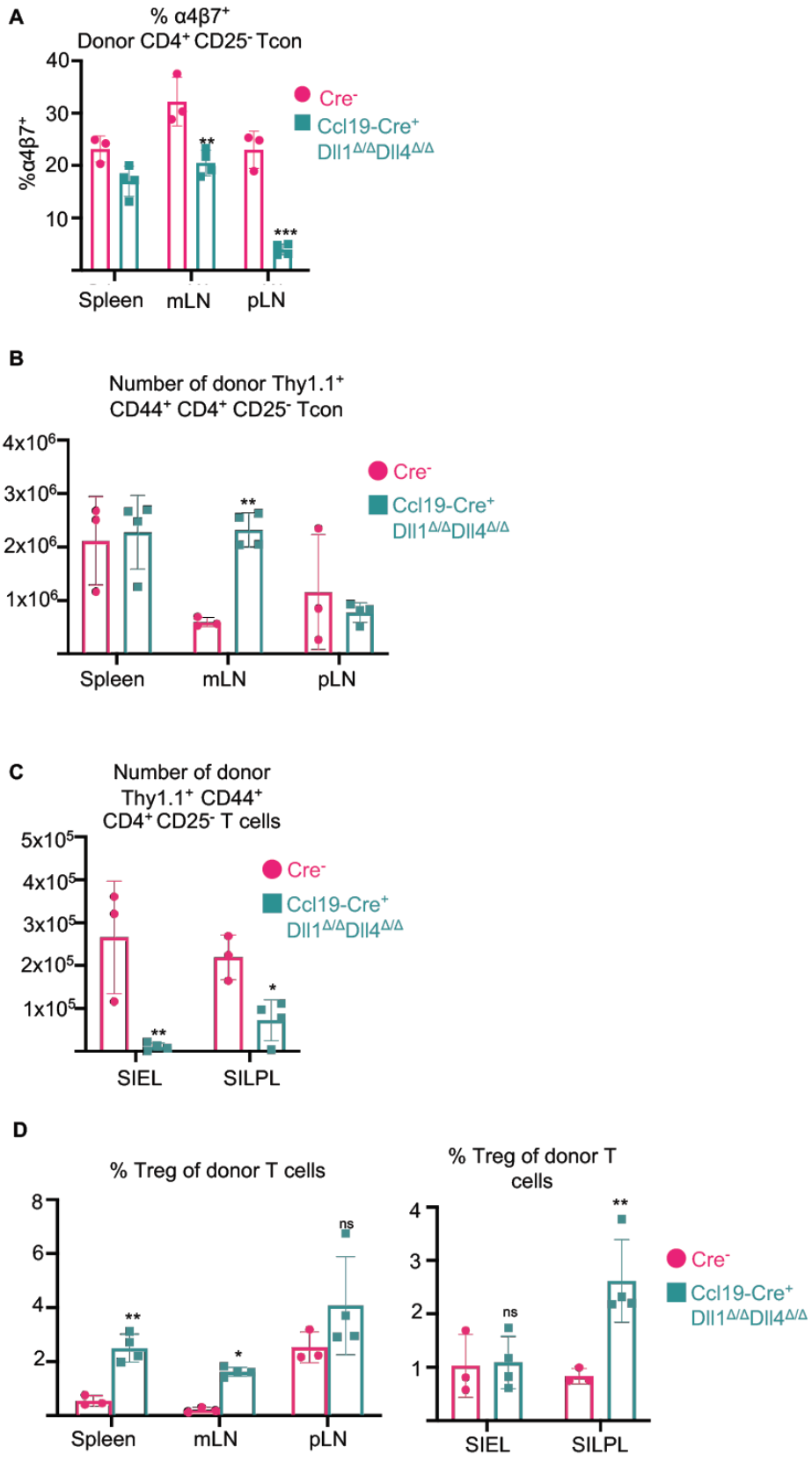

Fig 3.6. Delta-ligands from Ccl19-Cre lineage traced fibroblastic reticular cells are the critical source of Notch signals that drive alloreactive gut-homing program of CD4+ cells. Same experiment as Fig 3.5. (A) α4β7 expression in donor Thy1.1^{+} CD4^{+} CD25^{-} T con . Absolute number of donor CD4^{+} CD25^{-} T cells was quantified in secondary lymphoid organs (B) and small intestine (C). % CD25^{hi} CD4^{+} Tregs was quantified as a % of total donor T cells. n= at least 3 mice per group. *p<0.05, **p<0.01, ***p<0.001, one-way ANOVA with Tukey's post-hoc-tests. mLN = mesenteric lymph node. pLN = pooled peripheral (cervical, axial, brachial, inguinal) lymph nodes. SIEL = small intestinal epithelial lymphocyte fraction. SILPL = small intestinal lamina propria lymphocyte

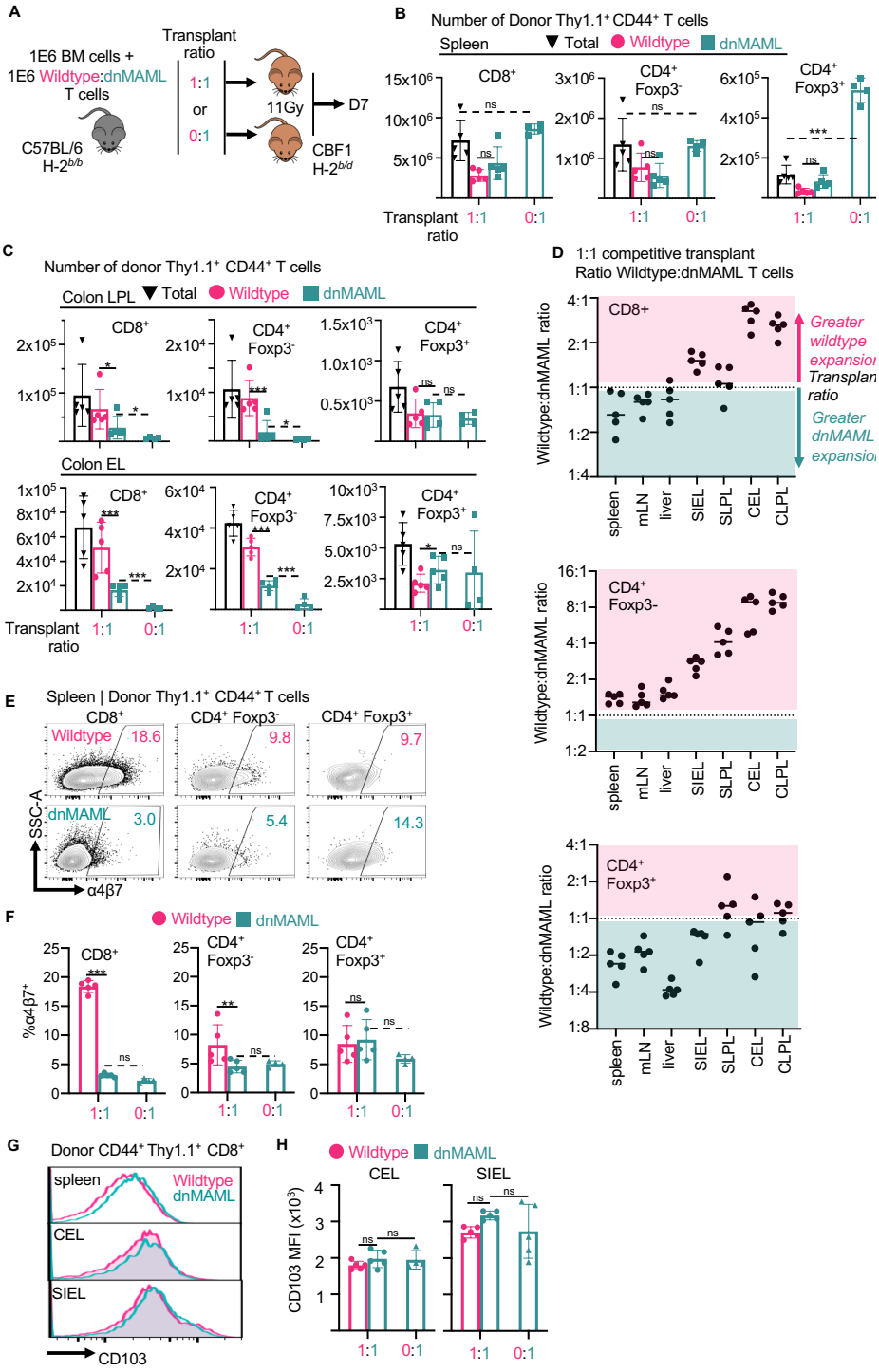

Fig 3.7 Notch drives gut-homing through cell-intrinsic and non-cell intrinsic mechanisms. Experimental Scheme. CBF1 recipients were transplanted with $1x10^6$ BM plus $1x10^6$ T cells at a ratio of 1:1 or a ratio of 0:1 wildtype:dnMAML. Donor T cell numbers in spleen (B) and colon lymphocyte fractions (C). Ratios of wildtype:dnMAML T cell subsets were calculated and plotted on a log2 axis with the initial 1:1 transplant ratio noted as a black dotted line (D). Flow cytometry plots of α4β7 expression in donor T cell subsets isolated from spleen (E) summarized in (F). Flow cytometric expression of CD103 in spleen and intestinal epithelium (G), summarized in (H). n= at least 4 mice per group. *p<0.05, **p<0.01, ***p<0.001, one-way ANOVA with Tukey's post-hoc-tests. mLN = mesenteric lymph node SIEL = small intestinal epithelial lymphocyte fraction. SILPL = small intestinal lamina propria lymphocyte fraction. CEL = colon epithelial lymphocyte fraction. CLPL = colon lamina propria lymphocyte fraction.

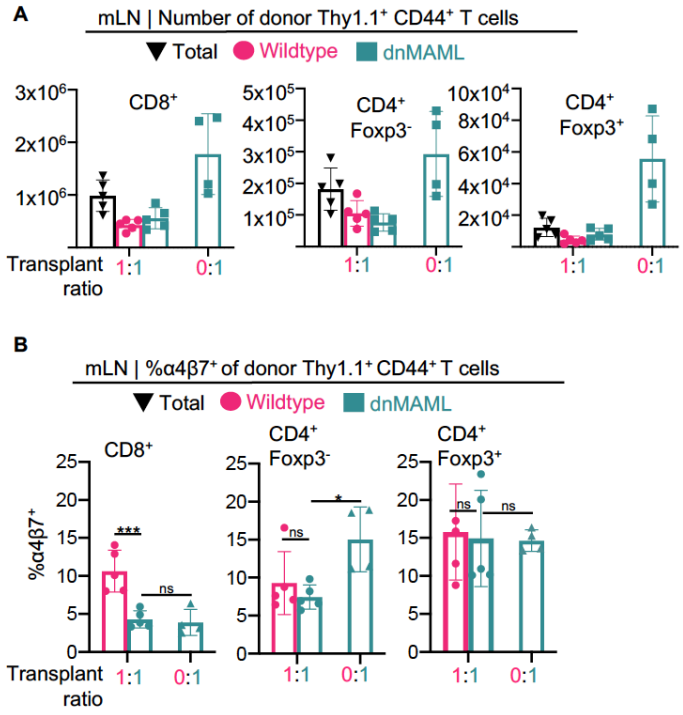

Fig 3.8 Notch drives T cell α4β7 expression cell-intrinsically in mLN. Same experiment as Fig 3.7. Absolute number of donor T cell subsets (A). Summarized α4β7 expression in T cell subsets (B). n=3 mice per group. *p<0.05, **p<0.01, ***p<0.001, one-way ANOVA with Tukey's post-hoc-tests. mLN = mesenteric lymph node.

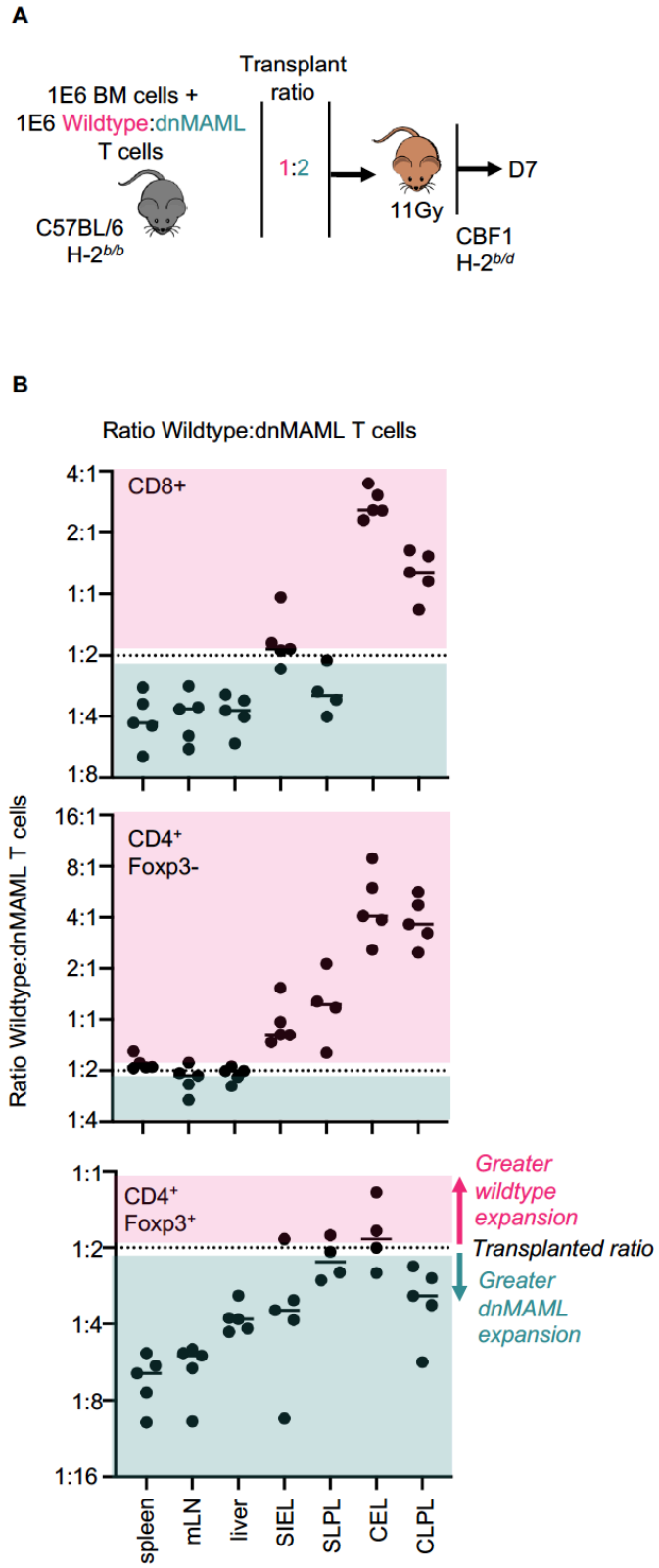

Fig 3.9 Notch drives cell-intrinsic effects on gut-homing (A) Experimental Scheme. CBF1 recipients as in Fig 3.7 but with a 1:2 wildtype:dnMAML ratio. Ratios of wildtype:dnMAML T cell subsets were calculated and plotted on log2 axis with the initial 1:2 transplant ratio noted as a dotted line (B). mLN = mesenteric lymph node SIEL = small intestinal epithelial lymphocyte fraction. SILPL = small intestinal lamina propria lymphocyte fraction. CEL = colon epithelial lymphocyte fraction. CLPL = colon lamina propria lymphocyte fraction.

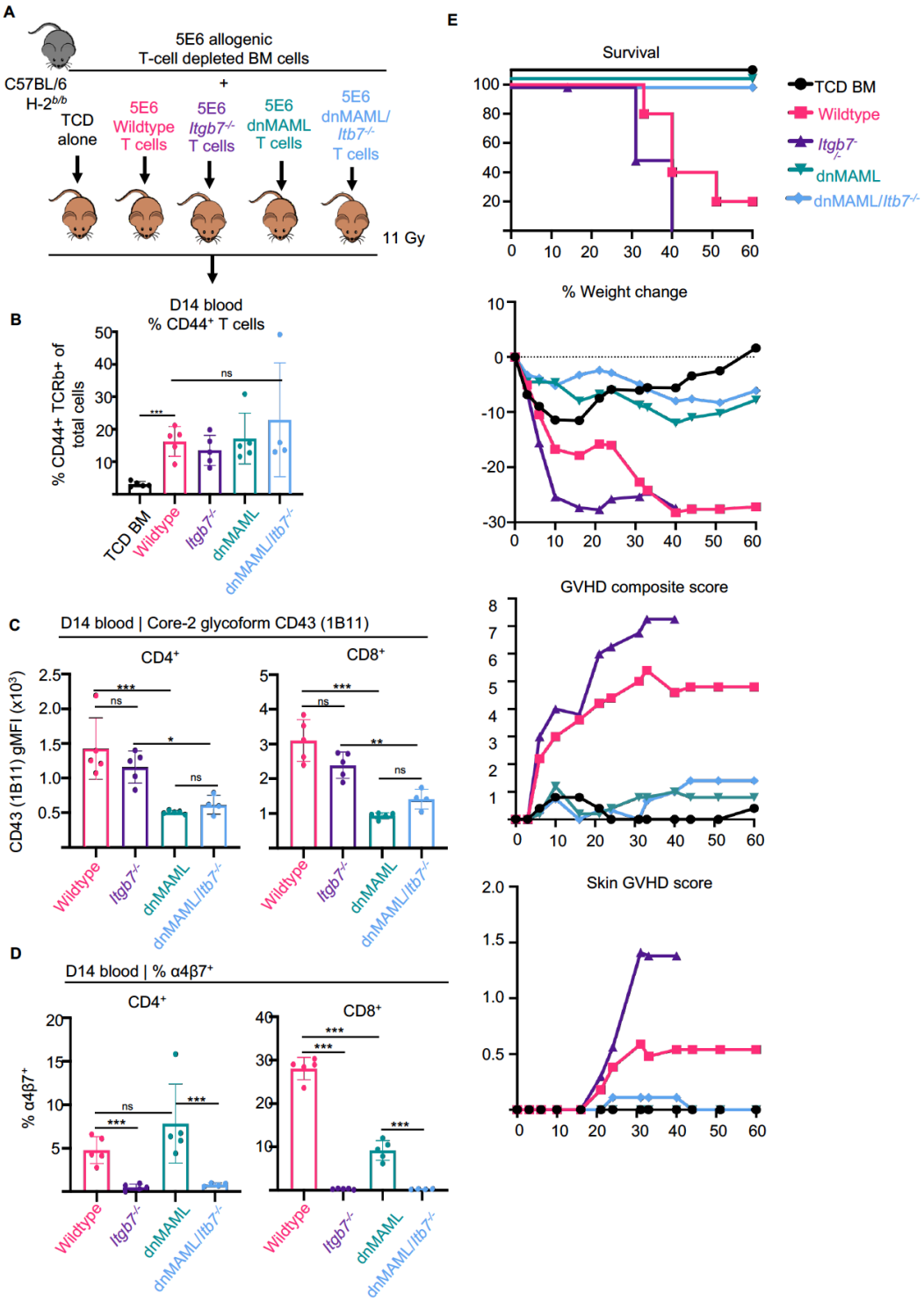

Figure 3.10. Notch loss of function selective regulates α4β7 in donor T cells and is protects mice more from GVHD compared to global *Itgb7* loss. (A) Experimental scheme. Recipient CBF1 mice were transplanted with $5x10^6$ BM cells plus $5x10^6$ T cells from indicated donors. Peripheral blood was analyzed at d14 post-transplant for % of alloactivated donor $CD44^+$ T cells (B). 1B11 (C) and α4β7 (D) expression was analyzed by flow cytometry. (E) Clinical GVHD was monitored throughout the course of allo-BMT. n=5 mice per group. *p<0.05, **p<0.01, ***p<0.001, one-way ANOVA with Tukey's post-hoc-tests.

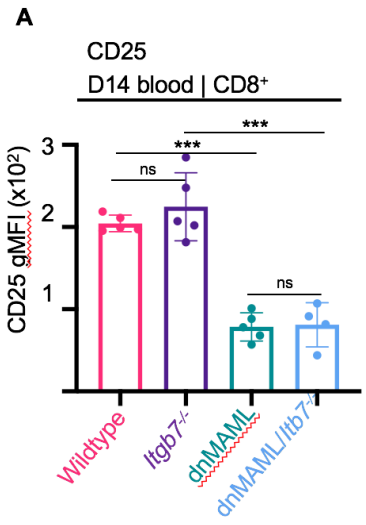

Fig 3.11. CD25 expression related to Fig 3.10.
CD25 expression in $CD44^+$ $CD8^+$ cells ***p<0.001, one-way ANOVA with Tukey's post-hoc-tests.

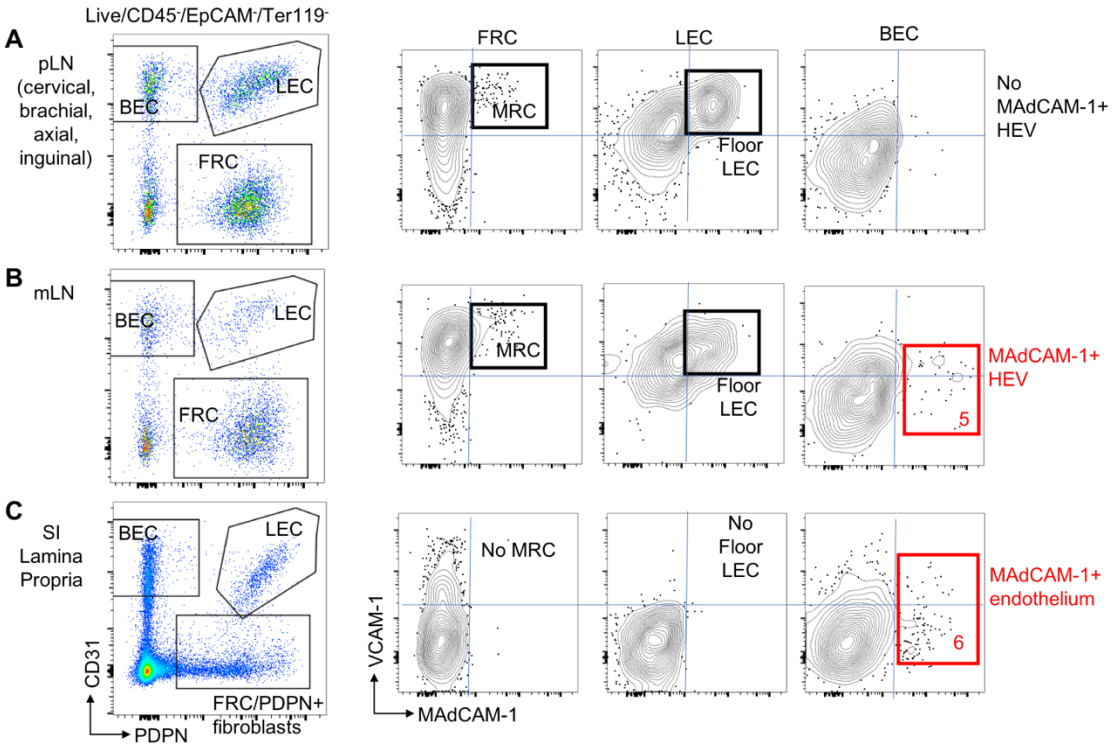

Fig 3.12. Expression of integrin ligands in secondary lymphoid organ and gut lamina propria stromal cells.
Pooled peripheral lymph nodes (cervical, brachial, axial, inguinal pLN), mesenteric lymph nodes (mLN), and small intestine lamina propria were digested with collagenase and non-epithelial non-hematopoietic $CD45^-EpCAM^-$ $Ter119^-$ stromal fractions were examine by flow cytometry. VCAM-1 and MAdCAM-1 expression was determined by flow cytometry. BEC = blood endothelial cells, LEC = lymphatic endothelial cells, FRC = fibroblastic reticular cells MRC = marginal reticular cells, HEV = high endothelial venule endothelial cells.

Chapter 4

Fibroblastic Reticular Cells Control T Cell Immunity through Dynamic Regulation of Delta-like Notch Ligands Independently of Antigen Presentation

4.1 Abstract

Graft-versus-host disease (GVHD) is the limiting immune complication of allogeneic bone marrow transplantation (allo-BMT). Fibroblastic reticular cells (FRCs) have recently been implicated as key initiators of GVHD pathogenesis through provision of Delta-like Notch ligands that drive lethal T cell alloreactivity. Here, we explore how the early allo-BMT environment shapes FRC biology. Allo-BMT rewired the transcriptome of FRC subsets to a pro-inflammatory state. This included the conversion of FRCs that previously expressed low levels of the Delta-like4 (DLL4) Notch ligand into FRCs that highly expressed DLL4, in addition to upregulation of DLL4 in subsets already expressing DLL4 at baseline. Conversion of $DLL4^{lo}$ FRCs to $DLL4^{hi}$ FRCs was driven by interaction with alloreactive T cells and was potentiated by the intensity of myeloablative conditioning. Furthermore, we show that FRCs upregulated MHC class II antigen presentation machinery after allo-BMT. Yet FRCs remained dispensable as a source of MHC class II alloantigen presentation in $CD4^+$ T cell-driven GVHD, suggesting that antigen and Notch ligands could be delivered by distinct cellular subsets during T cell activation. We confirmed this paradigm in a model of dendritic cell immunization where Notch ligands from FRCs but not DCs were

critical to drive the $CD8^+$ T cell effector response. Thus, we show that FRCs function as a critical third party in T cell:APC interactions that changes the outcome of the T cell response in allotransplantation and other immunological contexts.

4.2 Introduction

Graft-versus-host disease (GVHD) is a life-threatening complication of allogeneic bone marrow transplantation (allo-BMT) mediated by pathogenic donor T cells. Donor T cells encounter alloantigen presented by alloantigen-presenting cells (APCs), leading to activation, acquisition of effector function, and their ultimate role in driving pathology in GVHD target organs. There remains an ongoing debate about the nature of the critical APC subsets during GVHD **(**see **Chapter 1, section 1.6).** Several reports revealed that MHC class II alloantigen presentation by non-hematopoietic recipient tissues are critical to drive $CD4^+$ T cell mediated GVHD (66, 67, 82). A follow-up study in one model of allo-BMT showed that intestinal epithelial cells were the critical source of MHC class II alloantigen presentation (90). However, recipients lacking MHC class II in intestinal epithelial cells still developed severe skin GVHD and showed alloantigen-dependent expansion of donor T cells in secondary lymphoid organs, suggesting that other non-hematopoietic APCs might be important.

Our group recently identified fibroblastic reticular cells (FRCs) in secondary lymphoid organs as the critical source of Delta-like Notch ligands driving lethal T cell alloimmunity in multiple models of allo-BMT (25, 26). Notch signaling is a juxtracrine signaling pathway originally described as being critical for T cell development that emerged as a critical regulator of mature T cell function in multiple contexts (44). Cell-to-cell contact allows Notch receptor (Notch1-4) interaction with

agonistic Delta-like or Jagged ligands. This interaction causes cleavage and release of the Notch intracellular domain, which then translocates to the nucleus to mediate transcriptional activation of Notch target genes. We and others showed that Notch signals are crucial to drive T cell pathogenicity in several models of allo-BMT and organ transplantation (25, 26, 28–31, 47, 48, 52). Importantly, essential Notch signals were received within the first 48h of allo-BMT, suggesting that they are delivered around the same time as alloantigen. Thus, because FRCs provide critical juxtracrine Notch signals to alloreactive T cells through cell-to-cell interactions, we hypothesized that FRCs might function as critical alloantigen-presenting cells after allo-BMT through dynamic regulation of Notch ligand expression and MHC class II alloantigen presentation.

Fibroblastic reticular cells (FRCs) are a heterogenous group of cells that encompass several related non-hematopoietic and non-endothelial mesenchymal cell subsets in lymphoid tissues. While FRCs do serve structural purposes, as other fibroblasts, they are also specialized in organizing and orchestrating innate and adaptive immune responses. Distinct FRC subsets express unique combinations of chemokines, cytokines, and other signaling molecules that differentially attract, retain, and regulate mature immune cells including naïve T and B cells (202). New genetic tools, including use of transgenic mice expressing a Cre recombinase under the control of *Ccl19* regulatory elements has allowed precise targeting of FRCs in vivo (6, 8).

FRCs have also been shown to present self-antigens to both $CD8^+$ T cells (24, 203) and $CD4^+$ T cells (98, 204) to drive tolerance and expand $Foxp3^+$ T regulatory cells. In fact, immune-mediated damage to FRCs in acute GVHD correlates with loss of peripheral tolerance mechanisms and development of chronic GVHD (102). FRCs are also known to capture exosomal peptide-loaded

MHC class II from dendritic cells and present it on their surface to drive tolerance in $CD4^+$ T cells (205). However, this tolerance-inducing presentation of self-antigens might be turned on its head when donor T cells recognize what was once self-antigen as foreign.

Furthermore, little is known about how FRCs and other lymph node stromal cell subsets (LNSCs) are regulated at the onset of allo-BMT. Allo-BMT causes massive changes in innate and adaptive immune stimuli. The combined effects of tissue damage, translocation of microbial products across a damaged gut epithelium, and alloreactive T cell-derived inflammatory cytokines likely regulates both antigen presentation and expression of Notch ligands in FRCs (206). Thus, in order to understand how allo-BMT regulates FRC immune function, antigen presentation, and the Notch pathway, we profiled the transcriptome of several defined FRC subsets both at baseline and after allo-BMT. We found large changes in the transcriptome of FRC subsets after allo-BMT, including upregulated expression of interferon-related genes, MHC class I and MHC class II antigen presentation machinery, and the Delta-like4 (DLL4) Notch ligand. We show that allo-BMT increases DLL4 expression in $CD157^{hi}$ FRC subsets that previously expressed DLL4. In addition, allo-BMT converted $CD157^{hi}$ FRCs expressing low levels of DLL4 into cells expressing high amounts of DLL4. We show that this increase in the number of $DLL4^{hi}$ FRC was mediated by signals from allogeneic T cells and peaked at 12h post allo-BMT. Increases in DLL4 expression occurred in settings of both MHC-mismatched and MHC-matched allo-BMT and depended on the intensity of myeloablative conditioning. While we did not yet identify the signal(s) from alloreactive T cells that drive(s) this upregulation, our findings suggest the existence of a critical cross-talk between alloreactive T cells and FRCs that mediates increased Notch signaling in a feed-forward loop.

Allo-BMT also caused increases in both the transcriptomic and surface expression of MHC class II alloantigen presentation likely mediated by increases in expression of the Class II trans-activator (*Ciita)*. FRCs traced by the Ccl19-Cre were critical sources of Notch ligand that drove lethality in a monoclonal model of $CD4^+$ T cell mediated GVHD. However, in this same model, FRCs were not a necessary source of alloantigen presentation. This suggested that antigen and Notch ligands can be delivered from separate cellular sources *in trans* during T cell activation. To further test this tripartite model of T cell activation in another immunological context, we monitored $CD8^+$ T cell responses to DC-immunization. In this model, antigen presentation is limited to the DC, and we could restrict the cellular source of Delta-ligands to FRCs, DCs, both, or neither. In this context, FRCs and not DCs were the critical source of Delta-ligands that drove Notch-dependent generation of short-lived effector cells. Together, this work provides evidence for a three-cell model of T cell activation that operates in both allo-BMT and DC immunization. Thus, T cells require direct interaction with an APC to receive antigen and with a FRC to contact Notch ligands.

4.3 Results

4.3.1 Allogeneic bone marrow transplantation drives transcription of an inflammatory gene signature including *Dll4* in $CD157^{hi}$ FRCs

Our laboratory showed that FRCs, lineage traced by the Ccl19-Cre transgene, were the critical source of Delta-like Notch ligands that drove lethal GVHD after allo-BMT (25, 26). The highest abundance of Delta-like4 after allo-BMT was restricted to a subset of FRCs marked by high expression of CD157 and $CD21^+$ follicular dendritic cells. However, little is known about how

lymph node stromal cell subsets (LNSCs), including FRCs, respond to allo-BMT. Thus, we used transcriptomic profiling to 1. Determine how allo-BMT regulates gene expression in LNSCs and 2. Understand if DLL4-expressing FRCs had a distinct transcriptional profile. To this end, we used a double-reporter system where all cells that have activated the Ccl19-Cre transgene are lineage traced by a Rosa26^{eYFP} reporter (6) combined with a BAC transgenic reporter encoding the regulatory regions of *Dll4* fused to a mCherry reporter (207). Using this system, we defined four LNSC populations of interest for transcriptomic profiling. These included lymphatic endothelial cells (LECs) and three populations of FRCs lineage-traced by Ccl19-Cre: CD157$^-$ *Dll4*-mCherry$^-$ double negative fibroblastic reticular cells (DNFRC), CD157$^+$ *Dll4*-mCherry$^-$ single positive (SPFRC), and CD157$^+$ *Dll4*-mCherry$^+$ double positive (DPFRC) **(Fig 4.1A)**. C57BL/6 mice with this double-reporter system either received an MHC-mismatched allo-BMT with 11 Gy conditioning and 20 x 10^6 BALB/c splenocytes + 5 x 10^6 BM cells or were left untreated. LNSC subsets from pooled peripheral lymph nodes (cervical, brachial, axial, inguinal) were then sort purified 12h after allo-BMT. In each case, no less than 1,400 cells were sorted per population. RNA was isolated, cDNA was synthesized with oligo(dT) priming, and libraries were created with indices for Ilumina sequencing. Reads were pseudoaligned to an index constructed from the mouse transcriptome plus transgene sequences of Eyfp and mCherry with the kallisto program. Expression was converted to a log2 scale, normalized across samples, and genes with a low expression (<1 TPM in >5 samples) were filtered out prior to subsequent analysis. Expression of the LEC marker *Lyve1* and the fibroblast marker *Pdgfrb* along with *Bst1* (the gene encoding CD157) confirmed the identity of our sorted populations **(Fig 4.1 B, top panels)**.[3] Expression of

[3] Gene-wise expression data can be accessed at https://ericperkey.shinyapps.io/LNSC_Allo/

Eyfp revealed high expression in Ccl19-Cre^{+} lineage traced FRCs with lower expression in LECs, as expected, as a minor population of LECs expresses the Ccl19-Cre transgene (25). *Dll4*-mCherry expression was high in LECs and DPFRC, but low in DNFRC and SPFRC at baseline. Interestingly, there were trends for increased abundance of *mCherry* transcripts with allo-BMT although these did not reach significance **(Fig 4.1 B, bottom panels)**. Principal component analysis revealed large differences between LECs and FRCs with fewer differences among FRC subsets when examining the 1st principal component by the 2nd principal component **(Fig 4.1 C, top panel)**. When examining the 3rd principal component by the 2nd principal component, three distinct clusters (DNFRC, LEC, and combined DPFRC + SPFRC) were visible. These clusters all changed in similar directions after allo-BMT (**Fig 4.1 C, bottom panel**, arrows). To ascertain global differences in gene expression due to allo-BMT, we used limma/voom to identify differentially expressed genes due to allo-BMT in all LNSC subsets. There was upregulation of a strong interferon-associated gene signature including *Stat1, Cxcl9, Cxcl10, and Ly6a*. *Dll4* transcripts were increased as well (text in blue) **(Fig 4.1 D)**.

To ascertain if we could identify any differences between Delta-like4 expressing and non-expressing FRCs, we then compared SPFRCs and DPFRCs at baseline. As expected, *mCherry* and *Dll4* transcripts were significantly enriched in the DPFRC fraction. Also enriched were several genes highly expressed in MAdCAM-1^{+} marginal reticular cells (MRCs) including *Cxcl13, Tnfsf11, Ramp1,* and *Enpp2* (9, 15), suggesting that MRCs may be over-represented in the *Dll4*-mCherry^{+} FRC fraction **(Fig 4.1 E)**. Enrichment of *Cr2* transcripts in DPFRCs also suggested that follicular dendritic cells also are preferentially represented in the *Dll4*-mCherry^{+} FRC fraction. Conversely, SPFRCs were enriched for genes shown by others to be expressed preferentially

CCL19^{hi} T-zone FRCs including *Col14a1, Slc7a11, Stmn2*(9). We next examined the expression of Notch ligands in the LNSC populations. As expected, LECs had high levels and DNFRC low levels of *Dll4* transcripts, which were not changed by allo-BMT. On baseline, CD157^{+} *Dll4*-mCherry^{-} SPFRC also had low expression of *Dll4* compared to CD157^{+} *Dll4*-mCherry^{+} DPFRC **(Fig 4.1 F,** *cyan to purple comparison***)**. Allo-BMT drove upregulation of *Dll4* transcripts in CD157^{+} *Dll4*-mCherry^{+} DPFRC *(purple to magenta comparison)*. Unexpectedly, allo-BMT also caused significant upregulation of *Dll4* mRNA in CD157^{+} *Dll4*-mCherry^{-} SPFRC *(cyan to blue comparison)* so that they had similar levels to DPFRC *(blue to magneta comparison)*. This suggests that allo-BMT causes upregulated *Dll4* expression in FRCs that are already expressing *Dll4*, while also driving new expression of *Dll4* in FRCs that on baseline did not express it. It further suggests that regulation of *Dll4* mRNA occurs with faster kinetics than the abundance of mCherry protein. Allo-BMT did not regulate *Dll1* and *Jag2* expression and there were trends for decreased *Jag1* expression in all LNSC subsets, especially LECs. *Dll3* was not expressed in any subset.

Together, these data show that LNSCs dynamically respond to allo-BMT, leading to upregulated expression of many interferon and inflammation-associated genes. *Dll4*-mCherry positive FRCs are associated with a gene program seen in MRCs, suggesting that MRCs on baseline are enriched for *Dll4*. Allo-BMT leads to dramatic increases in *Dll4* expression in multiple CD157^{hi} FRC subsets. Significant upregulation of *Dll4* transcripts in FRCs still negative for *Dll4*-mCherry protein suggests a rapid increase in expression. It also raises the possibility that allo-BMT might convert FRC subsets that do not typically express DLL4 into cells expressing high amounts of

DLL4. This could increase the number of DLL4^{hi} FRC niches available to alloreactive T cell subsets, potentially driving Notch-dependent T cell pathology in GVHD.

4.3.2 Allogeneic but not syngeneic transplantation causes upregulation of Delta-like4 surface protein on CD157^{hi} FRCs, including both MAdCAM-1^{+} MRCs and MAdCAM-1^{-} subsets

Next, we sought to refine our observations by evaluating the abundance of cell surface DLL4 protein in distinct FRC subsets. To do this, we used a parent-to-F1 model of allo-BMT that requires Notch ligand expression in Ccl19-Cre^{+} FRCs to drive lethal T cell-mediated GVHD (26). We used a single flow cytometry panel to monitor DLL4 surface protein levels in distinct LNSC subsets as well as potential hematopoietic APCs **(Fig 4.2 A)**. Due to increases in non-specific staining with irradiation and allo-BMT, we calculated an adjusted geometric mean fluorescence intensity (gMFI) for Delta-like4 expression by subtracting the gMFI of an isotype control antibody for each replicate. Endothelial cells including blood endothelial cells (BECs, ii), MAdCAM-1^{-} LECs (iii), and especially MAdCAM-1^{+} (iv) subcapsular floor LECs expressed high levels of DLL4 on baseline (208), but without regulation after allo-BMT **(Fig 4.2 B**, top panel). CD21^{+} follicular dendritic cells expressed high levels of DLL4 (v) while there was minor but detectable DLL4 expression in CD157^{hi} FRCs (viii) and MRCs (ix) on baseline. Only CD157^{hi} FRCs and MRCs had significantly upregulation surface DLL4 at 12h post allo-BMT **(Fig 4.2 B**, middle panel). Hematopoietic cell subsets including B cells (x), CD11c^{hi}Class II^{int} resident dendritic cells (rDCs, xi), and CD11c^{int}MHCII^{hi} migratory DC (mDCs, xii) expressed low levels of DLL4 compared to LNSC subsets, but rDC and mDCs showed slight increases in DLL4 at 36h post allo-BMT **(Fig 4.2 B**, bottom panel).

To determine if the upregulation of DLL4 seen in CD157^{hi} fibroblasts (including both MAdCAM-1^{-} CD157^{hi} FRCs and MRCs) was due to damage caused by myeloablative conditioning, allotransplantation, or both, we transplanted CBF1 recipients as in Fig. 4.2A with syngeneic (CBF1), allogeneic (C57BL/6), or no cells. Significant upregulation of DLL4 was only seen when recipients were transplanted with allogeneic but not syngeneic cells in terms of both the percentage of FRCs that were positive for DLL4 (**Fig 4.2 C)** and their adjusted gMFI **(Fig 4.2 D)**. As above, this regulation remained restricted to the CD157^{hi} fibroblastic compartment.

These data suggest that specific CD157^{hi} subsets of FRCs dynamically upregulate surface DLL4 after allo-BMT. This regulation occurs in a defined time window peaking around 12h post allo-BMT, but decreasing by 36h post allo-BMT. DLL4 expression is lower and regulated with a different kinetics in hematopoietic cells. Furthermore, upregulation of DLL4 expression in CD157^{hi} fibroblasts only occurs with allogeneic transplantation, but not syngeneic transplantation or myeloablative conditioning alone.

4.3.3 Delta-like4 upregulation is controlled by signals from alloreactive T cells and myeloablative conditioning intensity potentiates this upregulation

In order to further understand the mechanisms of DLL4 upregulation in CD157^{hi} fibroblasts and identify the allograft cells involved, we examined expression of DLL4 in different allo-BMT models. First, we confirmed that the abundance of *Dll4* transcripts was increased by allogeneic but not syngeneic BMT by sorting CD157^{hi} fibroblasts and LECs at 12h post allo-BMT and assessing relative *Dll4* transcript levels by RT-qPCR **(Fig 4.3 A)**. CBF1 recipients were either transplanted

with allogeneic T cell-depleted bone marrow (TCD BM) alone, TCD BM + 20 x 10^6 splenocytes, or TCD BM + 5 x 10^6 purified T cells. Upregulated DLL4 expression was seen only when alloreactive splenocytes and T cells were transplanted. Furthermore, there was no significant difference between pure T cells versus bulk splenocytes, suggesting that alloreactive T cells were the main driver of DLL4 upregulation in FRCs **(Fig 4.3 B)**. Next, we wanted to understand if this regulation occurred in other models of allo-BMT and in recipients of different genetic backgrounds. Thus, we transplanted BALB/c (H-$2^{d/d}$) mice after 8 Gy irradiation with no cells, syngeneic cells (BALB/c), MHC-mismatched allogeneic cells (C57BL/6, H-$2^{b/b}$), or MHC-matched allogeneic cells (B10.D2, H-$2^{d/d}$). Both MHC-mismatched and MHC-matched allotransplantation, but not syngeneic transplantation, drove DLL4 upregulation in BALB/c CD157^{hi} fibroblasts **(Fig 4.3 C)**. While irradiation alone did not drive DLL4 upregulation **(Fig 4.2 C)**, we wanted to understand if the degree of myeloablative conditioning could affect DLL4 expression. We used the same parent-to-F1 model as in Fig 4.2. In this model, F1 recipients are tolerized to donor parental alloantigens, preventing rejection of donor cells without myeloablative conditioning. However, donor cells recognize the complementary parent's alloantigens as foreign and mediate a GVH reaction. We previously showed that such models still depend on Notch signals from Ccl19-Cre FRCs to drive lethal GVHD; however significantly more alloreactive T cells are required to drive lethality in these models (26, 28). We transplanted CBF1 recipients (or *Ccl19-Cre*$^+$ *Dll1*$^{f/f}$*Dll4*$^{f/f}$ as a control) with 20 x 10^6 C57BL/6 splenocytes + 5 x 10^6 BM with no conditioning, 3 Gy (300 rad), or 11 Gy (1100 rad). With no prior conditioning, we observed a slight trend for increased DLL4, but this did not reach statistical significance. However, with 3 Gy and 11 Gy conditioning, we observed dose-dependent increase in DLL4 expression **(Fig 4.3 D)**

Together, these data begin to unravel how DLL4 might be regulated in CD157^{hi} fibroblasts after allo-BMT. This upregulation depends on alloreactive T cells, independently of MHC mismatch. These data suggest that a very early factor released by alloantigen-activated T cells drives upregulation of DLL4 on FRCs. This signal is predicted to cooperate with the intensity of myeloablative conditioning, although how this cooperation occurs remains unknown.

4.3.4 Allogeneic transplantation drives upregulation of MHC class II antigen presentation machinery in FRCs

Multiple groups suggested that recipient nonhematopoietic cells rather than hematopoietic cells are the critical source of MHC class II-restricted alloantigen presentation that drives CD4$^+$ T cell mediated GVHD (66, 67, 82). The exact cell types involved are yet to be fully determined, although recent reports showed that intestinal epithelial cells can prime alloreactive CD4$^+$ T cells to initiate GI-GVHD (90). However, when MHC class II was deleted from intestinal epithelial cells in this model, alloreactive but not syngeneic T cells still expanded in secondary lymphoid organs and mice remained highly susceptible to skin GVHD. This suggests that there may be other important non-hematopoietic APCs that induce GHVD. Because Ccl19-Cre lineage traced FRCs engage in early cell-to-cell contact with alloreactive T cells to deliver Notch ligands (25, 26), we hypothesized that they may also present alloantigens to T cells. First, we explored the regulation of MHC class II presentation machinery in LNSC subsets including FRCs after allo-BMT. We examined transcriptomic profiles for expression of MHC class II genes encoded in the H-2 locus and found that allo-BMT drove upregulated expression of most of the genes in both LECS and all three FRC subsets **(Fig 4.4 A)**. Increased expression of the Class II transactivator (*Ciita)* in all four

stromal subsets may explain this upregulation **(Fig 4.4 B)**. *Ciita* has been shown to control endogenous expression of MHC class II genes in FRCs and other stromal subsets through induction by an IFN-γ sensitive promoter (pIV) (205). To build on these mRNA findings, we examined surface MHC class II expression by flow cytometry. We transplanted CBF1 recipients as in Fig 4.2 and monitored MHC class II expression with an antibody reactive to both I-A and I-E. On baseline, there were low but detectable levels of MHC class II in $CD157^{hi}$ FRCs, LECs, and BECs (blue lines) which was significantly upregulated at 36h post allo-BMT (red lines). Still, this expression was minor compared to that of B cells or DCs **(Fig 4.4 C)**. Interestingly, surface expression was not detectably upregulated at 12h, the time point at which we observed most DLL4 upregulation. Instead upregulation was only seen by 36h and continued to 50h post allo-BMT **(Fig 4.4 D).** Together, these data show that after allo-BMT, LNSC subsets including $CD157^{hi}$ FRCs upregulate MHC class II, which nominates them as candidate alloantigen-presenting cells. However, this upregulation occurred late compared to DLL4.

4.3.5 $CD4^+$ TEa TCR transgenic cells require Delta-like Notch signals from Ccl19-Cre lineage traced FRCs to drive lethal GVHD

We established that FRCs express heightened MHC class II antigen presentation machinery after allo-BMT. We next needed to establish a model to test whether this machinery was relevant to prime alloreactive $CD4^+$ T cells. Another group used TEa TCR transgenic cells to test the role of recipient hematopoietic cells versus nonhematopoietic cells in alloantigen presentation. The TEa TCR recognizes an allopeptide from $I\text{-}E^d$ processed and presented on $I\text{-}A^b$. C57BL/6 mice express $I\text{-}A^{b/b}$ but are null for I-E. BALB/c mice express both $I\text{-}A^{d/d}$ and $I\text{-}E^{d/d}$. CBF1 offspring of a C57B6/LxBALB/c cross will be $I\text{-}A^{b/d}$ and $I\text{-}E^{d/null}$. This allows expression and presentation of the

TEa allopeptide loaded on I-A^b. Using this model, past data showed that TEa cells primarily rely on recipient non-hematopoietic antigen-presenting cells (66). To use this model, we first needed to establish that it depended on a Ccl19-Cre lineage traced FRC source of Delta-like Notch ligands to drive GVHD. Thus, we transplanted 5 x 10^4 purified Thy1.1$^+$ TEa-TCR Tg cells with 5 x 10^6 BM cells into *Ccl19-Cre*$^+$ *Dll1*$^{f/f}$ *Dll4*$^{f/f}$ or Cre- CBF1 littermate controls. A group of Cre- mice received anti-DLL1/4 antibodies at day 0 and day 3 post allo-BMT while the other groups received control antibodies **(Fig 4.5 A)**. At day 7 post allo-BMT, expression of the core-2 O-glycoform of CD43 (1B11), previously shown to be sensitive indicator of Notch signaling (**Chapter 2**, (26)) was monitored in spleen (spl), mesenteric lymph node (mLN), and peripheral lymph nodes (pLN). Both anti-DLL1/4 and loss of the Delta-like ligands in Ccl19-Cre lineage traced cells blunted 1B11 to similar extent in CFSE diluted Thy1.1$^+$ CD4$^+$ TEa cells **(Fig 4.5 B)**. Likewise, CD25 expression, also regulated by Notch signaling in alloreactive T cells (47), was similarly decreased in the anti-DLL1/4-treated and *Ccl19-Cre*$^+$ *Dll1*$^{f/f}$ *Dll4*$^{f/f}$ recipients **(Fig 4.5 C)**. Next, we monitored GVHD lethality in a separate experiment. Mice with intact Notch signals succumbed to lethal GVHD, while anti-DLL1/4 antibodies were protective. Even better protected were *Ccl19-Cre*$^+$ *Dll1*$^{f/f}$*Dll4*$^{f/f}$ recipients, consistent with previous findings in polyclonal allo-BMT models (25). Together, these data establish that CD4$^+$ TEa cells require Notch ligands from Ccl19-Cre lineage traced FRCs to mediate lethal alloimmunity.

4.3.6 CD4$^+$ TEa TCR transgenic cells do not require alloantigen presentation from Ccl19-Cre$^+$ FRCs to drive lethal GVHD

After establishing that the TEa TCR Tg model of GVHD was dependent on a FRC source of Notch ligands, we asked if the same FRCs were the critical source of alloantigen in this model. Thus, we

generated CBF1 mice lacking the I-A^b MHC class II allele that presents allopeptide to TEa cells only in Ccl19-Cre lineage traced cells (**Fig 4.6 A**, Ccl19-Cre^+ I-$A^{b\Delta/d}$). We sought to retain other MHC class II alleles (I-A^d, I-E^d) on Ccl19-Cre lineage traced cells as other groups have shown tolerogenic roles for MHC class II antigen-presentation from Ccl19-Cre cells (22, 98, 102) and thus a loss of all MHC class II from these cells might affect mice even before allo-BMT. We confirmed that our genetic deletion strategy worked by examining I-A^b and I-A^d expression separately in different cellular subsets. Cre^- littermate controls had expression of both I-A^b and I-A^d d7 post allo-BMT. However, Ccl19-Cre^+ I-$A^{b\Delta/d}$ mice had nearly eliminated surface expression of I-A^b but preserved I-A^d expression (**Fig 4.6 B**). This selective loss of I-A^b occurred predominantly in $CD157^{hi}$ FRCs and to a lesser extent in LECs, a small fraction of which are traced by Ccl19-Cre (**Fig 4.6 C**). To test if expression of I-A^b by Ccl19-Cre^+ cells drives GVHD, we transplanted Ccl19-Cre^+ I-$A^{b\Delta/d}$ or littermate controls with TEa cells as in Fig 4.5. As a negative control, we also transplanted BALB/c mice (conditioned with 8 Gy), where only donor but not recipient antigen presentation can occur because they do not express I-A^b. Eliminating MHC class II alloantigen presentation from FRCs had no effect on overall survival, weight loss, or clinical GVHD scores (**Fig 4.6 D**). However, BALB/c mice still eventually succumbed to lethal GVHD suggesting that donor antigen presentation can mediate much of the lethality in this model. To determine if there were any subclinical effects on donor T cells themselves, we examined activation (CD44) and Notch surrogate (CD25, 1B11) read-outs in mice euthanized at day 6 post-transplant and found no differences (**Fig 4.6 E**).

These findings suggested that T cells that directly contact FRCs and receive all their Notch inputs from FRCs instead receive alloantigen stimulation from a separate cellular source. This finding

competes with a prevailing model suggesting that Notch ligands are delivered to T cells at the immune synapse with APCs (43, 49, 128, 209). To test if TEa cells could receive Notch ligands and antigen from distinct cellular sources, we turned to an in vitro system where we can provide Notch signals from an OP9 cell line (26). TEa cells were plated in vitro with bone marrow-derived DCs (BMDCs) isolated from poly(I:C)-induced *Mx-Cre*$^{+}$ *Dll1*$^{\Delta/\Delta}$*Dll4*$^{\Delta/\Delta}$ CBF1 mice, eliminating the possibility that TEa cells could receive Notch ligands from their source of alloantigen. Only activated TEa cells plated on OP9 stroma expressing DLL4 (OP9-DL4) and not control stroma (OP9-C) had higher ratios of the core-2 O-glycoform of CD43 (1B11) to total CD43 (S11), a measure that reflects Notch signaling. This increase in 1B11/S11 ratio was abrogated with anti-DLL4 treatment, indicating that it was dependent on Notch signaling (**Fig 4.6 F**). Together with our findings from Fig 4.5, this suggests that FRCs are dispensable sources of antigen presentation during GVHD while still being required as a source of Notch signals. This also demonstrates that T cells can receive separate juxtracrine signals, antigen and Notch ligands, from distinct cellular sources.

4.3.7 Notch ligands and antigen presentation derive from distinct cellular sources in CD8^{+} T cell responses to dendritic cell immunization

We were interested in further testing the hypothesis that Notch signals are derived from cellular sources distinct from antigen-presenting cells. To test this in a system where we could control the cellular source of antigen, we turned to a model of ovalbumin-specific CD8^{+} T cell response to BMDC immunization (DC-OVA). In this model, CD8^{+} T cell differentiation into KLRG1^{+}IL7R^{-} short-lived effector cells (SLECs) depends on Notch signals delivered by Delta-like ligands (26, 45, 46, 210) (**Chapter 2**). However, the generation of KLRG1^{-}IL7R^{-} early effector cells (EECs)

and KLRG1^{-}IL7R^{+} memory precursor cells (MPECs) remained intact in the absence of Notch signaling. One limitation of this model is that classical monocyte-derived BMDC matured with GM-CSF and IL-4 do not express high levels of Notch ligands (especially DLL4) even with lipopolysacchide (LPS) maturation (data not shown). However, FLT3L-matured DCs stimulated with LPS and resiquimod (R-848, TLR7/8 agonist) produced a mixture of DCs that express high levels of DLL4 (211). We used this FLT3L maturation protocol to produce DLL4^{hi} DCs from wild type or DLL4^{KO} DCs from *Mx-Cre*$^{+}$*Dll1*$^{\Delta/\Delta}$*Dll4*$^{\Delta/\Delta}$ C57BL/6 mice (after in vivo poly(I:C) treatment of both groups). After maturation and stimulation with LPS + R-848, BMDC cultures were purified through positive selection of CD11c^{+} cells and stained for cDC markers. Flow cytometry revealed a relatively pure population of CD11c^{+} Class II^{hi} cDC-like cells containing both CD24^{+} cDC1-like cells and SIRP1α^{+} cDC-2 like cells(212), both of which expressed high levels of DLL4 (**Fig 4.7 A**). We next tested if DLL4^{hi} DCs could provide a Notch stimulus in vitro. BALB/c DLL4^{hi} DCs were able to provide Notch signals to alloreactive eFluor 450 dilute C57BL/6 CD4^{+} T cells in an MLR. This was indicated by higher 1B11/S11 ratios in wild type but not dnMAML or N1$^{\Delta/\Delta}$N2$^{\Delta/\Delta}$ T cells when they were primed with DLL4^{hi} DCs versus DLL4^{KO} DCs (**Fig 4.7 B**). SIINFEKL-pulsed C57BL/6 DLL4^{hi} DCs compared to DLL4^{KO} DCs also drove higher 1B11/S11 ratios in CFSE dilute CD8^{+} OT-I cells, but not when Notch signals were blocked with anti-Notch1/2 antibodies (**Fig 4.7 C**).

We established that FLT3L DLL4^{hi} DC can provide both Notch stimulus and antigen in vitro. We next wanted to test their contribution to providing Notch ligands in vivo compared to FRCs. After pulsing DLL4^{hi} DC (red, '+') or *Mx-Cre*$^{+}$*Dll1*$^{\Delta/\Delta}$*Dll4*$^{\Delta/\Delta}$ *Dll4*^{KO} DC (blue, 'ko') with SIINFEKL we transferred 1 x 10^{5} DCs into *Ccl19-Cre*$^{+}$*Dll1*$^{\Delta/\Delta}$*Dll4*$^{\Delta/\Delta}$ ('ko') or *Cre*- (wild type, '+') littermate

controls. As a negative control for pan-T cell loss of Notch signaling, we also immunized CD4-Cre$^+$ dnMAML recipients **(Fig 4.8 A)**. SIINFEKL-specific responses were monitored by K^b-Ova staining at day 10 post immunization. There were no trends for reduced frequency of Ova-specific CD44$^+$ cells among all CD8$^+$ T cells with Notch blockade (**Fig 4.8 B**). In fact, loss of Notch ligands in FRCs (*Ccl19-Cre$^+$ Dll1$^{\Delta/\Delta}$Dll4$^{\Delta/\Delta}$*) or loss of the ability to receive Notch signals in T cells (*CD4-Cre$^+$ dnMAML*) caused a trend for increased frequency of antigen-specific cells, as previously reported (26, 45) (**Chapter 2)**. To assess Notch signals received by Ova-specific CD8$^+$ T cells, we assessed expression of the core-2 O-glycoform of CD43 (1B11), which we showed to be a sensitive indicator of Notch signaling (26). While deletion of Delta-ligands in DCs reduced 1B11 expression in Ova-specific CD8$^+$ T cells (**Fig 4.8 C,** red vs. blue filled histograms), greater effects were seen when deleting Delta-like ligands only in FRCs (**Fig 4.8 C**, red filled vs. red open histograms). This suggests that antigen-presenting DCs can provide Notch signals but cannot compensate for loss of Delta-like Notch inputs from FRCs. We next assessed differentiation into KLRG1$^+$IL7R$^-$ SLECs among antigen-specific CD8$^+$ T cells. In recipients whose FRCs expressed Delta-like ligands, ~30% of antigen-specific cells were SLECs irrespectively of priming by DLL4^{hi} or DLL4^{KO} DCs (**Fig 4.8 E**, top flow panels). However, if FRC were deficient for Delta-like ligands, SLECs were significantly reduced (~10% of antigen-specific cells), irrespective of their priming with DLL4^{hi} or DLL4^{KO} DCs (**Fig 4.8 E**, bottom flow panels). SLECs were further decreased in dnMAML recipients down to ~3%, suggesting other minor sources of Notch signals available to T cells neither derived from APCs or FRCs Delta-like ligands **(Fig 4.8 E**, right flow panel). Finally, to confirm that this effect was not due to differences in naïve T cell repertoire between our transgenic recipients, we pre-transferred 5 x 10^4 CD8$^+$ CD45.1$^+$ OT-I TCR transgenic cells into *Ccl19-Cre$^+$ Dll1$^{\Delta/\Delta}$Dll4$^{\Delta/\Delta}$* or Cre$^-$ littermate controls the day before BMDC immunization. We then assessed

$CD8^+$ $CD45.1^+$ $CD44^+$ OT-I cells at day 7 post immunization and confirmed that loss of Delta-like ligands on FRCs prevented SLEC differentiation **(Fig 4.8 G)** and diminished 1B11 expression **(Fig 4.8 H)**.

These experiments show that even in the context of antigen-presenting dendritic cells that have the capacity to provide Delta-like ligands in vitro, FRC niches remained the dominant source of Delta-like Notch signals that controlled $CD8^+$ T cells response *in vivo*. Viewed in context with our allo-BMT data, this suggests that T cells engage in tripartite interactions with both APCs and FRCs during early stages of in vivo priming. Cross-talk between FRCs and antigen-activated T cells drives DLL4 expression in FRCs, which may in turn drive further Notch signaling in T cells via a feed-forward loop.

4.4 Discussion

FRCs are critical initiators of T cell alloreactivity and GVHD lethality through the provision of Delta-like Notch ligands. Understanding their regulation and function during the initiation of GVHD is critical to develop new strategies to target them therapeutically. Furthermore, many of the rules that govern FRCs and Notch signaling during allo-BMT may apply to other immune contexts. Here, we explored how allo-BMT shaped FRC biology. We revealed that allo-BMT dramatically changes the transcriptional landscape of distinct FRC subsets. These changes included upregulation of inflammatory pathways including antigen presentation and the Notch ligand *Dll4*. FRC subsets that were previously expressed low amounts of *Dll4* rapidly expressed high amounts of *Dll4* within 12h of allo-BMT. This increase in percentage of $DLL4^{hi}$ FRCs depended on cross-talk with alloreactive T cells and was potentiated by the intensity of

myeloablative conditioning. Furthermore, allo-BMT increased FRC expression of the MHC class II antigen presentation machinery. However, while FRCs remained critical to drive T cell pathogenicity through Notch, they were dispensable as sources of alloantigen. This suggested that pathogenic T cell priming requires physical interaction of an alloreactive T cell with both an APC and a DLL4^{hi} FRC. We then tested this hypothesis in a DC immunization model. This allowed us to restrict antigen presentation to a known APC subset. We found that FRCs also provided the key source of Delta-like ligands that drove early effector response. Together, this highlights the primacy of the FRC niches in regulating T cell immune responses through the Notch pathway.

In this study, we ruled out the necessity of cell-intrinsic MHC class II antigen presentation by FRCs in order to drive GHVD. Instead, other cellular subsets may be sufficient to prime alloreactive T cells. Others have shown that intestinal epithelial cells directly prime alloreactive CD4^{+} T cells through MHC Class II (90). Yet, other nonhematopoietic cellular subsets could prime alloreactive T cells as well. For example, we showed that both blood and lymphatic endothelial cells upregulated MHC class II expression to a similar degree as FRCs. In the context of allo-BMT, expression and presentation of alloantigens may be broad enough to create redundancy in APC subsets, as others have shown with hematopoietic APCs in GVHD (76). However, an interesting possibility still exists that recipient FRCs can capture exosomal MHC class II from residual dendritic cells. In fact, this is the dominant form of MHC class II that exists on the surface of FRCs prior to transplantation (205). Ccl19-Cre mediated genetic excision of I-A^{b} would not rule out the possibility that FRCs pick up and express non-cell intrinsic exosomal derived MHC class II on their surface. To test this hypothesis, we are planning more refined imaging studies to

evaluate if T cells engage in immune synapses with FRCs displaying exosomally derived MHC class II.

If FRCs do not present alloantigens, then critical Notch signals can be delivered *in trans* to APCs from a distinct cellular subset. This challenges the current model of Notch signaling in mature T cells. Many other groups have suggested, although not often proven with genetic loss-of-function, that hematopoietic professional antigen-presenting cells (APCs) such as dendritic cells (DCs) are the critical cellular source of Notch signals to T cells (43, 49, 121, 128, 213). In fact, imaging studies suggested that Notch receptors and ligands interact between T cell:DC conjugates at the immune synapse (209). Yet, even when we immunized mice with DCs expressing high amounts of DLL4, they could not compensate for the loss of Notch ligand on FRCs. Why might FRCs be dominant sources of Notch ligands, when they likely do not form immune synapses with T cells? Antigen and costimulatory signals are most efficiently delivered *in cis* at the immune synapse. Only when the levels of costimulatory ligands are very high can bystander cells trigger costimulation *in trans* to APCs (214). The co-dependency of antigen and costimulatory signals at the immune synapse depends on colocalization and sharing of critical signal amplifying machinery, such as Lck, between the two pathways (215). However, canonical Notch signaling does not require participation in such amplification pathways and may be delivered to the nucleus just as well even if triggered outside of the immune synapse.

The dependency on FRC-derived Notch ligand may also be temporal. TCR signaling itself has been shown to trigger the Notch pathway (159, 216), thus APC provision of Notch ligands may be redundant with its provision of antigen. FRC provision of Notch ligands, however, may serve a

critical role just prior to T cell:APC encounter or after T cell:APC encounter has stopped. We have also shown that naïve $CD4^+$ T cells experience FRC-derived Notch signals **(Chapter 5),** suggesting that the former is possible. Less is known about the provision of Notch signals to activated T cells after DC interaction has ceased. Could ligand-dependent Notch signals be important only once initial TCR-induced Notch signals have ended? We are planning intravital imaging studies to track FRC-DC-T cell interactions at different timepoints after T cell activation to understand if T cells engage in close interactions with FRC even after DC interaction has ended.

We found that T cell alloactivation was required to drive DLL4 upregulation among FRCs. This indicates that antigen activation temporally precedes the peak delivery of Notch signals by T cells. Together, this suggests a model in which recently antigen-activated T cells shape their own $DLL4^{hi}$ FRC niche to control their further differentiate. This may coincide with the recruitment of recently activated but not yet divided $CXCR3^+$ T cells (217) by CXCL9 and CXL10, which are upregulated in FRCs during allo-BMT. The size of this niche and the level of Delta-like4 expression would control the magnitude of Notch-dependent T cell differentiation. We are currently exploring what T cell activation-associated signals might regulate DLL4 expression in FRCs to test this hypothesis further.

What other signals might FRCs provide to alloreactive T cells besides Notch signaling? We are still investigating other key immunomodulatory molecules upregulated during allo-BMT by FRCs. Interestingly, one of the genes with the greatest differential expression between baseline FRCs and allo-BMT FRCs is *Il15ra*. IL-15 signals are delivered through cell-to-cell contact requiring expression of *Il15ra* on the signal-sending cell. In allo-BMT, IL-15 signaling has been shown to

regulate $CD8^+$ T cell-mediated graft-versus-leukemia effects (218, 219). FRCs have been shown to be critical controllers of the IL-15 availability for ILC1s in the gut (220). Thus, FRCs might also regulate critical IL-15 signals that in turn differentially regulate pathogenic versus anti-leukemic T cell activity.

Altogether, our study reveals that distinct FRC subsets are differentially regulated by the allo-BMT environment, which in turn regulates T cell alloimmunity. We propose that alloreactive T cells drive the creation of their own pathogenic niche, dynamically upregulating DLL4 in FRCs through early activation-associated signals. These Delta-like4 Notch signals, in turn, program T cell pathogenicity in a feed-forward loop. We are actively exploring if upregulated expression of DLL4 on FRCs exists in other immunological contexts including immunization and acute infection. Interestingly, one study indicated that DLL4 is upregulated transcriptionally in FRCs post challenge with house dust mites (53). While we have previously shown that hematopoietic cells are dispensable sources of Notch ligands to drive T cell alloreactivity, we now show that FRCs are dispensable sources of alloantigen presentation. This is consistent with a model of T cell activation regulated by distinct cellular partners including DCs and FRCs. We believe that this model may not only be applicable to T cell alloreactivity, but also more broadly relevant to understand how FRCs govern T cell activation in other immune responses.

4.5 Figures

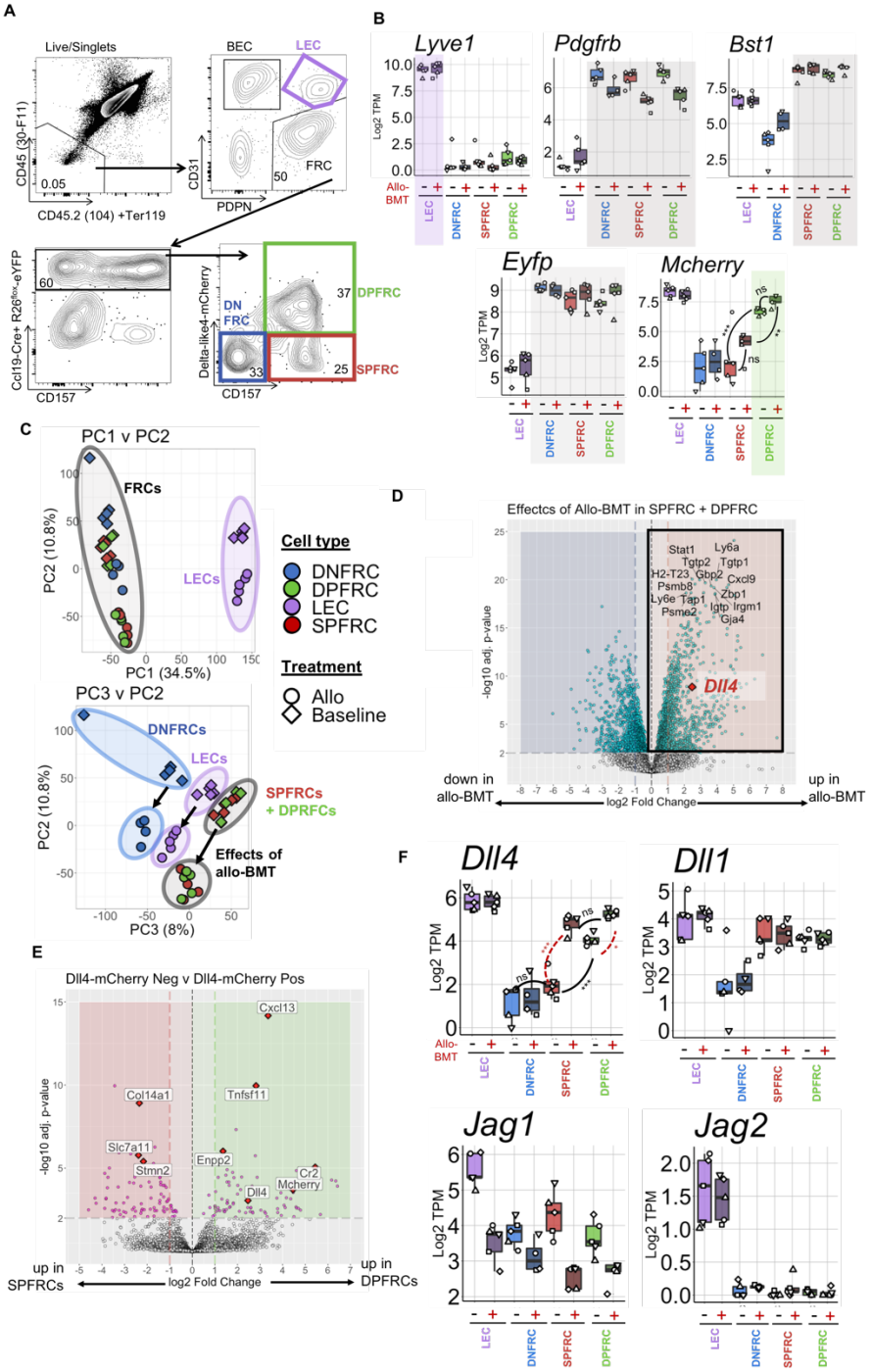

Fig 4.1. Allogeneic-BMT drives transcriptomic changes in lymph node stromal cell subsets including upregulation of Delta-like4 in CD157^{hi} fibroblastic reticular cells. C57BL/6 mice with Ccl19-Cre^{+} Rosa26^{eYFP} and *Dll4*-mCherry reporters were either transplanted with 20x10^{6} BALB/c splenocytes + 5x10^{6} BM cells after 11 Gy conditioning (allo-BMT) or not irradiated and not transplanted (baseline). Peripheral lymph nodes (cervical, brachial, axial, inguinal) were harvested 12h post allo-BMT or at baseline and different stromal cell subsets were isolated by FACS for transcriptomic analysis. (A) Flow cytometric gating of lymph node stromal cell subsets for analysis including lymphatic endothelial cells (LECs), *(Figure legend continued on next page)*

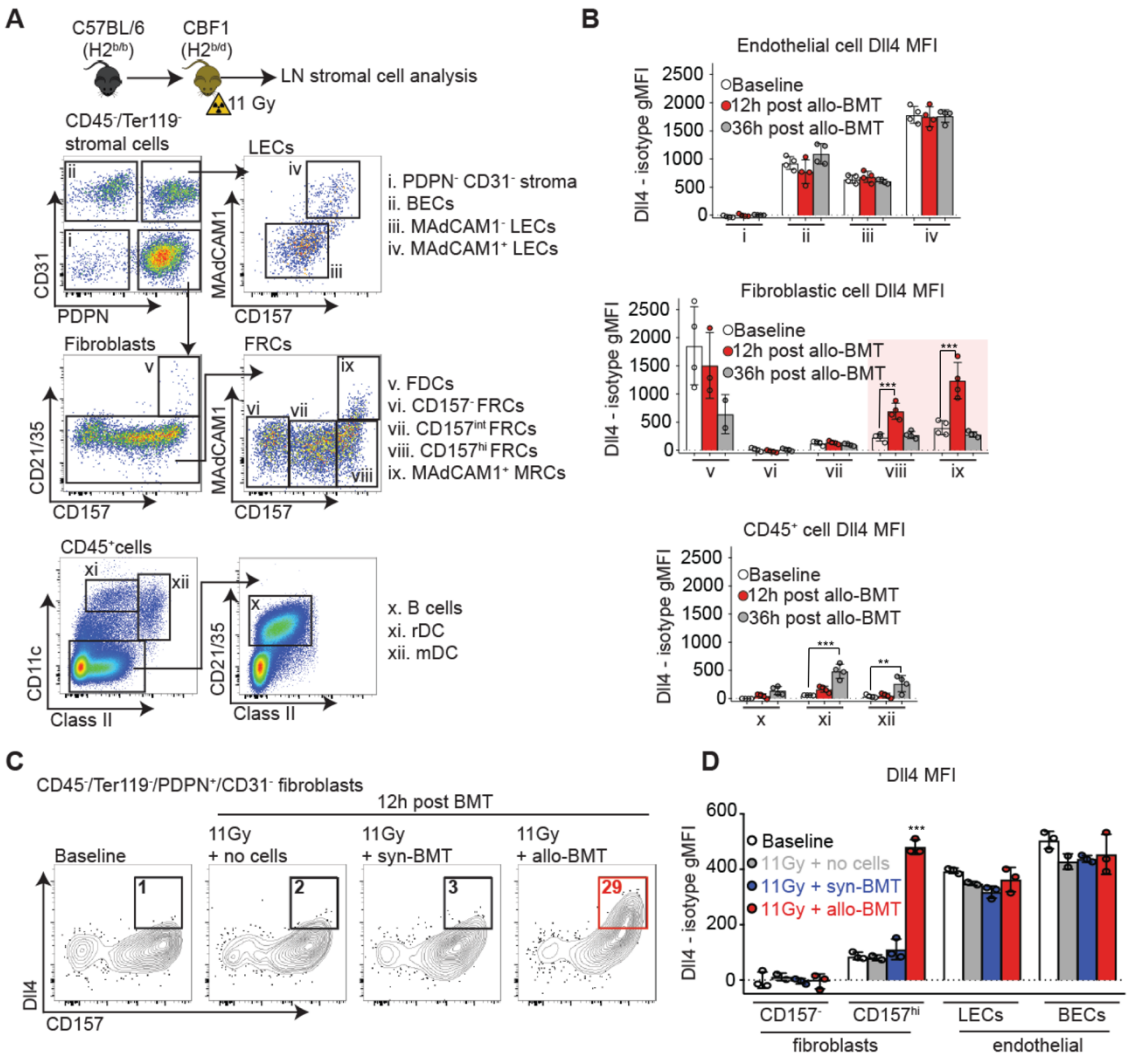

Fig 4.2 Allogeneic transplantation causes DLL4 upregulation in specific CD157^{hi} subsets of fibroblastic reticular cells. (A-B) CBF1 recipients were transplanted with 20x10^6 C57BL/6 splenocytes plus 5x10^6 BM cells after 11 Gy conditioning. pLN stromal and hematopoietic cell subsets were gated in the same panel (A) and assessed for DLL4 or isotype control staining summarized in (B). n=4 per group, representative of three independent experiments. (C-D) CBF1 recipients were irradiated with 11 Gy and transplanted with either syngeneic (CBF1, H-2$^{B/D}$) syn-BMT) or allogeneic (C57BL/6, H-2$^{B/B}$, allo-BMT) cells and assessed by flow cytometry at 12h post transplant as in (A). Representative plots of DLL4 staining in PDPN$^+$ CD31$^-$ fibroblasts with adjusted DLL4 MFI summarized in (D). n=3 per group, representative of two independent experiments. LECs = lymphatic endothleial cells. FRCs = fibroblastic reticular cells. MRCs = marginal reticular cells. rDC = CD11c^{hi}Class II^{int} resident dendritic cells. mDC = CD11c^{int}ClassII^{hi} migratory DCs. pLN = pooled peripheral lymph nodes (cervical, axial, brachial, inguinal).

(Fig 4.1 legend continued from previous page) CD157$^-$*Dll4*-mCherry$^-$ double negative fibroblastic reticular cells (DNFRC), CD157$^+$*Dll4*-mCherry$^-$ single positive (SPFRC), and CD157$^+$*Dll4*-mCherry$^+$ double positive (DPFRC). (B) Gene expression of stromal subset markers and transgenes as log2 transcripts-per-million (log2TPM). (C) Principal component clustering analysis of cell subsets shown by PC1 v PC2 (top) and PC3 v PC2 (bottom). (D) Volcano plots showing the global transcriptomic effects of allo-BMT v. baseline in pooled, indicating *Dll4* as a differentially expressed gene in blue. (E) Volcano plot showing global transcriptomic differences between *Dll4*-mCherry$^-$ SPFRC and mCherry$^+$ DPFRC, *Dll4* is noted in blue. (F) Expression of Notch ligands, of note *Dll3* was not detected. *p<0.05, **p<0.01, ***p<0.001 by empirical Bayes method in limma/voom.

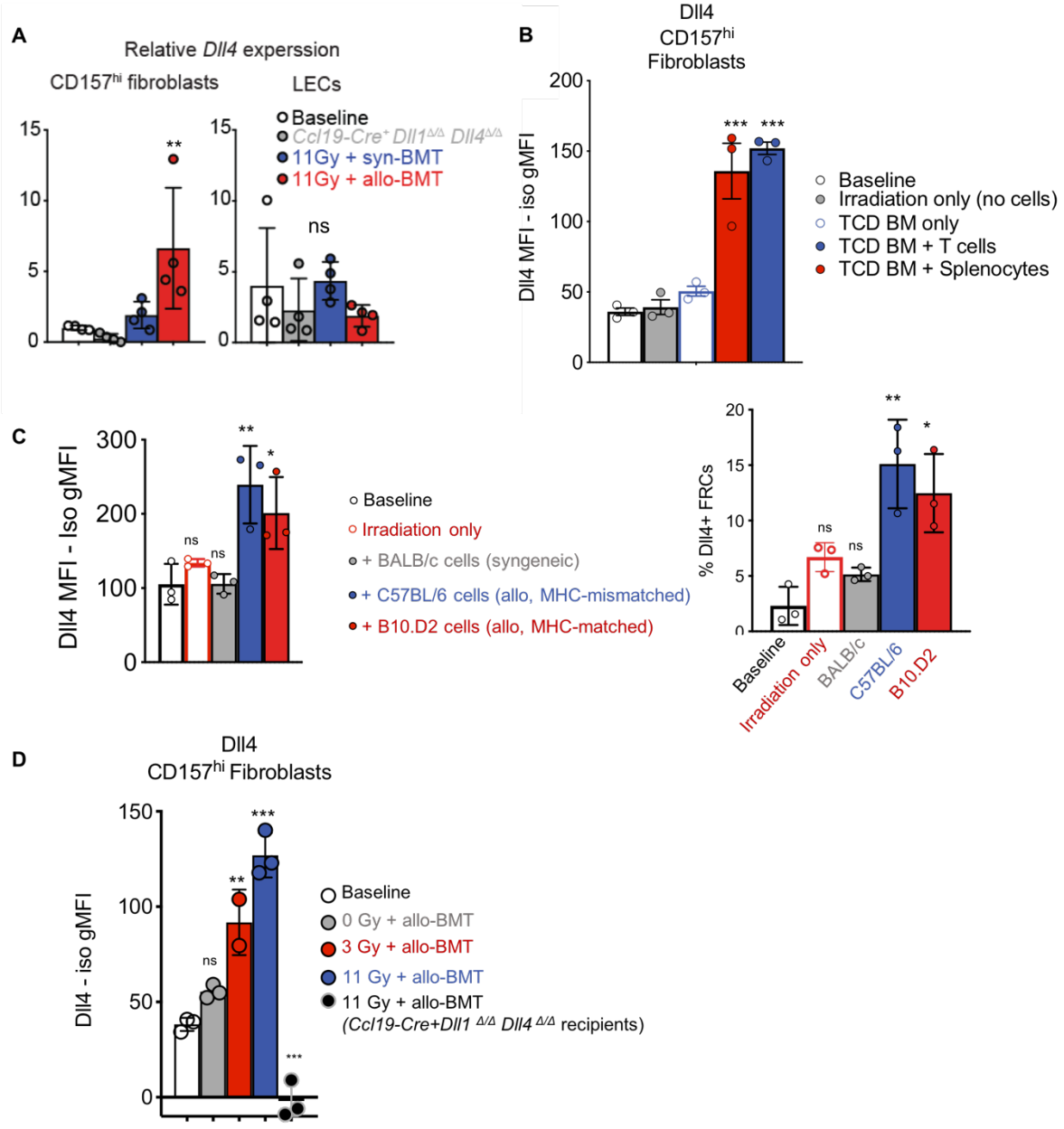

Fig 4.3 Upregulation of DLL4 in CD157^{hi} FRCs is driven by alloreactive T cells irrespective of MHC-mismatch and is potentiated by the degree of myeloablative conditioning. (A) *Ccl19-Cre+Dll1* $^{\Delta/\Delta}$ *Dll4* $^{\Delta/\Delta}$ or Cre- control CBF1 mice were transplanted as in Fig 4.2 C. Relative expression of *Dll4/Hprt* by RT-qPCR in FACS isolated CD157^{hi} FRCs or LECs, normalized to baseline CD157^{hi} FRCs. (B) Cell surface DLL4 expression was assessed by flow cytometry in CBF1 mice on baseline or 12h post 11 Gy irradiation alone, post allo-BMT with T-cell depleted (TCD) BM alone, TCD BM + 20 x 10^6 splenocytes, or TCD BM + 5 x 10^6 purified T cells. (C) BALB/c (H-$2^{D/D}$) recipients were irradiated (or not) with 8 Gy and transplanted with 5 x 10^6 BM + 10 x 10^6 splenocytes from BALB/c (H-$2^{D/D}$, syngeneic), C57BL/6 (H-$2^{B/B}$, MHC-mismatched allogeneic), or B10.D2 (H-$2^{D/D}$, MHC-matched allogeneic) mice. DLL4 MFI and % DLL4$^+$ FRCs were assessed by flow cytometry 12h post transplant. (D) CBF1 recipients were conditioned with increasing doses of irradiation (0 Gy, 3 Gy, 11 Gy) and transplanted as in Fig 4.2. DLL4 expression was assessed at 12h post transplantation. n=3 per experiment. *p<0.05, **p<0.01, ***p<0.001 by post-hoc Tukey tests following one-way ANOVA. TCD BM = T-cell depleted bone marrow.

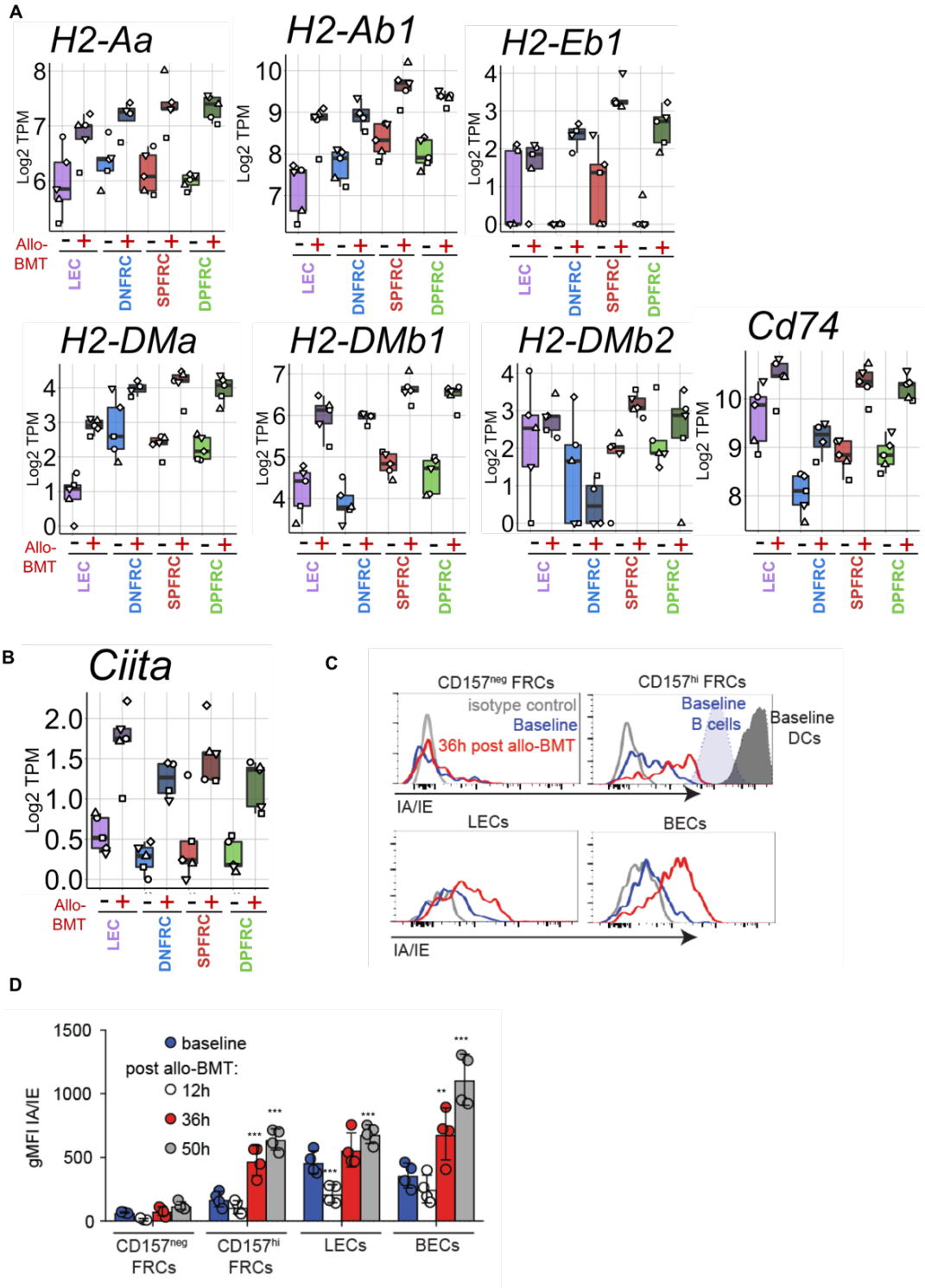

Fig 4.4. Allogeneic transplantation causes upregulation of MHC Class II Antigen presentation machinery in lymph node stromal cell subsets. Log2 transcript per million (TPM) expression data of (A) MHC Class II genes and (B) *Ciita* **from** transcriptomic profiling experiment in Fig 4.1. (C-D) CBF1 mice were transplanted as in Fig 4.2. MHC Class II expression in noted stromal and hematopoietic cell subsets at baseline and at varying timepoints post allo-BMT. N= 4 mice per group. Representative of two experiments. ***p<0.001, **p<0.01 by post-hoc Tukey test after one-way ANOVA, compared to baseline.

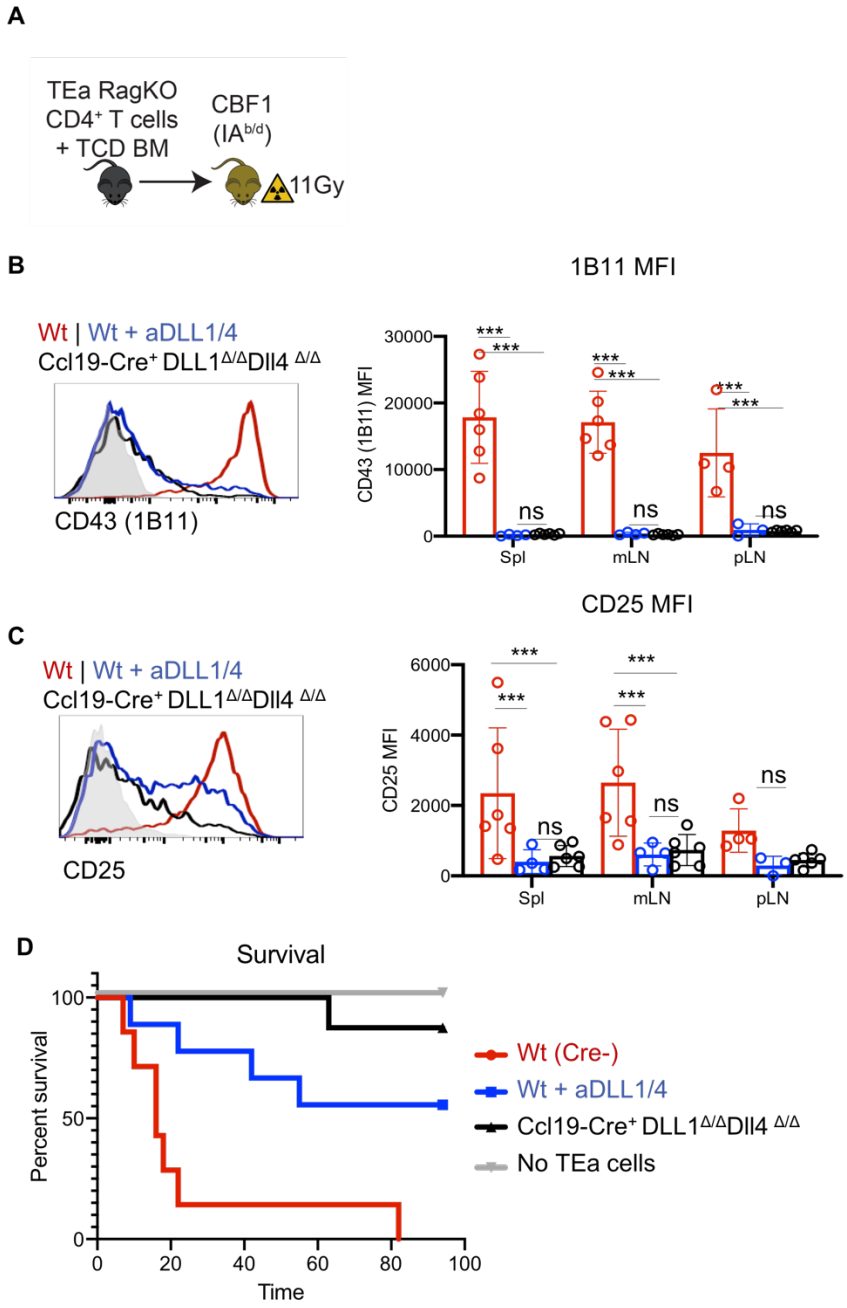

Fig 4.5. Ccl19-Cre lineage traced FRCs are the critical source of Delta-like Notch ligands that drives GVHD lethality after transplantation with monoclonal CD4+ TEa TCR-transgenic T cells. (A-D). CBF1 recipients were transplanted with 5 x 10^4 purified $CD4^+$ TEa cells + 5 x 10^6 TCD BM after 11 Gy irradiation. Recipients were *Ccl19-Cre+Dll1* $^{\Delta/\Delta}$ *Dll4* $^{\Delta/\Delta}$ or Cre^- littermate controls treated with or without 5mg/kg anti-DLL1/4 at d0 and d3 post allo-BMT. Mice not receiving anti-DLL1/4 were given an isotype control antibody. (A) Experimental scheme. (B-C) In one experiment mice were euthanized at day 7 post-transplant and Notch signaling surrogate readouts were assessed including (B) Core-2 O-glycosylated CD43 (1B11) and (C) CD25 expression in isolated CFSE dilute $Thy1.1^+CD4^+$ TEa cells. n = at least 4 per group. ***p<0.001 by post-hoc Tukey test after one-way ANOVA. (D) In another experiment overall survival was monitored post-transplant. n = 8 mice per group. Spl = spleen. mLN = mesenteric lymph node. pLN = pooled peripheral lymph nodes (cervical, brachial, axial, inguinal).

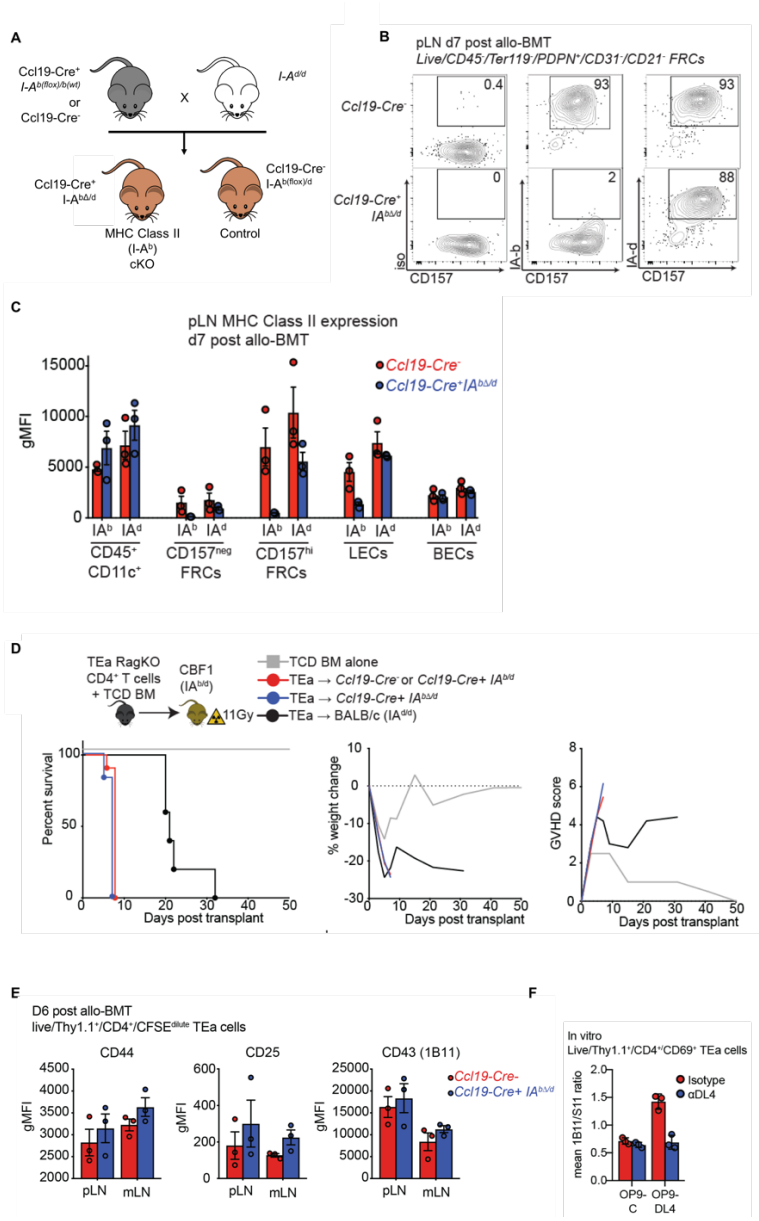

Fig 4.6. Ccl19-Cre lineage traced fibroblastic reticular cells are dispensable as a source of MHC Class II antigen-presentation that drives GVHD. (A) Mouse breeding scheme to generate Ccl19-Cre^{+} I-A$^{b\Delta/d}$ CBF1 mice lacking the I-A^{b} but not the I-A^{d} MHC Class II allele specifically in Ccl19-Cre lineage traced cells (MHC Class II cKO) or littermate control sufficient for both I-A^{b} and I-A^{d} in all cells (controls). Flow plots showing expression of I-A^{b} and I-A^{d} in fibroblastic reticular cells (B) and summary data showing MHC Class II expression in noted subsets (C) at 7 days post allo-BMT. (D-E) 5 x 10^{6} TCD BM + 5 x 10^{4} CD4^{+} Thy1.1^{+} TEa cells (recognizing alloantigen on I-A^{b}) were transplanted into Ccl19-Cre^{+} I-A$^{b\Delta/d}$ (I-A^{b} cKO, blue lines) recipients, littermate controls (intact I-A^{b}, red lines), or BALB/c mice (no recipient I-A^{b}, black lines). (D) GVHD was assessed through monitoring survival, % weight change, and composite GVHD score. N = 8 mice per group. Representative of two experiments. (E) In this experiment TEa cells were also CFSE labeled to monitor division. All cells diluted CFSE by day6 and CFSE^{dilute} TEa cell expression of CD44, CD25, and core-2 O-glycoform CD43 (1B11) was noted. (F) TEa cells were plated in-vitro with bone marrow derived DCs isolated from *Mx-Cre*$^{+}$ *Dll1*$^{\Delta/\Delta}$*Dll4*$^{\Delta/\Delta}$ CBF1 mice on a stromal feeder layer of OP9-C or OP9 cells expressing DLL4 (OP9-DL4). Wells were treated with anti-DLL4 antibody versus isotype control. At day 4 activated CD69^{+} TEa cells were assessed for Notch signals via the ratio of the core-2 O-glycoform of CD43 (1B11) to pan-CD43 (S11). N = 3 per group.

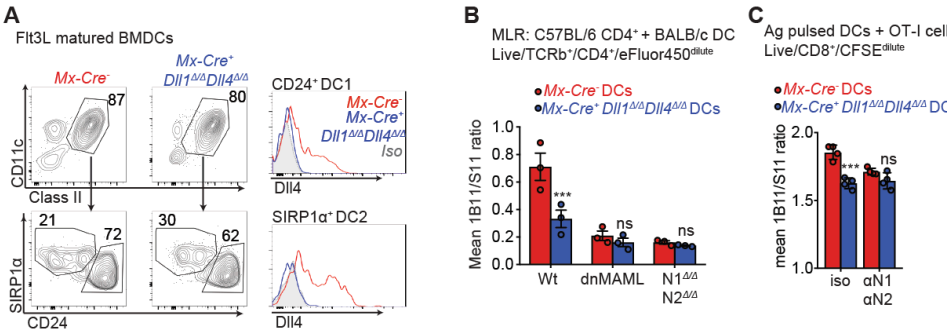

Fig 4.7 FLT3L matured bone marrow derived dendritic cells express high levels of DLL4 and provide Notch signals *in vitro*. Bone marrow from poly(I:C) induced *Mx-Cre*$^{+}$ *Dll1*$^{\Delta/\Delta}$*Dll4* $^{\Delta/\Delta}$ or Mx-Cre^{-} littermate controls was matured with FLT3L and stimulated with LPS + R848 to induce Delta-like4 expression. Bone marrow maturation protocol lead to the development of both DC1-like CD24+ and DC2-like SIRP1α^{+} cDCs. Expression of Delta-like4 in both subsets (A). (B) BALB/c FLT3L-DCs were used to stimulate polyclonal C57BL/7 CD4^{+} T cells (wild type, dnMAML, or *N1*$^{\Delta/\Delta}$*N2*$^{\Delta/\Delta}$) in an in vitro mixed-lymphocyte reaction. Proliferated eFluor450dilute CD4^{+} T cells were assessed for 1B11 and S11 expression. (C) SIINFEKL-pulsed FLT3L-DCs were used to stimulate CD8^{+} OT-I cells in-vitro and 1B11 and S11 expression was assessed by flow cytometry in CFSE dilute cells. *p<0.05, **p<0.01, ***p<0.001, one-way ANOVA with Tukey's post-hoc-tests.

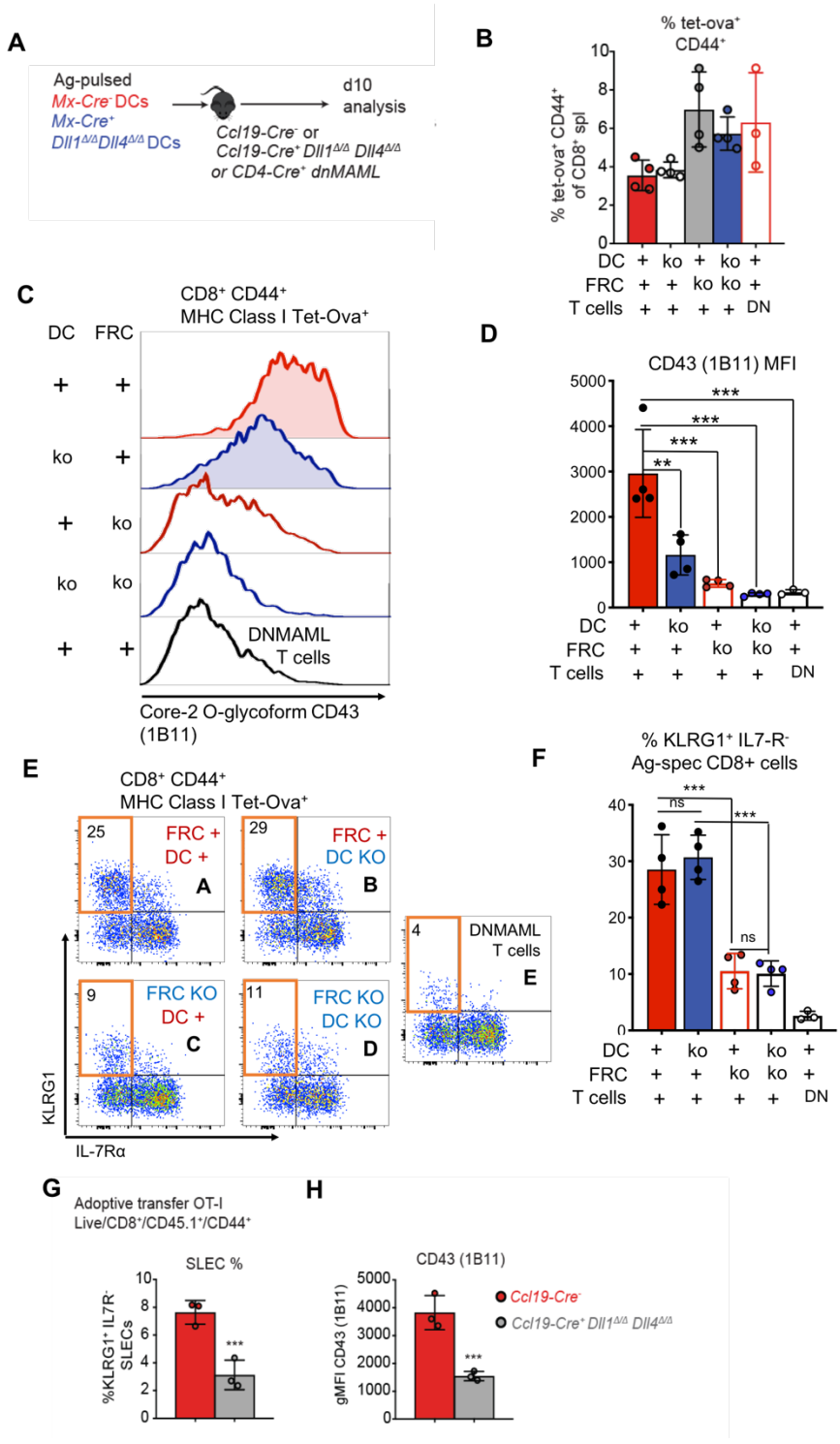

Fig 4.8 Ccl19-Cre lineage traced FRCs are the dominant source of Delta-like Notch ligands that control CD8$^+$ T cell responses to dendritic cell immunization. (A) FLT3L-DCs from Fig 4.7 were pulsed with SIINKFEKL and injected IV (1 x 10^5 cells) to stimulate endogenous CD8+ T cells in *Ccl19-Cre+Dll1$^{\Delta/\Delta}$ Dll4$^{\Delta/\Delta}$* , *CD4-Cre$^+$ dnMAML*, or wild type littermate controls (Ccl19-Cre-). Spleens were harvested at day 10 post immunization. (B) % of Ag-activated CD44$^+$ tetramer-ova$^+$ cells of total CD8$^+$ T cells. (C) The core-2 O-glycoform of CD43 (1B11) was assessed by flow cytometry and summarized in (D). (E) Representative flow cytometry plots of KLRG1$^+$ IL-7Rα$^-$ SLECs as a % of Ag-specific CD8$^+$ T cells, summarized in (F). (G-H) BMDC immunization was performed as in (A-F), but mice received 5 x 10^4 purified CD45.1$^+$ OT-I CD8$^+$ T cells by adoptive transfer one day before immunization. (G) % SLECs and (H) CD43 (1B11) gMFI of CD45.1$^+$ CD44$^+$ OT-I cells at day 7 post immunization. Data representative from two-independent experiments of at least n=3 per group. *p<0.05, **p<0.01, ***p<0.001, one-way ANOVA with Tukey's post-hoc-tests (D,F) or t-test (G,H). ko = genetic excision of *Dll1* and *Dll4*. DN = dnMAML. SLEC = short-lived effector cells.

Chapter 5

Fibroblastic reticular cells deliver Notch signals to naïve T cells

5.1 Abstract

The Notch signaling pathway is a critical regulator of T cell activation and function. In many contexts, Notch signals are thought to be delivered to T cells by antigen-presenting cells at the immune synapse. However, it is unclear if Notch signals can be triggered in mature T cells in the absence of antigen presentation, including in naïve T cells. Thus, we sought to understand the effects of Notch blockade on naïve $CD4^+$ T cells compared to alloantigen-activated T cells through transcriptomic profiling. Compared to alloantigen-activated cells where DLL1/4 blockade regulated the expression of ~200 genes, Notch signals in naïve $CD4^+$ T cells only controlled transcription at one genetic locus. This locus contained *Dtx1* and *Rasal1* as well as a previously described Notch-regulated enhancer element. Genetic loss of function revealed that fibroblastic reticular cells in secondary lymphoid organs were the critical source of Delta-like1/4 that provide Notch inputs to naïve $CD4^+$ T cells. Together, these results show that FRCs deliver Notch signals to naive T cells prior to antigen-mediated signaling, and that the T cell activation status shapes the gene expression signature regulated by Notch. These data lay the groundwork to further explore how Notch signals might regulate naïve T cell function and how Notch cooperates with other signals, including antigen and costimulation, to shape T cell activation.

5.2 Introduction

Notch is a conserved signaling pathway that links cell-to-cell interactions to transcriptional regulation. Upon physical interaction with a ligand from a neighboring cell, the Notch receptor is cleaved and the intracellular domain of Notch (ICN) traffics to the nucleus. ICN then forms a ternary transcriptional activation complex with the transcription factor RBP-Jκ and a co-activator of the Mastermind-like family (MAML). The Notch transcriptional complex binds consensus RBP-Jκ sites in gene regulatory regions to enhance transcription of target genes. While there are some shared Notch targets across cell types, many transcriptional targets of Notch signaling are thought to be cell-type and context-specific.

To better understand the effects of Notch signaling in T cells, our laboratory profiled the transcriptomic effects of Delta-like1/4 signals in alloreactive $CD4^+$ T cells early after alloantigen activation (149). Allogeneic (as opposed to syngeneic) transplantation led to profound changes in the transcriptional landscape of T cells affecting thousands of genes. This included the acquisition of a strong Th1 program defined by the transcription factor *Tbx21* and *Ifng* expression. The effects of Notch blockade were more limited, impacting a few hundred genes critical for pathogenic T cell function. Interestingly, Notch blockade significantly blunted *Ifng* without changing *Tbx21* expression. Transcriptomic effects of Notch signaling in an antigen-activated $CD4^+$ Th2 house dust mite allergen model of immunity (53) and antigen-specific $CD8^+$ response to influenza infection have also been explored systematically (221). Effects of Notch over-expression (31) and *Rbpj* deletion (222) have been profiled in $Foxp3^+$ Tregs. While there were some conserved effects of Notch signaling across of these studies, many immunologically important changes were unique. Viewed together, these studies suggest that Notch's function as a transcription factor is to amplify

transcription of genes in a cell-type and immunologic-context dependent manner that are ultimately controlled by other master transcription factors such as *Tbx21* (50). While there is an accumulating body of work on the molecular signature of Notch signaling in activated T cells, there has been little exploration of the effects that Notch signals might have in mature naïve T cells.

Much of the previous literature on Notch signaling in mature T cells assumed that Notch signals are delivered by antigen-presenting cells (APCs) concurrently to antigen-mediated stimulation of the T cell receptor (43, 209). However, we and others (17, 25) showed that the critical source of Notch ligand is derived from fibroblastic reticular cells (FRCs) lineage-traced by Ccl19-Cre in secondary lymphoid organs. Could FRCs provide Notch signals to naïve T cells as well? Imaging studies within secondary lymphoid organs showed that naïve T cells are in intimate contact with FRCs as they migrate along the desmin-rich extracellular matrix that FRCs ensheath (223). Thus, active Notch signals might be delivered to naïve T cells from the subsets of FRCs that also provide Notch ligands to antigen-activated T cells.

In this short chapter, we seek to understand if and how Notch signaling regulates naïve $CD4^+$ T cells. In contrast to the effects of Notch signaling during T cell activation where several hundred genes are regulated by Notch, we show that short-term blockade of Notch signaling in naïve $CD4^+$ T cells regulates expression of just one genetic locus containing *Dtx1* and *Rasal1*. However, naïve $CD4^+$ T cells from mesenteric lymph nodes compared to the spleen expressed the genetic hallmarks of an interferon signature, indicating that the organ site regulates naïve T cell transcription far more than Notch signaling. Furthermore, we show that Notch signals in vivo are delivered by

secondary lymphoid organ resident FRCs traced by a Ccl19-Cre transgene, the same cellular subset that provides Notch signals to alloreactive T cells during allo-BMT and to $CD8^+$ T cells during dendritic cell immunization **(Chapter 4)**. Together, these data establish that naïve T cells experience Notch signaling in vivo from fibroblastic niches.

5.3 Results

5.3.1 Naïve $CD4^+$ T cells in secondary lymphoid organs receive Notch signals, but only one genetic locus is transcriptionally regulated by Notch signaling

To understand the impact of Notch signaling in circulating naïve T cells, we turned to a monoclonal population of TCR transgenic $CD4^+$ T cells that we previously studied early after allogeneic transplantation (149). The $V\beta13^+$ 4C TCR recognizes allopeptides presented by the BALB/c MHC class II $I\text{-}A^d$ molecule, making it ideal to model naïve T cells, as it should not be activated by other peptides on the C57BL/6 ($I\text{-}A^b$) background. 4C TCR Tg mice were treated 12h or 36h prior with anti-DLL1/4 antibodies or 12h prior with control antibody (iso). We then sort purified $1x10^5$ $CD4^+$ $V\beta13^+$ $CD62L^+$ $CD44^-$ $CD25^-$ $CD69^-$ 4C naïve TCR transgenic cells from the spleens and mesenteric lymph nodes of C57BL/6 mice. RNA was extracted followed by cDNA synthesis with oligo(dT) priming and samples were index for library preparation for Ilumina sequencing. Reads were pseudoaligned to the mouse transcriptome with the kallisto program. Expression was converted to a log2 scale, normalized across samples, and genes with a low expression (<1 TPM in >3 samples) were filtered out prior to subsequent analysis **(Fig 5.1 A)**. Principal component analysis indicated that cells clustered predominantly by organ (mLN = circles vs. spleen = triangles), but not by Notch signaling status **(Fig 5.1 B)**. To ascertain global differences in gene

expression due to Notch signaling, we used limma/voom to compare all spleen and mLN samples treated with isotype control antibody to all spleen and mLN samples treated for 12h and 36h with anti-DLL1/4. Only two genes, *Dtx1* and *Rasal1,* showed significantly different mRNA abundance with Notch blockade **(Fig 5.1 C)**. Both genes were similarly regulated after either 12h or 36h of anti-DLL1/4 treatment, and there was no difference between organs **(Fig 5.1 D).** [4] *Dtx1* is a well-defined Notch target gene in T-ALL that is regulated by an RBP-Jκ-binding site containing enhancer in the second intron (224). This enhancer in the second intron of *Dtx1* corresponds to ATAC-seq data showing open chromatin regions present in both naïve and activated splenic $CD4^+$ T cells. *Rasal1* runs anti-parallel to *Dtx1* in very close proximity and could be regulated by the same enhancer **(Fig 5.1 E)**. Next, we re-examined the expression of these genes from our previous transcriptomic profiling in 4C T cells transplanted into syngeneic (Syn) or allogeneic recipients with or without anti-DLL1/4 (149). Using the same analysis pipeline and statistical cut-offs, Notch regulated the expression of far more genes in alloreactive cells (**Fig 5.2 A)** compared to naïve cells. Interestingly, alloantigenic stimulation downregulated expression of *Dtx1* (Syn-iso), although it was further downregulated by anti-DLL1/4 (iso-aDLL1/4). Alloantigen stimulation caused a trend towards *Rasal1* downregulated expression, but this did not reach statistical significance (perhaps due to its low expression).[5] **(Fig 5.2 B)**. Together, these findings show that active Notch signals

[4] Gene-wise expression data on effects of anti-DLL1/4 blockade on naïve 4C $CD4^+$ T cells can be accessed online at https://ericperkey.shinyapps.io/4C_Naive_App/

[5] Gene-wise expression data on effects of anti-DLL1/4 blockade on Allo-Ag activated $CD4^+$ 4C cells can be accessed at https://ericperkey.shinyapps.io/4CChung/

are delivered to naïve CD4$^+$ T cells in vivo. However, these signals have limited transcriptomic effects compared to signals delivered at the time of T cell activation.

5.3.2. Mesenteric lymph node resident naïve CD4$^+$ T cells have hallmarks of interferon signaling

To ascertain if there are organ-specific differences in naïve CD4$^+$ T cells, we performed differential expression analysis on cells isolated from spleen or mesenteric lymph nodes in mice treated with isotype control antibody. Interestingly, there were more genes regulated by the organ site than by Notch signaling **(Fig 5.3 A)**. *Vcam1* and *Slc40a1,* both markers of red pulp macrophage, were enriched in the spleen. This may represent minor contamination from FACS purification, although the master transcription factor of red pulp macrophage, *Spic* (225)*,* was not preferentially expressed in cells sorted from the spleen. Cells from the mesenteric lymph nodes had higher expression of many interferon-responsive genes including *Ifit1, Oasl2, Rsad, Mx1,* and *Ifi3* irrespective of Notch blockade **(Fig 5.3 B)**. GSEA performed on mesenteric lymph node-specific genes was enriched for both IFN-α and IFN-γ signatures **(Fig 5.3 C)**.

5.3.3 Delta-ligands from fibroblastic reticular cells are the cellular source of Notch signals to naïve CD4$^+$ T cells

We previously reported that alloreactive CD4$^+$ and CD8$^+$ T cells receive Delta-like Notch signals from non-hematopoietic secondary lymphoid organ fibroblastic reticular cells (FRCs) lineage traced by a Ccl19-Cre transgene (25). Conversely, others have suggested that the predominant source of Notch ligands during T cell activation are antigen-presenting dendritic cells (43, 49,

128). To determine the cellular source of Notch ligands that naive $CD4^+$ T cells receive, we purified naïve polyclonal $CD4^+$ from *Ccl19-Cre*$^+$*Dll1*$^{f/f}$*Dll4*$^{f/f}$ or Cre^- littermate controls treated with anti-DLL1/4 or isotype control. Expression of *Dtx1* in naïve $CD4^+$ cells isolated from spleen and peripheral lymph nodes was significantly blunted in *Ccl19-Cre*$^+$*Dll1*$^{f/f}$*Dll4*$^{f/f}$ mice. Furthermore, the abundance of *Dtx1* mRNA in *Ccl19-Cre*$^+$*Dll1*$^{f/f}$*Dll4*$^{f/f}$ mice was similar to that in mice treated with systemic anti-DLL1/4 antibodies **(Fig 5.4)**, indicating that there is no additional cellular source of Delta-like ligands that can compensate for loss of *Dll1 and Dll4* expression in FRCs. This indicates that Notch signals can be delivered by FRCs independently of antigen in secondary lymphoid organs.

5.4 Discussion

In this brief study, we have explored the effects of Notch signaling on naïve $CD4^+$ T cells with the goal of understanding if Notch signals can be delivered independently of antigen. A secondary goal of this study was to determine if and how Notch might regulate naïve T cell homeostasis and function. We conclusively show that naïve $CD4^+$ T cells experience active Notch signaling, although the transcriptomic effects were limited to the regulation of two genes at a single locus (*Dtx1* and *Rasal1)* with a well-known Notch-regulated enhancer. The transcriptomic program of naïve T cells was more impacted by their organ site, as cells recovered from mesenteric lymph nodes displayed a distinct interferon signature. FRCs, and no other cells, were the critical source of Notch ligands for naïve T cells, highlighting again their role in creating an immunological niche for T cells.

Pan-T cell Notch inhibition does not appear to cause defects in naïve T cells homeostasis in mouse models, although more data are needed (25). Conversely to pan-T cell inhibition, Treg-specific Notch inhibition without any particular antigenic challenge led to profound changes in Treg function, both positive (31) and negative (222) depending on the immunological context. It will also be important to study if "pre-loaded" Notch signals might become important during T cell activation. Notch signals might precede antigen-mediated activation, especially if Notch signals are delivered by FRCs and not antigen-presenting dendritic cells. Notch "pre-loaded" T cells might be primed to quickly react to an antigen stimulus, by analogy with how high levels of mTORC1 activity (perhaps itself driven by Notch2 signals) metabolically position marginal zone B cells to quickly differentiate into plasma cells (226). Interestingly, one group reported that freshly isolated naïve $CD4^+$ T cells had high levels of cleaved ICN, indicative of "pre-loaded" active Notch signals (159). In fact, this group needed to rest cells overnight, allowing enough time for ICN to decay, before being able to study the role of Notch signaling in vitro. They suggested that the presence of ICN was an artifact of the isolation process as EDTA-containing medium has been shown to cause Notch cleavage in vitro through the chelation of calcium away from the receptor (227). However, another intriguing explanation may be that these Notch signals are not artifactual and are instead delivered from a source in vivo. Such findings will need to be considered when designing in vitro T cell activation assays from freshly isolated naïve T cells.

Could the targets of Notch signals in naïve T cells have effects on T cell activation? Both *Dtx1* and *Rasal1* have been reported to increase the signaling threshold for T cell activation. DTX1 has E3 ubiquitin ligase function that degrades MEKK1, suppressing MAPK signals during T cell activation (228, 229). DTX1 has itself been shown to bind and degrade Notch receptors through

its tandem WWE domains. However, deletion of these domains did not prevent the ability of DTX1 to negatively regulate T cell, showing that DTX1 modifies T cell activation in a Notch-independent manner (229). RASAL1 is a GTPase activating protein that negatively regulates ERK signaling while also directly binding the ZAP-70 kinase domain to inhibit TCR signaling (230). Thus, Notch signals would be predicted to increase the threshold for T cell activation through upregulated expression of *Dtx1* and *Rasal1*. While this would be paradoxical with our current understanding that Notch drives T cell activation and effector function, we plan to conduct experiments with naïve T cells isolated from mice treated with or without Notch blockade to address this possibility.

Why are the transcriptomic effects of Notch limited in naïve as compared to activated T cells? This could be due to the nature of how Notch acts as a transcription factor. The amount of transcription by RNA polymerase at a given promoter is related to the frequency of transcriptional bursts and the size (duration and amplitude) of these bursts, which are in turn controlled by interactions with transcription factors bound to enhancers. Many transcriptional factors such as steroid hormone receptors increase mRNA expression by increasing the burst frequency of transcription (231). However, in Drosophila, increased ICN did not regulate this on-off frequency of transcription. Instead, Notch increased the length and amplitude of any given transcriptional burst. Importantly, Notch only drove these sustained increases in transcriptional burst size at enhancers already occupied by other tissue-specific transcription factors (41). Furthermore, the chromatin of naïve T cells is far less open than activated T cells. T cell activation causes a near doubling in the amount of accessible chromatin regions, dependent on the transcription factor AP-1 that is induced by costimulatory signaling (232). Thus, the closed chromatin of naïve T cells plus the absence of activation-associated transcription factors such as *Tbx21, Gata3,* and *Rorc* at

different enhancers may limit the genetic loci that are sensitive to loss of Notch signaling in naïve T cells.

Another recently described mechanism may come into play to limit the effects of Notch signaling in naïve T cells. The RBP-Jκ binding site at the *Dtx1/Rasal1* enhancer could be acting as a sink for ICN, recruiting and then actively degrading the Notch transcriptional complex to prevent its action at other loci. This phenomenon is related to variable thresholds of Notch transcriptional complexes needed for activation at different loci. Notch transcriptional activation complexes can dimerize and bind Suppressor of Hairless paired sites (SPS), which are two RBP-Jκ binding sites lying in head-to-head orientation and in close proximity. SPSs have a higher affinity for Notch transcriptional complexes compared to single RBP-Jκ binding sites. Curiously, introduction of a single synthetic SPS site in Drosophila led to a classic Notch loss-of-function wing phenotype (233). ICN captured by this SPS were degraded by CDK8, leading to less available ICN to bind to other RBP-Jκ sites. This caused a Notch loss-of-function phenotype, which could be rescued by over-expression of ICN. The *Dtx1/Rasal1* enhancer could in principle function as SPS "Notch-sink". In fact, B cells with mutant Notch receptors unable dimerize had decreased levels of *Dtx1* suggesting that the *Dtx1* enhancer is an SPS. However, these B cells had reciprocal increases in Notch-dependent *Myb* transcription, which was mediated by enhancers selectively bound by monomeric but not dimeric Notch transcriptional complexes (234). We hypothesize that a similar mechanism may be occurring during T cell activation. Epigenetic remodeling during T cell activation may decrease accessibility of Notch to the *Dtx1* locus, as evidenced by decreased *Dtx1* transcription post T cell activation. This closure of a "Notch-sink" may then increase the relative availability of Notch transcriptional complexes available at other loci. In summary, we show that

Notch has context-dependent effects on the transcriptome that depend on T cell activation. Still, what transcriptional effects of Notch signaling are directly regulated by the Notch transcriptional complex remains to be seen. Further epigenomic studies are ongoing to understand how T cell activation status regulates the occupancy of Notch transcriptional complexes at different target genes.

Why might naïve T cells in the mLN but not spleen have an interferon signature? While our mice should be immunologically naïve, gut-derived microbial products may trigger the release of type I interferons from innate immune cells present in the GI tract that in turn drive responses in naive T cells. Also, the interferon signature could be indicative of very early T cell activation. *Ifit3* was the top scoring gene in an interferon gene module uncovered by single-cell transcriptomic profiling of human T cells (235). While IFN-α induced *Ifit3* expression independently of TCR stimulation, *Ifit3* was also induced within 8h of TCR stimulation ex vivo. This interferon activation module depended on autocrine IFN-γ signals and preceded a later proliferation-associated activation module. However, this is unlikely in naïve 4C T cells as the 4C TCR should not be activated by any antigen in these mice. Furthermore, we did not detect any *Ifng* transcripts in our cells (data not shown). Still, presence of an interferon signature in mesenteric lymph nodes may predispose naïve $CD4^+$ T cells to the subsequent acquisition of Th1 phenotype after antigen stimulation, as others have reported (236), which may be relevant for GVHD pathology in the gut.

We revealed that sorted naïve polyclonal $CD4^+$ T cells from spleen and pLN expressed *Dtx1* which was abrogated when we deleted Delta-like ligands in FRCs. This demonstrates that naïve T cells experience Notch signals independently of antigen. Still, because we sorted bulk naive $CD4^+$ T

cells, it is unclear if all naïve T cells experience Notch signaling or only a subset experience Notch signals at any given time. Could there be a specific FRC niche that attracts and provides Notch signals to a limited number of naïve T cells? In the previous chapter, we showed that only specialized subsets of FRCs express DLL4 while other subsets had no expression (see **Chapter 4)**. These rare DLL4^{high} FRCs might set up a distinct immunological niche contributing to heterogeneity in the signals that naïve T cells receive. We are planning single-cell transcriptomic and imaging studies to understand if active Notch signals occur in all or only a subset of naïve T cells and if this subset might be located in specific FRC niches. If this is the case, FRCs that differ in DLL4 expression as well as other signaling molecules might construct distinct immunologic niches that could send naïve T cells down disparate differentiation trajectories.

5.5 Figures

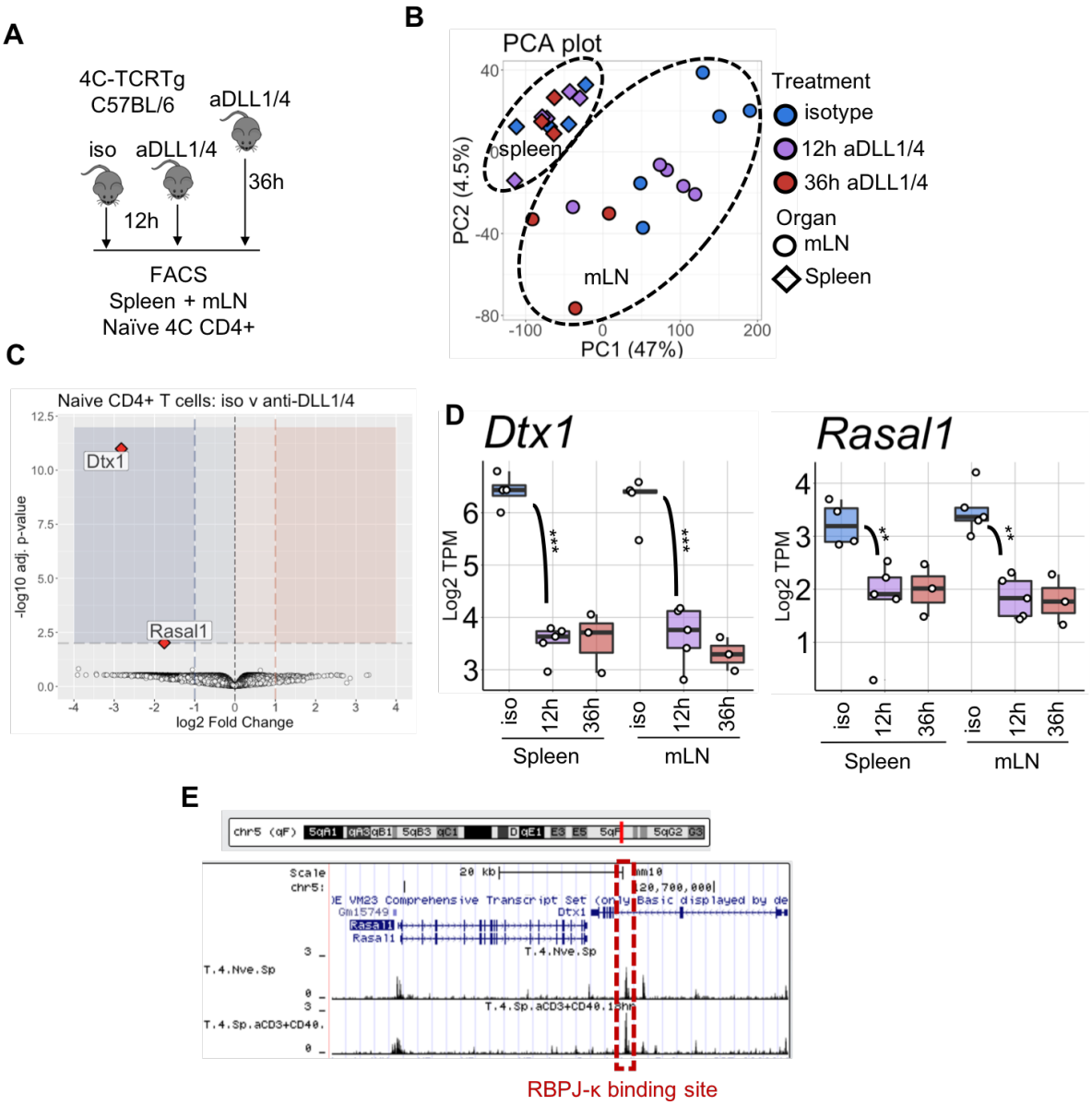

Fig 5.1 Notch blockade has distinct but limited effects on the transcriptome of naïve CD4$^+$ T cells. (A) Experimental scheme. C57BL/6 4C TCR-Tg mice were treated with intraperitoneal injections of anti-DLL1/4 (5 mg/kg) 12h or 36h before isolation or with 5mg/kg of isotype control antibody 12h before isolation. CD19$^-$CD8$^-$ CD4$^+$ Vβ13$^+$ CD62L$^+$ CD44$^-$ CD25$^-$ CD69$^-$ naïve 4C cells were FACS purified from spleen and mLN separately and transcriptomically profiled. (B) Principal component analysis reveals predominant clustering by organ but not by anti-DLL1/4 treatment (12h or 36h). (C) Volcano plot showing differentially expressed genes between pooled anti-DLL1/4 samples versus isotype control. (D) *Dtx1* and *Rasal1* expression in individual groups. (E) Genome browser tracks showing open chromatin ATAC-seq data from the Immgen database at the *Dtx1/Rasal1* locus in CD4$^+$ T cells. The RBP-Jκ-binding site is highlighted in red. mLN = mesenteric lymph node. **p<0.01, ***p<0.001 by empirical Bayes method in *limma*.

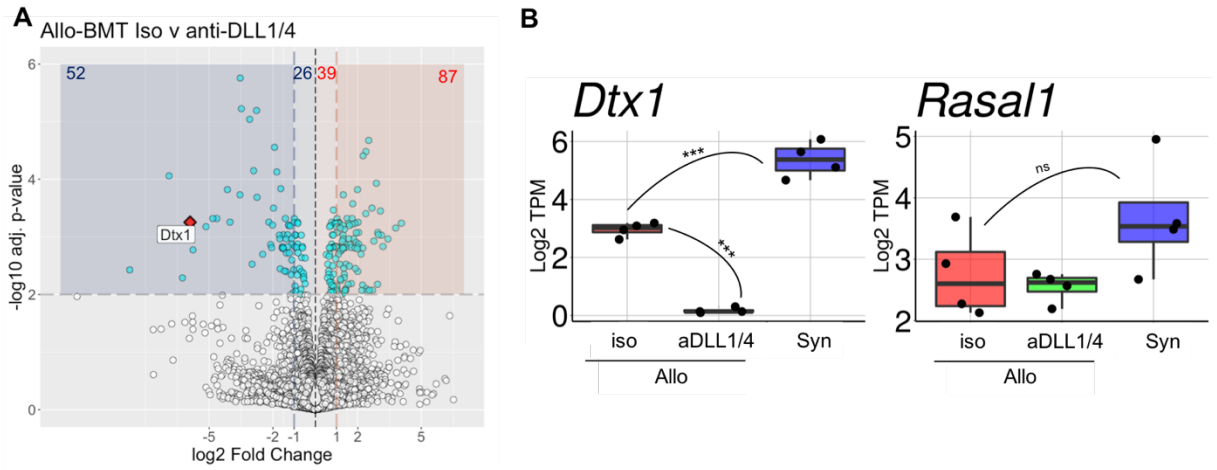

Fig 5.2 Transcriptomic effects of Notch blockade on alloreactive CD4$^+$ T cells. Reanalyzed data from Chung et. al.(149). 4C CD4$^+$ T cells were FACS purified 1.75 days after transplantation into syngeneic recipients or allogeneic recipients treated with anti-DLL1/4 (5mg/kg) or isotype control antibody (5mg/kg). (A) Volcano plot of global transcriptomic differences of between 4C cells transplanted into allogeneic recipients (allo) with and without anti-DLL1/4 blockade. Number of differentially expressed genes and *Dtx1* is noted in the volcano plot. (B) *Dtx1* and *Rasal1* expression. Syn = syngeneic. ***p<0.001 by empirical Bayes method in *limma*.

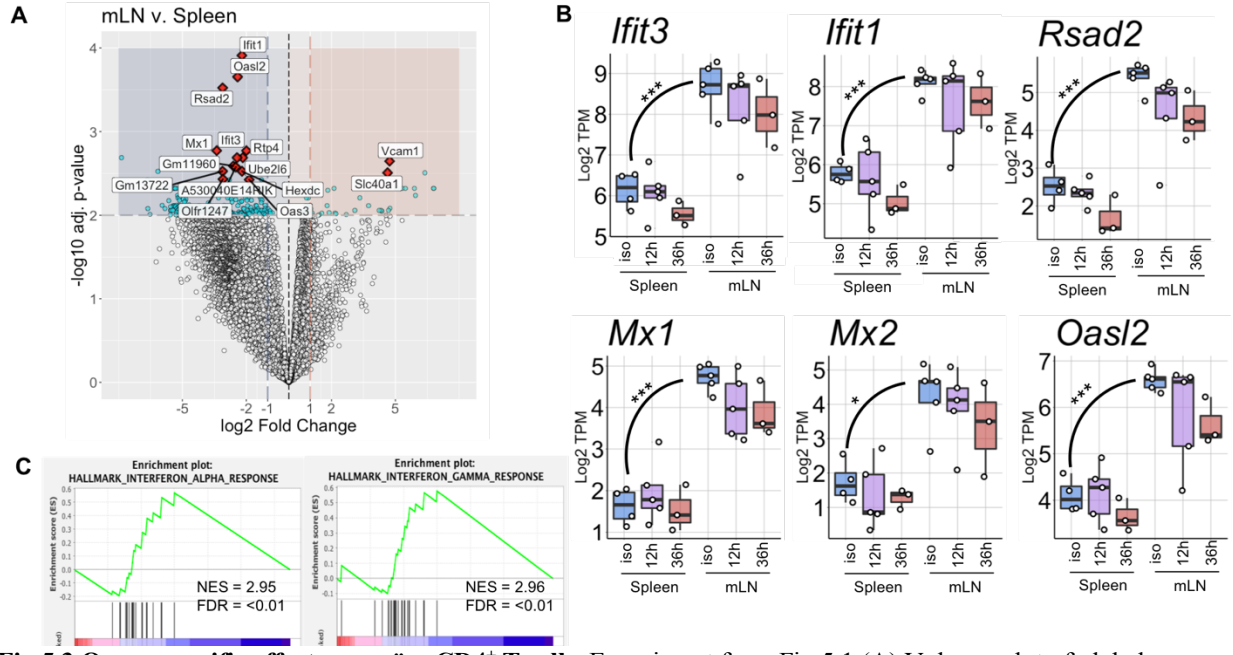

Fig 5.3 Organ specific effects on naïve CD4$^+$ T cells. Experiment from Fig 5.1 (A) Volcano plot of global transcriptomic differences between naïve 4C cells isolated from mesenteric lymph node (mLN) vs. spleen in mice treated with isotype control antibody. (B) Expression of selected differentially expressed genes associated with an interferon response signature. (C) GSEA analysis of differentially expressed genes ranked by log2 fold change. ***p<0.001 by empirical Bayes method in *limma*.

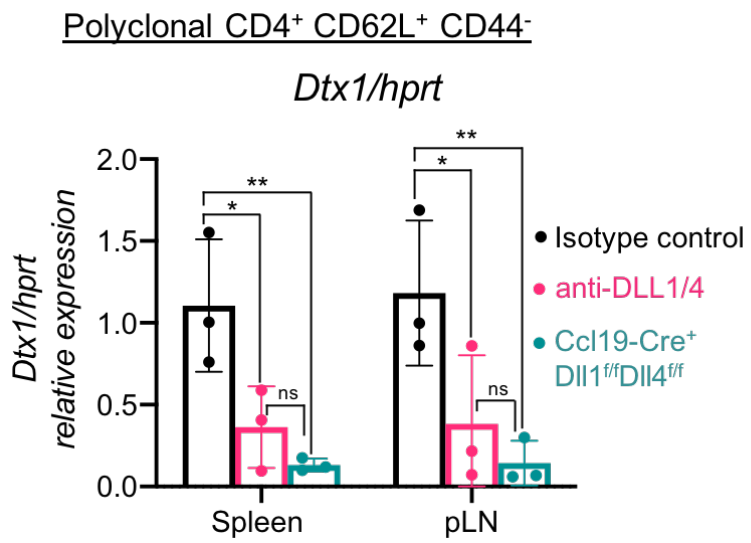

Fig 5.4 Ccl19-Cre lineage traced fibroblastic reticular cells provide Delta-like Notch signals to naïve CD4$^+$ T cells. Polyclonal CD44$^-$ CD62L$^+$ CD4$^+$ were FACS purified from *Ccl19-Cre*$^+$*Dll1*$^{\Delta/\Delta}$ *Dll4*$^{\Delta/\Delta}$ or Cre$^-$ littermate controls treated with anti-DLL1/4 or isotype control (5mg/kg). *Dtx1* expression was assessed by RT-qPCR. pLN = pooled (cervical, brachial, axial, inguinal) peripheral lymph nodes. **p<0.01, *p<0.05 by one-way ANOVA with post-hoc Tukey test.

Chapter 6

Conclusions and Perspectives

Notch inhibition is emerging as a novel pharmacological strategy to modulate pathogenic immune responses after allogeneic bone marrow transplantation, and thus prevent GVHD. In turn, findings in this context may apply to other immunological disorders, including organ rejection and autoimmunity. However, long-term systemic inhibition of Notch causes on-target toxicities including damage to blood endothelial cells (237) and the GI tract (238), which have limited the application of Notch inhibitors clinically. To expand the therapeutic window, new Notch inhibition strategies must be developed. These strategies could include blocking specific Notch receptor/ligands pairs, intervening in short but critical temporal windows, targeting only the key cellular subsets that provide Notch ligands, or inhibiting critical pathways that control ligand expression in these subsets. While much preclinical work has documented the role of Notch signaling in mature T cell responses, much less work has been done to carefully dissect the cellular sources and regulation of Notch ligands as well as the timing of their interaction with T cells. A full understanding of these questions will be critical to develop better therapeutic strategies that selectively modulate Notch signaling in immune disorders while preserving critical homeostatic functions of the pathway.

In this thesis, I explored the role that fibroblastic reticular cells (FRCs) in secondary lymphoid organs play in regulating T cell immune responses after allo-BMT and in other immunological contexts. First, using a novel cell surface indicator of Notch signaling, we documented the non-redundant role of FRCs in driving T cell alloimmunity through Delta-like Notch ligands during allotransplantation with reduced intensity or no myeloablative conditioning **(Chapter 2)**. This was an important finding, because it proved that even in a context when recipient hematopoietic cells were present, FRCs remained critical to drive Notch-dependent T cell pathology. Next, we showed that Delta-like Notch ligands from FRCs imprinted a gut-homing program in alloreactive effector T cells, including the acquisition of the critical integrin α4β7, that drove accumulation of alloreactive effector cells in the GI tract **(Chapter 3)**. I then turned to investigating how allo-BMT regulates FRC subsets. Allo-BMT caused upregulated expression of inflammatory genes and Delta-like4 in FRCs. This upregulation was restricted to specific subsets of $CD157^{hi}$ FRCs and was driven by alloreactive T cells. Allo-BMT also caused FRCs to upregulate the MHC class II antigen presentation machinery, suggesting that they may be involved in alloantigen presentation. However, while FRCs were critical to mediate lethal $CD4^+$ T cell alloimmunity through the provision of Notch ligands, they were dispensable as sources of alloantigen. This suggested that Notch signals and antigen can be delivered from separate cellular sources. We confirmed that this was the case in a DC immunization model, and thus not restricted to alloimmunity. FRCs acted as a critical non-redundant source of Notch ligands to drive effector $CD8^+$ T cell differentiation, even when they were primed by DCs highly expressing DLL4 **(Chapter 4)**. Furthermore, I showed that naïve $CD4^+$ T cells receive Notch signals in vivo from FRCs, independently of any antigen **(Chapter 5)**. Together, these studies highlight the critical roles of FRC niches in delivering Notch signals to T cells in different immunological contexts. In this chapter, I will discuss the

implications of my findings and provide a conceptual framework to understand the role of FRCs and Notch signaling in allo-BMT and other immune responses.

T cell-FRC crosstalk and regulation of the immunological niche during allo-BMT

We showed in **Chapter 4** that the FRC niche dynamically responds to signals from alloreactive T cells by upregulating expression of Delta-like4 within 12 hours of allotransplantation. This suggests that alloreactive T cells control expression of DLL4 in the FRC niche through production of yet-to-be-determined signals, that are in turn induced by antigen activation. In addition, these signals from alloreactive T cells may recruit previously DLL4$^{neg/lo}$ FRCs into the DLL4^{hi} FRC niche. The resulting expansion of DLL4 availability would allow a greater number of donor T cells to acquire a Notch-dependent pathogenic effector program. Thus, we propose the existence of a positive feedback loop model of alloactivation where T cells shape their own DLL4^{hi} niche that further endows them with pathogenic effector functions **(Fig 6.1).**

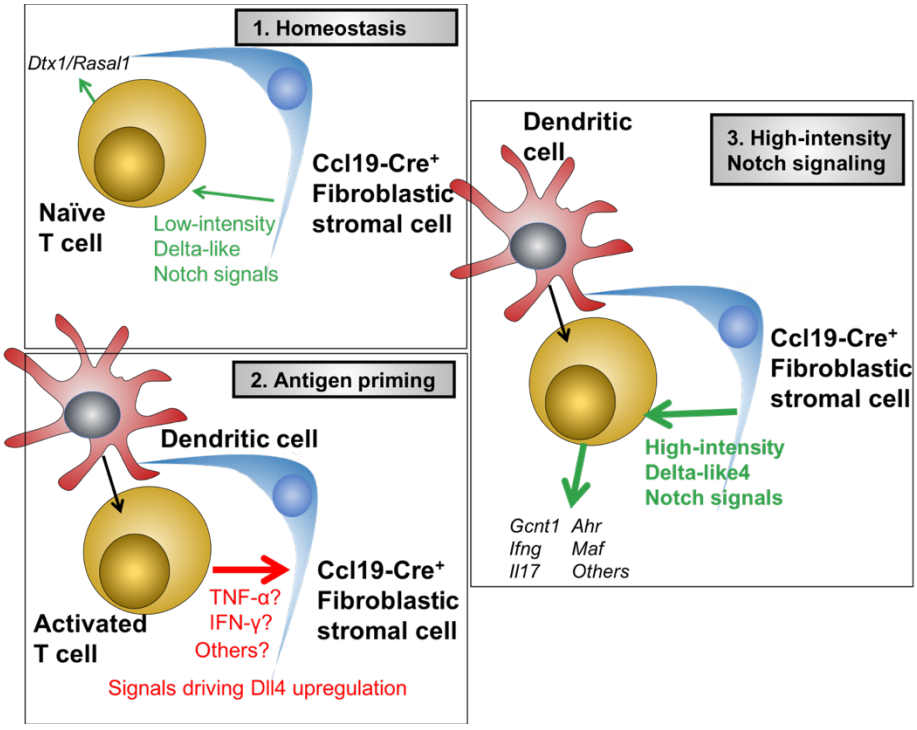

Fig 6.1 Proposed model of dynamic Notch signaling during T cell activation. (1) During recirculation through secondary lymphoid organs, naïve T cells interact with FRCs receiving Delta-like Notch ligands, which drives transcription of *Dtx1/Rasal1*. (2) During antigen priming, a T cell interacts with a dendritic cell or other APC inducing early activation-associated signals, such as TNF-α and IFN-γ that drive upregulation of Delta-like4 on FRCs. (3) Activated T cells continue to interact with FRCs, highly expressing Delta-like4, leading to the transcription of Notch target genes.

There is precedent for the concept that antigen-activated T cells control their own immunological niche. IL-17 derived from Th17 $CD4^+$ T cells cooperated with unknown inflammatory signals to drive survival and proliferation of FRCs. This, in turn, was required for expansion of the lymph node and subsequent B cell response (239). What might be the signal produced very early by alloreactive, but not syngeneic, T cells that drives upregulated expression of DLL4 in FRCs? We are currently exploring two candidates: TNF-α and IFN-γ. TNF-α has been shown to be produced within the first 5 hours of T cell activation (240), thus meeting the criteria to be a very early signal. While IFN-γ may not typically be thought to be released early after T cell activation, it has been shown that T cells can engage in autocrine IFN-γ signaling as soon as 12h after TCR stimulus (235). Based on our gene expression profiling, both TNF-α are IFN-γ are upregulated in alloreactive T cells at 42h post-transplant. Allo-BMT induced genes in FRCs after allo-BMT are also enriched for both IFN-γ and TNF-α gene-signatures by GSEA analysis **(Fig 6.2)**.

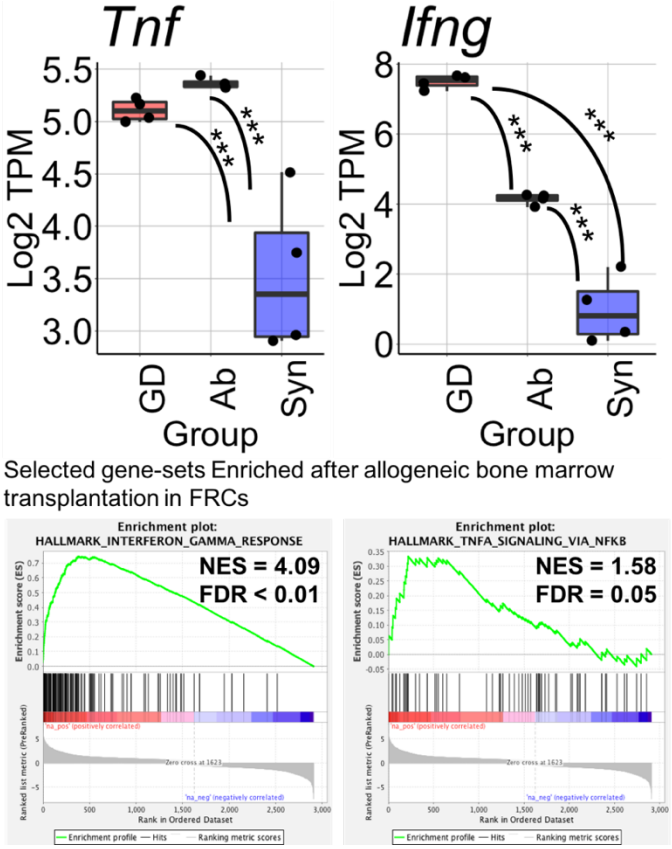

Fig 6.2 Potential IFN-γ and TNF-α cross-talk between alloreactive T cells and FRCs. Top. *Tnf* and *Ifng* transcript levels in 4C CD4+ alloreactive T cells at 42h post-transplant showing upregulation in alloreactive compared to syngeneic (Syn) transplant. *Tnf* is similarly upregulated irrespective of Notch blockade (GD v Ab) while *Ifng* is blunted with Notch blockade (GD v Ab). Bottom. GSEA analysis of genes differentially expressed in FRCs after allo-BMT showing enrichment for the "interferongamma_response" and "tnfa_signaling_via_nfkb" hallmark responses.

We are planning further experiments with T cells deficient in either TNF-α or IFN-γ to test if either signal could be important for DLL4 upregulation in FRCs. If neither signal regulates DLL4 upregulation, it will be interesting to profile the transcriptomic response of FRCs post allo-BMT, but now with allogeneic T cells deficient for both TNF-α and IFN-γ. Comparisons of the FRC gene signature in this setting to the gene signatures in the context of wild type allo-BMT, syngeneic-BMT, or myeloablative conditioning alone would reveal different gene response modules that may regulate DLL4 and other aspects of FRC biology.

We observed fine temporal control of DLL4 upregulation in FRCs. Surface expression, which was dramatically upregulated at 12h post-transplant returned to baseline levels by 36h post-transplant **(Chapter 4**, **Fig 4.2)**. This coincides with the time window during which we have shown that Notch signals are critical to drive T cell pathogenicity (25), as anti-DLL1/4 treatment provided limited clinical benefit if given 48h post allo-BMT. It will be interesting to further explore if this defined temporal pulse of DLL4 upregulation explains the time window of therapeutic anti-DLL1/4 intervention in alloreactive T cells. Once we identify signals that control DLL4 upregulation, we plan to use them to modify both the magnitude and temporal duration of DLL4 upregulation on FRCs to determine if this can control subsequent T cell responses.

What is the microanatomical localization of the DLL4^{hi} FRC niche both prior to and during allo-BMT? On baseline, we showed that DLL4 expression was predominantly restricted to MAdCAM-1^{-} CD157^{hi} FRCs, MAdCAM-1^{+} MRCs and FDCs by flow cytometry. We showed that *Dll4*-mCherry^{+} FRCs were enriched for both *Cxcl13* and *Tnfsf11* transcripts, markers of B-zone FRCs and MRCs. *Dll4*-mCherry^{-} CD157^{hi} FRCs, while low for *Dll4*, were enriched for transcripts such

as *Col14a, Slc7a11,* and *Stmn2*, all genes shown by single-cell RNAseq to be enriched in CCL19^{hi} T-zone FRCs (9). These observations imply that in resting lymph nodes many DLL4^{hi} FRCs are located far from the paracortex and the T cell zone. In fact, preliminary imaging studies in our lab have shown that *Ccl19-Cre* lineage-traced FRCs that were brightest for the *Dll4*-mCherry reporter were located close to the subcapsular sinus in resting lymph nodes and in interfollicular regions, consistent with MRCs and B-zone FRCs. Thus, paracortical T-zone FRCs may not express high levels of DLL4 on baseline. This might anatomically limit initial Notch-mediated priming of T cells in the T-zone during non-inflammatory response. In order to receive Notch signals, T cells may instead need to traffic towards the T-B border and interfollicular regions where DLL4^{hi} FRCs likely reside. Alternatively, strong initial TCR stimulus might lead to early production of signals that induce expression of DLL4 on T-zone FRCs, as we hypothesize it does in allo-BMT, providing a mechanism for antigen-mediated activation to drive subsequent Notch-dependent programming of T cells in the T-zone. We plan to study if T cell activation during immunization or anti-microbial responses also regulates DLL4 expression in FRCs, and if this regulation has consequences for the magnitude and quality of T cell responses.

The anatomical localization of DLL4 FRCs early after allo-BMT is unclear. We have previously detected DLL4 expression by immunofluorescence in splenic CD157^{hi} FRCs and CD21^{+} FDCs. Allo-BMT also dramatically alters the ultrastructure of FRC networks, increases relative FRC density, and changes surface maker expression of FRCs in the spleen and to a lesser degree in lymph nodes (25). Upregulated expression of DLL4 as detected by flow cytometry occurred predominantly in both MRCs and MAdCAM-1^{-} CD157^{hi} FRCs. This was documented as both an increase in the mean fluorescence intensity of DLL4 staining, but also as an increase in the

percentage of FRCs that were positive for any detectable surface DLL4 expression. Allo-BMT also drove upregulated expression of DLL4 in the FRC subsets that already express DLL4 at baseline, including MRCs and B-zone FRCs. However, it is unclear if allo-BMT also drives new FRC subsets in different microanatomical niches, such as the T-zone, to upregulate DLL4 expression. Curiously, we saw dramatic upregulation of endogenous *Dll4* mRNA in FRCs that were negative for *Dll4*-driven mCherry reporter expression. This suggests that *Dll4*-mCherry$^-$ FRCs or a subset of *Dll4*-mCherry$^-$ FRCs rapidly increased transcription of *Dll4* prior to transcription and expression of the mCherry protein. Thus, DLL4 expression, instead of being part of the cellular identity of particular FRC subsets, might instead be rapidly driven by the cellular activation status early after allo-BMT. This is also evidenced by the low-degree of global transcriptional differences between *Dll4*-mCherry$^+$ and *Dll4*-mCherry$^-$ CD157^{hi} FRC subsets on principal component analysis compared to differences between both CD157^{hi} FRC subsets and CD157$^-$ FRCs. These findings also urge caution when using the *Dll4-mCherry* reporter as marker of endogenous *Dll4* expression in settings where *Dll4* transcription may be rapidly regulated, such as after allo-BMT.

We have yet to define what physical interactions allow T cells to engage in contacts with FRCs in order to receive Notch signals. We hypothesized that expression of CCL19 may attract naïve CCR7$^+$ T cells to FRCs. CXCL13 expression may also play a role in attracting CXCR5$^+$ T cell subsets close to or into B cell follicles (e.g. for T follicular helper differentiation). In allo-BMT, increased *Dll4* expression also coincided with upregulation of many inflammatory molecules important in the immunological response including CXCL9, CXCL10, and CXCL11 **(Fig 6.3)**. Thus, these molecules may attract and retain recently antigen-activated CXCR3$^+$ T cells allowing

sustained Notch signaling (217), although it is unclear if and how FRC-derived CXCL9/10/11 might compete or cooperate with the same set of chemokines also produced by dendritic cells. It is also unclear if integrin interactions are required. FRCs express high levels of ICAM-1 and VCAM-1, while MRCs, the stromal subset with highest levels of DLL4, also express MAdCAM-1. We are planning to conduct T cell-specific loss-of-function experiments to determine if particular chemokine receptors and integrin interactions might facilitate delivery of Notch signals to T cells.

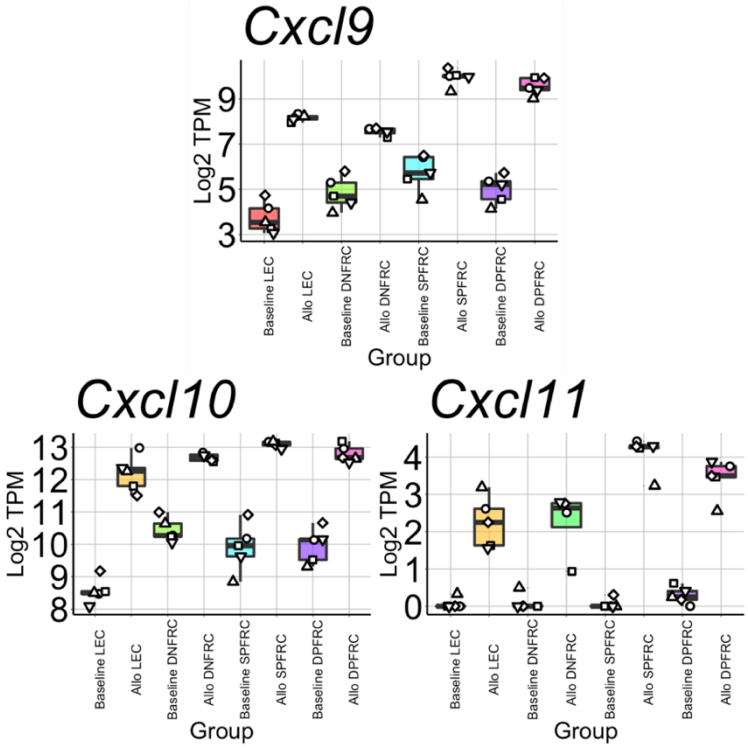

Fig 6.3 Upregulated expression of CXCL9/10/11 in lymph node stromal cell subsets post allo-BMT.

We previously documented a minor but still important role of DLL1 signals in driving T cell alloreactivity (29). *Dll1* expression was not regulated by allo-BMT in FRCs, but Ccl19-Cre lineage traced CD157^{hi} FRCs still expressed transcripts **(Chapter 4, Fig 4.1)**. It is unclear how DLL4 vs. DLL1 expression in FRCs might be controlled. Immunofluorescence imaging of mice with a *Dll1*-mCherry BAC reporter or an eGFP reporter knocked into the endogenous *Dll1* locus revealed

minimal expression of either reporter in FRC subsets in peripheral lymph nodes. However, both reporters revealed DLL1-reporter positive fibroblastic cells in the spleen. Ccl19-Cre lineage traced cells are also known to control marginal zone B cell and ESAM^{hi} cDC2 homeostasis through DLL1 in the spleen (17) but not lymph nodes, where neither cell subset exists. We plan to further explore the differential effects of DLL4 versus DLL1 with two novel mouse genetic systems that allow us to: 1. Swap the ectodomains of each ligand and 2. Overexpress each ligand in a Cre recombinase dependent manner. Such studies will determine if the dominance of DLL4 over DLL1 in control of T cell responses is due to differences in expression, microanatomical localization, or biochemical differences in how each ligand signals to Notch receptors (241–243).

The transcriptomic profiling described in this dissertation has already been a useful hypothesis-generating tool to launch further exploration of FRC biology in GVHD. This has allowed us to nominate other potential immunological niche factors that FRCs provide to alloreactive T cells. Candidate genes upregulated by FRCs in allo-BMT that are worth exploring include *Il15ra*, which is critical to present IL-15 *in trans* to other cells. IL-15 signaling will be interesting to explore as it has been shown to be differentially regulate GVHD versus graft-versus-leukemia effect (218). Regulation of genes involved in the MHC class I and class II antigen presentation pathways is also worth further exploration. We found that MHC class II antigen presentation by FRCs was dispensable to prime alloreactive T cells CD4$^+$ T cells. However, both MHC class II and MHC class I could be important to facilitate alloreactive CD4$^+$ and CD8$^+$-mediated killing of FRCs in GVHD. Such immune-mediated damage to FRCs was shown recently to contribute to the profound dysregulation of immunity seen in chronic GVHD (101, 102). Further work is required to fully understand how allo-BMT impacts FRC biology. We are planning imaging studies to assess the

microanatomical localization of DLL4-expressing FRCs after allo-BMT, as well as single-cell transcriptomic profiling, to understand further how the heterogeneity of FRC subsets might evolve in this context.

Notch transcriptional targets in mature T cells

In **Chapter 5**, I examined the role of the Notch signaling pathway in regulating naïve $CD4^+$ T cells. Notch signals were delivered to T cells by FRCs in secondary lymphoid organs and only controlled transcription of two genes in naïve T cells: *Dtx1* and its neighboring gene *Rasal1*. I compared this limited Notch-dependent transcriptomic footprint to the much larger Notch-dependent transcriptomic footprint seen in alloantigen-activated $CD4^+$ T cells (149). We believe that additional study on how the Notch transcriptional machinery differentially acts in naïve T cells versus T cells at different stages of activation will provide key mechanistic insights as to how both T cell subsets are regulated, but also as to how Notch transcriptional regulation occurs in general.

Notch mediates direct transcriptional "canonical" effects through the ICN/RBP-Jκ/MAML transcriptional complex. Direct transcriptional targets of Notch signaling have been carefully dissected in hematological malignancies, including T-ALL and B cell malignancies, using gamma-secretase inhibitor washout assays and ChIP-seq for members of the core Notch transcriptional complex, including RBP-Jκ and ICN itself (244, 245). Such techniques are difficult to execute in mature T cells, especially given the low numbers of antigen-specific T cells recovered from in vivo experiments early after antigen activation. Yet, genome-wide information will be essential to fully understand the role of Notch signaling in this context.

Notch signaling regulates T cell responses in diverse contexts and in ways that can seem contradictory (44). Only recently have the transcriptomic effects of Notch signaling in mature T cells been explored using loss-of-function methods. While some common effects were seen, Notch signals drove largely distinct signatures as it does in other biological contexts (31, 53, 149). Thus, Notch has context and cell-type specific effects. How can Notch accomplish such diverse transcriptional regulation of T cell subsets? One model is that Notch signals drive a similar set of direct transcriptional targets in all T cell subsets, irrespective of immunological context. The diverse phenotypic effects of Notch signaling would be secondary to other partners, which would be controlled by the cell type, cytokine milieu, or strength of TCR signaling. To ascertain what might be common Notch transcriptional targets, we identified genes that were consistently regulated by Notch loss-of-function in three separate transcriptomic profiling experiments. One was our laboratory's data examining the role of Notch signals in alloreactive $CD4^+$ T cells, which predominantly represents a Th1 response (149). The second was generated in a $CD4^+$ T cell Th2 allergic response to house dust mites (53). The third was derived from a $CD8^+$ T cell response to viral infection (unpublished data, in collaboration with the Nathalie Labrecque, University of Montreal). Consistent with our studies in **Chapter 2**, we found that *Gcnt1* expression was regulated in all three contexts **(Table 6.1 A)**. The previously described Notch targets *Trib2* and *Dtx1* were also regulated in all three contexts. Interestingly, expression of two transcription factors was consistently downregulated with Notch loss-of-function, including the *Ahr* (Aryl-hydrocarbon receptor) and *Maf* (c-MAF), both of which have been shown to be regulated by Notch in other T cell contexts (54, 246). Future research should evaluate if Notch's different transcriptional effects could be due to how *Ahr* and *Maf* cooperate with other cell-type and immunologic-context specific transcription factors.

A. Transcripts down with Notch loss of function	*Ahr, Dgkh, Dtx1, Frmd4b, Gcnt1, Il10, Maf, Trib2*
B. Transcripts up with Notch loss of function	*Ltb, Itgb1, Ncf1, Ramp1, Rgs2, Sema4c, Tnfsf10*

Table 6.1 A common Notch transcriptional signature in activated T cells

Another model for how Notch controls transcription is that the direct transcriptional targets of the Notch transcriptional complex may vary depending on the epigenetic landscape of the cell. In *Drosophila,* Notch has been shown to only substantially increase transcription at enhancers already occupied by tissue-specific transcription factors (41). Furthermore, the fact that Notch signals have a limited effect on naïve $CD4^+$ T cells could reflect the closed chromatin state of these T cells. Notch transcriptional complexes might only have access to multiple Notch-responsive enhancers once T cell activation has dramatically reshaped the chromatin landscape (232). Cell-type specific (e.g. short-lived effector vs. memory precursor $CD8^+$ vs. $CD4^+$ Th1, Th2, Th17, Tfh, Treg, etc.) epigenetic regulation may further determine what enhancers Notch binds and regulates, as others have proposed (50). In this model, Notch would act as a transcriptional co-stimulator only at "primed enhancers" (41). In reality, a combination of the two models involving both ubiquitous and context-specific Notch transcriptional targets may better explain the effects of Notch in T cell biology. We are actively developing methods to further explore how Notch might directly regulate its transcriptional targets within the epigenetic landscape of mature T cells, including low cell number input cut-and-run techniques, to elucidate where the Notch transcriptional complex binds.

In **Chapter 3**, I showed that Notch signals delivered by FRCs drove a gut homing program in alloreactive effector T cells including the acquisition of α4β7, an integrin critical for T cell migration into intestinal target tissues during GVHD. However, it is not clear how this is regulated by Notch signals. When we examined gene expression of *Itga4* and *Itgb7* in our transcriptomic

profiling of alloreactive T cells, both were strongly downregulated with alloantigen activation, and Notch inhibition mildly increased the abundance of transcripts from both genes (149) (**Fig 6.4)**. Interestingly, *Itgb1* is consistently upregulated with Notch loss-of-function in multiple immunological contexts **(Table 6.1 B)**, suggesting a conserved role of Notch in downregulating *Itgb1* in antigen activated T cells. High expression of integrin β1 has been shown to negatively regulate the expression of α4β7 by outcompeting β7 for pairing with α4 (201). While retinoic acid signaling has been shown to control α4β7 expression (and acquisition of other gut-homing molecules in T cells) (170), this was accomplished through transcriptional regulation of *Itga4* not *Itgb1* or *Itgb7* (201). Thus, by decreasing levels of *Itgb1,* Notch signaling may represent a novel mechanism to indirectly upregulate α4β7 expression independently of retinoic acid by increasing the pairing frequency of α4 with β7. We are currently planning experiments to test the effects of Notch inhibition on expression of individual integrin chains to determine if this mode of regulation is occurring.

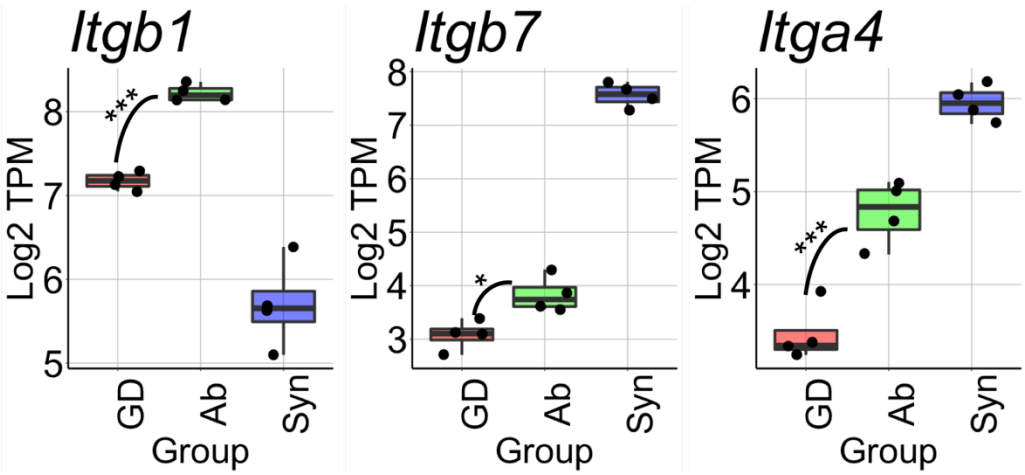

Fig 6.4 Regulation of integrin transcription in alloreactive CD4$^+$ T cells. Expression of Itgb1, Itgb7, and Itga4 in 4C CD4+ TCR transgenic alloreactive T cells(149) at 42h post allogeneic or syngeneic-BMT. Ab = anti-DLL1/4 treatment. GD = isotype control. Syn = syngeneic-BMT.

The role of Notch signals from the FRC niche in broader immunological contexts

Our studies defined a dominant role for FRC-derived Notch ligands compared with other cellular subsets in allo-BMT, regardless of the degree of conditioning intensity **(Chapter 2)**. FRCs were also non-redundant sources of Notch ligands after DC immunization even when DCs expressed high levels of DLL4 **(Chapter 4)**. Finally, FRCs provided Notch ligands independently of antigen to naïve $CD4^+$ T cells **(Chapter 5).** This is consistent with work documenting the critical role of FRCs in driving T follicular helper cell differentiation through Delta-like4 ligands (17), while dendritic cells were largely dispensable for this function (246). Together, these findings suggest a three-cell model of T cell priming where distinct cell-to-cell contacts with both APCs and FRCs control the outcome of T cell differentiation and function.

Yet, it is unclear if this model extends to other T cell immune responses. Much of the evidence that antigen-presenting cells are a source of Notch ligands has been correlative or from in vitro co-culture experiments. However, some studies have used in vivo genetic loss-of-function approaches to show roles for dendritic cell-derived Notch ligands in regulating T cell immunity. For example, H-Y antigen-specific Marilyn TCR transgenic $CD4^+$ T transferred into male recipients with CD11c-Cre deletion of *Dll4* expressed less activation markers and were smaller compared to cells transferred into Cre- controls (49). Another study showed that DLL1 expressed by DCs was critical for the survival of memory $CD4^+$ T cells (247). Yet another study showed that deletion of *Dll1* but not *Jag2* in DCs impaired tumor clearance (128). Our laboratory has also assessed the necessity of Ccl19-Cre^+ FRC-derived Notch ligands in a $CD4^+$ T cell-driven model of experimental autoimmune encephalitis, which we have previously shown depends on Notch (133). In this model, mice still had clinical disease when Notch ligands were deleted from FRCs. This suggested that

there may be alternative sources of pathogenic Notch ligands, perhaps in the blood brain barrier, that drove pathogenic T cell function (unpublished data).

Altogether, we continue to uncover new roles for FRC-derived Notch ligands in many aspects of T cell immunobiology. In a heterotopic model of cardiac allograft rejection that depends on Notch signals in T cells, we showed that Delta-ligands from FRC controlled pathogenesis (unpublished data). In ongoing collaborative studies, we have identified that Notch-ligands from splenic FRCs control the balance of progenitor versus terminally exhausted $CD8^+$ T cells during chronic viral infection. Current experiments are ongoing to understand the contribution of FRC-derived Notch ligands in driving $CD8^+$ T cell responses to acute bacterial and viral infections.

FRCs control other immunological processes through Notch signals. Delta-like1 ligands from FRCs control the development and maintenance of marginal zone B cells and $ESAM^{hi}$ cDC2 subsets in the spleen (17). Thus, we are exploring if elimination of Delta-like ligands from FRCs could impact DC function in our DC immunization model. Ongoing ligand-dependent Notch signals are critical in sustaining certain hematological malignancies, including those driven by mutations in the PEST domain of Notch. These mutations decrease the degradation of intracellular Notch, generating an oncogenic gain-of-function allele. However, these Notch mutants still require ligand to drive the initial proteolytic cleavage of the Notch receptor. Close observations of lymph node biopsies from angioimmunoblastic T-cell lymphoma and chronic lymphocytic leukemia with and even without PEST-domain mutations have revealed distinct positive staining for cleaved intracellular Notch in cancer cells within the lymph node, while cancer cells that had traversed the lymph node capsule into extra-nodal tissue lacked intracellular Notch staining (248). If FRCs

provide the critical Notch inputs to sustain Notch-driven malignancies, it would suggest another therapeutic application of targeting either stromal ligands or the pathways controlling their expression.

Chapter 7

Materials and Methods

Mice

C57BL/6 (B6, H-$2^{b/b}$, Thy1.2), C57BL/6 x BALB/cJ F1 (CBF1, H-$2^{b/d}$, Thy1.2), C57BL/6-Thy1.1/2 (B6, H-$2^{b/b}$, Thy1.1/2), and B10.D2 (H-$2^{d/d}$) mice were bred at the University of Michigan and the University of Pennsylvania. BALB/cJ mice were purchased from Jackson Laboratories. *Itgb7*$^{-/-}$ (249) mice were purchased from Jackson Laboratories and bred in house. Mx1-Cre, Ccl19-Cre (6), Cd4-Cre, *Dll1*$^{f/f}$, *Dll4*$^{f/f}$, *Notch1*$^{f/f}$, *Notch2*$^{f/f}$ and *ROSA26*^{DNMAMLf},*Rosa26*^{eYPF} alleles (abbreviated DNMAML) were described previously (25, 28). 4C *Rag1*$^{-/-}$TCR transgenic mice on the B6 background reactive to I-A^d were previously described (250). *Gcnt1*-deficient mice were previously described (251). OT-I TCR transgenic mice recognize the Ovalbumin (OVA) peptide SIINFEKL and were maintained on the B6 background. E8I-Cre$^+$*Notch1*$^{f/f}$*Notch2*$^{f/f}$ lack *Notch1/2* genes in $CD8^+$ T cells, as described (45). TEa TCR transgenic mice were a gift from Dr. Todd Brennan (Cedar-Sinai Medical Center) and were previously described (66). Mice carrying a Delta-like4-mCherry BAC reporter construct were a gift from Dr. Iannis Aifantis (NYU) and were previously described (207). Mice with a conditional I-A^{bflox} allele were previously described (90). For transplantation experiments, cohoused littermate controls were used as donors and recipients at the University of Michigan or the University of Pennsylvania, per protocols approved by the University of Pennsylvania's Office of Regulatory Affairs and the University of Michigan's Committee on Use and Care of Animals. For *Listeria monocytogenes*

and LCMV infection, experimental mice were housed at the Maisonneuve-Rosemont Hospital Research Center Facility, Montreal, QC and treated in accordance with the Canadian Council on Animal Care guidelines.

Bone marrow transplantation, systemic antibody-mediated Notch inhibition, and GVHD assessment.

For transplantation, CBF1 or C57BL/6 recipients were irradiated using a Cesium-137 source with titrated doses: high-intensity myeloablative conditioning (11 Gy, split into two doses separated by 3h), reduced-intensity non-myeloablative conditioning (3 Gy), or no conditioning. BALB/c recipients received 8 Gy in a single dose. Recipients were 8-16 weeks old. Both female and male mice were used as recipients and equally distributed among experimental groups. T cell-depleted BM (TCD BM) prepared with anti-Thy1.2 antibodies and complement (Cedar Lane Laboratories) was injected i.v. with or without splenocytes and/or purified T cells, as described (29). Cell numbers infused for each experiment are noted in the text and figure legends. For experiments with 4C or TEa $CD4^+$ T cells, T cells were purified with negative magnetic selection for $CD4^+$ T cells (Stem Cell Technologies) and labeled with eFluor450 cell proliferation dye. For polyclonal experiments, wild-type, *Gcnt1*-deficient, *Itgb7*$^{-/-}$, or dnMAML T cells were purified with negative magnetic selection for T cells (Stem Cell Technologies) and labeled with eFluor450 or CFSE cell proliferation dye (Invitrogen). For long-term experiments, mice received noted doses of splenocytes and/or lymph node cells with TCD BM. Clinical GVHD scores and weight changes were monitored at least once weekly, as described (103). In selected experiments, recipient mice received humanized IgG1 mAbs specific for DLL1 or DLL4 i.p. (5 mg/kg) (29). A human IgG1 Ab to Herpes Simplex Virus gD glycoprotein was used as isotype control. Each antibody batch

was tested for specificity and efficacy by assessing loss of Dll4-dependent T cell progenitors (36) or DLL1-dependent marginal zone B cells in vivo (252).

BMDC generation, immunization, Listeria monocytogenes infection, chronic Lymphocytic Choriomeningitis Virus infection (LCMV clone 13), and analysis of T cell response.

Bone-marrow derived DCs were generated with GM-CSF and IL-4 as previously described(45), matured with LPS (100 ng/mL; Sigma) and the TLR7/8 agonist R-848 (100 ng/mL; Sigma) and loaded with $OVA_{257-264}$ peptide (SIINFEKL, 2 μg/mL; Sigma). A total of $5x10^5$ DCs were i.v. injected. For experiments with OT-I cells, 5 x 10^4 purified (Stem Cell Technologies) $CD45.1^+$ OT-I $CD8^+$ T cells were adoptively transferred the day before DC immunization. For FLT3L-BMDC experiments, FTL3L was added in culture as described (211) and DCs were stimulated with LPS + R-848. Cells were then purified via positive $CD11c^+$ selection prior to use in vitro or in vivo. To assay anti-infectious response, *L. monocytogenes* expressing ovalbumin (Lm-OVA) was grown, as described (45). A sublethal dose of 2 x 10^3 CFUs was i.v. injected. The endogenous $CD8^+$ T cell response was monitored with K^b-OVA staining. To monitor responses to chronic viral infection, mice were infected with LCMV clone 13 (2 x 10^6 PFU i.v.) and virus-specific $CD8^+$ T cells were assayed at day 8 and day 30 post-infection with K^b-gp33 tetramer staining.

In vitro 4C, TEa, OT-I, polyclonal$^+$ T cell stimulation on OP9 stroma.

OP9 cell lines overexpressing DLL1 and DLL4 have been described before (253, 254). The night before the experiment, 1 x 10^4 OP9 cells were seeded onto 96-well flat-bottom plates in 20% FCS + αMEM. 4C wild-type $CD4^+$ T cells and 4C dnMAML $CD4^+$ T cells were purified, labeled with eFluor450 proliferation dye and plated in a ratio of 2:2:1 with BMDCs from poly(I:C)-induced

Mx1-Cre$^{+/-}$ *Dll1$^{f/f}$ Dll4$^{f/f}$* CBF1 mice in complete RPMI (10% FCS) + 2β-mercaptoethanol. Blocking antibodies (anti-DLL1, anti-DLL4, both, or isotype control) were added at a concentration of 25 μg/mL. Cells were harvested at day 4 post-plating. In other experiments purified TEa CD4$^+$ cells were used with CBF1 BMDCs. In yet other experiments, purified polyclonal C57BL/6 CD4$^+$ cells were stimulated with BALB/c BMDCs. In selected experiments, purified CD8$^+$ OT-I T cells were stimulated with C57BL/6 BMDCs pulsed with SIINFEKL peptide.

Preparation of single-cell suspensions from lymphoid and GVHD target organs.

Single-cell suspensions of cells from spleen, mesenteric lymph node, or pooled peripheral lymph nodes (cervical, brachial, axial, inguinal) were prepared by physical disruption through 70 μm cell strainers. Single-cell suspensions were prepared from liver (132), intestinal lamina propria, and intestinal epithelium (28) as previously described.

Antibodies, flow cytometry, and cell sorting.

The following antibodies were from Biolegend: anti-CD4 (clone GK1.5); CD8α (clone 53-6.7); CD44 (clone IM7); CD25 (clone PC61); CD45.1 (clone A20); CD45.2 (clone 104); Thy1.1 (clone OX-7); Thy1.2 (clone 30-H12); H-2K^b (clone AF6-88.5); H-2K^d (clone SF1-1.1); IFNγ (clone XMG1.2); IL-17A (clone TC11-18H10.1); pan-CD43 (clone S11), core-2 O-glycosylation CD43 (clone 1B11); KLRG1 (clone 2F1); CD127/IL7Rα (clone A7R34); CD11c (clone N418); MHC II (clone M5/114.15.2); PDPN/gp38 (clone 8.1.1); CD31 (clone 390); Ter119 (clone TER-119); CD157 (clone BP-3); CD21/35 (clone 7E9); CD45 (clone 30-F11); MAdCAM-1 (clone MECA-367); VCAM-1 (clone 429); I-A^b (clone KH74); I-A^d (clone 39-10-8); α4β7 (clone DATK32); CD103 (clone 2E7); CD24 (clone 30-F1), SIRP1α (clone P84). Anti-FoxP3 (clone FJK-16s) was from eBioscience. Anti-Vβ13 (clone MR12-3) and Dll4 (clone 9A1.5) was from BD Biosciences.

SIINFEKL peptide loading on H-2K^b MHC and conjugation to PE was done as previously described (255). Non-viable cells were excluded from analysis with Zombie Aqua Fixable Viability Dye (Biolegend), or DAPI (Sigma-Aldrich). For intranuclear staining, FoxP3/Transcription Factor Staining Buffer (eBioscience) set was used per manufacturer's protocol. Assessment of intracellular T cell cytokine production after short ex vivo stimulation was previously described (25). Flow cytometric analysis was performed using a 4 or 5-laser Fortessa (BD). Sorting of T cells was performed using a 4-laser FACSAria II/III (BD). Alloreactive or naive 4C T (Thy1.1$^+$ CD4$^+$), naïve OT-I CD8$^+$ T cells (CD8$^+$CD44^{lo}), and day 3 OT-I effector CD8$^+$ T cells (CD8$^+$CD45.2$^+$CD44^{hi}) were sorted directly into TRIzol Reagent (Invitrogen).

Lymph node stromal cell preparation and sorting

Stromal cells were isolated as described previously (25). Briefly, pooled peripheral lymph nodes (cervical, axial, brachial, inguinal) were harvested from mice, diced into small slices with a scalpel, and incubated at 37C for 15 mins in RPMI media containing 1mg/mL collagenase IV (Invitrogen), 40 μg/mL DNAse I (Roche), 5% of FBS, and 25 mM HEPES. Samples were pipetted gently and incubated for two more rounds of 15 min digestion. After each round, the supernatant was collected and filtered into flow cytometry buffer, replacing digestion media. Stromal cell populations were sorted directly into TRizol.

Quantitative real-time PCR

Total RNA was extracted from TRIzol with phenol/chloroform and purified with RNeasy Micro Kit (QIAGEN). cDNA was generated with SuperScript II (Invitrogen) using poly-dT primers and subjected to quantitative PCR with TaqMan reagents (Applied Biosystems). Gene expression analysis was performed using the following primers: *Gcnt1* (Mm02010556_s1); *St3gal1*

(Mm00501483_m1)*;* *Hprt* (Mm03024075_m1); *Dll4* (Mm00444619_m1). Relative gene expression was determined using the ΔΔCt method, with normalization to *Hprt.*

RNA-sequencing

Cell populations were sorted with a BD ARIA II directly into TRIzol supplemented with 0.5% 2-ME and then frozen at -80C. RNA was extracted per the published TRIzol protocol (Thermo-Fisher) using glycogen as a carrier. RNA abundance was quantified using Qubit RNA high sensitivity fluorometric assay. Selected RNA samples were assessed for quality by Agilent TapeStation using HSRNA assay. The Takara Clonetech SMART-seq HT RNA kit was used to synthesize cDNA using recommended inputs. RNA-seq libraries were prepared using the Illumina Nextera XT kit with 150ng cDNA input. Libraries were individually quality controlled and quantified using a TapeStation DNA assay and Qubit DNA fluorometric assay. The molarity of each library was calculated based on these data and libraries were pooled at equal molar ratios prior to sequencing on an Illumina Nextseq500 (75 bp SE v 2).

Pseudoalignment and gene expression analysis

Transcript abundance using calculated using pseudoalignment to an index built from the mouse transcriptome by the Kallisto program (256). For pseudoalignment of sequences from lymph node stromal cells samples, the sequences for mCherry, eYFP, and human CD4 were added to the index. Transcript per million (TPM) values were then log2 transformed, normalized, and genes with low expression were filtered out. Gene-wise expression was then fit to a linear model by empirical Bayes method using the Voom (257) and Limma (258) R packages. Differential gene expression was defined as a Benjemini and Hochberg corrected *p*-value of <0.01 and a log2 fold change >1.

Gene Set Enrichment Analysis

GSEA was completed using the Broad institute GSEA program against curated genes sets with a pre-linked list containing differentially expressed genes weighted for log2 fold change (259).

Statistical analysis

Sample size for in vivo mouse experiments was determined empirically based on prior experience of known effect sizes and variation and used to calculate power with "pwr" statistical package in R. All statistical tests were performed using Prism software (GraphPad Prism version 8). Unless otherwise noted, data with more than one group was analyzed for differences with one-way ANOVA or two-way ANOVA depending on the number of factors. If a factor significantly explained the variation of the data multiple comparisons between groups were made with Tukey's test assuming $\alpha = 0.05$ and adjusted p-values were reported. The multiple comparisons performed are represented in the figures by lines between groups. Data with only two groups were compared with an unpaired, 2-tailed Student's *t*-test. If variance between the two groups differed significantly by an F test, Welch's correction for *t*-tests was applied. Survival curves were compared using a log-rank (Mantel-Cox) test. Unless otherwise noted graphs were generated in GraphPad Prism and presented as mean +/- one standard deviation. Unless otherwise noted, adjusted p-values for comparisons were reported as *p<0.05, **p<0.01, ***p<0.001.

References

1. Schofield, R. 1977. The relationship between the spleen colony-forming cell and the haemopoietic stem cell. *Blood Cells* 4(1-2): 7-25.

2. de Cuevas, M., and E. L. Matunis. 2011. The stem cell niche: Lessons from the Drosophila testis. *Development* 138: 2861–2869.

3. Morrison, S. J., and D. T. Scadden. 2014. The bone marrow niche for haematopoietic stem cells. *Nature* 505: 327–334.

4. Plaks, V., N. Kong, and Z. Werb. 2015. The cancer stem cell niche: How essential is the niche in regulating stemness of tumor cells? *Cell Stem Cell* 16: 225–238.

5. Taylor, C. T., and S. P. Colgan. 2017. Regulation of immunity and inflammation by hypoxia in immunological niches. *Nat. Rev. Immunol.* 17: 774–785.

6. Chai, Q., L. Onder, E. Scandella, C. Gil-Cruz, C. Perez-Shibayama, J. Cupovic, R. Danuser, T. Sparwasser, S. Luther, V. Thiel, T. Rülicke, J. Stein, T. Hehlgans, and B. Ludewig. 2013. Maturation of Lymph Node Fibroblastic Reticular Cells from Myofibroblastic Precursors Is Critical for Antiviral Immunity. *Immunity* 38: 1013–1024.

7. Schaeuble, K., M. R. Britschgi, L. Scarpellino, S. Favre, Y. Xu, E. Koroleva, T. K. A. Lissandrin, A. Link, M. Matloubian, C. F. Ware, S. A. Nedospasov, A. V. Tumanov, J. G. Cyster, and S. A. Luther. 2017. Perivascular Fibroblasts of the Developing Spleen Act as LTα1β2-Dependent Precursors of Both T and B Zone Organizer Cells. *Cell Rep.* 21: 2500–2514.

8. Cheng, H. W., L. Onder, M. Novkovic, C. Soneson, M. Lütge, N. Pikor, E. Scandella, M. D. Robinson, J. ichi Miyazaki, A. Tersteegen, U. Sorg, K. Pfeffer, T. Rülicke, T. Hehlgans, and B. Ludewig. 2019. Origin and differentiation trajectories of fibroblastic reticular cells in the splenic white pulp. *Nat. Commun.* 10: 1–14.

9. Rodda, L. B., E. Lu, M. L. Bennett, A. D. Luster, C. J. Ye, J. G. Cyster, L. B. Rodda, E. Lu, M. L. Bennett, C. L. Sokol, X. Wang, S. A. Luther, B. A. Barres, A. D. Luster, C. J. Ye, and J. G. Cyster. 2018. Single-Cell RNA Sequencing of Lymph Node Stromal Resource Single-Cell RNA Sequencing of Lymph Node Stromal Cells Reveals Niche-Associated Heterogeneity. *Immunity* 48: 1014-1028.

10. Onder, L., P. Narang, E. Scandella, Q. Chai, M. Iolyeva, K. Hoorweg, C. Halin, E. Richie, P. Kaye, J. Westermann, T. Cupedo, M. Coles, and B. Ludewig. IL-7-producing stromal cells are critical for lymph node remodeling. *Blood* 120: 4675–4683.

11. Cremasco, V., M. C. Woodruff, L. Onder, J. Cupovic, J. M. Nieves-Bonilla, F. A. Schildberg, J. Chang, F. Cremasco, C. J. Harvey, K. Wucherpfennig, B. Ludewig, M. C. Carroll, and S. J. Turley. 2014. B cell homeostasis and follicle confines are governed by fibroblastic reticular cells. *Nat. Immunol.* 15: 1–11.

12. Rodda, L. B., O. Bannard, B. Ludewig, T. Nagasawa, and J. G. Cyster. 2015. Phenotypic and Morphological Properties of Germinal Center Dark Zone Cxcl12-Expressing Reticular Cells. *J. Immunol.* 195: 4781–4791.

13. Wang, X., B. Cho, K. Suzuki, Y. Xu, J. A. Green, J. An, and J. G. Cyster. Follicular dendritic cells help establish follicle identity and promote B cell retention in germinal centers. *J. Exp. Med.* 208: 2497–2510.

14. Huang, H. Y., A. Rivas-Caicedo, F. Renevey, H. Cannelle, E. Peranzoni, L. Scarpellino, D. L. Hardie, A. Pommier, K. Schaeuble, S. Favre, T. K. Vogt, F. Arenzana-Seisdedos, P. Schneider, C. D. Buckley, E. Donnadieu, and S. A. Luther. 2018. Identification of a new subset of lymph node stromal cells involved in regulating plasma cell homeostasis. *Proc. Natl. Acad. Sci. U. S. A.* 155(29): 6826-6835.

15. Katakai, T. 2012. Marginal reticular cells: a stromal subset directly descended from the lymphoid tissue organizer. *Front. Immunol.* 3: 200.

16. Jarjour, M., A. Jorquera, I. Mondor, S. Wienert, P. Narang, M. C. Coles, F. Klauschen, and M. Bajénoff. 2014. Fate mapping reveals origin and dynamics of lymph node follicular dendritic cells. *J. Exp. Med.* 211: 1109–22.

17. Fasnacht, N., H.-Y. Y. Huang, U. Koch, S. Favre, F. Auderset, Q. Chai, L. Onder, S. Kallert, D. D. Pinschewer, H. R. MacDonald, F. Tacchini-Cottier, B. Ludewig, S. A. Luther, and F. Radtke. 2014. Specific fibroblastic niches in secondary lymphoid organs orchestrate distinct Notch-regulated immune responses. *J. Exp. Med.* 211: 2265–79.

18. Siegert, S., H.-Y. Huang, C.-Y. Yang, L. Scarpellino, L. Carrie, S. Essex, P. J. Nelson, M. Heikenwalder, H. Acha-Orbea, C. D. Buckley, B. J. Marsland, D. Zehn, and S. A. Luther. 2011. Fibroblastic reticular cells from lymph nodes attenuate T cell expansion by producing nitric oxide. *PLoS One* 6: e27618.

19. Lukacs-Kornek, V., D. Malhotra, A. L. Fletcher, S. E. Acton, K. G. Elpek, P. Tayalia, A. Collier, and S. J. Turley. Regulated release of nitric oxide by nonhematopoietic stroma controls expansion of the activated T cell pool in lymph nodes. *Nat. Immunol.* 12: 1096–1104.

20. Schaeuble, K., H. Cannelle, S. Favre, H. Y. Huang, S. G. Oberle, D. E. Speiser, D. Zehn, and S. A. Luther. 2019. Attenuation of chronic antiviral T-cell responses through constitutive COX2-dependent prostanoid synthesis by lymph node fibroblasts. *PLoS Biol.* 17(7): e3000072

21. Brown, F. D., D. R. Sen, M. W. LaFleur, J. Godec, V. Lukacs-Kornek, F. A. Schildberg, H. J. Kim, K. B. Yates, S. J. H. Ricoult, K. Bi, J. D. Trombley, V. N. Kapoor, I. A. Stanley, V. Cremasco, N. N. Danial, B. D. Manning, A. H. Sharpe, W. N. Haining, and S. J. Turley. 2019. Fibroblastic reticular cells enhance T cell metabolism and survival via epigenetic remodeling. *Nat. Immunol.* 20: 1668-1680.

22. Nakayama, Y., C. C. Brinkman, and J. S. Bromberg. 2015. Murine Fibroblastic Reticular Cells From Lymph Node Interact With CD4+ T Cells Through CD40-CD40L. *Transplantation* 99(8): 1561-1567.

23. Malhotra, D., A. L. Fletcher, and S. J. Turley. 2013. Stromal and hematopoietic cells in secondary lymphoid organs: Partners in immunity. *Immunol. Rev.* 251(1): 160-176.

24. Fletcher, A. L., V. Lukacs-Kornek, E. D. Reynoso, S. E. Pinner, A. Bellemare-Pelletier, M. S. Curry, A.-R. R. Collier, R. L. Boyd, and S. J. Turley. 2010. Lymph node fibroblastic reticular cells directly present peripheral tissue antigen under steady-state and inflammatory conditions. *J. Exp. Med.* 207: 689–697.

25. Chung, J., C. L. C. L. C. L. Ebens, E. Perkey, V. Radojcic, U. Koch, L. Scarpellino, A. Tong, F. Allen, S. Wood, J. Feng, A. Friedman, D. Granadier, I. T. I. T. Tran, Q. Chai, L. Onder, M. Yan, P. Reddy, B. R. B. R. B. R. Blazar, A. Y. A. Y. Huang, T. V. T. V. Brennan, D. K. K. Bishop, B. Ludewig, C. W. C. W. Siebel, F. Radtke, S. A. S. A. S. A. Luther, and I. Maillard. 2017. Fibroblastic niches prime T cell alloimmunity through Delta-like Notch ligands. *J. Clin. Invest.* 127: 1574–1588.

26. Perkey, E., D. Maurice De Sousa, L. Carrington, J. Chung, A. Dils, D. Granadier, U. Koch, F. Radtke, B. Ludewig, B. R. Blazar, C. W. Siebel, T. V. Brennan, J. Nolz, N. Labrecque, and I. Maillard. 2020. GCNT1-Mediated O -Glycosylation of the Sialomucin CD43 Is a Sensitive Indicator of Notch Signaling in Activated T Cells . *J. Immunol.* 204: 1674–1688.

27. Kovall, R. A., B. Gebelein, D. Sprinzak, and R. Kopan. 2017. The Canonical Notch Signaling Pathway: Structural and Biochemical Insights into Shape, Sugar, and Force. *Dev. Cell* 41(3): 228-241.

28. Zhang, Y., A. R. Sandy, J. Wang, V. Radojcic, G. T. Shan, I. T. Tran, A. Friedman, K. Kato, S. He, S. Cui, E. Hexner, D. M. Frank, S. G. Emerson, W. S. Pear, and I. Maillard. 2011. Notch signaling is a critical regulator of allogeneic CD4+ T-cell responses mediating graft-versus-host disease. *Blood* 117: 299–308.

29. Tran, I. T., A. R. Sandy, A. J. Carulli, C. Ebens, J. Chung, G. T. Shan, V. Radojcic, A. Friedman, T. Gridley, A. Shelton, P. Reddy, L. C. Samuelson, M. Yan, C. W. Siebel, and I. Maillard. 2013. Blockade of individual notch ligands and receptors controls graft-versus-host disease. *J. Clin. Invest.* 123: 1590–1604.

30. Wood, S., J. Feng, J. Chung, V. Radojcic, A. R. Sandy-Sloat, A. Friedman, A. Shelton, M. Yan, C. W. Siebel, D. K. Bishop, and I. Maillard. 2015. Transient blockade of delta-like Notch ligands prevents allograft rejection mediated by cellular and humoral mechanisms in a mouse model of heart transplantation. *J. Immunol.* 194: 2899–908.

31. Charbonnier, L.-M., S. Wang, P. Georgiev, E. Sefik, and T. A. Chatila. 2015. Control of peripheral tolerance by regulatory T cell–intrinsic Notch signaling. *Nat. Immunol.* 16: 1162–1173.

32. Auderset, F., S. Schuster, M. Coutaz, U. Koch, F. Desgranges, E. Merck, H. R. MacDonald, F. Radtke, and F. Tacchini-Cottier. 2012. Redundant Notch1 and Notch2 signaling is necessary for IFN secretion by T helper 1 cells during infection with Leishmania major. *PLoS Pathog.* 8: e1002560.

33. Shin, H. M., L. M. Minter, O. H. Cho, S. Gottipati, A. H. Fauq, T. E. Golde, G. E. Sonenshein, and B. A. Osborne. Notch1 augments NF-κB activity by facilitating its nuclear retention. *Embo J* 25: 129-138.

34. Ellisen, L. W., J. Bird, D. C. West, A. L. Soreng, T. C. Reynolds, S. D. Smith, and J. Sklar. 1991. TAN-1, the human homolog of the Drosophila Notch gene, is broken by chromosomal translocations in T lymphoblastic neoplasms. *Cell* 66(4): 649-661.

35. Radtke, F., A. Wilson, G. Stark, M. Bauer, J. Meerwijk, H. R. MacDonald, and M. Aguet. Deficient T cell fate specification in mice with an induced inactivation of Notch1. *Immunity* 10(5): 547-558.

36. Hozumi, K., C. Mailhos, N. Negishi, K. Hirano, T. Yahata, K. Ando, S. Zuklys, G. A. Holländer, D. T. Shima, S. Habu, G. A. Hollander, D. T. Shima, and S. Habu. 2008. Delta-like 4 is indispensable in thymic environment specific for T cell development. *J Exp Med* 205: 2507–13.

37. Koch, U., E. Fiorini, R. Benedito, V. Besseyrias, K. Schuster-Gossler, M. Pierres, N. R. Manley, A. Duarte, H. R. Macdonald, and F. Radtke. Delta-like 4 is the essential, nonredundant ligand for Notch1 during thymic T cell lineage commitment. *J Exp Med* 205(11): 2515-2523.

38. Radtke, F., H. R. MacDonald, and F. Tacchini-Cottier. 2013. Regulation of innate and adaptive immunity by Notch. *Nat. Rev. Immunol.* 13: 427–37.

39. Wang, H., C. Zang, L. Taing, K. L. Arnett, Y. J. Wong, W. S. Pear, S. C. Blacklow, X. S. Liu, and J. C. Aster. NOTCH1-RBPJ complexes drive target gene expression through dynamic interactions with superenhancers. *Proc Natl Acad Sci U S A* 111(2): 705-710.

40. Herranz, D., A. Ambesi-Impiombato, T. Palomero, S. A. Schnell, L. Belver, A. A. Wendorff, L. Xu, M. Castillo-Martin, D. Llobet-Navas, and C. Cordon-Cardo. A NOTCH1-driven MYC enhancer promotes T cell development, transformation and acute lymphoblastic leukemia. *Nat Med* 20: 1130-1137.

41. Falo-Sanjuan, J., N. C. Lammers, H. G. Garcia, and S. J. Bray. 2019. Enhancer Priming Enables Fast and Sustained Transcriptional Responses to Notch Signaling Correspondence. *Dev. Cell* 50: 411–425.

42. Palaga, T., L. Miele, T. E. Golde, and B. A. Osborne. 2003. TCR-mediated Notch signaling regulates proliferation and IFN-gamma production in peripheral T cells. *J. Immunol.* 171: 3019–24.

43. Amsen, D., J. M. Blander, G. R. Lee, K. Tanigaki, T. Honjo, and R. a. Flavell. 2004. Instruction of distinct CD4 T helper cell fates by different notch ligands on antigen-presenting cells. *Cell* 117: 515–526.

44. Brandstadter, J. D., and I. Maillard. 2019. Notch signalling in T cell homeostasis and differentiation. *Open Biol.* 9: 190187.

45. Mathieu, M., F. Duval, J.-F. Daudelin, and N. Labrecque. 2014. The Notch Signaling Pathway Controls Short-Lived Effector CD8+ T Cell Differentiation but Is Dispensable for Memory Generation. *J. Immunol.* 194: 5654–62.

46. Backer, R. a, C. Helbig, R. Gentek, A. Kent, B. J. Laidlaw, C. X. Dominguez, Y. S. de Souza, S. E. van Trierum, R. van Beek, G. F. Rimmelzwaan, A. ten Brinke, a M. Willemsen, A. H. C. van Kampen, S. M. Kaech, J. M. Blander, K. van Gisbergen, and D. Amsen. 2014. A central role for Notch in effector CD8+ T cell differentiation. *Nat. Immunol.* 15: 1143–1151.

47. Sandy, A. R., J. Chung, T. Toubai, G. T. Shan, I. T. Tran, a Friedman, T. S. Blackwell, P. Reddy, P. D. King, and I. Maillard. 2013. T cell-specific notch inhibition blocks graft-versus-host disease by inducing a hyporesponsive program in alloreactive CD4+ and CD8+ T cells. *J. Immunol.* 190: 5818–5828.

48. Magee, C. N., N. Murakami, T. J. Borges, T. Shimizu, K. Safa, S. Ohori, S. Cai, A. Uffing, J. Azzi, W. Elyaman, L.-M. Charbonnier, K. Liu, D. Toprak, G. Visner, T. A. Chatila, C. W. Siebel, N. Najafian, and L. V. Riella. 2019. Notch-1 Inhibition Promotes Immune Regulation in Transplantation via Treg-Dependent Mechanisms. *Circulation* 140(10): 846-863.

49. Laky, K., S. Evans, A. Perez-Diez, and B. J. J. Fowlkes. 2015. Notch Signaling Regulates Antigen Sensitivity of Naive CD4+ T Cells by Tuning Co-stimulation. *Immunity* 42: 80–94.

50. Bailis, W., Y. Yashiro-Ohtani, T. Fang, R. D. Hatton, C. T. Weaver, D. Artis, and W. S. Pear. 2013. Notch Simultaneously Orchestrates Multiple Helper T Cell Programs Independently of Cytokine Signals. *Immunity* 39: 148–159.

51. Minter, L. M., D. M. Turley, P. Das, H. M. Shin, I. Joshi, R. G. Lawlor, O. H. Cho, T. Palaga, S. Gottipati, J. C. Telfer, L. Kostura, A. H. Fauq, K. Simpson, K. A. Such, L. Miele, T. E. Golde, S. D. Miller, and B. A. Osborne. 2005. Inhibitors of gamma-secretase block in vivo and in vitro T helper type 1 polarization by preventing Notch upregulation of Tbx21. *Nat. Immunol.* 6: 680–8.

52. Roderick, J. E., G. Gonzalez-Perez, C. A. Kuksin, A. Dongre, E. R. Roberts, J. Srinivasan, C. Andrzejewski, A. H. Fauq, T. E. Golde, L. Miele, and L. M. Minter. 2013. Therapeutic targeting of NOTCH signaling ameliorates immune-mediated bone marrow failure of aplastic anemia. *J. Exp. Med.* 210: 1311–29.

53. Tindemans, I., A. van Schoonhoven, A. KleinJan, M. J. W. de Bruijn, M. Lukkes, M. van Nimwegen, A. van den Branden, I. M. Bergen, O. B. J. Corneth, W. F. J. van IJcken, R. Stadhouders, and R. W. Hendriks. 2020. Notch signaling licenses allergic airway inflammation by promoting Th2 cell lymph node egress. *J. Clin. Invest. 10.1172/JCI128310*.

54. Alam, M. S., Y. Maekawa, A. Kitamura, K. Tanigaki, T. Yoshimoto, K. Kishihara, and K. Yasutomo. 2010. Notch signaling drives IL-22 secretion in CD4+ T cells by stimulating the aryl hydrocarbon receptor. *Proc Natl Acad Sci U S A* 107: 5943–8.

55. Neal, L. M., Y. Qiu, J. Chung, E. Xing, W. Cho, A. N. Malachowski, A. R. Sandy-Sloat, J. J. Osterholzer, I. Maillard, and M. A. Olszewski. 2017. T Cell–Restricted Notch Signaling Contributes to Pulmonary Th1 and Th2 Immunity during Cryptococcus neoformans Infection . *J. Immunol.* 199: 643–655.

56. Lindahl, K., and D. Wilson. 1977. Histocompatibility antigen-activated cytotoxic T lymphocytes. *J. Exp. Med.* 145(3): 508-22.

57. Macdonald, W. A., Z. Chen, S. Gras, J. K. Archbold, F. E. Tynan, C. S. Clements, M. Bharadwaj, L. Kjer-Nielsen, P. M. Saunders, M. C. J. Wilce, F. Crawford, B. Stadinsky, D. Jackson, A. G. Brooks, A. W. Purcell, J. W. Kappler, S. R. Burrows, J. Rossjohn, and J. McCluskey. 2009. T Cell Allorecognition via Molecular Mimicry. *Immunity* 31: 897–908.

58. Colf, L. A., A. J. Bankovich, N. A. Hanick, N. A. Bowerman, L. L. Jones, D. M. Kranz, and K. C. Garcia. 2007. How a single T cell receptor recognizes both self and foreign MHC. *Cell* 129: 135–146.

59. Sprent, J., M. Schaefer, D. Lo, and R. Korngold. Properties of purified T cell subsets. *II. vivo responses to Cl. I vs. Cl. II H-2. J. Exp. Med.* 163(4): 998-1011.

60. Takemoto, S. K., P. I. Terasaki, D. W. Gjertson, and J. M. Cecka. Twelve years' experience with national sharing of HLA-matched cadaveric kidneys for transplantation. *N Engl J Med* 343: 1078-1084.

61. Wang, W., L. Meadows, J. den Haan, N. Sherman, Y. Chen, E. Blokland, J. Shabanowitz, A. Agulnik, R. Hendrickson, C. Bishop, and et al. 1995. Human H-Y: a male-specific histocompatibility antigen derived from the SMCY protein. *Science.* 269(5230): 1588-1590.

62. Martin, P. J., D. M. Levine, B. E. Storer, E. H. Warren, X. Zheng, S. C. Nelson, A. G. Smith, B. K. Mortensen, and J. A. Hansen. 2017. Genome-wide minor histocompatibility matching as related to the risk of graft-versus-host disease. *Blood* 129(6): 791-798.

63. Spierings, E., Y.-H. H. Kim, M. Hendriks, E. Borst, R. Sergeant, A. Canossi, M. Oudshoorn, P. Loiseau, H. Dolstra, M. Markiewicz, M. S. Leffell, N. Pereira, B. Kircher, H. Turpeinen, J.-F. F. Eliaou, T. Gervais, D. Laurin, J. Enczmann, M. Martinetti, J. Thomson, F. Oguz, S. Santarone, J. Partanen, U. Siekiera, E. P. Alessandrino, S. Kalayoglu, R. Brand, and E. Goulmy. 2013. Multicenter analyses demonstrate significant clinical effects of minor Histocompatibility Antigens on GvHD and GvL after HLA-matched related and unrelated Hematopoietic stem cell transplantation. *Biol. Blood Marrow Transplant.* 19(8): 1244–1253.

64. Miconnet, I., T. Roger, M. Seman, M. Bruley-Rosset, M. Bruley-Rosset Eur, I. Miconnet, T. Roger, M. Seman, M. Bruley-Rosset INSERM, and H. Paul Brousse. 1995. Critical role of endogenous Mtv in acute lethal graft-versus-host disease. *Eur J Immunol* 25(2): 364–368.

65. Shlomchik, W. D., M. S. Couzens, C. B. Tang, J. McNiff, M. E. Robert, J. Liu, M. J. Shlomchik, and S. G. Emerson. 1999. Prevention of graft versus host disease by inactivation of host antigen-presenting cells. *Science* 285(5426): 412–415.

66. Koyama, M., R. D. Kuns, S. D. Olver, N. C. Raffelt, Y. a Wilson, A. L. J. Don, K. E. Lineburg, M. Cheong, R. J. Robb, K. a Markey, A. Varelias, B. Malissen, G. J. Hämmerling, A. D. Clouston, C. R. Engwerda, P. Bhat, K. P. a MacDonald, and G. R. Hill. 2011. Recipient nonhematopoietic antigen-presenting cells are sufficient to induce lethal acute graft-versus-host disease. *Nat. Med.* 18: 135–142.

67. Toubai, T., I. Tawara, Y. Sun, C. Liu, E. Nieves, R. Evers, T. Friedman, R. Korngold, and P. Reddy. 2012. Induction of acute GVHD by sex-mismatched H-Y antigens in the absence of functional radiosensitive host hematopoietic-derived antigen-presenting cells. *Blood* 119: 3844–53.

68. Matte, C. C., J. Liu, J. Cormier, B. E. Anderson, I. Athanasiadis, D. Jain, J. McNiff, and W. D. Shlomchik. 2004. Donor APCs are required for maximal GVHD but not for GVL. *Nat. Med.* 10: 987–992.

69. Markey, K. a, T. Banovic, R. D. Kuns, S. D. Olver, A. L. J. Don, N. C. Raffelt, Y. A. Wilson, L. J. Raggatt, A. R. Pettit, J. S. Bromberg, G. R. Hill, K. P. A. MacDonald, P. Kelli, A. Macdonald, and W. Dc. 2009. Conventional dendritic cells are the critical donor APC presenting alloantigen after experimental bone marrow transplantation. *Blood* 113: 5644–9.

70. Anderson, B. E., J. M. McNiff, D. Jain, B. R. Blazar, W. D. Shlomchik, J. Shlomchik, W. Dc, and M. J. Shlomchik. 2005. Distinct roles for donor- and host-derived antigen-presenting cells and costimulatory molecules in murine chronic graft-versus-host disease: requirements depend on target organ. *Blood* 105: 2227–34.

71. Koyama, M., M. Cheong, K. A. Markey, K. H. Gartlan, R. D. Kuns, K. R. Locke, K. E. Lineburg, B. E. Teal, L. Leveque-El Mouttie, M. D. Bunting, S. Vuckovic, P. Zhang, M. W. L. Teng, A. Varelias, S.-K. Tey, L. F. Wockner, C. R. Engwerda, M. J. Smyth, G. T. Belz, S. R. McColl, K. P. A. MacDonald, and G. R. Hill. 2015. Donor colonic CD103+ dendritic cells determine the severity of acute graft-versus-host disease. *J. Exp. Med.* 212: 1303–21.

72. Leveque-El mouttie, L., M. Koyama, L. Le Texier, K. A. Markey, M. Cheong, R. D. Kuns, K. E. Lineburg, B. E. Teal, K. A. Alexander, A. D. Clouston, B. R. Blazar, G. R. Hill, K. P. A. MacDonald, L.-E. M. T. L, K. M, L.-E. M. T. L, M. KA, C. M, K. RD, L. KE, T. BE, A. KA, and C. AD. 2016. Corruption of dendritic cell antigen presentation during acute GVHD leads to regulatory T-cell failure and chronic GVHD. *Blood* 128: 794–804.

73. Wikstrom, M. E., P. Fleming, R. D. Kuns, I. S. Schuster, V. Voigt, G. Miller, A. D. Clouston, S. K. Tey, C. E. Andoniou, G. R. Hill, and M. A. Degli-Esposti. 2015. Acute GVHD results in a severe DC defect that prevents T-cell priming and leads to fulminant cytomegalovirus disease in mice. *Blood* 126: 1503–1515.

74. Teshima, T., R. Ordemann, P. Reddy, S. Gagin, C. Liu, K. R. Cooke, and J. L. M. Ferrara. 2002. Acute graft-versus-host disease does not require alloantigen expression on host epithelium. *Nat. Med.* 8: 575–581.

75. Duffner, U. A., Y. Maeda, K. R. Cooke, P. Reddy, R. Ordemann, C. Liu, J. L. M. Ferrara, and T. Teshima. 2004. Host Dendritic Cells Alone Are Sufficient to Initiate Acute Graft-versus-Host Disease. *J. Immunol.* 172: 7393–7398.

76. Li, H., A. J. Demetris, J. McNiff, C. Matte-Martone, H. S. Tan, D. M. Rothstein, F. G. Lakkis, and W. D. Shlomchik. 2012. Profound depletion of host conventional dendritic cells, plasmacytoid dendritic cells, and B cells does not prevent graft-versus-host disease induction. *J. Immunol.* 188: 3804–11.

77. Koyama, M., D. Hashimoto, K. Aoyama, K. Matsuoka, K. Karube, H. Niiro, M. Harada, M. Tanimoto, K. Akashi, and T. Teshima. 2009. Plasmacytoid dendritic cells prime alloreactive T cells to mediate graft-versus-host disease as antigen-presenting cells. *Blood* 113: 2088–2095.

78. Weber, M., B. Rudolph, P. Stein, N. Yogev, M. Bosmann, H. Schild, and M. P. Radsak. 2014. Host-Derived CD8(+) Dendritic Cells Protect Against Acute Graft-versus-Host Disease after Experimental Allogeneic Bone Marrow Transplantation. *Biol. Blood Marrow Transplant.* 20: 1696–704.

79. Teshima, T., P. Reddy, K. P. Lowler, M. A. KuKuruga, C. Liu, K. R. Cooke, and J. L. Ferrara. Flt3 ligand therapy for recipients of allogeneic bone marrow transplants expands host CD8 alpha(+) dendritic cells and reduces experimental acute graft-versus-host disease. *Blood* 99: 1825-1832.

80. Zhang, Y., J.-P. Louboutin, J. Zhu, A. J. Rivera, and S. G. Emerson. 2002. Preterminal host dendritic cells in irradiated mice prime CD8+ T cell-mediated acute graft-versus-host disease. *J. Clin. Invest.* 109: 1335–44.

81. Matte-martone, C., J. Liu, D. Jain, J. McNiff, and W. D. Shlomchik. 2008. CD8+ but Not CD4+ T Cells Require Cognate Interactions With Target Tissues to Mediate GVHD Across Only Minor H Antigens, Whereas Both CD4+ and CD8+ T Cells Require Direct Leukemic Contact to Mediate GVL. *Blood* 111(7): 3884–3892.

82. Jones, S. C., G. F. Murphy, T. M. Friedman, and R. Korngold. 2003. Importance of minor histocompatibility antigen expression by nonhematopoietic tissues in a CD4+ T cell-mediated graft-versus-host disease model. *J. Clin. Invest.* 112: 1880–6.

83. Tawara, I., W. D. Shlomchik, A. Jones, W. Zou, E. Nieves, C. Liu, T. Toubai, R. Duran-Struuck, Y. Sun, S. G. Clouthier, R. Evers, K. P. Lowler, R. B. Levy, and P. Reddy. 2010. A crucial role for host APCs in the induction of donor CD4+CD25+ regulatory T cell-mediated suppression of experimental graft-versus-host disease. *J Immunol* 185: 3866–72.

84. Steimle, V., L. A. Otten, M. Zufferey, and B. Mach. 1993 Complementation cloning of an MHC class II transactivator mutated in hereditary MHC class II deficiency (or bare lymphocyte syndrome. *Cell* 75(1): 135-146.

85. Steimle, V., C. A. Siegrist, A. Mottet, B. Lisowska-Grospierre, and B. Mach. Regulation of MHC class II expression by interferon-gamma mediated by the transactivator gene CIITA. *Science.* 265(5168): 106-109.

86. Li, H., C. Matte-Martone, H. S. Tan, S. Venkatesan, J. McNiff, A. J. Demetris, D. Jain, F. Lakkis, D. Rothstein, and W. D. Shlomchik. 2011. Graft-versus-host disease is independent of innate signaling pathways triggered by pathogens in host hematopoietic cells. *J. Immunol.* 186: 230–241.

87. Barrera, C. A., I. V. Pinchuk, J. I. Saada, G. Suarez, D. A. Bland, E. Beswick, P. A. Adegboyega, R. C. Mifflin, D. W. Powell, and V. E. Reyes. 2004. Class II MHC-expressing myofibroblasts play a role in the immunopathogenesis associated with staphylococcal enterotoxins. *Ann. N. Y. Acad. Sci.* 1029: 313–318.

88. Pinchuk, I. V., J. I. Saada, E. J. Beswick, G. Boya, S. M. Qiu, R. C. Mifflin, G. S. Raju, V. E. Reyes, D. W. Powell, S. Pinchuk IV, B. JI, B. EJ, Q. G, M. SM, R. RC, R. GS, VE, and D. W. Powell. 2008. PD-1 ligand expression by human colonic myofibroblasts/fibroblasts regulates CD4+ T-cell activity. *Gastroenterology* 135(4): 1228-1237.

89. Saada, J. I., I. V Pinchuk, C. a Barrera, P. a Adegboyega, G. Suarez, R. C. Mifflin, J. F. Di Mari, V. E. Reyes, and D. W. Powell. 2006. Subepithelial myofibroblasts are novel nonprofessional APCs in the human colonic mucosa. *J. Immunol.* 177: 5968–5979.

90. Koyama, M., P. Mukhopadhyay, I. S. Schuster, A. S. Henden, J. Hülsdünker, A. Varelias, M. Vetizou, R. D. Kuns, R. J. Robb, P. Zhang, B. R. Blazar, R. Thomas, J. Begun, N. Waddell, G. Trinchieri, R. Zeiser, A. D. Clouston, M. A. Degli-Esposti, and G. R. Hill. 2019. MHC Class II Antigen Presentation by the Intestinal Epithelium Initiates Graft-versus-Host Disease and Is Influenced by the Microbiota. *Immunity* 51(5): 885-898.

91. Mayer, L., and R. Shlien. 1987. Evidence for function of Ia molecules on gut epithelial cells in man. *J Exp Med* 166: 1471–83.

92. Hershberg, R. M., D. H. Cho, A. Youakim, M. B. Bradley, J. S. Lee, P. E. Framson, and G. T. Nepom. 1998. Highly polarized HLA class II antigen processing and presentation by human intestinal epithelial cells. *J Clin Invest* 102: 792–803.

93. Westendorf, A. M., D. Fleissner, L. Groebe, S. Jung, a D. Gruber, W. Hansen, and J. Buer. 2009. CD4+Foxp3+ regulatory T cell expansion induced by antigen-driven interaction with intestinal epithelial cells independent of local dendritic cells. *Gut* 58: 211–219.

94. Silva, I. A., K. Olkiewicz, D. Askew, J. M. Fisher, M. N. Chaudhary, K. M. Vannella, D. T. Deurloo, S. W. Choi, E. M. Pierce, S. G. Clouthier, C. Liu, and K. R. Cooke. 2010. Secondary Lymphoid Organs Contribute to , but Are Not Required for the Induction of Graft-versus-Host Responses following Allogeneic Bone Marrow Transplantation : A shifting Paradigm for T Cell. *Biol. Blood Marrow Transplant.* 16: 598–611.

95. Beilhaek, A., S. Schulz, J. Baker, G. F. Beilhack, R. Nishimura, E. M. Baker, G. Landan, E. I. Herman, E. C. Butcher, C. H. Contag, and R. S. Negrin. 2008. Prevention of acute graft-versus-host disease by blocking T-cell entry to secondary lymphoid organs. *Blood* 111: 2919–2928.

96. Beilhack, A., S. Schulz, J. Baker, G. F. Beilhack, C. B. Wieland, E. I. Herman, E. M. Baker, Y. A. Cao, C. H. Contag, and R. S. Negrin. 2005. In vivo analyses of early events in acute graft-versus-host disease reveal sequential infiltration of T-cell subsets. *Blood* 106: 1113–1122.

97. Malhotra, D., A. L. Fletcher, J. Astarita, V. Lukacs-Kornek, P. Tayalia, S. F. Gonzalez, K. G. Elpek, S. K. Chang, K. Knoblich, M. E. Hemler, M. B. Brenner, M. C. Carroll, D. J. Mooney, S. J. Turley, Y. Zhou, S. a Shinton, R. R. Hardy, N. a Bezman, J. C. Sun, C. C. Kim, L. L. Lanier, J. Miller, B. Brown, M. Merad, A. L. Fletcher, K. G. Elpek, A. Bellemare-Pelletier, D. Malhotra, S. J. Turley, K. Narayan, K. Sylvia, J. Kang, R. Gazit, B. Garrison, D. J. Rossi, V. Jojic, D. Koller, R. Jianu, D. Laidlaw, J. Costello, J. Collins, N. Cohen, P. Brennan, M. B. Brenner, T. Shay, A. Regev, F. Kim, T. N. Rao, A. Wagers, E. L. Gautier, C. Jakubzick, G. J. Randolph, P. Monach, A. J. Best, J. Knell, A. Goldrath, T. Heng, T. Kreslavsky, M. Painter, D. Mathis, and C. Benoist. 2012. Transcriptional profiling of stroma from inflamed and resting lymph nodes defines immunological hallmarks. *Nat. Immunol.* 13: 499–510.

98. Abe, J., S. Shichino, S. Ueha, S. -i. Hashimoto, M. Tomura, Y. Inagaki, J. V. Stein, and K. Matsushima. 2014. Lymph Node Stromal Cells Negatively Regulate Antigen-Specific CD4+ T Cell Responses. *J. Immunol.* 193: 1636–44.

99. Dubrot, J., F. V. Duraes, L. Potin, F. Capotosti, D. Brighouse, T. Suter, S. LeibundGut-Landmann, N. Garbi, W. Reith, M. A. Swartz, and S. Hugues. 2014. Lymph node stromal cells acquire peptide-MHCII complexes from dendritic cells and induce antigen-specific $CD4^+$ T cell tolerance. *J. Exp. Med.* 211: 1153–1166.

100. Kündig, T. M., M. F. Bachmann, C. DiPaolo, J. J. Simard, M. Battegay, H. Lother, A. Gessner, K. Kühlcke, P. S. Ohashi, H. Hengartner, T. M. Kundig, M. F. Bachmann, C. DiPaolo, J. J. Simard, M. Battegay, H. Lother, A. Gessner, K. Kuhlcke, P. S. Ohashi, and H. Hengartner. 1995. Fibroblasts as efficient antigen-presenting cells in lymphoid organs. *Science* 268: 1343–7.

101. Suenaga, F., S. Ueha, J. Abe, M. Kosugi-Kanaya, Y. Wang, a. Yokoyama, Y. Shono, F. H. W. Shand, Y. Morishita, J. Kunisawa, S. Sato, H. Kiyono, and K. Matsushima. 2014. Loss of Lymph Node Fibroblastic Reticular Cells and High Endothelial Cells Is Associated with Humoral Immunodeficiency in Mouse Graft-versus-Host Disease. *J. Immunol.* 194: 398–406.

102. Dertschnig, S., P. Evans, P. Santos e Sousa, T. Manzo, I. R. Ferrer, H. J. Stauss, C. L. Bennett, and R. Chakraverty. 2020. Graft-versus-host disease reduces lymph node display of tissue-restricted self-antigens and promotes autoimmunity. *J. Clin. Invest.* 130: 1896–1911.

103. Hill, G. R., J. M. Crawford, K. R. Cooke, Y. S. Brinson, L. Pan, and J. L. Ferrara. 1997. Total body irradiation and acute graft-versus-host disease: the role of gastrointestinal damage and inflammatory cytokines. *Blood* 90: 3204–13.

104. Artis, D., and H. Spits. The biology of innate lymphoid cells. *Nature* 517: 293-301.

105. Hanash, A. M., J. A. Dudakov, G. Hua, M. H. O'Connor, L. F. Young, N. V Singer, M. L. West, R. R. Jenq, A. M. Holland, and L. W. Kappel. Interleukin-22 protects intestinal stem cells from immune-mediated tissue damage and regulates sensitivity to graft versus host disease. *Immunity* 37: 339-350.

106. Dudakov, J. A., A. M. Hanash, R. R. Jenq, L. F. Young, A. Ghosh, N. V Singer, M. L. West, O. M. Smith, A. M. Holland, and J. J. Tsai. Interleukin-22 drives endogenous thymic regeneration in mice. *Science.* 336(6077): 91-95.

107. Clift, R. A., C. D. Buckner, F. R. Appelbaum, S. I. Bearman, F. B. Petersen, L. D. Fisher, C. Anasetti, P. Beatty, W. I. Bensinger, and K. Doney. Allogeneic marrow transplantation in patients with acute myeloid leukemia in first remission: a randomized trial of two irradiation regimens. *Blood* 76(9): 1867-1871.

108. Eriguchi, Y., S. Takashima, H. Oka, S. Shimoji, K. Nakamura, H. Uryu, S. Shimoda, H. Iwasaki, N. Shimono, and T. Ayabe. Graft-versus-host disease disrupts intestinal microbial ecology by inhibiting Paneth cell production of alpha-defensins. *Blood* 120(1): 223-231.

109. Jenq, R. R., C. Ubeda, Y. Taur, C. C. Menezes, R. Khanin, J. A. Dudakov, C. Liu, M. L. West, N. V Singer, and M. J. Equinda. Regulation of intestinal inflammation by microbiota following allogeneic bone marrow transplantation. *J Exp Med* 209(5): 903-911.

110. Jenq, R. R., Y. Taur, S. M. Devlin, D. M. Ponce, J. D. Goldberg, K. F. Ahr, E. R. Littmann, L. Ling, A. C. Gobourne, and L. C. Miller. Intestinal Blautia Is Associated with Reduced Death from Graft-versus-Host Disease. *Biol Blood Marrow Transpl.* 21(8): 1373-1383.

111. Shono, Y., M. D. Docampo, J. U. Peled, S. M. Perobelli, E. Velardi, J. J. Tsai, A. E. Slingerland, O. M. Smith, L. F. Young, J. Gupta, S. R. Lieberman, H. V. Jay, K. F. Ahr, K. A. Porosnicu Rodriguez, K. Xu, M. Calarfiore, H. Poeck, S. Caballero, S. M. Devlin, F. Rapaport, J. A. Dudakov, A. M. Hanash, B. Gyurkocza, G. F. Murphy, C. Gomes, C. Liu, E. L. Moss, S. B. Falconer, A. S. Bhatt, Y. Taur, E. G. Pamer, M. R. M. Van Den Brink, and R. R. Jenq. 2016. Increased GVHD-related mortality with broad-spectrum antibiotic use after allogeneic hematopoietic stem cell transplantation in human patients and mice. *Sci. Transl. Med.* 8(339): 339ra71.

112. Takashima, S., M. Kadowaki, K. Aoyama, M. Koyama, T. Oshima, K. Tomizuka, K. Akashi, and T. Teshima. 2011. The Wnt agonist R-spondin1 regulates systemic graft-versus-host disease by protecting intestinal stem cells. *J Exp Med* 208: 285–294.

113. Lindemans, C. A., M. Calafiore, A. M. Mertelsmann, M. H. O'Connor, J. A. Dudakov, R. R. Jenq, E. Velardi, L. F. Young, O. M. Smith, and G. Lawrence. Interleukin-22 promotes intestinal-stem-cell-mediated epithelial regeneration. *Nature* 528(7583): 560-564.

114. Fu, Y.-Y. Y., A. Egorova, C. Sobieski, J. Kuttiyara, M. Calafiore, S. Takashima, H. Clevers, and A. M. Hanash. 2019. T Cell Recruitment to the Intestinal Stem Cell Compartment Drives Immune-Mediated Intestinal Damage after Allogeneic Transplantation. *Immunity* 51: 90-103.

115. Takashima, S., M. L. Martin, S. A. Jansen, Y. Fu, J. Bos, D. Chandra, M. H. O'Connor, A. M. Mertelsmann, P. Vinci, J. Kuttiyara, S. M. Devlin, S. Middendorp, M. Calafiore, A. Egorova, M. Kleppe, Y. Lo, N. F. Shroyer, E. H. Cheng, R. L. Levine, C. Liu, R. Kolesnick, C. A. Lindemans, and A. M. Hanash. 2019. T cell-derived interferon-γ programs stem cell death in immune-mediated intestinal damage. *Sci. Immunol.* 4(42): pii: eaay8556.

116. Levine, J. E., E. Huber, S. T. Hammer, A. C. Harris, J. K. Greenson, T. M. Braun, J. L. Ferrara, and E. Holler. Low Paneth cell numbers at onset of gastrointestinal graft-versus-host disease identify patients at high risk for nonrelapse mortality. *Blood* 122(8): 1505-1509.

117. Sato, T., J. H. Es, H. J. Snippert, D. E. Stange, R. G. Vries, M. Born, N. Barker, N. F. Shroyer, M. Wetering, and H. Clevers. Paneth cells constitute the niche for Lgr5 stem cells in intestinal crypts. *Nature* 469(7330):415-418.

118. Vaishnava, S., M. Yamamoto, K. M. Severson, K. A. Ruhn, X. Yu, O. Koren, R. Ley, E. K. Wakeland, and L. V Hooper. The antibacterial lectin RegIIIgamma promotes the spatial segregation of microbiota and host in the intestine. *Science.* 334(6053): 255-258.

119. Ferrara, J. L. M., A. C. Harris, J. K. Greenson, T. M. Braun, E. Holler, T. Teshima, J. E. Levine, S. W. J. Choi, E. Huber, K. Landfried, K. Akashi, M. Vander Lugt, P. Reddy, A. Chin, Q. Zhang, S. Hanash, and S. Paczesny. 2011. Regenerating islet-derived 3-alpha is a biomarker of gastrointestinal graft-versus-host disease. *Blood* 118: 6702–6708.

120. Riella, L. V., T. Ueno, I. Batal, S. A. De Serres, R. Bassil, W. Elyaman, H. Yagita, J. O. Medina-Pestana, A. Chandraker, N. Najafian, S. A. De Serres, R. Bassil, W. Elyaman, H. Yagita, J. O. Medina-Pestana, A. Chandraker, and N. Najafian. 2011. Blockade of Notch ligand delta1 promotes allograft survival by inhibiting alloreactive Th1 cells and cytotoxic T cell generation. *J Immunol* 187: 4629.

121. Mochizuki, K., F. Xie, S. He, Q. Tong, Y. Liu, I. Mochizuki, Y. Guo, K. Kato, H. Yagita, S. Mineishi, and Y. Zhang. 2013. Delta-like ligand 4 identifies a previously uncharacterized population of inflammatory dendritic cells that plays important roles in eliciting allogeneic T cell responses in mice. *J. Immunol.* 190: 3772–82.

122. Wong, K. K., M. J. Carpenter, L. L. Young, S. J. Walker, G. McKenzie, A. J. Rust, G. Ward, L. Packwood, K. Wahl, L. Delriviere, G. Hoyne, P. Gibbs, B. R. Champion, J. R. Lamb, and M. J. Dallman. 2003. Notch ligation by Delta1 inhibits peripheral immune responses to transplantation antigens by a CD8+ cell-dependent mechanism. *J. Clin. Invest.* 112: 1741–1750.

123. Hoyne, G. F., I. Le Roux, M. Corsin-Jimenez, K. Tan, J. Dunne, L. M. Forsyth, M. J. Dallman, M. J. Owen, D. Ish-Horowicz, and J. R. Lamb. 2000. Serrate1-induced notch signalling regulates the decision between immunity and tolerance made by peripheral CD4(+) T cells. *Int Immunol* 12(2): 177-185.

124. Yvon, E. S., S. Vigouroux, R. F. Rousseau, E. Biagi, P. Amrolia, G. Dotti, H. J. Wagner, and M. K. Brenner. 2003. Over expression of the Notch ligand, Jagged-1 induces alloantigen-specific human regulatory T cells. *Blood* 102(10): 3815-3821).

125. Vigouroux, S., E. Yvon, H. J. Wagner, E. Biagi, G. Dotti, U. Sili, C. Lira, C. M. Rooney, and M. K. Brenner. Induction of antigen-specific regulatory T cells following overexpression of a Notch ligand by human B lymphocytes. *J Virol* 77(20:10872-10880.

126. Poe, J. C., W. Jia, H. Su, S. Anand, J. J. Rose, P. V. Tata, A. N. Suthers, C. D. Jones, P. F. Kuan, B. G. Vincent, J. S. Serody, M. E. Horwitz, V. T. Ho, S. Z. Pavletic, F. T. Hakim, K. Owzar, D. Zhang, B. R. Blazar, C. W. Siebel, N. J. Chao, I. Maillard, and S. Sarantopoulos. 2017. An aberrant NOTCH2-BCR signaling axis in B cells from patients with chronic GVHD. *Blood* 130(19): 2131-2145.

127. Reynolds, N. D., N. W. Lukacs, N. Long, and W. J. Karpus. Delta-like ligand 4 regulates central nervous system T cell accumulation during experimental autoimmune encephalomyelitis. *J Immunol* 187(5):2803-2813.

128. Tchekneva, E. E., M. U. L. Goruganthu, R. V. Uzhachenko, P. L. Thomas, A. Antonucci, I. Chekneva, M. Koenig, L. Piao, A. Akhter, M. T. P. de Aquino, P. Ranganathan, N. Long, T. Magliery, A. Valujskikh, J. V. Evans, R. R. Arasada, P. P. Massion, D. P. Carbone, A. Shanker, and M. M. Dikov. 2019. Determinant roles of dendritic cell-expressed Notch Delta-like and Jagged ligands on anti-tumor T cell immunity. *J. Immunother. Cancer* 7(1): 95.

129. Vijayaraghavan, J., and B. A. Osborne. 2018. Notch and T Cell Function – A Complex Tale.*Adv. Exp. Med. Biol.* 1066: 339–354.

130. Sugimoto, K., Y. Maekawa, A. Kitamura, J. Nishida, A. Koyanagi, H. Yagita, H. Kojima, S. Chiba, M. Shimada, and K. Yasutomo. 2010. Notch2 signaling is required for potent antitumor immunity in vivo. *J. Immunol.* 184: 4673–8.

131. Sierra, R. A., P. Thevenot, P. L. Raber, Y. Cui, C. Parsons, A. C. Ochoa, J. Trillo-Tinoco, L. Del Valle, and P. C. Rodriguez. 2014. Rescue of Notch-1 Signaling in Antigen-Specific CD8+ T Cells Overcomes Tumor-Induced T-cell Suppression and Enhances Immunotherapy in Cancer. *Cancer Immunol. Res.* 2: 800–811.

132. Radojcic, V., K. Paz, J. Chung, J. Du, E. T. Perkey, R. Flynn, S. Ivcevic, M. Zaiken, A. Friedman, M. Yan, M. A. Pletneva, S. Sarantopoulos, C. W. Siebel, B. R. Blazar, and I. Maillard. 2018. Notch signaling mediated by Delta-like ligands 1 and 4 controls the pathogenesis of chronic GVHD in mice. *Blood* 132: 2188–2200.

133. Sandy, A. R., J. Stoolman, K. Malott, P. Pongtornpipat, B. M. Segal, and I. Maillard. 2013. Notch signaling regulates T cell accumulation and function in the central nervous system during experimental autoimmune encephalomyelitis. *J. Immunol.* 191: 1606–13.

134. Minter, L., D. Turley, P. Das, H. Shin, … I. J.-N., and B.A. Osborne. 2005. Inhibitors of γ-secretase block in vivo and in vitro T helper type 1 polarization by preventing Notch upregulation of Tbx21. *Nat. Immunol.* 6(7): 660-668.

135. Dell'Aringa, M., and R. L. Reinhardt. 2018. Notch signaling represents an important checkpoint between follicular T-helper and canonical T-helper 2 cell fate. *Mucosal Immunol.* 11: 1079–1091.

136. Baecher-Allan, C., J. Kemp, K. Dorfman, R. Barth, and J. Frelinger. 1993. Differential epitope expression of Ly-48 (mouse leukosialin). *Immunogenetics* 37: 183–192.

137. Hobbs, S. J., and J. C. Nolz. 2017. Regulation of T Cell Trafficking by Enzymatic Synthesis of O-Glycans. *Front. Immunol.* 8: 600.

138. Barran, P., W. Fellinger, C. E. Warren, J. W. Dennis, and H. J. Ziltener. 1997. Modification of CD43 and other lymphocyte O-glycoproteins by core 2 N-acetylglucosaminyltransferase. *Glycobiology* 7: 129–136.

139. Carlow, D. A., M. J. Williams, and H. J. Ziltener. 2005. Inducing P-Selectin Ligand Formation in CD8 T Cells: IL-2 and IL-12 Are Active In Vitro but Not Required In Vivo. *J. Immunol.* 174: 3959–3966.

140. Nolz, J. C., and J. T. Harty. 2014. IL-15 regulates memory CD8+ T cell O-glycan synthesis and affects trafficking. *J. Clin. Invest.* 124: 1013–1026.

141. Osborn, J. F., J. L. Mooster, S. J. Hobbs, M. W. Munks, C. Barry, J. T. Harty, A. B. Hill, and J. C. Nolz. 2017. Enzymatic synthesis of core 2 O-glycans governs the tissue-trafficking potential of memory CD8 $^{+}$ T cells. *Sci. Immunol.* 2: eaan6049.

142. Harrington, L. E., M. Galvan, L. G. Baum, J. D. Altman, and R. Ahmed. 2000. Differentiating between memory and effector CD8 T cells by altered expression of cell surface O-glycans. *J. Exp. Med.* 191: 1241–1246.

143. Ellies, L. G., A. T. Jones, M. J. Williams, and H. J. Ziltener. 1994. Differential Regulation of Cd43 Glycoforms on Cd4(+) and Cd8(+) T-Lymphocytes in Graft-Versus-Host Disease. *Glycobiology* 4: 885–893.

144. Bagˇriaçik, E. Ü., M. D. Armstrong, M. Okabe, and J. R. Klein. 1999. Differential expression of CD43 isoforms on murine T cells and their relationship to acute intestinal graft versus host disease: studies using enhanced-green fluorescent protein transgenic mice. *Int. Immunol.* 11: 1651–1662.

145. Kansas, G. S., M. E. Ebel, O. Awe, and M. H. Kaplan. 2015. MAPK α Cells via p38 T Selectin Ligand Expression on Murine CD4 Diverse Inflammatory Cytokines Induce. *J Immunol Ref.* 194: 5781–5788.

146. Snapp, K. R., C. E. Heitzig, L. G. Ellies, J. D. Marth, and G. S. Kansas. 2001. Differential requirements for the O-linked branching enzyme core 2 1-6-N-glucosaminyltransferase in biosynthesis of ligands for E-selectin and P-selectic. *Blood* 87(12):3806-3811.

147. Lim, Y. C., H. Xie, C. E. Come, S. I. Alexander, M. J. Grusby, A. H. Lichtman, and F. W. Luscinskas. 2001. IL-12, STAT4-dependent up-regulation of CD4(+) T cell core 2 beta-1,6-n-acetylglucosaminyltransferase, an enzyme essential for biosynthesis of P-selectin ligands. *J. Immunol.* 167: 4476–84.

148. Carlow, D. A., M. J. Williams, and H. J. Ziltener. 2005. Inducing P-selectin ligand formation in CD8 T cells: IL-2 and IL-12 are active in vitro but not required in vivo. *J. Immunol.* 174: 3959–66.

149. Chung, J., V. Radojcic, E. Perkey, T. J. Parnell, Y. Niknafs, X. Jin, A. Friedman, N. Labrecque, B. R. Blazar, T. V. Brennan, C. W. Siebel, and I. Maillard. 2019. Early Notch Signals Induce a Pathogenic Molecular Signature during Priming of Alloantigen-Specific Conventional CD4+ T Cells in Graft-versus-Host Disease. *J. Immunol.* 203: 557–568.

150. Weng, A. P., A. A. Ferrando, W. Lee, J. P. Morris, L. B. Silverman, C. Sanchez-Irizarry, S. C. Blacklow, A. T. Look, and J. C. Aster. 2004. Activating mutations of NOTCH1 in human T cell acute lymphoblastic leukemia. *Science* 306: 269–71.

151. Wang, H., J. Zou, B. Zhao, E. Johannsen, T. Ashworth, H. Wong, W. S. Pear, J. Schug, S. C. Blacklow, K. L. Arnett, B. E. Bernstein, E. Kieff, and J. C. Aster. 2011. Genome-wide analysis reveals conserved and divergent features of Notch1/RBPJ binding in human and murine T-lymphoblastic leukemia cells. *Proc. Natl. Acad. Sci.* 108: 14908–14913.

152. Maillard, I., A. P. Weng, A. C. Carpenter, C. G. Rodriguez, H. Sai, L. Xu, D. Allman, J. C. Aster, and W. S. Pear. 2004. Mastermind critically regulates Notch-mediated lymphoid cell fate decisions. 104: 1696–1702.

153. Kumar, R., R. Camphausen, F. Sullivan, D. C.- Blood, and undefined 1996. Core2 beta-1, 6-N-acetylglucosaminyltransferase enzyme activity is critical for P-selectin glycoprotein ligand-1 binding to P-selectin. *Blood* 88(10):3872-3879.

154. Li, F., P. P. Wilkins, S. Crawley, J. Weinstein, R. D. Cummings, and R. P. McEver. 1996. Post-translational modifications of recombinant P-selectin glycoprotein ligand-1 required for binding to P- and E-selectin. *J. Biol. Chem.* 271: 3255–64.

155. Lu, S. X., A. M. Holland, I.-K. Na, T. H. Terwey, O. Alpdogan, J. L. Bautista, O. M. Smith, D. Suh, C. King, A. Kochman, V. M. Hubbard, U. K. Rao, N. Yim, C. Liu, A. C. Laga, G. Murphy, R. R. Jenq, J. L. Zakrzewski, O. Penack, L. Dykstra, K. Bampoe, L. Perez, B. Furie, B. Furie, and M. R. M. van den Brink. 2010. Absence of P-selectin in recipients of allogeneic bone marrow transplantation ameliorates experimental graft-versus-host disease. *J. Immunol.* 185: 1912–9.

156. Adler, S. H., E. Chiffoleau, L. Xu, N. M. Dalton, J. M. Burg, A. D. Wells, M. S. Wolfe, L. A. Turka, and W. S. Pear. 2003. Notch signaling augments T cell responsiveness by enhancing CD25 expression. *J. Immunol.* 171: 2896–903.

157. Boulet, S., J.-F. Daudelin, and N. Labrecque. 2014. IL-2 induction of Blimp-1 is a key in vivo signal for CD8+ short-lived effector T cell differentiation. *J. Immunol.* 193: 1847–54.

158. Ellies, L. G., A. T. Jones, M. J. Williams, and H. J. Ziltener. 1994. Differential regulation of CD43 glycoforms on $CD4^+$ and $CD8^+$ T lymphocytes in graft-versus-host disease. *Glycobiology* 4: 885–893.

159. Steinbuck, M. P., K. Arakcheeva, and S. Winandy. 2018. Novel TCR-Mediated Mechanisms of Notch Activation and Signaling. *J. Immunol.* 200: 997–1007.

160. Mukasa, R., T. Homma, T. Ohtsuki, O. Hosono, A. Souta, T. Kitamura, M. Fukuda, S. Watanabe, and C. Morimoto. 1999. Core 2-containing O-glycans on CD43 are preferentially expressed in the memory subset of human CD4 T cells. *Int. Immunol.* 11: 259–268.

161. Fox,', R. I., M. Hueniken, S. Fong, S. Behar, I. Royston, S. K. Singhal, + And, L. Thompson, L. Jo//, and R. I. Fox. 1983. A novel cell surface antigen (T305) found in increased frequency on acute leukemia cells and in autoimmune disease states. *J. Immunol.* 131: 762–767.

162. Naymagon, S., L. Naymagon, S. Y. Wong, H. M. Ko, A. Renteria, J. Levine, J. F. Colombel, and J. Ferrara. 2017. Acute graft-versus-host disease of the gut: Considerations for the gastroenterologist. *Nat. Rev. Gastroenterol. Hepatol.* 14: 711–726.

163. Berlin, C., E. L. Berg, M. J. Briskin, D. P. Andrew, P. J. Kilshaw, B. Holzmann, I. L. Weissman, A. Hamann, and E. C. Butcher. 1993. α4β7 integrin mediates lymphocyte binding to the mucosal vascular addressin MAdCAM-1. *Cell* 74: 185–195.

164. Nakache, M., E. Lakey Berg, P. R. Streeter, and E. C. Butcher. 1989. The mucosal vascular addressin is a tissue-specific endothelial cell adhesion molecule for circulating lymphocytes. *Nature* 337: 179–181.

165. Cohen, J. N., E. F. Tewalt, S. J. Rouhani, E. L. Buonomo, A. N. Bruce, X. Xu, S. Bekiranov, Y.-X. Fu, and V. H. Engelhard. 2014. Tolerogenic Properties of Lymphatic Endothelial Cells Are Controlled by the Lymph Node Microenvironment. *PLoS One* 9: e87740.

166. Waldman, E., S. X. Lu, V. M. Hubbard, A. A. Kochman, J. M. Eng, T. H. Terwey, S. J. Muriglan, T. D. Kim, G. Heller, G. F. Murphy, C. Liu, O. Alpdogan, and M. R. M. Van Den Brink. 2006. Absence of β7 integrin results in less graft-versus-host disease because of decreased homing of alloreactive T cells to intestine. *Blood* 107: 1703–1711.

167. Schreder, A., G. L. Moschovakis, S. Halle, J. Schlue, C. W. Lee, A. Schippers, S. David, G. Bernhardt, A. Ganser, O. Pabst, R. Förster, and C. Koenecke. 2015. Differential Effects of Gut-Homing Molecules CC Chemokine Receptor 9 and Integrin-β7 during Acute Graft-versus-Host Disease of the Liver. *Biol. Blood Marrow Transplant.* 21: 2069–2078.

168. Petrovic, J., P. Formosa-Jordan, J. C. Luna-Escalante, G. Abelló, M. Ibañes, J. Neves, and F. Giraldez. 2014. Ligand-dependent Notch signaling strength orchestrates lateral induction and lateral inhibition in the developing inner ear. *Development* 141: 2313–2324.

169. Beilhack, A., S. Schulz, J. Baker, G. F. Beilhack, R. Nishimura, E. M. Baker, G. Landan, E. I. Herman, E. C. Butcher, C. H. Contag, and R. S. Negrin. 2015. Prevention of acute graft-versus-host disease by blocking T-cell entry to secondary lymphoid organs. 111: 2919–2929.

170. Iwata, M., A. Hirakiyama, Y. Eshima, H. Kagechika, C. Kato, and S.-Y. Song. 2004. Retinoic Acid Imprints Gut-Homing Specificity on T Cells. *Immunity* 21(4): 527-538.

171. Coombes, J. L., K. R. R. Siddiqui, C. V. Arancibia-Cárcamo, J. Hall, C. M. Sun, Y. Belkaid, and F. Powrie. 2007. A functionally specialized population of mucosal CD103+ DCs induces Foxp3+ regulatory T cells via a TGF-β -and retinoic acid-dependent mechanism. *J. Exp. Med.* 204: 1757–1764.

172. Hammerschmidt, S. I., M. Ahrendt, U. Bode, B. Wahl, E. Kremmer, R. Förster, and O. Pabst. 2008. Stromal mesenteric lymph node cells are essential for the generation of gut- Homing T cells in vivo. *J. Exp. Med.* 205: 2483–2490.

173. Bascones Gleave, S., G. Magri, L. Cassis, L. Comerma, M. Gentile, C. Barra, I. Puga, and A. Cerutti. 2015. Splenic MAdCAM-1+ marginal reticular cells deliver antibody-inducing signals and confer gut-homing properties to human marginal zone B cells (IRC5P.622). *J. Immunol.* 194: 58.5.

174. Mucida, D., Y. Park, G. Kim, O. Turovskaya, I. Scott, M. Kronenberg, and H. Cheroutre. 2007. Reciprocal TH17 and regulatory T cell differentiation mediated by retinoic acid. *Science* 317: 256–260.

175. Aoyama, K., A. Saha, J. Tolar, M. J. Riddle, R. G. Veenstra, P. A. Taylor, R. Blomhoff, A. Panoskaltsis-Mortari, C. A. Klebanoff, G. Socie, D. H. Munn, W. J. Murphy, J. S. Serody, L. M. Fulton, T. Teshima, R. A. Chandraratna, E. Dmitrovsky, Y. Guo, R. J. Noelle, and B. R. Blazar. 2013. Inhibiting retinoic acid signaling ameliorates graft-versus-host disease by modifying T-cell differentiation and intestinal migration. *Blood* 122: 2125–2134.

176. Chen, X., J. Dodge, R. Komorowski, and W. R. Drobyski. 2013. A critical role for the retinoic acid signaling pathway in the pathophysiology of gastrointestinal graft-versus-host disease. *Blood* 121: 3970–3980.

177. Holzmann, B., B. W. McIntyre, and I. L. Weissman. 1989. Identification of a murine Peyer's patch-specific lymphocyte homing receptor as an integrin molecule with an α chain homologous to human VLA-4α. *Cell* 56: 37–46.

178. Kim, S. V., W. V. Xiang, C. Kwak, Y. Yang, X. W. Lin, M. Ota, U. Sarpel, D. B. Rifkin, R. Xu, and D. R. Littman. 2013. GPR15-mediated homing controls immune homeostasis in the large intestine mucosa. *Science* 340: 1456–1459.

179. Modur, V., G. A. Zimmerman, S. M. Prescott, and T. M. McIntyre. 1996. Endothelial cell inflammatory responses to tumor necrosis factor α: Ceramide-dependent and -independent mitogen-activated protein kinase cascades. *J. Biol. Chem.* 271: 13094–13102.

180. Palomo, M., M. Diaz-Ricart, C. Carbo, M. Rovira, F. Fernandez-Aviles, C. Martine, G. Ghita, G. Escolar, and E. Carreras. 2010. Endothelial Dysfunction after Hematopoietic Stem Cell Transplantation: Role of the Conditioning Regimen and the Type of Transplantation. *Biol. Blood Marrow Transplant.* 16: 985–993.

181. Schreder, A., G. L. Moschovakis, S. Halle, J. Schlue, C.-W. Lee, A. Schippers, S. David, G. Bernhardt, A. Ganser, O. Pabst, R. Förster, and C. Koenecke. 2015. Differential effects of gut-homing molecules CC chemokine receptor 9 and integrin-beta7 during acute GvHD of the liver. *Biol. Blood Marrow Transplant* 21(12): 2069-2078.

182. Petrovic, A., O. Alpdogan, L. M. Willis, J. M. Eng, A. S. Greenberg, B. J. Kappel, C. Liu, G. J. Murphy, G. Heller, and M. R. M. Van Den Brink. 2004. LPAM (α4β7 integrin) is an important homing integrin on alloreactive T cells in the development of intestinal graft-versus-host disease. *Blood* 103: 1542–1547.

183. Chen, Y.-B., N. N. Shah, A. S. Renteria, C. Cutler, J. Jansson, M. Akbari, C. Chen, S. Quadri, A. Parfionovas, and S. M. Devine. 2019. Vedolizumab for prevention of graft-versus-host disease after allogeneic hematopoietic stem cell transplantation. *Blood Adv.* 3: 4136–4146.

184. Furlan, S. N., B. Watkins, V. Tkachev, R. Flynn, S. Cooley, S. Ramakrishnan, K. Singh, C. Giver, K. Hamby, L. Stempora, A. Garrett, J. Chen, K. M. Betz, C. G. K. Ziegler, G. K. Tharp, S. E. Bosinger, D. E. L. Promislow, J. S. Miller, E. K. Waller, B. R. Blazar, and L. S. Kean. 2015. Transcriptome analysis of GVHD reveals aurora kinase A as a targetable pathway for disease prevention. *Sci. Transl. Med.* 7: 315ra191.

185. Tkachev, V., S. N. Furlan, B. Watkins, D. J. Hunt, H. Betty Zheng, A. Panoskaltsis-Mortari, K. Betz, M. Brown, J. B. Schell, K. Zeleski, A. Yu, I. Kirby, S. Cooley, J. S. Miller, B. R. Blazar, D. Casson, P. Bland-Ward, and L. S. Kean. 2017. Combined OX40L and mTOR blockade controls effector T cell activation while preserving Treg reconstitution after transplant. *Sci. Transl. Med.* 9(408): eaan3085.

186. Tkachev, V., F. Kuhnert, S. N. Furlan, H. Zheng, D. J. Hunt, L. Colonna, J. M. Carlson, A. Taraseviciute, A. Panoskaltsis-Mortari, V. Hoglund, K. Betz, A. Yu, B. R. Blazar, S. Carpenter, O. Harari, G. Thurston, I. Maillard, and L. Kean. 2018. Pharmacologic Blockade of Notch/Delta-like Ligand 4 Signaling Protects from Gastrointestinal Acute Graft-Versus-Host Disease in Non-Human Primates. *Blood* 132: 2027–2027.

187. Chandar, A. K., S. Singh, M. H. Murad, L. Peyrin-Biroulet, and E. V. Loftus. 2015. Efficacy and safety of natalizumab and vedolizumab for the management of Crohn's disease: A systematic review and meta-analysis. *Inflamm. Bowel Dis.* 21: 1695–1708.

188. Zundler, S., E. Becker, C. Weidinger, and B. Siegmund. 2017. Anti-adhesion therapies in inflammatory bowel disease-molecular and clinical aspects. *Front. Immunol.* 8: 891.

189. Zundler, S., A. Fischer, D. Schillinger, M.-T. Binder, R. Atreya, T. Rath, R. Lopez-Pósadas, C. J. Voskens, A. Watson, I. Atreya, C. Neufert, and M. F. Neurath. 2017. The a4b1 Homing Pathway Is Essential for Ileal Homing of Crohn's Disease Effector T Cells In Vivo. *Inflamm. Bowel Dis.* 23(3): 379-391.

190. Maaser, C., S. Schoeppner, T. Kucharzik, M. Kraft, E. Schoenherr, W. Domschke, and N. Lügering. 2001. Colonic epithelial cells induce endothelial cell expression of ICAM-1 and VCAM-1 by a NF-κB-dependent mechanism. *Clin. Exp. Immunol.* 124: 208–213.

191. Eyrich, M., G. Burger, K. Marquardt, W. Budach, K. Schilbach, D. Niethammer, and P. G. Schlegel. 2005. Sequential expression of adhesion and costimulatory molecules in graft-versus-host disease target organs after murine bone marrow transplantation across minor histocompatibility antigen barriers. *Biol. Blood Marrow Transplant.* 11: 371–382.

192. Norton, J., J. P. Sloane, N. Al-Saffar, and D. O. Haskard. 2008. Expression of adhesion molecules in human intestinal graft- versus- host disease. *Clin. Exp. Immunol.* 87: 231–236.

193. Shirota, T., and M. Tavassoli. 1992. Alterations of bone marrow sinus endothelium induced by ionizing irradiation: Implications in the homing of intravenously transplanted marrow cells. *Blood Cells* 18: 197–214.

194. Berg, E. L., L. M. McEvoy, C. Berlin, R. F. Bargatze, and E. C. Butcher. 1993. L-selectin-mediated lymphocyte rolling on MAdCAM-1. *Nature* 366: 695–698.

195. Nguyen, L. P., J. Pan, T. T. Dinh, H. Hadeiba, E. O'hara, A. Ebtikar, A. Hertweck, M. R. Gökmen, G. M. Lord, R. G. Jenner, E. C. Butcher, and A. Habtezion. 2015. Role and species-specific expression of colon T cell homing receptor GPR15 in colitis. *Nat. Immunol.* 16: 207–213.

196. Adamczyk, A., D. Gageik, A. Frede, E. Pastille, W. Hansen, A. Rueffer, J. Buer, J. Büning, J. Langhorst, and A. M. Westendorf. 2017. Differential expression of GPR15 on T cells during ulcerative colitis. *JCI Insight* 2(8): 90585.

197. Nawaz, F., L. R. Goes, J. C. Ray, R. Olowojesiku, A. Sajani, A. A. Ansari, I. Perrone, J. Hiatt, D. Van Ryk, D. Wei, M. Waliszewski, M. A. Soares, K. Jelicic, M. Connors, S. A. Migueles, E. Martinelli, F. Villinger, C. Cicala, A. S. Fauci, and J. Arthos. 2018. MAdCAM costimulation through Integrin-α4β7 promotes HIV replication. *Mucosal Immunol.* 11: 1342–1351.

198. Engelhardt, B. G., M. Jagasia, B. N. Savani, N. L. Bratcher, J. P. Greer, A. Jiang, A. A. Kassim, P. Lu, F. Schuening, S. M. Yoder, M. T. Rock, and J. E. Crowe. 2011. Regulatory T cell expression of CLA or α 4 B 7 and skin or gut acute GVHD outcomes. *Bone Marrow Transplant.* 46: 436–442.

199. Chen, Y. B., S. McDonough, H. Chen, J. Kennedy, C. Illiano, E. C. Attar, K. K. Ballen, B. R. Dey, S. L. McAfee, M. Jagasia, R. Soiffer, T. R. Spitzer, and J. Ritz. 2013. Expression of α4β7 integrin on memory CD8 + T cells at the presentation of acute intestinal GVHD. *Bone Marrow Transplant.* 48: 598–603.

200. Gerriets, V. A., R. J. Kishton, M. O. Johnson, S. Cohen, P. J. Siska, A. G. Nichols, M. O. Warmoes, A. A. De Cubas, N. J. MacIver, J. W. Locasale, L. A. Turka, A. D. Wells, and J. C. Rathmell. 2016. Foxp3 and Toll-like receptor signaling balance T reg cell anabolic metabolism for suppression. *Nat. Immunol.* 17: 1459–1466.

201. DeNucci, C. C., A. J. Pagán, J. S. Mitchell, and Y. Shimizu. 2010. Control of α4β7 Integrin Expression and CD4 T Cell Homing by the β1 Integrin Subunit. *J. Immunol.* 184: 2458–2467.

202. Perez-Shibayama, C., C. Gil-Cruz, and B. Ludewig. 2019. Fibroblastic reticular cells at the nexus of innate and adaptive immune responses. *Immunol. Rev.* 289: 31–41.

203. Lee, J.-W., M. Epardaud, J. Sun, J. E. Becker, A. C. Cheng, A. Yonekura, J. K. Heath, and S. J. Turley. Peripheral antigen display by lymph node stroma promotes T cell tolerance to intestinal self. *Nat. Immunol.* 8: 181–190.

204. Baptista, A. P., R. Roozendaal, R. M. Reijmers, J. J. Koning, W. W. Unger, M. Greuter, E. D. Keuning, R. Molenaar, G. Goverse, M. M. S. Sneeboer, J. M. M. den Haan, M. Boes, and R. E. Mebius. 2014. Lymph node stromal cells constrain immunity via MHC class II self-antigen presentation. *Elife* 3: 04433.

205. Dubrot, J., F. V. Duraes, L. Potin, F. Capotosti, D. Brighouse, T. Suter, S. LeibundGut-Landmann, N. Garbi, W. Reith, M. A. Swartz, and S. Hugues. 2014. Lymph node stromal cells acquire peptide-MHCII complexes from dendritic cells and induce antigen-specific CD4+ T cell tolerance. *J. Exp. Med.* 211: 1153–1166.

206. Perkey, E., and I. Maillard. 2018. New Insights into Graft-Versus-Host Disease and Graft Rejection. *Annu. Rev. Pathol. Mech. Dis* 13: 219–45.

207. Tikhonova, A. N., I. Dolgalev, H. Hu, K. K. Sivaraj, E. Hoxha, Á. Cuesta-Domínguez, S. Pinho, I. Akhmetzyanova, J. Gao, M. Witkowski, M. Guillamot, M. C. Gutkin, Y. Zhang, C. Marier, C. Diefenbach, S. Kousteni, A. Heguy, H. Zhong, D. R. Fooksman, J. M. Butler, A. Economides, P. S. Frenette, R. H. Adams, R. Satija, A. Tsirigos, and I. Aifantis. 2019. The bone marrow microenvironment at single-cell resolution. *Nature* 569: 222–228.

208. Cordeiro, O. G., M. Chypre, N. Brouard, S. Rauber, F. Alloush, M. Romera-Hernandez, C. Bénézech, Z. Li, A. Eckly, M. C. Coles, A. Rot, H. Yagita, C. Léon, B. Ludewig, T. Cupedo, F. Lanza, and C. G. Mueller. 2016. Integrin-Alpha IIb Identifies Murine Lymph Node Lymphatic Endothelial Cells Responsive to RANKL. *PLoS One* 11: e0151848.

209. Luty, W. H., D. Rodeberg, J. Parness, and Y. M. Vyas. 2007. Antiparallel Segregation of Notch Components in the Immunological Synapse Directs Reciprocal Signaling in Allogeneic Th:DC Conjugates. *J. Immunol.* 179: 819–829.

210. De Sousa, D. M., F. Duval, J.-F. Daudelin, S. Boulet, and N. Labrecque. 2019. The Notch signaling pathway controls CD8+ T cell differentiation independently of the classical effector HES1. *PLoS One* 14: e0215012.

211. Mochizuki, K., L. Meng, I. Mochizuki, Q. Tong, S. He, Y. Liu, J. Purushe, H. Fung, M. R. Zaidi, Y. Zhang, R. Reshef, B. R. Blazar, H. Yagita, S. Mineishi, and Y. Zhang. 2016. Programming of donor T cells using allogeneic delta-like ligand 4-positive dendritic cells to reduce GVHD in mice. *Blood* 127(25): 3270-3280.

212. Brown, C. C., H. Gudjonson, Y. Pritykin, D. Deep, V. P. Lavallée, A. Mendoza, R. Fromme, L. Mazutis, C. Ariyan, C. Leslie, D. Pe'er, and A. Y. Rudensky. 2019. Transcriptional Basis of Mouse and Human Dendritic Cell Heterogeneity. *Cell* 179: 846-863.

213. Meng, L., Z. Bai, S. He, K. Mochizuki, Y. Liu, J. Purushe, H. Sun, J. Wang, H. Yagita, S. Mineishi, H. Fung, G. A. Yanik, R. Caricchio, X. Fan, L. M. Crisalli, E. O. Hexner, R. Reshef, Y. Y. Zhang, and Y. Y. Zhang. 2015. The Notch Ligand DLL4 Defines a Capability of Human Dendritic Cells in Regulating Th1 and Th17 Differentiation. *J. Immunol.* 196(3): 1070-1080.

214. Ding, L., and E. M. Shevach. 1994. Activation of CD4+ T cells by delivery of the B7 costimulatory signal on bystander antigen-presenting cells (trans-costimulation). *Eur. J. Immunol.* 24: 859–866.

215. Bashour, K. T., J. Tsai, K. Shen, J.-H. Lee, E. Sun, M. C. Milone, M. L. Dustin, and L. C. Kam. 2014. Cross Talk between CD3 and CD28 Is Spatially Modulated by Protein Lateral Mobility. *Mol. Cell. Biol.* 34: 955–964.

216. Guy, C. S., K. M. Vignali, J. Temirov, M. L. Bettini, A. E. Overacre, M. Smeltzer, H. Zhang, J. B. Huppa, Y.-H. Tsai, C. Lobry, J. Xie, P. J. Dempsey, H. C. Crawford, I. Aifantis, M. M. Davis, and D. A. A. Vignali. 2013. Distinct TCR signaling pathways drive proliferation and cytokine production in T cells. *Nat. Immunol.* 14: 262–270.

217. Groom, J. R., and A. D. Luster. 2011. CXCR3 in T cell function. *Exp. Cell Res.* 317: 620–631.

218. Sauter, C. T., C. P. Bailey, M. M. Panis, C. S. Biswas, T. Budak-Alpdogan, A. Durham, N. Flomenberg, and O. Alpdogan. 2013. Interleukin-15 administration increases graft-versus-tumor activity in recipients of haploidentical hematopoietic SCT. *Bone Marrow Transplant.* 48(9): 1237-1242.

219. Mathew, N. R., F. Baumgartner, L. Braun, D. O'Sullivan, S. Thomas, M. Waterhouse, T. A. Müller, K. Hanke, S. Taromi, P. Apostolova, A. L. Illert, W. Melchinger, S. Duquesne, A. Schmitt-Graeff, L. Osswald, K. L. Yan, A. Weber, S. Tugues, S. Spath, D. Pfeifer, M. Follo, R. Claus, M. Lübbert, C. Rummelt, H. Bertz, R. Wäsch, J. Haag, A. Schmidts, M. Schultheiss, D. Bettinger, R. Thimme, E. Ullrich, Y. Tanriver, G. L. Vuong, R. Arnold, P. Hemmati, D. Wolf, M. Ditschkowski, C. Jilg, K. Wilhelm, C. Leiber, S. Gerull, J. Halter, C. Lengerke, T. Pabst, T. Schroeder, G. Kobbe, W. Rösler, S. Doostkam, S. Meckel, K. Stabla, S. K. Metzelder, S. Halbach, T. Brummer, Z. Hu, J. Dengjel, B. Hackanson, C. Schmid, U. Holtick, C. Scheid, A. Spyridonidis, F. Stölzel, R. Ordemann, L. P. Müller, F. Sicre-De-Fontbrune, G. Ihorst, J. Kuball, J. E. Ehlert, D. Feger, E. M. Wagner, J. Y. Cahn, J. Schnell, F. Kuchenbauer, D. Bunjes, R. Chakraverty, S. Richardson, S. Gill, N. Kröger, F. Ayuk, L. Vago, F. Ciceri, A. M. Müller, T. Kondo, T. Teshima, S. Klaeger, B. Kuster, D. H. Kim, D. Weisdorf, W. Van Der Velden, D. Dörfel, W. Bethge, I. Hilgendorf, A. Hochhaus, G. Andrieux, M. Börries, H. Busch, J. Magenau, P. Reddy, M. Labopin, J. H. Antin, A. S. Henden, G. R. Hill, G. A. Kennedy, M. Bar, A. Sarma, D. McLornan, G. Mufti, B. Oran, K. Rezvani, O. Shah, R. S. Negrin, A. Nagler, M. Prinz, A. Burchert, A. Neubauer, D. Beelen, A. Mackensen, N. Von Bubnoff, W. Herr, B. Becher, G. Socié, M. A. Caligiuri, E. Ruggiero, C. Bonini, G. Häcker, J. Duyster, J. Finke, E. Pearce, B. R. Blazar, and R. Zeiser. 2018. Sorafenib promotes graft-versus-leukemia activity in mice and humans through IL-15 production in FLT3-ITD-mutant leukemia cells. *Nat. Med.* 24: 282–291.

220. Gil-Cruz, C., C. Perez-Shibayama, L. Onder, Q. Chai, J. Cupovic, H.-W. Cheng, M. Novkovic, P. A. Lang, M. B. Geuking, K. D. McCoy, S. Abe, G. Cui, K. Ikuta, E. Scandella, and B. Ludewig. 2016. Fibroblastic reticular cells regulate intestinal inflammation via IL-15-mediated control of group 1 ILCs. *Nat. Immunol.* 17(12): 1388-1396.

221. Backer, R. A., P. Hombrink, C. Helbig, and D. Amsen. 2018. The Fate Choice Between Effector and Memory T Cell Lineages: Asymmetry, Signal Integration, and Feedback to Create Bistability. *Adv. Immunol.* 137: 48-82.

222. Delacher, M., C. Schmidl, Y. Herzig, M. Breloer, W. Hartmann, F. Brunk, D. Kägebein, U. Träger, A. C. Hofer, S. Bittner, D. Weichenhan, C. D. Imbusch, A. Hotz-Wagenblatt, T. Hielscher, A. Breiling, G. Federico, H. J. Gröne, R. M. Schmid, M. Rehli, J. Abramson, and M. Feuerer. 2019. Rbpj expression in regulatory T cells is critical for restraining TH2 responses. *Nat. Commun.* 10: 1621.

223. Bajénoff, M., J. G. Egen, L. Y. Koo, J. P. P. Laugier, F. Brau, N. Glaichenhaus, and R. N. Germain. 2006. Stromal cell networks regulate lymphocyte entry, migration, and territoriality in lymph nodes. *Immunity* 25: 989–1001.

224. Pinnell, N., R. Yan, H. J. Cho, T. Keeley, M. J. Murai, Y. Liu, A. S. Alarcon, J. Qin, Q. Wang, R. Kuick, K. S. J. J. Elenitoba-Johnson, I. Maillard, L. C. Samuelson, T. Cierpicki, and M. Y. Chiang. 2015. The PIAS-like Coactivator Zmiz1 Is a Direct and Selective Cofactor of Notch1 in T Cell Development and Leukemia. *Immunity* 43: 870–883.

225. Kohyama, M., W. Ise, B. T. Edelson, P. R. Wilker, K. Hildner, C. Mejia, W. A. Frazier, T. L. Murphy, and K. M. Murphy. 2009. Role for Spi-C in the development of red pulp macrophages and splenic iron homeostasis. *Nature* 457: 318–321.

226. Gaudette, B. T., D. D. Jones, A. Bortnick, Y. Argon, and D. Allman. 2020. mTORC1 coordinates an immediate unfolded protein response-related transcriptome in activated B cells preceding antibody secretion. *Nat. Commun.* 11: 723.

227. Rand, M. D., L. M. Grimm, S. Artavanis-Tsakonas, V. Patriub, S. C. Blacklow, J. Sklar, and J. C. Aster. 2000. Calcium Depletion Dissociates and Activates Heterodimeric Notch Receptors. *Mol. Cell. Biol.* 20: 1825–1835.

228. Liu, W.-H., and M.-Z. Lai. 2005. Deltex Regulates T-Cell Activation by Targeted Degradation of Active MEKK1. *Mol. Cell. Biol.* 25: 1367–1378.

229. Hsiao, H. W., W. H. Liu, C. J. Wang, Y. H. Lo, Y. H. Wu, S. T. Jiang, and M. Z. Lai. 2009. Deltex1 Is a Target of the Transcription Factor NFAT that Promotes T Cell Anergy. *Immunity* 31: 72–83.

230. Thaker, Y. R., M. Raab, K. Strebhardt, and C. E. Rudd. 2019. GTPase-activating protein Rasal1 associates with ZAP-70 of the TCR and negatively regulates T-cell tumor immunity. *Nat. Commun.* 10: 4804.

231. Larson, D. R., C. Fritzsch, L. Sun, X. Meng, D. S. Lawrence, and R. H. Singer. 2013. Direct observation of frequency modulated transcription in single cells using light activation. *Elife* 2:

e00750.

232. Yukawa, M., S. Jagannathan, S. Vallabh, A. V. Kartashov, X. Chen, M. T. Weirauch, and A. Barski. 2020. AP-1 activity induced by co-stimulation is required for chromatin opening during T cell activation. *J. Exp. Med.* 217: e20182009.

233. Kuang, Y., O. Golan, K. Preusse, B. Cain, C. J. Christensen, J. Salomone, I. Campbell, F. V Okwubido-Williams, M. R. Hass, Z. Yuan, N. Eafergan, K. H. Moberg, R. A. Kovall, R. Kopan, D. Sprinzak, and B. Gebelein. 2020. Enhancer architecture sensitizes cell-specific responses to Notch gene dose via a bind and discard mechanism. *Elife* 9: e53659.

234. Kobia, F. M., K. Preusse, Q. Dai, N. Weaver, P. Chaturvedi, S. J. Stein, W. S. Pear, Z. Yuan, R. A. Kovall, Y. Kuang, N. Eafergen, D. Sprinzak, B. Gebelein, E. Brunskill, and R. Kopan. 2020. Exposure to Mites Sensitizes Intestinal Stem Cell Maintenance, Splenic Marginal Zone B Cell Homeostasis, And Heart Development to Notch Dosage and Cooperativity. *bioRxiv*. preprint. https://doi.org/10.1101/2020.02.13.948224

235. Szabo, P. A., H. M. Levitin, M. Miron, M. E. Snyder, T. Senda, J. Yuan, Y. L. Cheng, E. C. Bush, P. Dogra, P. Thapa, D. L. Farber, and P. A. Sims. 2019. Single-cell transcriptomics of human T cells reveals tissue and activation signatures in health and disease. *Nat. Commun.* 10: 4706.

236. Brinkmann, V., T. Geiger, S. Alkan, and C. H. Heusser. 1993. Interferon α increases the frequency of interferon γ-producing human CD4+ T cells. *J. Exp. Med.* 178: 1655–1663.

237. Kumano, K., S. Chiba, A. Kunisato, M. Sata, T. Saito, E. Nakagami-Yamaguchi, T. Yamaguchi, S. Masuda, K. Shimizu, T. Takahashi, S. Ogawa, Y. Hamada, and H. Hirai. 2003. Notch1 but not Notch2 is essential for generating hematopoietic stem cells from endothelial cells. *Immunity* 18: 699–711.

238. Carulli, A. J., T. M. Keeley, E. S. Demitrack, J. Chung, I. Maillard, and L. C. Samuelson. 2015. Notch receptor regulation of intestinal stem cell homeostasis and crypt regeneration. *Dev. Biol.* 402: 98–108.

239. Majumder, S., N. Amatya, S. Revu, C. V. Jawale, D. Wu, N. Rittenhouse, A. Menk, S. Kupul, F. Du, I. Raphael, A. Bhattacharjee, U. Siebenlist, T. W. Hand, G. M. Delgoffe, A. C. Poholek, S. L. Gaffen, P. S. Biswas, and M. J. McGeachy. 2019. IL-17 metabolically reprograms activated fibroblastic reticular cells for proliferation and survival. *Nat. Immunol.* 20(5): 534-545.

240. Brehm, M. A., K. A. Daniels, and R. M. Welsh. 2005. Rapid Production of TNF-α following TCR Engagement of Naive CD8 T Cells. *J. Immunol.* 175: 5043–5049.

241. Tveriakhina, L., K. Schuster-Gossler, S. M. Jarrett, M. B. Andrawes, M. Rohrbach, S. C. Blacklow, and A. Gossler. 2018. The ectodomains determine ligand function in vivo and selectivity of DLL1 and DLL4 toward NOTCH1 and NOTCH2 in vitro. *Elife* 7: e40045.

242. Nandagopal, N., L. A. Santat, L. LeBon, D. Sprinzak, M. E. Bronner, and M. B. Elowitz. 2018. Dynamic Ligand Discrimination in the Notch Signaling Pathway. *Cell* 172(4): 869-880.

243. Hirano, K. I., A. Suganami, Y. Tamura, H. Yagita, S. Habu, M. Kitagawa, T. Sato, and K. Hozumi. 2020. Delta-like 1 and delta-like 4 differently require their extracellular domains for triggering notch signaling in mice. *Elife* 9: e50979.

244. Weng, A. P., J. M. Millholland, Y. Yashiro-Ohtani, M. L. Arcangeli, A. Lau, C. Wai, C. Del Bianco, C. G. Rodriguez, H. Sai, J. Tobias, Y. Li, M. S. Wolfe, C. Shachaf, D. Felsher, S. C. Blacklow, W. S. Pear, and J. C. Aster. 2006. c-Myc is an important direct target of Notch1 in T-cell acute lymphoblastic leukemia/lymphoma. *Genes Dev.* 20(15): 2096-2109.

245. Ryan, R. J. H., J. Petrovic, D. M. Rausch, Y. Zhou, C. A. Lareau, M. J. Kluk, A. L. Christie, W. Y. Lee, D. R. Tarjan, B. Guo, L. K. H. Donohue, S. M. Gillespie, V. Nardi, E. P. Hochberg, S. C. Blacklow, D. M. Weinstock, R. B. Faryabi, B. E. Bernstein, J. C. Aster, and W. S. Pear. 2017. A B Cell Regulome Links Notch to Downstream Oncogenic Pathways in Small B Cell Lymphomas. *Cell Rep.* 21(3): 784-797.

246. Dell'aringa, M., and R. Lee Reinhardt. 2018. Notch signaling represents an important checkpoint between follicular T-helper and canonical T-helper 2 cell fate article. *Mucosal Immunol.* 11: 1079–1091.

247. Maekawa, Y., C. Ishifune, S. Tsukumo, K. Hozumi, H. Yagita, and K. Yasutomo. 2015. Notch controls the survival of memory CD4 + T cells by regulating glucose uptake. *Nat. Med.* 21: 55–61.

248. Kluk, M. J., T. Ashworth, H. Wang, B. Knoechel, E. F. Mason, E. A. Morgan, D. Dorfman, G. Pinkus, O. Weigert, J. L. Hornick, L. R. Chirieac, M. Hirsch, D. J. Oh, A. P. South, I. M. Leigh, C. Pourreyron, A. J. Cassidy, D. J. DeAngelo, D. M. Weinstock, I. E. Krop, D. Dillon, J. E. Brock, A. J. F. Lazar, M. Peto, R. J. Cho, A. Stoeck, B. B. Haines, S. Sathayanrayanan, S. Rodig, and J. C. Aster. 2013. Gauging NOTCH1 Activation in Cancer Using Immunohistochemistry. *PLoS One* 8(6): e67306.

249. Wagner, N., J. Lohler, E. J. Kunkel, K. Ley, E. Leung, G. Krissansen, K. Rajewsky, and W. Muller. 1996. Critical role for β7 integrins in formation of the gut-associated lymphoid tissue. *Nature* 382: 366–370.

250. Brennan, T. V., V. Hoang, K. R. Garrod, F.-C. Liu, T. Hayden, J. Kim, and S.-M. Kang. 2008. A new T-cell receptor transgenic model of the CD4+ direct pathway: level of priming determines acute versus chronic rejection. *Transplantation* 85: 247–255.

251. Ellies, L. G., S. Tsuboi, B. Petryniak, J. B. Lowe, M. Fukuda, and J. D. Marth. 1998. Core 2 Oligosaccharide Biosynthesis Distinguishes between Selectin Ligands Essential for Leukocyte Homing and Inflammation. *Immunity* 9: 881–890.

252. Hozumi, K., N. Negishi, D. Suzuki, N. Abe, Y. Sotomaru, N. Tamaoki, C. Mailhos, D. Ish-Horowicz, S. Habu, and M. J. Owen. 2004. Delta-like 1 is necessary for the generation of marginal zone B cells but not T cells in vivo. *Nat. Immunol.* 5: 638–644.

253. Schmitt, T. M., and J. C. Zúñiga-Pflücker. 2002. Induction of T cell development from hematopoietic progenitor cells by delta-like-1 in vitro. *Immunity* 17: 749–756.

254. Schmitt, T. M., and J. C. Zúñiga-Pflücker. 2006. T-cell development, doing it in a dish. *Immunol. Rev.* 209: 95–102.

255. Lacombe, M. H. M.-H., M.-P. M. P. Hardy, J. Rooney, and N. Labrecque. 2005. IL-7 receptor expression levels do not identify CD8+ memory T lymphocyte precursors following peptide immunization. *J. Immunol.* 175: 4400–4407.

256. Bray, N. L., H. Pimentel, P. Melsted, and L. Pachter. 2016. Near-optimal probabilistic RNA-seq quantification. *Nat. Biotechnol.* 34(5): 525-527.

257. Law, C. W., Y. Chen, W. Shi, and G. K. Smyth. 2014. Voom: Precision weights unlock linear model analysis tools for RNA-seq read counts. *Genome Biol.* 15(2):R29.

258. Ritchie, M. E., B. Phipson, D. Wu, Y. Hu, C. W. Law, W. Shi, and G. K. Smyth. 2015. Limma powers differential expression analyses for RNA-sequencing and microarray studies. *Nucleic Acids Res.* 43(7):e47.

259. Subramanian, A., P. Tamayo, V. K. Mootha, S. Mukherjee, B. L. Ebert, M. A. Gillette, A. Paulovich, S. L. Pomeroy, T. R. Golub, E. S. Lander, and J. P. Mesirov. 2005. Gene set enrichment analysis: A knowledge-based approach for interpreting genome-wide expression profiles. *Proc. Natl. Acad. Sci. U. S. A.* 102(43): 15545-15550.